

THE UNIVERSITY OF HULL

The Synthesis of Liquid Crystalline Materials for
Organic Semiconductor Device Applications

being a Thesis submitted for the Degree of

Doctor of Philosophy (PhD)

in the University of Hull

by

Mark S. Dixon B.Sc. (Hons), M.Sc.

June 2009

Acknowledgements

I would like to express my thanks and appreciation and I gratefully acknowledge the assistance, guidance and support given to me by my supervisor, Professor S. M. Kelly, throughout the course of this research.

I wish to thank Dr. Martin Heeney, from Merck Chemicals Ltd., and Elliot J. Firth and Allen Pang from the University of Hull for synthesising, under my supervision, some of the intermediates and final products detailed in this thesis.

In addition to which, my thanks go to Dr. Panagiotis Vlachos for synthesising some of the intermediates detailed in this thesis first and for the helpful discussions he provided. Additional thanks go to Dr. Stuart Kitney for the help and assistance that he provided.

I would like to thank the technical staff at the University of Hull for performing the necessary analysis on the reaction intermediates and final products detailed in this thesis. These include Mrs. Brenda Worthington and Mr. Bob Knight (NMR), Mr. Dave Hannan (MS) and Mrs. Carol Kennedy (Elemental Analysis). I would also like to thank Mr. Martin Cawley for his help and assistance in obtaining the necessary IR spectra.

I would like to acknowledge and thank the EPSRC and Merck Chemicals Ltd. for providing funding for this research project.

Special thanks go to my colleague, Nayyar Aziz, in C217 for his advice, friendship and support and finally, I would like to thank my parents for their support and encouragement throughout my PhD programme.

Abstract

This research is based on the synthesis and evaluation of novel photo- and chemically-reactive, liquid crystalline monomers (reactive mesogens) with improved charge-transporting properties. Low-molar-mass (LMM) liquid crystalline monomers, based on a series of substituted dibenzothiophenes, thiophenes, [2,2']-bithiophenes, thieno[3,2-b]thiophenes, benzo-2,1,3-thiadiazoles and fluorenes have been synthesised. These materials incorporate photo-polymerisable (non-conjugated diene and methacrylate) and chemically-polymerisable (oxetane) end-groups, attached by aliphatic spacer units of varying length to an aromatic core. These photo- and chemically-polymerisable end-groups are situated at the peripheries of the molecular structure, allowing the potential fabrication of multi-layer, organic semiconductor devices due to the insoluble, cross-linked polymer network obtained after polymerisation of the analogous reactive mesogens (RMs).

Ultra-violet (UV) radiation can be used, without the requirement of photoinitiators, to polymerise and cross-link the RMs with the non-conjugated diene and methacrylate end-groups by a radical mechanism, to form insoluble liquid crystalline polymer networks. The oxetane polymerisable end-groups require a suitable chemical initiator, such as a boron trifluoride-THF or -diethyl ether complex to initiate polymerisation via an ionic mechanism. These cross-linked, insoluble polymer networks can then be used as the charge-transporting layer of multi-layer, organic semiconductor devices. It is envisaged that this approach, using highly cross-linked, insoluble polymer networks, can achieve high charge-carrier mobility, due to a high degree of order within the solid polymer network with liquid crystalline order.

A secondary focus of this research was to identify potential structure-property relationships for the novel organic LMM materials synthesised, such as the dependence of liquid crystalline transition temperatures and charge-transport or mobility on molecular structure. The correlation between molecular structure and charge-transporting properties was to be achieved by synthesising a series of related compounds with different central chromophores, enabling clear comparisons of the efficiency of each of the chromophores to be established. Furthermore, the

incorporation of different end-groups and aliphatic spacer unit lengths into a number of compounds with the same chromophore allowed their effect upon the physical properties stated above to be studied.

Despite the synthetic difficulties encountered, a wide range of charge-transporting RMs, for organic semiconductor device applications, have been successfully synthesised. Many of these new materials form nematic and predominantly smectic liquid crystalline or crystal- or quasi-smectic phases over significant temperature ranges. Significantly lower liquid crystalline and crystal-smectic transition temperatures were attained for those RMs incorporating branched photo- and chemically-polymerisable groups at the ends of the spacers and fluorine atoms in the 2-position on the phenyl rings in the respective material structures. From this work, it has been observed that the mesophases, melting points, liquid crystalline and crystal-smectic transition temperature ranges and clearing points observed for the RMs synthesised can be manipulated by synthetically altering the structure of the RM.

The [2,2']-bithiophene class of materials generally exhibited smectic and crystal-smectic mesophases. However, a nematic mesophase was observed when photo-polymerisable methacrylate end-groups were incorporated in a lateral position and fluorine atoms incorporated adjacent to the molecular core, into the materials structure (compound **76**). LCs incorporating the 2,7-disubstituted-9,9-dialkylfluorene unit tend to form nematic mesophases due to steric effects. Consequently materials containing these units tend to have lower viscosities than analogous materials forming smectic and crystal-smectic mesophases due to the absence of a layer structure. This was intended to allow the new nematic liquid crystalline semiconductors to be aligned more easily than the standard smectic and crystal-smectic semiconductors for practical devices.

Apart from the disubstituted fluorene-based material (compound **115**), which exhibits a glass transition temperature at -3 °C, there was no evidence for the formation of stable glasses, at or above room temperature, by any of the other materials synthesised. The formation of a stable glass by a material is an attractive property for organic semiconductors, as it would allow device fabrication based on anisotropic polymer networks to be carried out at or above room temperature.

Contents

Acknowledgements	(i)
Abstract	(ii) - (iii)
1.0 Introduction	1
1.1 A brief history of organic semiconductor devices	1 - 5
1.1.1 Semiconductors	5 - 6
1.2 Device parameters	7
1.2.1 Device structure	7 - 8
1.2.2 Device physics and operation	8 - 9
1.2.3 Field effect mobility and on/off current ratio	9 - 10
1.2.4 Insulator-semiconductor interface	10
1.2.5 Microstructure-mobility interplay	10 - 11
1.3 Device manufacturing methods	11 - 12
1.3.1 Vacuum sublimation	12
1.3.2 Solution processing methods	12
1.3.2.1 Spin coating	13
1.3.3 Printing and stamping methods	13 - 14
1.3.3.1 Microcontact printing (stamping)	14
1.3.3.2 Inkjet printing	14 - 15
1.4 Materials previously used for organic semiconductor devices	15 - 17
1.4.1 Low molar mass (LMM) materials	17 - 22
1.4.2 Polymeric materials (PMs)	22 - 25
1.4.3 Stability and reliability of organic semiconductor devices	25 - 26
1.5 Liquid crystals (LCs)	27 - 28
1.5.1 Structure property relationships	28 - 30
1.5.2 Thermotropic liquid crystals	30
1.5.2.1 Calamitic liquid crystals	30 - 33
1.5.2.2 The nematic (N) phase	33 - 34
1.5.2.3 The chiral nematic (N*) phase	35

1.5.2.4 The smectic phase	36
1.5.2.5 The smectic A (SmA) phase	37
1.5.2.6 The smectic C (SmC) phase	37 - 38
1.5.2.7 The crystal-smectic phases	38
1.5.2.7.1 Crystals B and E	38 - 39
1.5.2.7.2 Crystals J and G	39
1.5.2.7.3 Crystals H and K	39 - 40
1.5.3 Columnar liquid crystals	40
1.5.4 Liquid crystalline polymers (LCPs)	40 - 41
1.5.5 Mesophase identification	41
1.5.5.1 Optical polarising microscopy	41 - 43
1.5.5.2 Differential scanning calorimetry (DSC)	43 - 44
1.5.5.3 X-ray diffraction	44
1.6 Liquid crystals and organic semiconductors	45
1.6.1 Calamitic liquid crystals as charge-carrier transport layers	45 - 47
1.6.2 Liquid crystalline polymer networks	47 - 50
1.7 References	51 - 58

2.0 Aims of the Research 59 - 61

2.1 References	62
--------------------------	----

3.0 Experimental 63

3.1 Material evaluation	63 - 68
3.2 Experimental discussion	69 - 77
3.3 Reaction schemes	78 - 92
3.4 Material synthesis	93 - 146
3.5 References	147 - 148

4.0 Results and Discussion 149 - 151

4.1 Reaction scheme two	152 - 155
4.2 Reaction schemes three and four	156 - 160
4.3 Reaction schemes five a and b	161

4.4 Reaction schemes six a and b	162 - 164
4.5 Reaction schemes three, four and thirteen	165 - 167
4.6 Reaction scheme seven	168 - 170
4.7 Reaction schemes eight and nine	171 - 178
4.7.1 Charge-carrier mobility	179 - 180
4.8 Reaction schemes eleven and twelve	181 - 184
4.9 Reaction scheme fourteen	185
4.10 Reaction scheme fifteen	186 - 188
4.11 Cyclic Voltammetry (CV)	189 - 190
4.12 References	191 - 192
5.0 Conclusions	193 - 195



Chapter One



Introduction



•

•

•

1.0 Introduction

1.1 A Brief History of Organic Semiconductor Devices

Monocrystalline silicon has been the most popular semiconductor over the last 30 years. It has a single and continuous crystal lattice structure with no grain boundary defects or impurities allowing it to obtain significantly greater charge-carrier mobilities ($300\text{-}900\text{ cm}^2\text{ V}^{-1}\text{ s}^{-1}$) when compared to poly ($50\text{-}100\text{ cm}^2\text{ V}^{-1}\text{ s}^{-1}$) or amorphous ($1\text{ cm}^2\text{ V}^{-1}\text{ s}^{-1}$) silicon. However, the high price per unit area and some inherent mechanical fragility make the use of monocrystalline silicon difficult in applications where large area coverage, mechanical toughness and low cost are required. It is with such applications in mind that researchers have been exploring, with growing interest, the properties of organic semiconductor materials.

The discovery of conducting organic polymers has proven to be not only of intrinsic scientific interest, but also of great technological promise. The goal of all-polymer electronics has motivated an increasing number of research groups for the past 25 years. These groups hope to provide plastics, which have the advantages of low cost processing, flexibility and toughness, with the electronic properties needed for practical circuitry. Organic semiconductors have the potential to be adapted to continuous feed manufacturing methods, such as reel to reel printing or screen printing, allowing low cost mass production of electronic devices.

Organic devices need several key innovations to achieve their market potential. Firstly, ongoing improvement in materials is necessary, with regards to improved conductivity and charge-carrier mobility, which would increase the range of potential applications. Improved chemical and mechanical stability would simplify packaging and allow the use of organic devices in harsh environments. Predictable and consistent material properties are also necessary for potential commercial applications.

Secondly, many of the potential applications of organic devices are unlikely to be cost-effective without innovations in manufacturing methods. Semiconductor

formulations compatible with existing printing methods can greatly reduce the manufacturing costs, particularly for large area or high-volume devices. Innovations in manufacturing methods are the key to the success of organic semiconductor devices. As long as these devices require rigid glass or plastic substrates, they will offer only limited advantages relative to existing silicon technology. Robust films on flexible or semi-flexible substrates will help organic devices serve applications that silicon cannot reach. Manufacturing innovations could also allow organic semiconductor devices to take advantage of the extremely low cost, high volume methods currently employed by the printing industry.

The commercial prospects for organic semiconductors depend on their technical capabilities. They will succeed or fail not because they can compete with silicon devices on sheer processing power, but because they can do things that silicon devices cannot. While silicon should continue to dominate the performance orientated segments of the semiconductor market, organic semiconductors offer simpler processing and more physically robust devices. Organic materials may be able to win a niche in low cost, highly portable, applications.

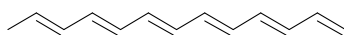
Thin films formed by conjugated aromatic polymers and oligomers, as previously stated, can be simple and inexpensive to manufacture. These organic films have good mechanical properties (strength, robustness and flexibility) and good physical and chemical properties (durability, solvent and corrosion resistance, UV light stability and resistance to oxidative degradation), in addition to being lightweight. Devices such as field effect transistors (FETs) and thin film transistors (TFTs) manufactured partially or entirely with polymeric or oligomeric materials, are today a reality.

Main chain polymers can exhibit good processing properties and high glass transition temperatures (T_g), of which the latter, tends to enhance the stability of the material. Polyacetylene is the simplest type of conjugated main chain polymer consisting of methine hydrogens linked by one C-C single bond to one C-C double bond and can exist in two main isomeric forms, *cis*- and *trans*-, with *trans*-polyacetylene being the most thermodynamically stable isomer at room temperature.

Shirakawa et al^[1] discovered that it was possible to control the proportions of *cis*- and *trans*-isomers present in polyacetylene by changing the reaction conditions of the polymerisation. By increasing the concentration of a Ziegler-Natta catalyst or varying the temperature either pure *trans*- or pure *cis*-polyacetylene, could be obtained, see figure 1.1. The conductivity of polyacetylene was found to increase by over seven orders of magnitude (from 3.2×10^{-6} to $38 \Omega^{-1}\text{cm}^{-1}$), when *trans*-polyacetylene was chemically doped with electron acceptors (*p*-doping) such as iodine^[2], or with electron donors (*n*-doping) such as sodium. The values of electrical conductivity obtained were extremely high and in the region of metallic behaviour^[3].



(A) - *cis*-polyacetylene



(B) - *trans*-polyacetylene

Figure 1.1 - A structural representation of the *cis*- (A) and *trans*- (B) isomers of polyacetylene

There are however problems associated with polyacetylene as a conducting polymer in a practical device in that it reacts rapidly and irreversibly with oxygen, it is insoluble in organic solvents and unlike many other polymers, cannot be melted and is consequently difficult to process. Progress was made with the discovery of poly(*para*-phenylenevinylene)^[4] (PPV) and polythiophene^[5-6], see figure 1.2. Long alkyl chains could be attached to the backbones of these polymers^[7-10], making them soluble in non-polar organic solvents and thus easier to process and they are inherently less sensitive than polyacetylene to oxidative degradation. A variety of PPV derivatives containing different substituents have also been synthesised^[11-13].

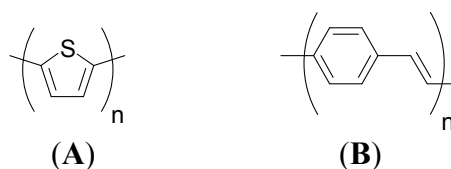


Figure 1.2 - Structural representations of polythiophene (A) and poly(*para*-phenylenevinylene) (PPV) (B)

A further ten years passed, after this initial breakthrough, before the first practical FETs were demonstrated. In 1986, Tsumura et al.^[14] produced such a device, which used electrochemically-prepared polythiophene as the semiconducting layer. These devices gave charge-carrier mobilities of the order of $10^{-5} \text{ cm}^2 \text{ V}^{-1} \text{ s}^{-1}$. Then in 1988, functional polymer TFTs were demonstrated by Burroughes et al.^[15] using doped polyacetylene as the conjugated, polymeric semiconductor material. These devices produced carrier mobilities of the order of $10^{-4} \text{ cm}^2 \text{ V}^{-1} \text{ s}^{-1}$, an order of magnitude greater than those produced by Tsumura.

The performance of organic FETs (OFETs) and TFTs (OTFTs) has improved dramatically since such devices were demonstrated and optimised electronic devices now show electrical characteristics approaching or even exceeding those of amorphous silicon (aSi) TFTs, that is they have mobilities approaching or exceeding $1 \text{ cm}^2 \text{ V}^{-1} \text{ s}^{-1}$. This has been made possible by the development of new, more stable conducting polymeric materials.

Plastic chips have the potential to be much less expensive than the equivalent silicon chips. Not only are the materials cheaper than silicon to produce, the manufacturing process is also less complex. In addition, being printed on plastic would make potential products flexible and more robust than traditional devices manufactured on rigid substrates. Such inexpensive, but less powerful devices, could have potential applications in consumer products and markets where many separate devices are needed, but do not demand excessive individual computing power, e.g., airline luggage and inventory control tags. Plastic chips have the potential to store more information than standard bar codes, making them useful for consumer packaging as well.

Other potential applications of plastic electronics include large area flat panel displays (TVs, monitors and advertising), small area displays (automotive and consumer electronics), laptops and PDAs (personal digital assistants), Radio Frequency Identification (RFID), smart cards and programmable credit cards, cell phones and digital cameras, organic solar cells and large area sensors. OFETs and OTFTs are likely to be appropriate for other applications where cost is critical and performance requirements are secondary.

Applications of organic semiconductors in packaging and RFID tags may be the closest to technological feasibility. These devices require only limited numbers of transistors and are compatible with current semiconductor manufacturing methods. However, silicon RFID tags are already well established, cost very little and are backed by a large manufacturing infrastructure. Packaging applications of organic semiconductors may be more promising in the short term, with computerised clothing and electronic luggage tag applications likely to emerge more slowly, as they face significant cost and technological barriers. However, these applications face little direct competition from silicon devices.

Even though polymeric materials have carrier mobilities that are several orders of magnitude less than monocrystalline silicon, the carrier mobilities observed for polymeric materials are sufficient for the applications described above. In addition to which, they can be easily processed by the low cost methods characteristic of polymer technology, principally solution processing techniques such as spin coating. The major reason for the great commercial potential of semiconductor polymers is that they can be produced quickly and cheaply. Electronic components based on polymers and polymer integrated circuits (ICs) will soon find their place in consumer products where low processing costs will be more important than high speeds.

1.1.1 Semiconductors

Metals are good conductors because they have their upper energy or valence band (VB) partly filled. Because the VB is partly filled, electrons can flow and hence conduct electricity. By contrast, insulators have their VB completely filled, consequently, for electrons to flow they must occupy the next available empty energy

level. This is typically a few electron volts (eV) above the VB and is called the conduction band (CB).

The energy gap between the VB and the CB is large in insulators and hence electrons cannot ordinarily occupy the CB and there is no electrical conduction. In semiconductors however, the energy gap between the VB and the CB is smaller. This means that some electrons can be excited, either thermally or through an applied field, from the VB to the CB and hence they can conduct electricity, see figure 1.3.

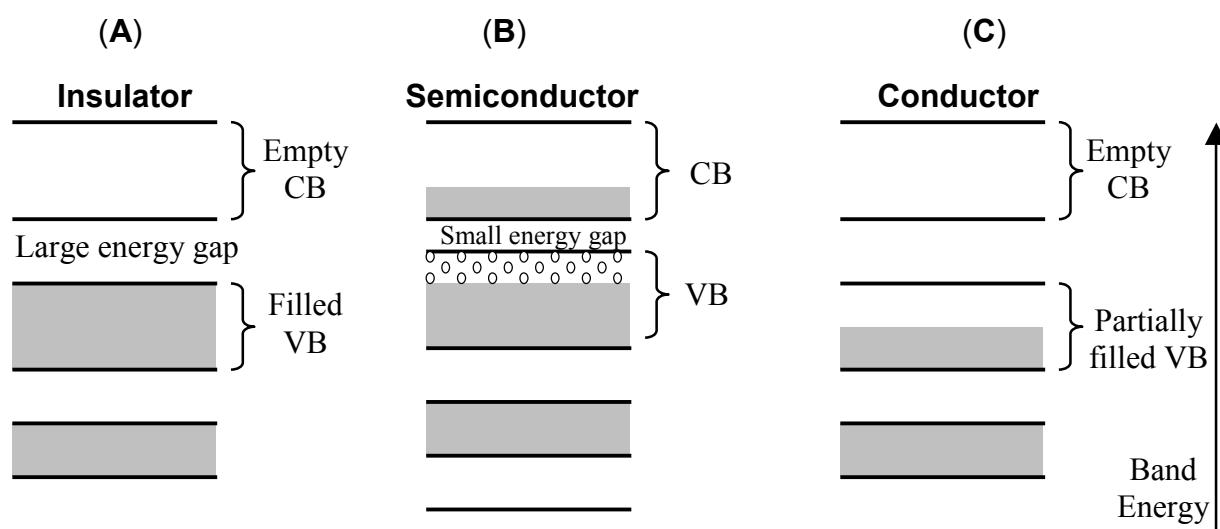


Figure 1.3 - Energy bands in an inorganic insulator (A), semiconductor (B) and conductor (C)

Organic molecules are known generally to be insulators, but when a high degree of conjugation is present they may act as semiconductors. This is because in a C-C double bond, the sp_z orbitals overlap to form a pair of π molecular orbitals (MOs). The lower energy level π orbital is the bonding MO and the higher energy π^* orbital is the anti-bonding MO. In terms of semiconductors, the bonding and anti-bonding orbitals can be referred as the VB and CB respectively and there is therefore a bandgap between them.

1.2 Device Parameters

There are several organic semiconducting device parameters that need to be considered and these are discussed in the following sections.

1.2.1 Device Structure

OTFTs based on organic semiconductors can be manufactured in one of two configurations. A top gate arrangement, as shown in figure 1.4(a) or a bottom gate arrangement, as shown in figure 1.4(b).

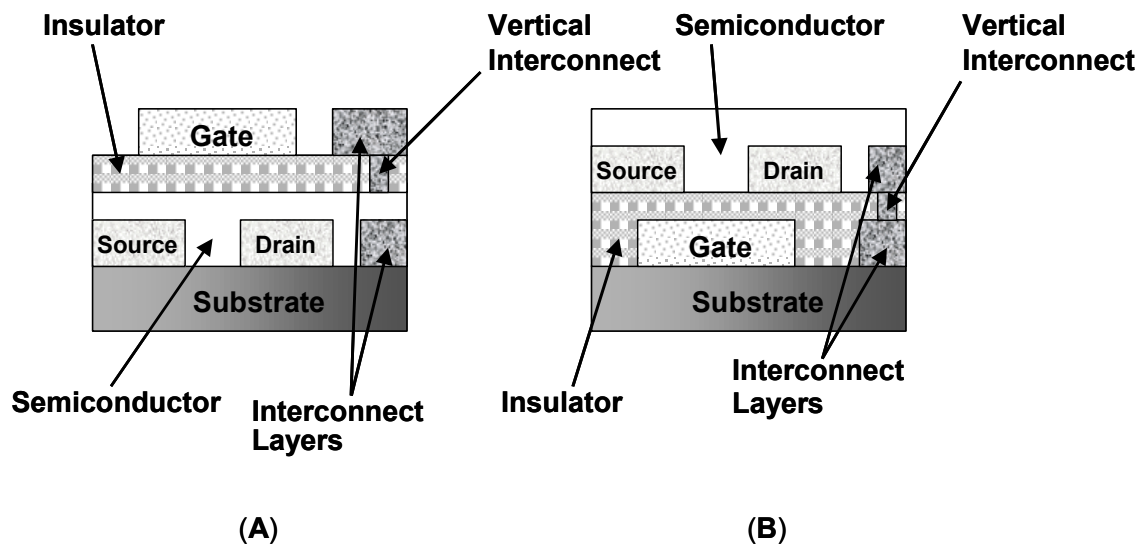


Figure 1.4 - Top (A) and bottom (B) gate approach to OTFT manufacture

The top gate arrangement has the advantage of protecting both the gate dielectric or insulator layer and the layer of semiconductor material, which chemically are the most sensitive to environmental influence. The electronic properties of the materials used for these layers can degrade rapidly when exposed to oxygen or water vapour. It does however, have two main disadvantages. Firstly the gate dielectric has to be deposited and structured on top of the semiconductor and this process must preserve the semiconductor material layer. Secondly, vertical interconnects (*vias*) between the conductive layers have to be built through the gate dielectric, potentially a difficult technological task.

To manufacture an OTFT in the bottom gate arrangement, the gate electrode is first deposited onto an insulating substrate followed by the deposition of the gate insulator, which can consist of either an organic or inorganic dielectric film. Source and drain electrodes are deposited onto the gate dielectric film, which is then followed by the deposition of the thin film channel layer. This thin film channel layer can contain either a molecular or polymeric semiconductor, which connects the source and drain electrodes. A reverse of this sequence is followed to manufacture an OTFT in the top gate arrangement.

The thin film of semiconducting material can be easily applied to the device. The electrodes however, require patterning and for inorganic materials such as metals, that step has traditionally been performed with lithographic and etching techniques. For low cost plastics however, photolithography is not a good choice because it is relatively expensive, incompatible with some polymers, difficult to apply on uneven substrates and not appropriate for reel-to-reel processing. These drawbacks have motivated the search for alternative printing methods, see section 1.3.3.

1.2.2 Device Physics and Operation

The principals on which a TFT works are the same, regardless of whether the device is silicon-based or polymer-based. An OTFT has three contacts or electrodes: the source, the drain and the gate. Considering an OTFT in which the semiconductor is *p*-type, that is the charge-carriers are holes (h^+), in the “on” state, figure 1.5(a), the gate electrode is made negative and this induces a positive charge in the insulating dielectric layer immediately next to the gate. This sets up a field in the dielectric, so at its opposite side, adjacent to the semiconductor, a negative charge builds up. This induces a positive charge in the semiconductor, which, in turn, makes the semiconductor more conducting. This creates a conducting channel, allowing charge to flow from the source to the drain. In the “off” state, the gate voltage is set so that there is no conducting channel set up in the semiconducting layer, see figure 1.5(b). This means that no current can flow between the source and drain electrodes, even if there is a voltage difference between them.

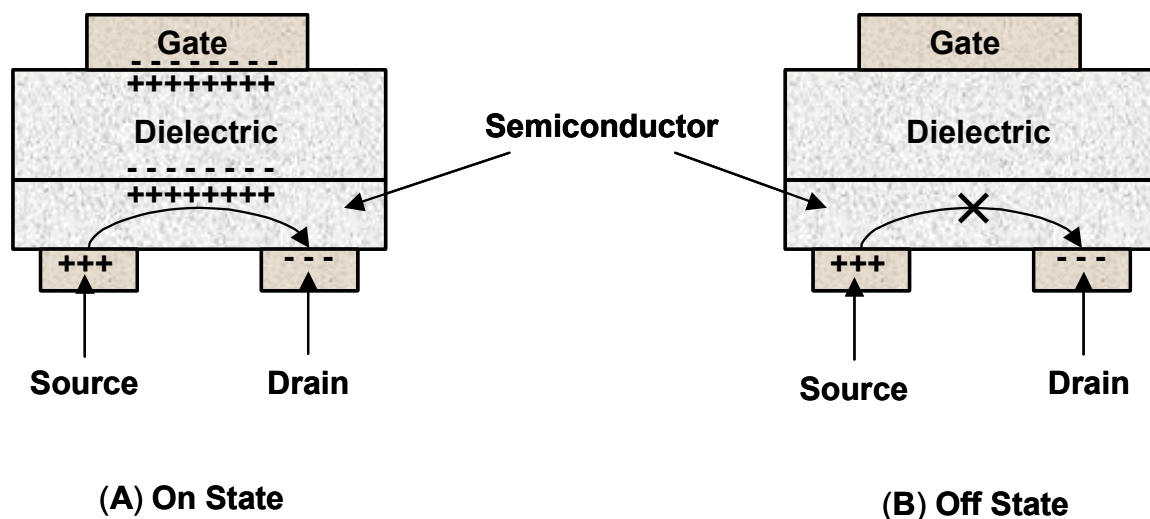


Figure 1.5 - OTFT operation in the on (A) and off (B) states (Note: the current shown in figure 1.5(a) - the “on” state - is shown as a flow of holes since the semiconductor is *p*-type)

1.2.3 Field Effect Mobility and On/Off Current Ratio

One of the major problems in achieving adequate operating speeds is the mobility of the charge-carriers in the semiconducting material layer. The field effect mobility (FEM) of an OTFT describes how easily charge-carriers (free electrons or holes) are able to move through the organic semiconducting material and is typically determined by a time of flight (TOF) technique^[16-18]. This in turn determines the magnitude of the transistor current and the switching speed of the device or the maximum speed at which the circuit can process electrical signals. When holes (h^+) are the dominant charge-carriers the semiconductor material can be regarded as a *p*-type material, an example of which is polythienylenevinylene (PTV), see figure 1.6. OTFTs manufactured from spin-coated solutions of PTV precursors^[19] have shown hole mobilities in the range of $5 \times 10^{-4} - 10^{-3} \text{ cm}^2 \text{ V}^{-1} \text{ s}^{-1}$.

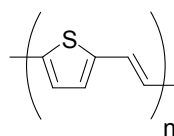


Figure 1.6 - Structural representation of polythienylenevinylene (PTV)

An example of an organic *n*-type material, where electrons (e^-) are the dominant charge-carriers, is copper hexadecafluorophthalocyanine^[20]. However, *n*-type materials tend to be unstable and have rarely been used in OTFT devices to date. The performance of an OTFT is also characterised by its on/off current ratio, which is the ratio of the current in the on-state to that in the off-state. A high performance OTFT should have a high FEM and a high on/off current ratio.

1.2.4 Insulator-Semiconductor Interface

The interface between the insulator (gate dielectric) and the semiconductor material is the most important part of the device to configure correctly. The cleanliness of the insulating layer is also important, ensuring it is free from static charges. The flatness of a substrate is also important, in order to avoid local electric fields, which can potentially disrupt the formation of the accumulation regime. The accumulation regime describes the situation where the majority carriers (free electrons or holes) are attracted to the insulator-semiconductor interface when a negative voltage is applied to the gate electrode, which in turn allows a significant current to flow between the source and drain electrodes *via* the semiconducting material.

1.2.5 Microstructure-mobility Interplay

There is a definite relationship between the microstructure of a semiconducting material and the mobility in an OTFT. Most of the work with OTFTs to date has been carried out on disordered amorphous polymers, where the polymer chains tend to be tangled which results in highly-localised charge-carriers and hence mobilities that are lower than those required. This represents a major obstacle to developing workable applications. However, work published by Sirringhaus et al.^[21-22] has provided experimental evidence that in some polymers, which tend to self-organise, the charge-carriers are more extended than usual. These papers show that the π - π stacking direction gives very good mobility, $0.1 \text{ cm}^2 \text{ V}^{-1} \text{ s}^{-1}$ for vacuum evaporated films of regioregular poly(3-hexylthiophene) (rr-P3HT), see figure 1.7(a). Regioregularity denotes the percentage of stereoregular head to tail attachments of the hexyl side chains to the 3-position of the thiophene rings, see figure 1.7(b).

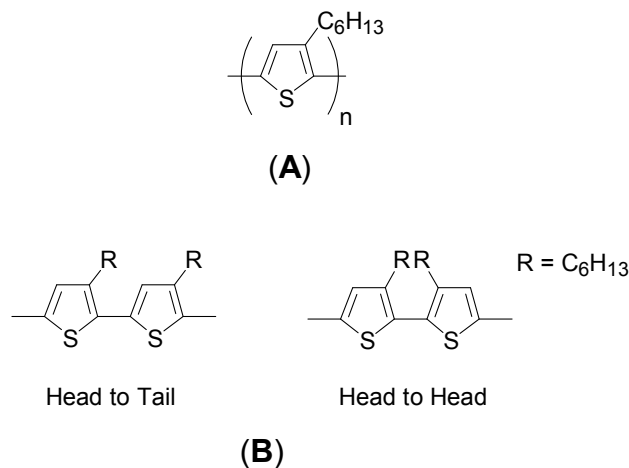


Figure 1.7 - Structural representation of (A) rr-P3HT and (B) the head to tail and head to head orientation of the hexyl side chains in the 3-position on the thiophene rings in rr-P3HT

rr-P3HT is much more ordered than its regiorandom counterparts and has achieved mobilities as high as $4.5 \times 10^{-2} \text{ cm}^2 \text{ V}^{-1} \text{ s}^{-1}$ even in OTFTs manufactured from solution cast films^[23]. However, rr-P3HT is very sensitive to oxygen and OTFTs manufactured with this polymer degrade within a short time period in the presence of air and light^[19].

1.3 Device Manufacturing Methods

Semiconducting polymers might not compete with silicon for speed and durability in electronic circuits, but they are candidates for applications in which low cost and flexibility are paramount. The challenge is to produce low performance, low cost electronics, focussing on inexpensive methods to manufacture and pattern the organic films. Fortunately, organic electronics have the potential to be reasonably cheap, but ultimately there are trade-offs to be had between the manufacturing technique used and the subsequent costs and performance.

When small molecule organic semiconductors, such as pentacene, are processed by single crystal growth or vacuum deposition, the molecules often arrange themselves in well-ordered layers, enhancing the overlap between adjacent molecular orbitals and increasing the probability that the charge-carriers can hop from one molecule to another, which subsequently enhances the charge-carrier mobility. Vacuum deposited

films can be expensive to produce due to the patterning and processing required of the subsequent films. By contrast, oligomers and polymers can be applied from solution and patterned using low cost stamping or printing techniques. However, the carrier mobility is often quite low due to the increased disordered nature of the molecules in the resulting material.

1.3.1 Vacuum Sublimation

Most of the high performance organic semiconductors discovered to date are low molecular weight materials (small molecules) with high melting points (in excess of 250 °C) and low solubility. They are generally aromatic molecules with extended and conjugated π -systems or fused ring structures. The most common method for thin film deposition of these materials is vacuum sublimation. In this method, the material is heated inside a vacuum chamber and the evaporated organic vapour condenses on the desired substrate forming a thin film. The deposition process can also, in some cases, further enhance the purity of the evaporated material. Highly ordered, polycrystalline films are obtained, which is essential in achieving high FEMs. Vacuum deposition methods do not involve organic solvents and multilayer films can be deposited without dissolving the previous layers during subsequent depositions. However, there are drawbacks associated with vacuum sublimation techniques, e.g., the process requires a lag time period to attain a high vacuum (high cost), it is difficult to deposit films over large areas and in addition, patterning and photomasks are also required for this technique.

1.3.2 Solution Processing Methods

Solution-based processing methods, such as spin coating and printing, can potentially reduce fabrication costs and lead to large-area, reel-to-reel production. Printing methods are particularly desirable since the deposition and patterning steps can be combined into one single step. The following sections summarise several reported solution-based processing methods, involving solution-processable materials.

1.3.2.1 Spin Coating

In addition to vacuum deposition, the application of semiconducting materials, in solution, onto a substrate can take place by spin coating. Spin coating is a technique that provides an almost perfectly homogenous organic film with a thickness of 100-200 nm. The substrate takes the form of a disc that rotates rapidly and when a drop of the required organic semiconductor solution falls onto the disc, it spreads out immediately into an homogenous film. When the solvent evaporates, the organic film becomes taut and the substrate gains a coating of the appropriate material. Spin coating has the advantage that there is virtually no restriction in terms of the size of component that can be produced.

1.3.3 Printing and Stamping Methods

The technology believed to have the potential to produce the lowest manufacturing costs is the use of soluble organic semiconductors combined with large-area stamping or printing techniques. In the quest for cheap polymer electronics, researchers have progressed from making single, rudimentary all-polymer transistors^[24] to manufacturing high performance ICs made partially^[25] or entirely^[19, 26-27] from polymeric materials.

Two research groups of note have demonstrated cheap printing methods. John Rogers and co-workers from Bell Laboratories, Lucent Technologies have used a rubber-like stamp to pattern an active matrix of 256 polymer transistors on the back plane of a flexible optical display^[28]. In contrast, Richard Friend and colleagues at the University of Cambridge have employed high-resolution inkjet printing to produce OTFT circuits with fewer transistors, but with electrical interconnections (*vias*) between layers^[29].

The critical dimension of an OTFT is the distance that the field-induced charges must traverse, that is the distance between the source and drain electrodes. For the oligomeric and polymeric materials typically used, this distance must be of the order of 10 μm to give acceptably high drive current and switching speeds. Microcontact printing (stamping), with elastomeric or rubber-like stamps, possesses the required

resolution and has been used by the Bell Laboratories group to pattern organic transistors^[30-31]. Inkjet printing, until recently, did not have the required 10 μm resolution, a problem resolved by Friend and colleagues at the University of Cambridge.

1.3.3.1 Microcontact Printing (Stamping)

A low-resolution stamp is first used to define the gate pattern (the transistors in the Bell Laboratories array have the gate electrode on the bottom - see figure 1.4(b)), in a layer of indium tin oxide (ITO) that covers a Mylar substrate. The resulting gate electrodes are then coated with a layer of glass, which serves as the dielectric. Next is the critical step of printing the source and drain electrodes, which requires a higher resolution pattern to keep the source-drain separation to the required 10 μm resolution. The electrodes are made from gold rather than a polymeric material, because gold has been shown to work well with the inks that are used in the stamping process. The stamp applies a hexadecanethiol ink to a thin film of gold that has been evaporated onto the glass. The ink forms a self-assembled monolayer on the gold, covering the desired areas with minimal defects and well-defined edges. The unstamped regions of gold are then etched away, the remaining ink is evaporated and a layer of semiconducting polymer is then spin cast on top.

There are two notable disadvantages with this process. Firstly, photolithography is required to pattern the elastomeric stamp. Once the stamp is made however, it can be used again and again to manufacture numerous circuits. Secondly, the use of a gold film is not compatible with all-solution processing, but the Bell Laboratories group have shown that they can deposit silver metal from solution to manufacture organic transistors^[32].

1.3.3.2 Inkjet Printing

Friend and colleagues from the University of Cambridge use a top gate approach, see figure 1.4(a), to manufacture its transistors by depositing droplets of a conducting polymer in solution onto the required positions of a suitable substrate. The droplets tend to spread out when they come into contact with the substrate, so to maintain a

minimal separation of 5 μm between the source and drain electrodes, the droplets are confined within small “walls” of the hydrophobic polymer, polyimide. This technique, however, requires an initial photolithography step to define the desired pattern in the polyimide. Once deposited, the source and drain electrodes are covered with a layer of semiconducting polymer, followed by an insulating dielectric layer. The gate electrode is then placed on top utilising inkjet printing once more.

The University of Cambridge group have also developed a way to make another key component of a complex IC, *via* hole interconnections, which link the gate and drain electrodes in different layers of the transistor structure. This was achieved by using the inkjet to deposit successive droplets of a suitable solvent (isopropanol), which dissolves the insulating layer and creates a hole that can be subsequently filled with a conducting polymer.

Inkjet printing offers several advantages including a large degree of flexibility in the choice of materials that can be printed in any of the various layers of the transistor structure and it can provide accurate registration over large areas. As the technique is currently implemented, however, it still relies on an initial lithography step and inkjet printing has not, as yet, been demonstrated for an IC.

1.4 Materials Previously Used for Organic Semiconductor Devices

Organic materials for charge-carrier transport devices can be synthesised in great variety to match the different requirements of a particular organic semiconductor. Materials can be designed on a molecular level for a specific function, e.g. hole- or electron-transport and the HOMO-LUMO band gap can be modified through the synthesis of different molecular structures to achieve greater charge-carrier mobility.

There is a wide range of organic compounds that are suitable as organic semiconductors, which fortunately, can be easily categorised. There are two major classes of materials, firstly LMM materials and secondly conjugated mainchain polymeric materials (PMs). The main difference between the two is the way in which they are deposited onto a substrate to make the organic transistor. LMM materials are deposited by vacuum deposition at high vacuum (10^{-5} Torr), whereas PMs are

deposited by spin coating a solution of a soluble polymer or polymer precursor onto a suitable substrate.

LMM materials predominantly form polycrystalline films. These films often contain crystal grain boundaries, which can act as quenching sites for charge-carriers and consequently, charge-carrier transport is reduced. The main advantage of PMs is the ability to form stable glasses with high glass transition temperatures. Such glassy films tend to lack these defects. PMs are potentially more commercially attractive because of their advantageous processability, scalability, cost and mechanical properties.

LMM materials can be purified to a high degree in comparison with polymers where purification is often a problem. PMs are difficult to purify because they cannot be sublimed, distilled or recrystallised. The insufficient purity of polymers can be detrimental to the performance of an organic transistor device. LMM materials deposited as thin film layers by vapour deposition can produce thin, pure solid films but are very expensive to produce and are difficult to pattern, especially over large areas. By contrast, many polymers and precursor polymers have now been prepared, which are soluble in most common solvents, making the deposition of thin films *via* spin coating possible. The spin coating technique is cheaper and can allow large areas to be coated in a continuous batch process.

In LMM materials, it is generally considered that charge is transported by an intermolecular hopping mechanism. Most conjugated organic materials are electron rich, and therefore these materials transport holes (cation radicals), rather than electrons (anion radicals). Efficient hole injection requires a material with a low ionisation potential, whereas materials with a high electron affinity, such as electron-deficient nitrogen-heterocycles tend to be used where electron-transport is required.

The mobility values found in LMM materials tend to be higher than those of polymers, due primarily to the order present in LMM materials. Charge-transport in polymeric materials has been found to be typically in the region of 10^{-8} - 10^{-3} $\text{cm}^2 \text{V}^{-1} \text{s}^{-1}$ and can be attributed to larger hopping distances, increased disorder and also to the effects associated with traps^[3]. For the same reasons, LMM materials tend to exhibit

lower mobility values when compared to the high order present in organic single crystals. The mobility values for single crystals tend to be in the order of 10^{-1} - $1 \text{ cm}^2 \text{ V}^{-1} \text{ s}^{-1}$. Organic single crystals however, are difficult and costly to process and thus are unsuitable for commercial applications.

1.4.1 Low Molar Mass (LMM) Materials

Advances in organic electronics is often measured in terms of charge-carrier mobility. In organic semiconductors the mobility, as previously stated, is dictated by the ease with which the majority charge-carriers (free electrons (e^-) for *n*-type device materials and holes (h^+) for *p*-type device materials) can hop from one molecule to another. The last few years has seen substantial improvements in the mobility of organic transistors due primarily to the synthesis of materials with enhanced chemical purity, that are more stable to environmental influences, such as oxygen and water vapour and are more structurally ordered. Organic materials that are currently used in organic semiconductor devices can now achieve mobility values that equal, or in some cases, exceed that of amorphous silicon ($1 \text{ cm}^2 \text{ V}^{-1} \text{ s}^{-1}$).

What follows is a brief discussion of some of the different types of materials, based on LMM and oligomeric and polymeric materials, used as the semiconducting component of organic transistor devices, the methods used to deposit the films of these materials and the mobilities achieved.

Evaporated films of pentacene^[33-34], see figure 1.8, have achieved mobilities comparable to and exceeding that of amorphous silicon. Mobilities as large as $1.5 \text{ cm}^2 \text{ V}^{-1} \text{ s}^{-1}$ and on/off ratios larger than 10^8 have been achieved using two layers of pentacene as the active material, deposited at different substrate temperatures, in a stacked pentacene layer OTFT device structure^[35]. In addition, high purity pentacene single crystals grown by physical vapour transport in a stream of hydrogen^[36], have shown mobilities of $2.7 \text{ cm}^2 \text{ V}^{-1} \text{ s}^{-1}$ at room temperature in the accumulation regime (hole transport). Pentacene OTFTs manufactured by the spin coating of soluble precursors^[19] have shown mobilities of $0.01 \text{ cm}^2 \text{ V}^{-1} \text{ s}^{-1}$, which were also stable in air. Pentacene's high mobility can be attributed to its highly ordered intermolecular structure, which can be polycrystalline or more significantly monocrystalline.

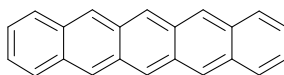


Figure 1.8 - Structural representation of pentacene

Pentacene has also been shown to exhibit ambipolar characteristics^[36], that is the ability to transport both holes and electrons. The FEMs achieved with OFETs based on pentacene single crystals, prepared with an amorphous aluminium oxide gate insulator, increased from 2.7 and 1.7 $\text{cm}^2 \text{V}^{-1} \text{s}^{-1}$ at room temperature to 1200 and 320 $\text{cm}^2 \text{V}^{-1} \text{s}^{-1}$ at low temperatures for hole and electron transport respectively. However, pentacene is not a polymer and therefore is relatively fragile and difficult to coat with other materials, which could cause potential problems in the manufacture of commercial devices. Other groups have also shown that organic semiconducting materials can exhibit superconductivity^[37] at low temperatures. It has also been found that solution cast films of regioregular poly(3-hexylthiophene) (rr-P3HT) formed relatively well-ordered films, owing to self-organisation, exhibited charge-carrier mobilities of 0.05-0.1 $\text{cm}^2 \text{V}^{-1} \text{s}^{-1}$ at room temperature. At low temperatures, below 2.35 K, however, the polythiophene film became superconducting, achieving sheet-carrier densities exceeding $2.5 \times 10^{14} \text{cm}^2 \text{V}^{-1} \text{s}^{-1}$.

The conjugated oligomer, α,ω -dihexyl sexithiophene (α,ω -DH6T), see figure 1.9, shows good mobility when vacuum evaporated. The sexithiophene (6T) oligomer without substituents has a mobility of 0.002 $\text{cm}^2 \text{V}^{-1} \text{s}^{-1}$. When hexyl groups are substituted on both terminal positions however, the mobility of α,ω -DH6T increases by a factor of 25 to 0.05 $\text{cm}^2 \text{V}^{-1} \text{s}^{-1}$. The addition of hexyl groups in the α and ω positions tend to induce self-assembling properties and increase the long range ordering inside the film of the material^[38].

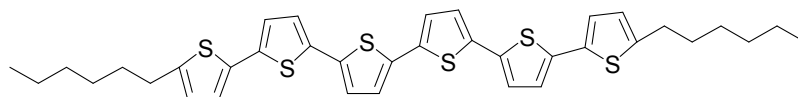


Figure 1.9 - Structural representation of α,ω -DH6T

α,ω -Dihexylquaterthiophene (DH α 4T)^[39], see figure 1.10, has also been used as the semiconducting component of OTFTs and has exhibited mobilities of 0.16, 0.12, 0.23 and 0.046 cm² V⁻¹ s⁻¹ when deposited at the different substrate temperatures of RT, 50, 80 and 100 °C respectively for a channel width to length ratio of 1.5:1. The 80 °C mobility is the highest observed to date for an oligothiophene and is an order of magnitude higher than the highest reported mobility of the parent α 4T. As with pentacene, it is believed that the high mobility observed is correlated with the single-crystal^[40] nature of the organic semiconducting film^[41].

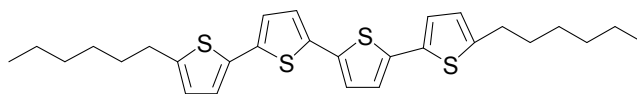


Figure 1.10 - Structural representation of DH α 4T

A conjugated polymer that shows good electrical properties, due to the solid state ordering that it achieves, is regioregular poly(3-hexylthiophene)^[42] (rr-P3HT), see figure 1.11. rr-P3HT is much more ordered than its regiorandom counterparts, and has consequently achieved mobilities upto 0.045 cm² V⁻¹ s⁻¹ in organic transistors manufactured from solution cast films.

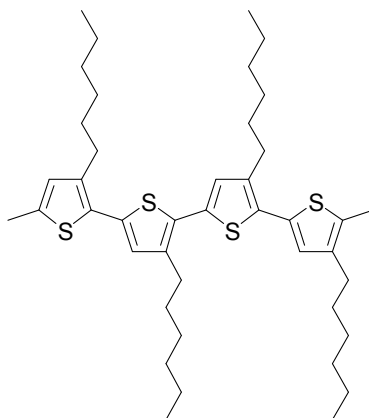


Figure 1.11 - Structural representation of rr-P3HT

Other groups^[43-44] have also investigated the use of solution processable rr-P3HT as the semiconducting component of OFETs. The high mobilities achieved, 0.05-0.1 cm² V⁻¹ s⁻¹ are due to the formation of extended states brought about by a greater conjugation length and also π - π stacking of adjacent chains as a result of the lamellar

type packing, see figure 1.12. Unfortunately, rr-P3HT is extremely sensitive to oxygen and organic transistors made with this polymer degrade rapidly when operated in air^[19].

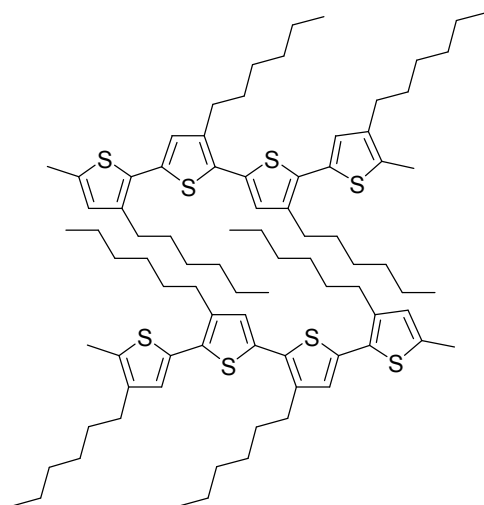


Figure 1.12 - Structural representation of the lamellar type packing in rr-P3HT

Significant research effort has gone into synthesising thiophene oligomers, indicated by the large amount of literature available in this area^[45-49], that produce chemically purer products and avoid unwanted side products by non-selective couplings and ionic residues from the reaction process. This, to a large extent, has enabled thiophene oligomers to be one of the most investigated and successful class of organic semiconductor materials used in transistor devices^[50-52] to date.

Highly ordered polycrystalline, vacuum-deposited films of α,ω -dihexyl anthradithiophene (DHADT), see figure 1.13, have also been manufactured^[53]. These films, when incorporated into a suitable organic transistor device structure have shown mobilities as high as $0.15 \text{ cm}^2 \text{ V}^{-1} \text{ s}^{-1}$, the highest reported value to date for a polycrystalline, organic material.

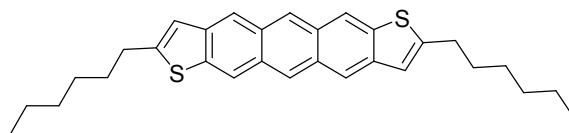


Figure 1.13 - A structural representation of α,ω -dihexylanthradithiophene (DHADT)

The torsional freedom and structure of the molecule and the organisation of the molecules in the bulk are important properties in determining a materials efficacy for charge-carrier transport. It has been demonstrated that planar molecules tend to exhibit high charge-carrier mobilities. A dimer of fused benzodithiophene, see figure 1.14, has been synthesised by the Bell Labs^[54-55] and shows high hole mobilities of $0.04 \text{ cm}^2 \text{ V}^{-1} \text{ s}^{-1}$.

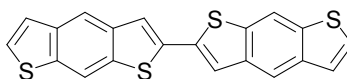


Figure 1.14 - A structural representation of the benzodithiophene dimer

The dimer is planar because the benzodithiophene molecules are fused and therefore lack torsional freedom. The planarity allows the molecules to pack with close proximity and increases the overlap of intermolecular π -orbitals. This allows charges to “hop”, from molecule to molecule, more easily and consequently results in relatively high charge mobilities.

Similar to the benzothiophene dimer above, a conjugated and fused thiophene oligomer, bis(dithienothiophene)^[56-57] (BDT), see figure 1.15, has been synthesised and deposited by vacuum sublimation as the active layer in OTFTs by Sirringhaus and colleagues at the University of Cambridge, and has shown FEMs in the range of 0.02 - $0.05 \text{ cm}^2 \text{ V}^{-1} \text{ s}^{-1}$ and high on/off ratios of 10^8 . The good performance associated with this material can be explained by the favourable coplanar π - π stacking, which differs from the herringbone stacking observed in oligothiophenes.

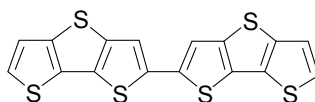


Figure 1.15 - A structural representation of BDT

In addition, two α,α' -disubstituted BDT derivatives have also been synthesised^[58] These derivatives were also deposited by vacuum sublimation as the active layers in OTFTs. The devices exhibit high on/off ratios 10^6 and 10^8 and FEMs of 1×10^{-3} and $2 \times 10^{-2} \text{ cm}^2 \text{ V}^{-1} \text{ s}^{-1}$, respectively, for dithiohexyl (DTH-BDT) and dioctyl (DO-BDT) substituted bis(dithienothiophene), see figure 1.16. DTH-BDT was found to be considerably more soluble than the unsubstituted BDT.

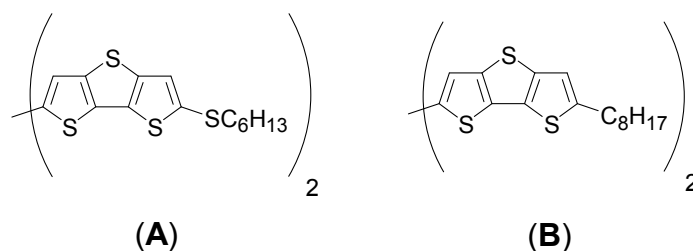


Figure 1.16 - Structural representations of **(A)** DTH-BDT and **(B)** DO-BDT

Organic-inorganic hybrid materials have also been demonstrated and promise both the superior charge-carrier mobility of inorganic semiconductors and the processability of organic materials. Hybrids based on the perovskite structure crystallise from solution to form orientated molecular composites of alternating organic and inorganic sheets. Organic transistor device structures with spin coated thin films of the semiconducting perovskite material, phenethylamine-tin iodide, $[(\text{C}_6\text{H}_5\text{C}_2\text{H}_4\text{NH}_3)\text{SnI}_4]$, have demonstrated mobilities in the region of $0.6 \text{ cm}^2 \text{ V}^{-1} \text{ s}^{-1}$ ^[59].

1.4.2 Polymeric Materials (PMs)

In semiconducting conjugated polymers, it is generally considered that charge is transported intramolecularly along the direction of the polymer chain, in which polarons are the principal charge-carriers. Most conjugated polymers are electron rich

and therefore transport holes rather than electrons. Charge-transport in polymers has been found to be typically less than $10^{-4} \text{ cm}^2 \text{ V}^{-1} \text{ s}^{-1}$ and can be attributed to larger hopping distances, increased disorder and also to the effects associated with traps as previously discussed.

Polymers such as PPV and its derivatives, have found commercial interest as materials for transistor devices since the mid-1980s. However, such materials possess some disadvantageous properties for electronic devices as outlined previously. Numerous charge-transport polymers have been developed over the years. For electron transport, oxadiazole based compounds^[60] have shown excellent electron-transport/hole-blocking properties. An example of a polymer incorporating oxadiazole^[55,61-62] heterocyclic rings is shown in figure 1.17.

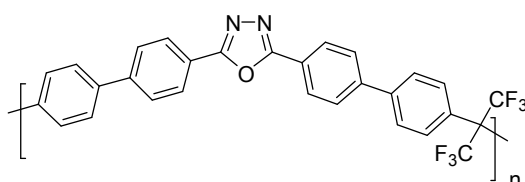


Figure 1.17 - A structural representation of an oxadiazole-based electron transporting polymer

Electron-transporting polymers can be synthesised by incorporating electron-deficient nitrogen atoms or electron-withdrawing groups, such as CF_3 and CN , into the polymer backbone. Polymers incorporating oxadiazole^[63] and triazole^[63] moieties have been synthesised and have shown good electron-transporting properties. However, their performance in electronic devices has generally been found to be inadequate^[64].

One of the most successful and efficient materials currently used for a hole transport layer is poly(dioxyethylenethienylene) (PEDOT) doped with polystyrenesulphonic acid (PSS)^[65], see figure 1.18.

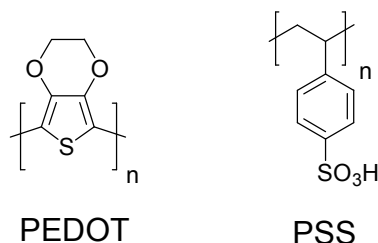


Figure 1.18 - A structural representation of a mixed PEDOT/PSS based electron-transporting polymer

Liquid crystals (LCs)^[66-71], see section 1.5, display unique properties that can be exploited in transistor devices as a third class of organic semiconductors. Characteristic features of LCs include the anisotropy of charge transport and the tendency to form homogeneous monodomains as uniform films on suitable alignment layers. In addition, photopolymerisable molecular glasses^[72-73] have been shown to be attractive alternatives to traditional polymeric materials for electrooptic device applications. A comprehensive review of functional organic molecular glasses has been published^[74]. The formation of a polymer network using UV light, after spin coating, results in an insoluble film that allows additional layers to be spin coated on top of the initial organic film, with minimal disruption to the lower layer. The use of photopolymerisable LCs is discussed in section 1.6.2.

An important criterion for aligning liquid crystalline polymers (LCPs) is the formation of a monodomain thin film, which is usually achieved by quenching from the liquid crystalline state into a glassy state on rubbed polyimide. The formation of a glass, allows the liquid crystalline order to be preserved and stabilised. Unfortunately, thermal annealing over several hours is usually required to achieve uniform alignment of the whole sample.

Isotropic 9,9-dioctylfluorene (PFO) exhibits hole mobilities of $3 \times 10^{-4} \text{ cm}^2 \text{ V}^{-1} \text{ s}^{-1}$ at room temperature. Bradley^[75] demonstrated that charge mobilities could be improved by an order of magnitude, compared to isotropic PFO, using liquid crystalline PFO aligned on rubbed polyimide. Hole mobilities of $1 \times 10^{-3} \text{ cm}^2 \text{ V}^{-1} \text{ s}^{-1}$ were attained at room temperature. High charge-carrier mobilities were found by Sirringhaus^[76] in a liquid crystalline copolymer, poly-(9,9-dioctylfluorene-co-bithiophene) (F8T2). A

thin film transistor was fabricated using F8T2 and enhanced mobilities of $0.01 \text{ cm}^2 \text{ V}^{-1} \text{ s}^{-1}$ were demonstrated.

Other types of materials, such as porphyrin based compounds^[77], phthalocyanines^[61] and more recently fluorocarbon-substituted oligothiophenes^[78] have all demonstrated good charge transporting properties. These, however, will not be discussed here, but are cited in order to highlight that the variety of material types in this area is extensive.

1.4.3 Stability and Reliability of Organic Semiconductor Devices

The organic materials used in electronic devices are semiconductors and therefore thin films ($\approx 100 \text{ nm}$) of material are necessary for low voltage operation and low power consumption. Such thin films, however, are prone to defects and short-circuits caused by dust particles on the surface of the substrate. Oxygen and water vapour are also known to lead to device failure, through the degradation of the materials used in these devices.

Both LMM materials and PMs are sensitive to environmental conditions during device operation. The effects of oxygen and water vapour can lead to the photo-degradation of the organic materials, particularly polymeric materials, and can have damaging effects on the electrodes, which ultimately leads to the reduction in the lifetime of the device. PPV for example, is very susceptible to photo-oxidation due to the presence of C-C double bonds (vinylene groups) in between the aromatic rings. The oxidation and subsequent cleavage of these double bonds, resulting in a reduction of the conjugation length of the polymer, can occur in the presence of highly reactive singlet oxygen.

Most conjugated polymers have a sufficiently high T_g to prevent the polymer from crystallising over a long period of time. Although most LMM materials do form an amorphous glass, they have a tendency to crystallise more easily and over a shorter period of time than conjugated polymers. This tendency to crystallise is accelerated due to heating of the transistor device during operation. This partial crystallisation subsequently leads to the formation of crystal grain boundaries and non-uniformity in

the organic film. These defects behave as traps and quenching sites and reduce the efficiency of the device. This crystallisation can also affect the electrode/organic-material interface^[79]. These problems associated with LMM materials can be solved by using photopolymerisable materials^[80-85], which are discussed in section 1.6.2.

However, the observed types of degradation mentioned above are more apparent in atmospheric conditions and most of the studies to date have been conducted without special encapsulation procedures, which lead to the exclusion of oxygen and moisture. The issues of stability and reliability of organic materials are directed towards the need for pure materials, careful encapsulation and the requirement of new materials with improved structural stability against photodegradation. The understanding of the degradation mechanisms involved in electronic devices and in the organic semiconducting materials from which they are manufactured, is an essential part of this development.

1.5 Liquid Crystals (LCs)^[86]

The name LC is given to materials that exhibit intermediate phases between the crystal and isotropic liquid states. A number of these LC phases exist, which differ by the degree of positional and orientational order of the constituent molecules in relation to one another. The term mesophase, coined by Friedel^[87], is used to describe a liquid crystalline phase. Compounds that exhibit such phases are therefore referred to as mesogens. However, not all mesophases are liquid crystalline. The crystal- or quasi-smectic phases exhibit 3-dimensional long-range positional order and are therefore not fluid. They do, however, vary considerably in molecular orientational order and are consequently referred to as crystalline mesophases, rather than liquid crystalline mesophases.

The molecules in a crystalline solid have long-range positional and orientational order. When heated the molecular interactions between the molecules begin to breakdown, and if all of the interactions breakdown simultaneously, an isotropic liquid is formed. However, if the interactions breakdown in stages, either side-to-side or end-to-end, then intermediate phases are formed between the solid and liquid states. These intermediate phases are characteristic of LCs. Mesophases are characterised by the partial ordering of the molecules. The molecular axes of the molecules possess different degrees of orientational order, but little or no positional order. LCs exhibit a strong anisotropy in many of their physical properties, that is their magnitude depends on the direction of measurement, either parallel or perpendicular, to the long molecular axis.

There are two main categories of LCs: thermotropic and lyotropic, see figure 1.19. If transitions between the phases depend on temperature, then thermotropic LCs are formed. If the phase transitions depend on the addition and concentration of a solvent, lyotropic LCs are formed. Lyotropic LCs do not form part of this thesis and will not be discussed further.

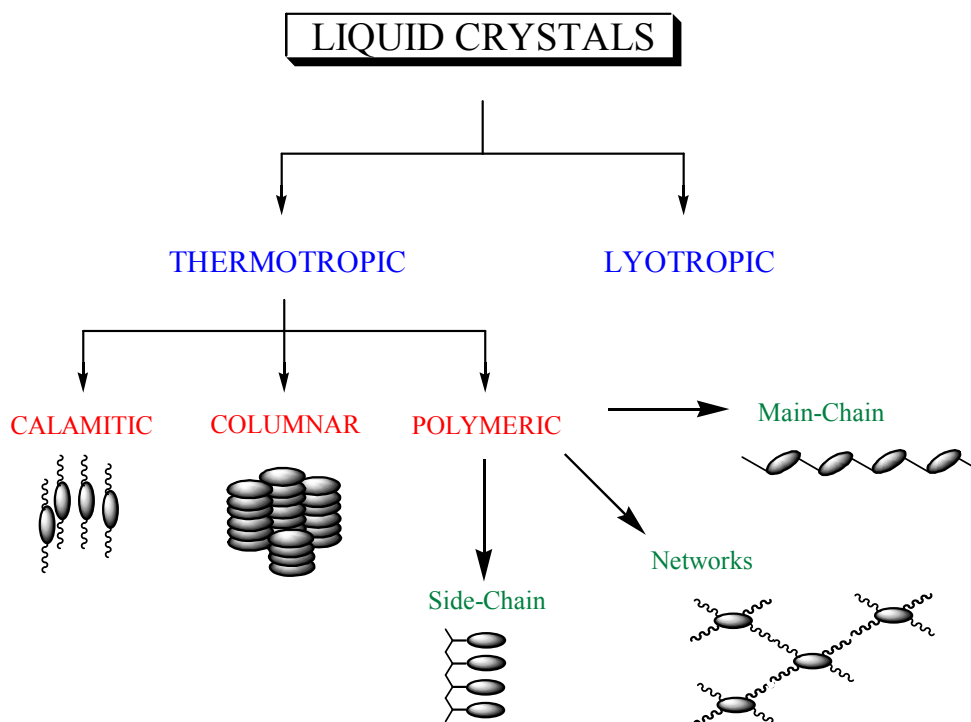


Figure 1.19 - A general classification of LCs

1.5.1 Structure Property Relationships^[86, 88]

All calamitic thermotropic LCs have a characteristic geometric, rod- or rath-like shape, which leads to anisotropic intermolecular forces with the interactions between the ends of the molecules being weaker than those of the lateral interactions. Liquid crystalline phases tend to be exhibited by materials of specific molecular structures. The combination of structural moieties determines the physical properties of a material, which in turn confers a certain phase morphology and particular values of melting point and phase transition temperatures.

All of these factors have to be taken into account when the design and synthesis of LCs is undertaken in order to ensure the desired physical properties are generated. Generally, structural features that give reasonable rigidity to an almost linear molecule should be conducive to LC formation. The main structural features include increased core length, terminal groups, linking groups and small lateral groups.

The generally accepted archetypal structure of a calamitic, rod-like liquid crystalline compound has two flexible aliphatic chains attached to a rigid aromatic core or quasi-rigid alicyclic core^[89]. The general template of a calamitic LC is shown in figure 1.20.

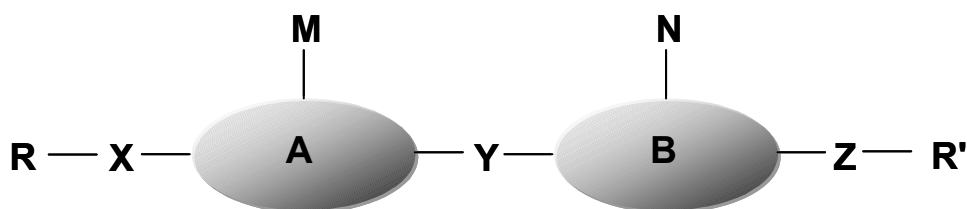


Figure 1.20 - The general structural template for a calamitic LC, where A and B are core units, Y is a core linking group, R and R' are terminal chains, X and Z are chain linking groups and M and N are lateral substituents

A and B represent the core of the material, sometimes these are linked by a linking group (Y) or more frequently they are directly bonded together by a C-C bond. Similarly, the terminal chains (R and R') may be linked directly to the core, or linked via other groups (X and Z). The mesophase morphology and the physical properties of the material are further modified by the presence of lateral substituents (M and N). The units that are used and the combination in which they are used determine the mesophases formed by a compound and its physical properties.

A certain rigidity is necessary to give the anisotropic molecular structure, this is usually provided by linearly linked ring systems (A and B). Rings A and B are generally aromatic rings, but they can also be alicyclic. The rings, joined directly or via a linking group (Y), maintain the linearity of the core and, if unsaturated, extend the conjugation between the rings. Common linking groups include an ester linkage (-C(O)-O-) or Schiff base (-CH=N-), however, other groups can also be used including, -C≡C-, -CH₂-CH₂- and -N≡N-.

The rigid core is usually too rigid to give rise to liquid crystalline phases and terminal chains are used to induce a degree of flexibility into a compound. Furthermore, they

ensure reasonably low melting points and stabilise the molecular alignment within the mesophase structure. The terminal chains are commonly straight alkyl or alkoxy chains, however one of the substituents is commonly a small polar group, for example -CN, -F, -NCS or -NO₂. The terminal chains may also be branched, with the branching group being non-polar, such as -CH₃ or polar, for example -CN, -F or -CF₃. Branching groups are usually incorporated in to molecules to induce chirality.

The physical properties of a compound may be altered by the introduction of lateral substituents, which tend to cause a significant reduction in the melting and clearing points. The most commonly used lateral substituent is the fluoro group because of its small size and high electronegativity, but other groups are also used, for example -Cl, -CN or -CH₃. Despite the small size of fluorine, it can potentially have a dramatic effect on the smectic thermal stability by diminishing the efficiency of the packing of the molecules in layers^[90-91]. Substituents larger than fluorine usually destabilise the smectic phase to a larger degree whilst giving compounds with lower clearing points.

1.5.2 Thermotropic Liquid Crystals

Thermotropic LCs can be divided into three general classes: calamitic, columnar and polymeric LCs. Calamitic LCs will be discussed in detail as they are the primary focus of this thesis, columnar and polymeric LCs will only be discussed briefly.

1.5.2.1 Calamitic Liquid Crystals^[92-94]

Calamitic LCs usually consist of rod-like shaped molecules, which contain a semi-rigid core and flexible end groups. They can be subdivided into two main categories: nematics and smectics. Both types have chiral versions with a range of variants having been reported for the smectic mesophase. The usual sequence of liquid crystalline mesomorphic behaviour for a typical calamitic LC is summarised in figure 1.21.

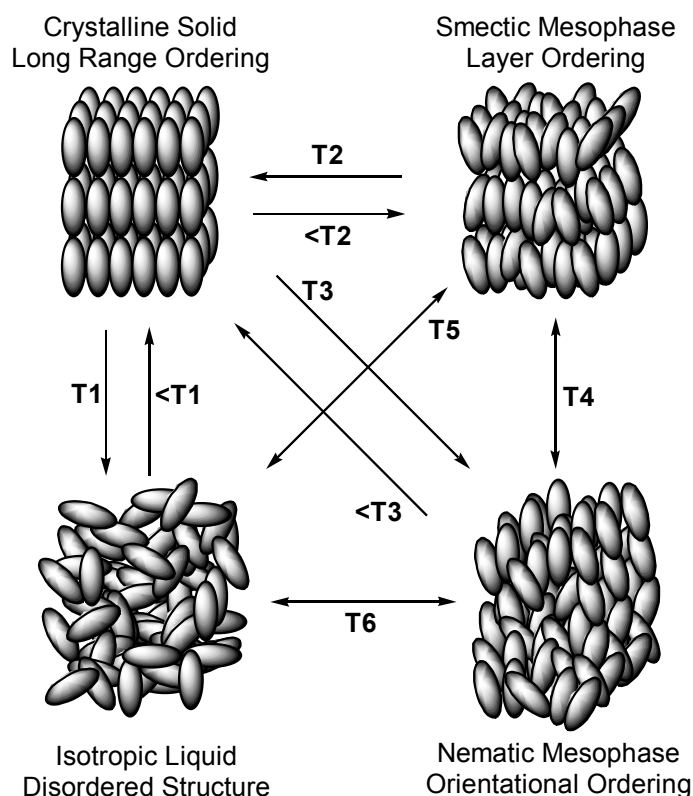


Figure 1.21 - Mesomorphic behaviour for a typical calamitic LC

As the heat increases the first possibility for the breakdown in the structure of the organised solid is for the molecules to start to rotate about their long molecular axes. The increase in heat leads to a transition from the crystal to a soft-crystal or quasi-smectic phase. There are several crystal-smectic phases that can be formed, with the packing arrangement and layer ordering of the molecules used to classify each of these phases. Within the layers, the molecules have long-range positional order. Similarly the out-of-phase ordering is also long-range. The long axes of the molecules can be either orthogonal or tilted with respect to the layer planes. The letters B, E, J, G, H and K are used to denote these crystal-smectic phases^[95].

When a liquid crystalline material is heated in the solid state the molecules begin to vibrate. When the vibrational energy overcomes the attractive forces between the molecules, this is known as the melting point. This is the case for **T1**, in figure 1.21, where the crystalline solid gives rise to an isotropic liquid. In **T2**, the attractive forces between the ends of the molecules are overcome, while interaction between their long

molecular axes is still maintained. This gives rise to a layered structure where the molecules are still parallel to each other. **T2** is known as a crystal to smectic (Cr-Sm) transition.

This further heating of the material results in a phase transition where the periodic ordering of the molecules break down. This change in order can produce a number of phases, the smectic phases, where the molecules are still organised in layers, but there is only short-range positional order of the molecules in the plane of the layers. The molecules maintain the same orientation order from layer to layer, but there is no out-of-plane ordering of the molecules. Despite these constraints, the molecules in these phases are able to rotate rapidly about their axes, pass from layer to layer and tumble in a restricted manner about their long axes.

The smectic phases are subdivided into a number of groups depending on the local packing of the molecules. The molecules may be tilted with respect to the layer planes, as in the SmC mesophase and also have local hexagonal packing, as in SmI and SmF mesophases. Alternatively, the molecules can have their long axes orthogonal to the layer planes, as is the case for the SmA mesophase or local packing, as in the SmB mesophase.

In **T3** both the attractive forces between the molecules and the interaction between their long molecular axes are overcome giving rise to a non-layered structure but the molecules still point, on average, in the same direction. This is known as a crystal to nematic (Cr-N) transition. In the nematic phase the molecules do not have either positional or layer ordering. The molecules do, however, possess orientational ordering, which is the only structural feature that distinguishes the nematic phase from the isotropic liquid. The long axes of the molecules tend to lie approximately parallel to one another, even though the molecules are free to tumble and slide past one another.

Once in the smectic phase, the lateral interaction between the molecules may be overcome due to further heating giving rise to the nematic phase. This is shown in **T4** and is known as the smectic to nematic (Sm-N) transition. If all the remaining attractive forces are overcome, whether in the smectic or nematic phase then the

molecules are free to move in a random order, giving rise to the isotropic liquid (I). This is shown in **T5** and **T6** respectively. Both of the transitions, (Sm-I) and (N-I), are known as the clearing point. The mesophases that are observed above the melting point (heating) are called enantiotropic, whereas those mesophases that are observed below the melting point (cooling) are called monotropic.

When a liquid crystalline compound is heated it does not necessarily have to melt through all of the described stages before going into the isotropic liquid phase. For example, a particular material may only exhibit a nematic phase, whereas another material may pass through several smectic phases before going into the nematic phase and then the isotropic liquid. Furthermore, no liquid crystalline material has been discovered that exhibits all of the recognised liquid crystalline phase types, but many exhibit a number of the known phase types.

Additionally, chiral examples of both nematic and smectic phases exist^[86, 96]. Consequently, when a liquid crystalline material contains chiral groups, a variety of new phases are formed which have different properties from their achiral analogues. Current knowledge^[96] indicates that the thermodynamic ordering of the phases, in sequence of increasing order, from the isotropic liquid (Iso) to the crystalline solid (Cr) is as follows:

Iso - N - SmA - SmC - [SmB, SmI] - B - SmF - J - G - E - K - H - Cr

The type of liquid crystalline phase that is formed by a mesomorphic material essentially depends on the molecular properties of the substance^[97], with the overall shape of the compound being the primary factor in the formation of liquid crystalline phases. To form calamitic LCs, the associated molecules have to sweep-out rotational volumes in the shape of an ellipsoid^[98].

1.5.2.2 The Nematic (N) Phase^[86, 96]

The nematic phase derives its name from the Greek word *nematos*, meaning thread-like, with respect to thread-like textures observed under an optical polarizing microscope. The rod-like molecules tend to align parallel to one another with their

long axes pointing roughly in the same direction, see figure 1.22. The molecules are orientationally ordered, but there is no long-range positional ordering of the molecules. As such, the nematic phase is considered essentially to be a one-dimensionally ordered elastic fluid, which is the least ordered and most fluid-like (least viscous) of all the liquid crystalline phases.

The average direction along which the molecules point is called the director of the phase and is usually given the symbol n . The rod-like molecules in the nematic phase are free to rotate about their short molecular axes and to some degree about their long molecular axes. The degree of alignment of the molecules relative to the director, n , is called the order parameter, S , and is defined by equation (1):

$$S = \left\langle \frac{1}{2} (3 \cos^2 \theta - 1) \right\rangle \quad (1)$$

Where θ is the angle made between the long axis of each molecule and the director, and the angled brackets indicate that the equation represents an average taken over a large number of molecules. The order parameter S can range from 0 to 1. An order parameter of 1 indicates that the phase is completely ordered and the molecules are aligned with the director. If the molecules are randomly orientated about the director, i.e., isotropic, then $S = 0$. Typically for a nematic mesophase the value of the order parameter varies from 0.3 to 0.75. The director can be forced by an applied electric or magnetic field to change its direction.

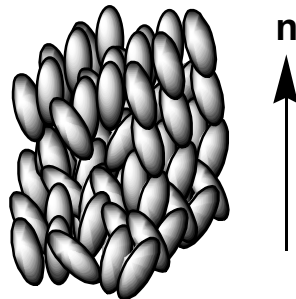


Figure 1.22 - A schematic representation of the nematic mesophase

1.5.2.3 The Chiral Nematic (N*) Phase^[86, 89, 99]

The use of molecules with at least one chiral centre adds a further dimension to LC behaviour. The presence of optically active chiral centres in a LC promotes the formation of helical structures, in both nematic and smectic mesophases. The addition of small amounts (approximately 1-5%) of optically active molecules, usually referred to as chiral dopants, to an achiral mixture converts that mixture to its chiral equivalent. This has commercial benefits, since chiral molecules are much more expensive to synthesise than achiral molecules.

The chiral nematic or cholesteric phase (N*) arises when one or more chiral centres are incorporated into the constituent molecules of a nematic material. It can be thought of as a stack of nematic layers with their directors rotating constantly from layer to layer, see figure 1.23. This variation of the director forms a helix with a pitch length, p , which is defined as the distance required for the director to rotate through 360° .

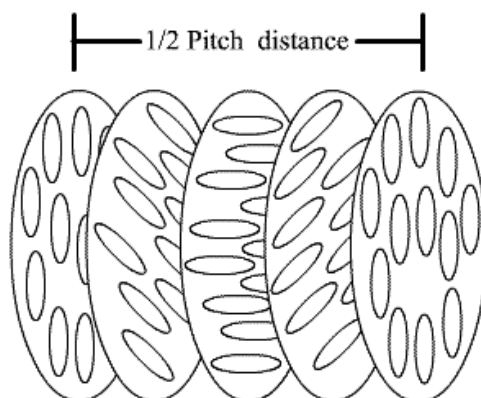


Figure 1.23 - A schematic representation of the chiral nematic phase

The pitch length can vary considerably in a chiral nematic material, from 1.0×10^{-7} m to almost infinity. When the pitch length is close to the wavelength of visible light the phase will selectively reflect light. Chiral nematic LCs are widely used for thermochromic applications as the pitch length changes with varying temperature and as a result, the colour of light reflected varies with temperature^[100].

1.5.2.4 The Smectic Phase^[97]

The smectic phase, named by Friedel, derives its name from the Greek word *smectos*, meaning soap-like. Smectic phases are more ordered than nematic phases, having two degrees of order, positional and orientational. The constituent molecules in a smectic phase form a layered structure, where the molecules are free to move within the layer and to a lesser extent translate from one layer to another. The molecular long axis can be orthogonal or tilted with respect to the layer plane. This type of mesophase can be viewed as a set of two-dimensional liquid layers, stacked on one another, with well-defined spacing.

Unlike the nematic phase several different types of smectic phases have been identified, reflecting the mobility of the layers and the differing orientation of the molecules within the layers. Some of these phases are true liquid crystals, whereas others are crystal-smectic phases, which exhibit long range positional order in 3-dimensions and do not exhibit any fluid properties. The constituent molecules can be arranged orthogonal with respect to the layers (SmA) or they can be tilted, by a temperature dependent angle θ , with respect to the layers (SmC).

Within the layers the molecules can also pack into hexagonal or orthorhombic arrays, which adds an extra degree of order. It is important to note that for some phases the hexagonal networks do not correlate with neighbouring layers, which maintains a degree of fluidity, albeit of very high viscosity. The molecules within the arrays can also be orthogonal (SmB) or tilted with respect to the layers. For the hexagonal tilted phases the molecules can adopt one of two arrangements, they can be tilted towards the side of the hexagon (SmF) or tilted towards the hexagon's apex (SmI). Other smectic phases with long-range in-layer correlations are known and are referred to as crystal-smectic phases and include the crystals B and E, which tend to have their molecular long axis orthogonal with respect to the layer plane and the crystals J, G, H and K, which tend to have their molecular long axis tilted with respect to the layer plane.

1.5.2.5 The Smectic A (SmA) Phase^[86, 97]

In the SmA mesophase, the molecules are free to rotate about their molecular long axis and the director is perpendicular to the smectic plane with no particular positional order within the layers, as a result the layers are then free to slide over each other, see figure 1.24. The molecules within the mesophase can move from one layer to another and there is no correlation between the layers.

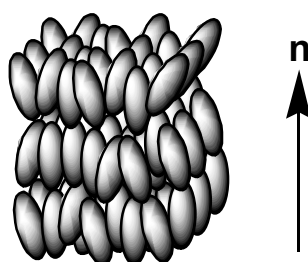


Figure 1.24 - A schematic representation of the SmA phase

The SmA phase is the least ordered of the smectic phases. If a molecule exhibits a SmA phase in addition to other smectic phases, the SmA phase is always observed at higher temperatures.

1.5.2.6 The Smectic C (SmC) Phase^[96- 97, 101]

In SmC LCs the constituent molecules are arranged in diffuse layers. Within the phase, the molecular long axes of the constituent molecules are tilted with respect to the layer planes. Furthermore, the molecules are packed in an unstructured way within the layers. The SmC phase is therefore the tilted analogue of the SmA phase. The molecules within the SmC mesophase are arranged as in the SmA mesophase, but the director makes a tilt angle with respect to the normal smectic plane, see figure 1.25. As a consequence of the tilt angle, the layer spacing of the SmC phase is smaller compared to that of the corresponding SmA phase.

The molecules within each layer exist in a close packed hexagonal array with respect to the director of the phase. The close packed hexagonal array ordering is short-range. Consequently over large distances the molecules are randomly packed, with the molecules being tilted in roughly the same direction in one domain. The tilt orientational ordering between successive layers is, therefore, preserved over long distances.

The optically active equivalent of the SmC phase is the SmC* phase formed by molecules incorporating an optically active center. The SmC* phase exhibits a helical structure similar to that of the chiral nematic phase, but with an additional layer structure.

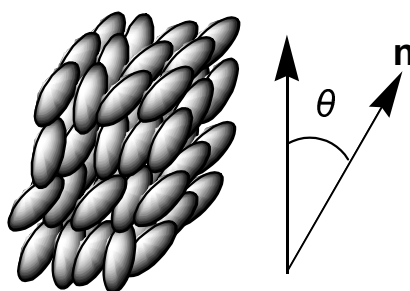


Figure 1.25 - A schematic representation of the SmC phase

1.5.2.7 Crystal-Smectic Phases

1.5.2.7.1 Crystals B and E^[86, 96]

In the crystal B phase the molecules are arranged in layers with their long axes orthogonal to the layer planes. The molecules undergo rapid re-orientational motion about their long axes. In this phase, like the SmB phase, the molecules are arranged hexagonally, but unlike the SmB phase, the positions of the hexagonal lattices are predictable over a long range in three dimensions.

As with the crystal B phase, the molecules in the crystal E phase are also arranged so that their long axes are perpendicular to the layer planes. Locally, the molecules pack in an orthorhombic array. The molecules within the phase cannot undergo free

rotation about their long axes^[102] because of the restricted distance between the molecules. This contraction of the hexagonal lattice confers a herringbone-like structure with restricted rotation. The molecules themselves undergo rapid re-orientational motion about their long axes whilst having long-range in-plane and out-of-plane periodic order.

1.5.2.7.2 Crystals J and G^[86, 101]

The crystal J and G phases are tilted analogues of the crystal B phase in addition to being the crystalline analogues of the SmI and SmF phases respectively. In the crystal J phase the molecules are arranged in layers where their long axes are tilted with respect to the layer planes. Along the tilt direction of the phase, the molecules are arranged in a pseudohexagonal packing structure, with the tilt being directed towards the apex of the array.

The molecules have long-range periodic ordering within and between the layers. The phase therefore has long-range orientational ordering in three dimensions as well as long-range positional ordering. The major difference between the crystal J and crystal G phases is that for the crystal G phase the tilt is directed towards the edge of the hexagonal packing array, whereas in the crystal J phase it is towards the apex. Due to the extent of the positional ordering these phases are crystalline. The molecules are, however, undergoing rapid re-orientational motion about their long axes^[103]. The molecular dynamics of these phases are therefore different from those normally observed in crystals.

1.5.2.7.3 Crystals H and K^[101]

The crystal H and crystal K phases are both similar to the crystal E phase except for the molecules being tilted with respect to the layer planes. The molecules are arranged in layers so that they possess long-range periodic ordering. The interlayer packing is also correlated over long distances, producing a crystalline structure. The packing arrangement is monoclinic with the tilt being towards the shorter edge of the crystal H phase and to the longer edge of the packing net in the crystal K phase. In these phases

the molecules are still undergoing rapid re-orientational motion about their long axes, but in this case it is assumed to be oscillatory in nature^[102].

1.5.3 Columnar Liquid Crystals

A columnar liquid crystalline phase is made up of columns of liquid crystalline molecules. Two types of material principally exhibit columnar phases, those that have a flat disc-like molecular core and those that have a polycatenar structure. The disc-like molecules form stacks or columns and the columns self assemble forming two-dimensional lattice structures. The molecules may also be arranged randomly within the stacks giving a disordered structure. The arrangement of the molecules within the columns and the arrangement of the columns themselves lead to varying types of mesophase. The different types of columnar phase include columnar hexagonal, col_h ; rectangular, col_r ; and oblique, col_{ob} , which are either ordered, col_o or disordered col_d . For a schematic representation of a columnar phase, see figure 1.26.

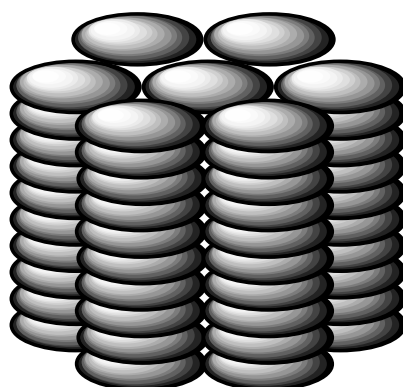


Figure 1.26 - A schematic representation of a columnar phase

1.5.4 Liquid Crystalline Polymers (LCPs)

LCPs can be subdivided in side chain and main chain polymers. Main chain LCPs are linear and consist of repeating monomeric units. Side chain LCPs have mesogenic repeating units appended to the polymer backbone. These units can be either calamitic or discotic LCs, see figure 1.27.

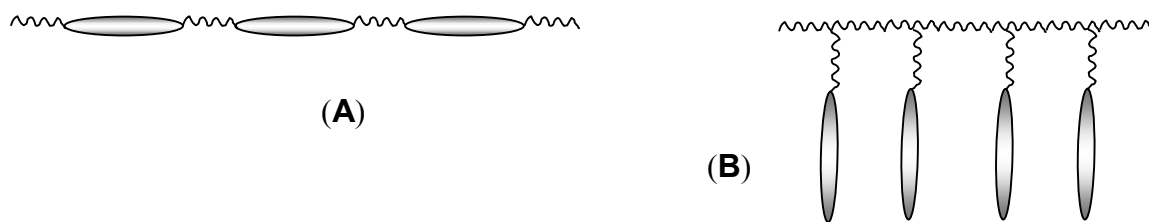


Figure 1.27 - A schematic representation of main chain **(A)** and side chain **(B)** LCPs

Liquid crystalline monomers, that incorporate a polymerisable group at the end of two or more flexible spacer units, have the potential to form polymer networks (see section 1.6.2). Polymer networks are formed by the polymerisation of each reactive end-group with its nearest neighbour, resulting in an insoluble and intractable polymer network, with a high degree of cross-linking between the polymer chains.

1.5.5 Mesophase Identification^[86, 89]

Liquid crystalline phase identification can be a complex and difficult process, as such, LC phases are identified using a number of different techniques including optical polarising microscopy, differential scanning calorimetry (DSC), X-Ray diffraction, neutron scattering, and miscibility studies. Perhaps the most commonly used method is thermal optical polarising microscopy, however, one technique alone is not usually sufficient for precise mesophase identification and so several techniques may be used in collaboration.

1.5.5.1 Optical Polarising Microscopy^[97, 104]

Optical polarising microscopy is one of the most simple, useful and widely used techniques for phase identification. Mesophase types formed by liquid crystalline materials are usually identified by investigations of the texture that they form, as each different LC phase has a distinct optical texture. These textures are a result of the anisotropic molecular orientation of the domains within the mesophase.

Texture identification entails placing a thin sample of the material under investigation on a microscope slide with a cover slip. The slide is then placed in a small variable

and accurate temperature-controlled oven (hot stage), which is then placed under a microscope between polarisers crossed at an angle of 90° . With no sample (or with an isotropic liquid) in place, the crossed polarisers extinguish all light passing through them and the field of view is black. However, if an anisotropic, birefringent medium, such as a crystal or liquid crystal, is placed between them, then light is not extinguished and the orientation of the polarised light is altered within the medium and a texture is observed that gives information relating to the arrangement of the molecules within that medium.

The textures exhibited depend upon the orientation of the LC between the glass substrates and also on the defects, which are characteristic of each phase. The classification of the defects is made when the sample is cooled from the isotropic liquid into its mesophase or mesophases. The defects obtained in this way are characteristic of the mesophase and not the crystal, therefore allowing preliminary identification of the mesophase. Under these conditions, LCs generate a coloured texture or pattern. From this it is relatively straight forward to identify the simpler, more common liquid crystalline phases, such as nematic, SmA and SmC. However, the more complicated phases are more difficult to determine and a large amount of practice is required to distinguish one from another.

The most distinctive feature of the nematic phase occurs on cooling from the isotropic liquid. Small droplets form, which coalesce, forming the colourful *schlieren* texture. This characteristic phenomenon is unique to the nematic phase and is therefore very useful in the identification of nematic phases. The nematic phase may also be characterised by the above mentioned *schlieren* texture, which consists of two and four point brush defects, see figure 1.28. The threaded defect texture is also commonly observed. The SmC phase exhibits a schlieren texture of 4 point brush defects and appears much more viscous than the nematic phase. The smectic A phase exhibits a focal conic texture.

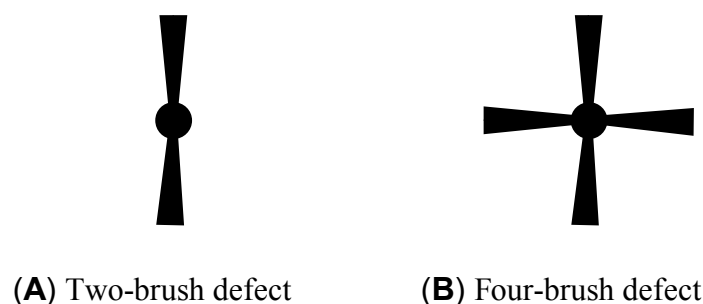


Figure 1.28 - A schematic representation of two- (A) and four- (B) brush defects

The *schlieren* texture is usually highly coloured and exhibits two types of defect, the point singularity and the line singularity. The point singularity gives rise to two and four *schlieren* brushes. The *schlieren* brushes arise from the arrangement of the director around the point defect. When the director is aligned parallel to either one of the crossed-polarisers, then there is an area of extinction, which appears black.

The second type of defect is the line singularity, also known as the line disclination, which appear as thin “thread like” lines. They are the result of two point defects on the surface being joined by a defect line that runs parallel to the supporting surface. Optical discontinuities are associated with a sudden alteration of the angle of the director. The molecules that make up the discontinuity line are in an isotropic state, hence the thread is optically extinct and appears black.

1.5.5.2 Differential Scanning Calorimetry (DSC)^[105]

This method is used to confirm the number, the enthalpy of transition and the temperature ranges of the transitions between the phases, in addition to melting and clearing points exhibited by LCs. The technique involves measuring the enthalpy changes at LC transitions, by having two micro-furnaces linked together each with a separate heater and temperature sensor. One of the furnaces contains a reference material, which has a known heat of fusion, usually Al_2O_3 . The other contains the sample under investigation.

After calibration with a standard material, usually indium, heat energy is supplied to both samples and the heating rates of the samples are maintained at an identical rate.

At the melting transition, extra heat is supplied to the sample in order to maintain a uniform heating rate. The extra energy input is measured by the instrument and converted to a value for the enthalpy change (ΔH). DSC is useful for identifying the presence of phase transitions, which can then be assigned using optical microscopy, and for measuring glass transition temperatures (T_g) of small molecules, oligomers and polymers.

The information obtained is displayed as a thermogram of power versus temperature with a peak for each transition temperature. The position of the peak gives the transition temperature and the area of the peak represents the enthalpy change involved. This technique, however, does not identify a particular phase type, but the enthalpy change can provide valuable information as to the phase structure.

1.5.5.3 X-Ray Diffraction^[106]

X-Ray diffraction studies can be used to determine the phase structure in a mesophase and so identify the phase type. The basic process of X-Ray diffraction works by X-Rays being scattered by individual atoms in the sample, which then interfere with one another to give a characteristic pattern of intensities. The patterns produced can be interpreted in terms of the location of atoms in the molecule, thus giving valuable information about the molecular structure of the sample. As a result, X-Ray diffraction maps out the exact molecular positions within the structure at each given temperature and thus identifies the liquid crystalline phase type at each temperature. As such X-Ray diffraction is the ultimate tool for the identification of liquid crystalline phases. Aligned samples are necessary to distinguish and classify highly-ordered phases.

To identify, unambiguously, a certain liquid crystalline phase may require several of the above mentioned techniques. Usually, thermal optical polarising microscopy and DSC are used in conjunction with each other to elucidate phases.

1.6 Liquid Crystals and Organic Semiconductors

Whilst in their mesophase, LCs exhibit significant molecular order and have the ability to self-organise^[107]. They can form homogeneous thin films and can be macroscopically oriented. A microsegregation phenomenon^[108] can take place in a mesophase that results in a more favourable long-range π -overlap between the LC molecules. These properties make LCs excellent candidates for use in organic semiconductor device applications with improved charge-transport characteristics. Several research groups have observed enhanced charge-transport in the liquid crystalline state^[109-111].

The charge-carrier mobility in ordered lamellar smectic phases of LMM organic compounds has been found to be high. This is due to the high degree of molecular order present in the layered smectic mesophase. In the liquid crystalline state, charges hop from one molecular site to another neighbouring site distributed energetically and spatially. Therefore enhanced charge transport is expected in an aligned smectic mesophase, see figure 1.29.

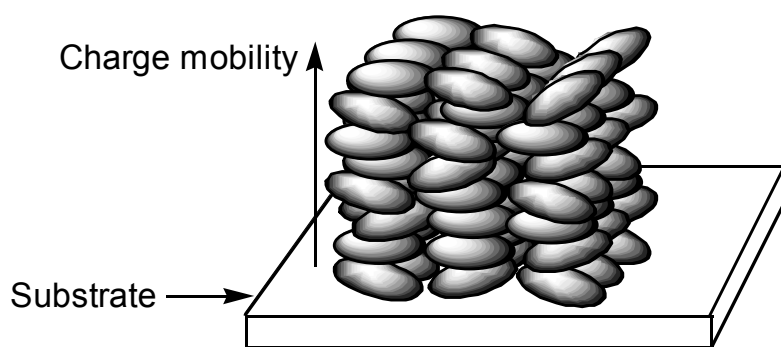


Figure 1.29 - A SmA phase homogeneously oriented on a substrate

1.6.1 Calamitic Liquid Crystals as Charge-Carrier Transport Layers

Organic semiconductor devices require efficient charge-carrier transporting materials, therefore there is a critical need for new materials with improved charge-carrier transport properties. The self-organising ability and the tendency not to form grain-

boundary defects and traps that are associated with polycrystalline materials and amorphous solids, make LCs an attractive prospect for organic semiconductor device applications. Examples of charge-carrier transporting calamitic LCs are shown in figure 1.30 and are subsequently discussed below.

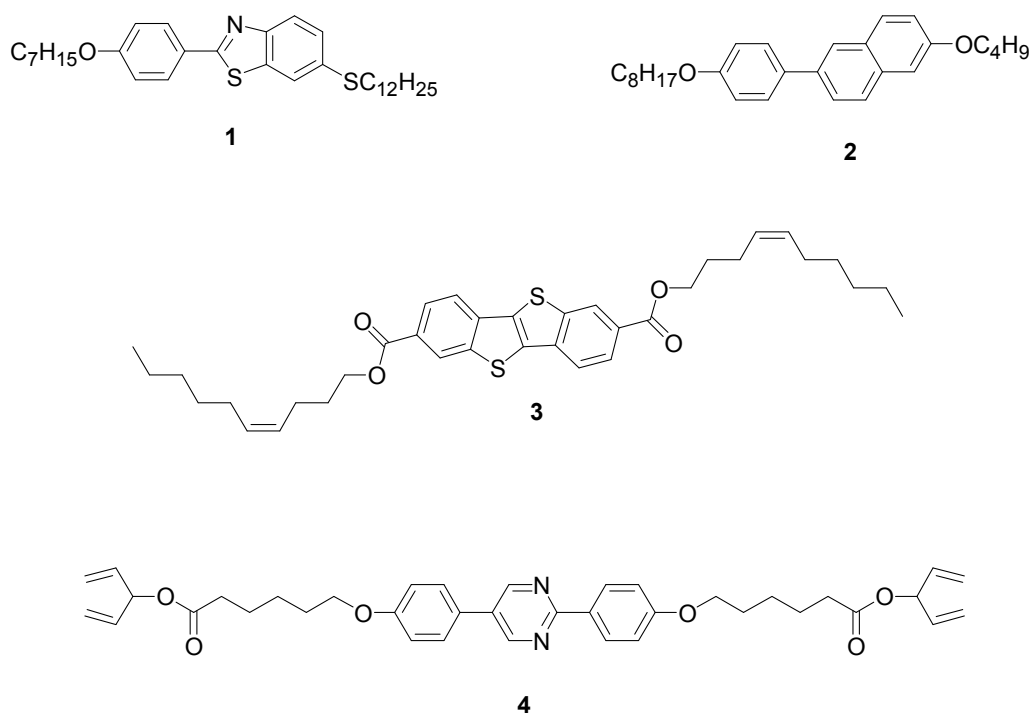


Figure 1.30 - Examples of charge-carrier transporting calamitic LCs

Compound **1**^[112-114] [Cr 90 °C SmA 100 °C I] has a low ionisation potential and contains heteroatoms in the aromatic core, which assists hole transport. It has been found that the charge mobility in the SmA mesophase is two orders of magnitude greater than in the isotropic state^[114]. The hole mobility was found to be $5 \times 10^{-3} \text{ cm}^2 \text{ V}^{-1} \text{ s}^{-1}$. Compound **2**^[109] shows numerous smectic phases [Cr 55 °C CrE 125 °C SmA 129 °C I] and in addition in the CrE mesophase, exhibits high ambipolar carrier-transport with carrier mobilities of $1.0 \times 10^{-2} \text{ cm}^2 \text{ V}^{-1} \text{ s}^{-1}$. There is less order in the SmA mesophase and consequently charge mobilities tend to be lower ($4 \times 10^{-4} \text{ cm}^2 \text{ V}^{-1} \text{ s}^{-1}$). The high charge-carrier mobilities can be accounted for, at least in part, by the molecular ordering and packing in the CrE mesophase. In addition, the fused planar naphthalene ring aids charge-transport by allowing the molecular π -orbitals of adjacent molecules to come close to one another. A sanidic LC has also been

synthesised, compound **3**, that shows high ambipolar mobilities ($2 \times 10^{-3} \text{ cm}^2 \text{ V}^{-1} \text{ s}^{-1}$) in the lamello-columnar mesophase^[115-117].

Although efficient charge-transport has been demonstrated in the liquid crystalline phases of the materials above, they are all crystals at room temperature and therefore unsuitable for practical semiconductor device applications. Compound **4**^[111] [Cr 25 °C SmC 124 °C I], however, has the advantage of being liquid crystalline at room temperature and can be stabilised by photopolymerisation of the diene end-groups to form an insoluble and intractable polymer network. Compound **4** has exhibited electron mobilities of $1.5 \times 10^{-5} \text{ cm}^2 \text{ V}^{-1} \text{ s}^{-1}$.

The performance of an organic semiconductor is largely controlled by the charge-carrier mobility of both electrons and holes. Generally, a hole transporting material must have a low ionisation potential for easy loss of an electron to produce a hole in the conduction process. By contrast, an electron transporting material must have a high ionisation potential.

Ionic impurities tend to exert a strong influence as charge-carriers during the electrical conduction process in materials, particularly in liquids because of their viscosity-dependent charge mobility. Electronic conduction may be masked by ionic conduction, even if the organic materials only contain a small concentration of ionic impurities. Consequently, not only pure, but also chemically stable materials, are required for organic semiconductor device applications that do not degrade to produce ionic impurities. Ionic impurities can lead to low on/off ratios and often dielectric breakdown and low device lifetimes.

1.6.2 Liquid Crystalline Polymer Networks^[118-120]

The two most common methods to construct organic semiconductor devices are vacuum deposition and spin coating. Vacuum deposition allows well-defined, thin layers to be produced, but is a time consuming and expensive method. Spin coating is cheap and large areas can be coated, but interlayer mixing can occur during the

deposition of each layer. In order to facilitate multilayer fabrication *via* spin coating the solubility of the layers must be reduced after deposition.

A possible solution is polymerisable LCs or RMs, which are LMM liquid crystalline materials that possess polymerisable groups at the end of aliphatic spacer units attached to an aromatic core. The reactive LCs can be aligned and stabilised by polymerisation to form an insoluble anisotropic polymer network, see figure 1.31. The liquid crystalline state of the monomer remains in the polymer network after polymerisation. If the LC has more than one polymerisable group then a network can be produced with a high cross-link density^[121]. The resulting film is solid, robust and insoluble.

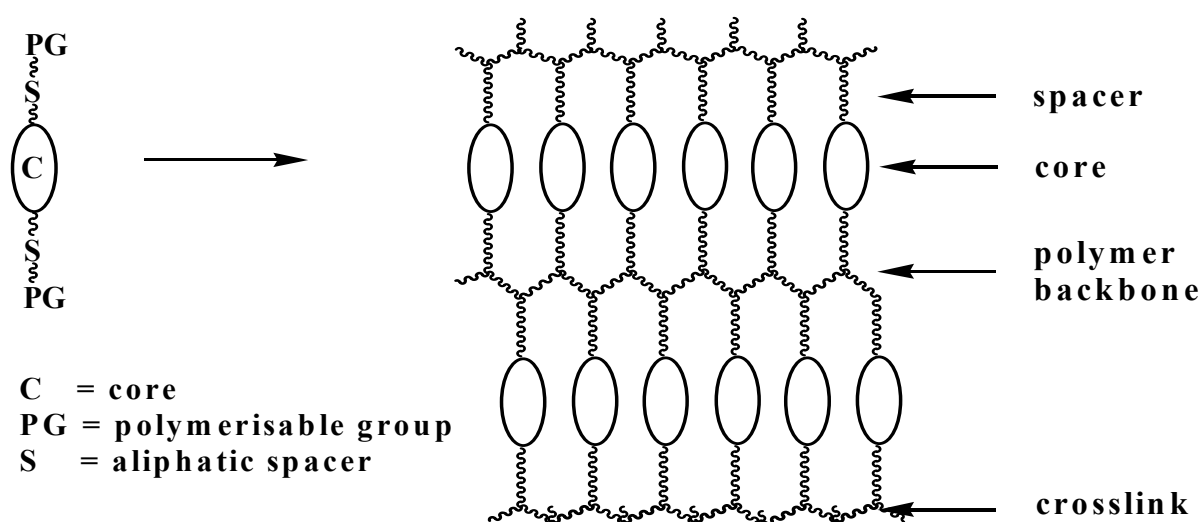


Figure 1.31 - A schematic representation of a cross-linked polymer network

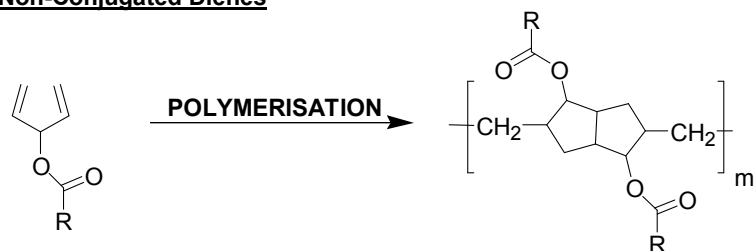
RMs can be polymerised by chemical, thermal or photochemical methods, with the latter being more attractive for potential semiconductor device applications. RMs have been reported in the literature using various polymerisable groups, such as acrylates^[122-123], methacrylates^[124], oxetanes^[125] and conjugated dienes^[126-127]. During this research non-conjugated diene and methacrylate photo-polymerisable and oxetane chemically-polymerisable end-groups respectively, have been incorporated into liquid crystalline monomers in order to produce polymer networks via the action of UV light or suitable chemical initiators.

The advantages associated with non-conjugated dienes include their thermal stability at elevated temperatures. This prevents degradation during the photopolymerisation process. Dienes also tend to promote liquid crystallinity^[70] and generally lead to lower melting points than those LCs with straight alkyl chains of similar length^[82]. Also the polymerisation can take place without using a photoinitiator, which is beneficial for device applications, because residues from the initiator may be detrimental to the device performance and stability.

Charge-transporting RMs are a promising class of materials for semiconductor device applications. They can form uniform thin films, either in the liquid crystalline phase or as a liquid crystalline glass. Upon polymerisation, the liquid crystalline film is made insoluble and the highly cross-linked structure prevents crystallisation, a problem associated with amorphous materials. This approach combines the advantages associated with polymers, such as deposition from solution, principally spin coating, whilst eliminating the problems associated with amorphous materials. They possess unambiguous molecular structures with definite molecular weights, monodispersity and good chemical purity is readily achievable. Photopolymerisation allows the fabrication of photopatternable multilayer organic semiconductor devices that can be manufactured relatively cheaply.

Non-conjugated diene monomers polymerise, *via* a radical intra- and inter-molecular cyclopolymerisation mechanism, to form an inert cyclic polymer backbone. Methacrylates and acrylates polymerise by an intermolecular radical chain mechanism to form a linear backbone. Oxetanes polymerise forming a linear polymer backbone *via* a cationic ring opening mechanism using a suitable chemical initiator, such as a boron trifluoride-THF or –diethyl ether complex. Figure 1.32 shows the structure of each starting monomer, non-conjugated diene, methacrylate and oxetane and the resulting inert polymer backbone that is formed once polymerisation has taken place.

Non-Conjugated Dienes



Methacrylates



Oxetanes

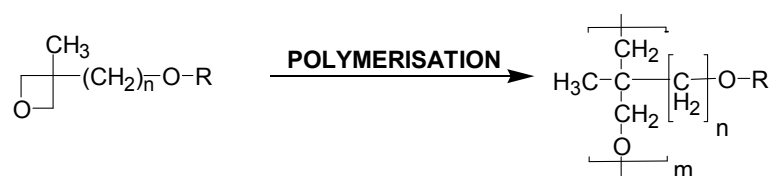


Figure 1.32 - The structures of the non-conjugated diene, methacrylate and oxetane monomers and the resulting polymers formed after polymerisation

1.7 References

- 1 T. Ito, H. Shirakawa and S. Ikeda, *J. Polym. Sci. Polym. Chem. Ed.*, 1974, **12** (1), 11.
- 2 H. Shirakawa, E. J. Louis, A. G. MacDiarmid, C. K. Chiang and A. J. Heeger, *J. Chem. Soc., Chem. Commun.*, 1977, **16**, 578.
- 3 N. C. Greenham and R. H. Friend, *Semiconductor Device Physics of Conjugated Polymers, Solid State Physics*, 1995, **49**.
- 4 J. H. Burroughes, D. D. C. Bradley, A. R. Brown, R. N. Marks, K. Mackay, R. H. Friend, P. L. Burn and A. B. Holmes, *Nature*, 1990, **347**, 539.
- 5 G. B. Street and T. C. Clarke, *IBM J. Res. Dev.*, 1981, **25**, 51.
- 6 G. Schopf and G. Koßmehl, *Adv. Polym. Sci.*, 1997, **129**, 1.
- 7 R. D. McCullough and R. D. Lowe, *J. Chem. Soc., Chem. Commun.*, 1992, **1**, 70.
- 8 T.-A. Chen, R. A. O'Brien and R. D. Rieke, *Macromolecules*, 1993, **26** (13), 3462.
- 9 M. Hamaguchi and K. Yoshino, *Jpn. J. Appl. Phys.*, 1994, **33**, L1478.
- 10 M. Hamaguchi and K. Yoshino, *Jpn. J. Appl. Phys.*, 1995, **34**, L712.
- 11 C. Zhang, S. Höger, K. Pakbaz, F. Wudl, and A. J. Heeger, *J. Electron Mater.*, 1993, **22** (4), 413.
- 12 S. T. Kim, D.-H. Hwang, X. C. Li, J. Grüner, R. H. Friend, A. B. Holmes and H. K. Shim, *Adv. Mater.*, 1996, **8** (12), 979.
- 13 S. Höger, J. J. McNamara, S. Schricker and F. Wudl, *Chem. Mater.*, 1994, **6** (2), 171.
- 14 A. Tsumura, H. Koezuka and T. Ando, *Appl. Phys. Lett.*, 1986, **49** (18), 1210.
- 15 J. H. Burroughes, C. A. Jones and R. H. Friend, *Nature*, 1988, **335**, 137.
- 16 G. Horowitz, R. Hajlaoui, R. Bourguiga and M. Hajlaoui, *Synth. Met.*, 1999, **101**, 401.
- 17 N. Karl, *Synth. Met.*, 2003, **133-134**, 649.
- 18 H. E. Katz and Z. Boa, *J. Phys. Chem. B*, 2000, **104** (4), 671.
- 19 G. H. Gelinck, T. C. T. Geuns and D. M. de Leeuw, *Appl. Phys. Lett.*, 2000, **77** (10), 1487.

- 20 J. A. Rogers, Z. Boa, A. Dodabalapur and A. Makhija, *IEEE Electron Dev. Lett.*, 2000 **21** (3), 100.
- 21 H. Sirringhaus, P. J. Brown, R. H. Friend, M. M. Nielsen, K. Bechgaard, B. M. W. Langeveld-Voss, A. J. H. Spiering, R. A. J. Janssen, E. W. Meijer, P. Herwig and D. M. de Leeuw 1999, *Nature*, **401**, 685.
- 22 H. Sirringhaus, P. J. Brown, R. H. Friend, M. M. Nielsen, K. Bechgaard, B. M. W. Langeveld-Voss, A. J. H. Spiering, R. A. J. Janssen and E. W. Meijer, *Synth. Met.*, 2000, **111-112**, 129.
- 23 Z. Boa, A. Dodabalapur, A. J. Lovinger and A. Makhija, *Appl. Phys. Lett.*, 1996, **69** (26), 4108.
- 24 F. Garnier, R. Hajlaoui, A. Yassar, and P. Srivastava, *Science*, 1994, **265**, 1684.
- 25 B. Crone, A. Dodabalapur, Y.-Y. Lin, R. W. Filas, Z. Boa, A. LaDuca, R. Sarpeshkar, H. E. Katz and W. Li, *Nature*, 2000, **403**, 521.
- 26 C. J. Drury, C. M. J. Mutsaers, C. M. Hart, M. Matters and D. M. de Leeuw, *Appl. Phys. Lett.*, 1998, **73** (1), 108.
- 27 M. Matters, D. M. de Leeuw, M. J. C. M. Vissenberg, C. M. Hart, P. T. Herwig, T. Geuns, C. M. J. Mutsaers and C. J. Drury, *Optical Materials*, 1999, **12** (2-3), 189.
- 28 J. A. Rogers, Z. Boa, K. Baldwin, A. Dodabalapur, B. Crone, V. R. Raju, V. Kuck, H. E. Katz, K. Amundson, J. Ewing and P. Drzaic, *Proceedings of the National Academy of Sciences*, 2001, **98** (9), 4835.
- 29 H. Sirringhaus, T. Kawase, R. H. Friend, T. Shimoda, M. Inbasekaran, W. Wu and E. P. Woo, *Science*, 2000, **290**, 2123.
- 30 J. A. Rogers, Z. Boa, A. Makhija, and P. Braun, *Adv. Mater.*, 1999, **11** (9), 741.
- 31 J. A. Rogers, A. Dodabalapur, Z. Boa and H. E. Katz, *Appl. Phys. Lett.*, 1999, **75** (7), 1010.
- 32 J. Tate, J. A. Rogers, C. D. W. Jones, B. Vyas, D. W. Murphy, W. Li, Z. Boa, R. E. Slusher, A. Dodabalapur and H. E. Katz, *Langmuir*, 2000, **16** (14), 6054.
- 33 D. J. Gundlach, Y.-Y. Lin, T. N. Jackson, S. F. Nelson and D. G. Schlom, *IEEE Electron Dev. Lett.*, 1997, **18** (3), 87.

- 34 Y.-Y. Lin, D. J. Gundlach, S. F. Nelson and T. N. Jackson, *IEEE Trans. Electron Dev.*, 1997, **44** (8), 1325.
- 35 Y.-Y. Lin, D. J. Gundlach, S. F. Nelson and T. N. Jackson, *IEEE Electron Dev. Lett.*, 1997, **18** (12), 606.
- 36 J. H. Schön, S. Berg, Ch. Kloc and B. Batlogg, *Science*, 2000, **287**, 1022.
- 37 J. H. Schön, A. Dodabalapur, Z. Boa, Ch. Kloc, O. Schenker and B. Batlogg, *Nature*, 2001, **410**, 189.
- 38 F. Garnier, A. Yassar, R. Hajlaoui, G. Horowitz, F. Deloffre, B. Servet, S. Ries and P. Alnot, *J. Am. Chem. Soc.*, 1993, **115** (19), 8716.
- 39 B. Wegewijs, M. P. de Haas, D. M. de Leeuw, R. Wilson and H. Sirringhaus, *Synth. Met.*, 1999, **101**, 534.
- 40 J. H. Schön, Ch. Kloc, R. A. Laudise and B. Batlogg, *Phys. Rev. B*, 1998, **58** (19), 12952.
- 41 H. E. Katz, A. J. Lovinger and J. C. Laquindanum, *Chem. Mater.*, 1998, **10** (2), 457.
- 42 Z. Boa, A. Dodabalapur and A. J. Lovinger, *Appl. Phys. Lett.*, 1996, **69** (26), 4108.
- 43 P. J. Brown, H. Sirringhaus, M. Harrison, M. Shkunov and R. H. Friend, *Phys. Rev. B*, 2001, **63** (12), 125204.
- 44 P. J. Brown, H. Sirringhaus and R. H. Friend, *Synth. Met.*, 1999, **101**, 557.
- 45 P. Bäuerle, F. Pfau, H. Schlupp, F. Würthner, K.-U. Gaudl, M. B. Caro and P. Fischer, *J. Chem. Soc. Perkin Trans. 2*, 1993, **3**, 489.
- 46 L. L. Miller and Y. Yu, *J. Org. Chem.*, 1995, **60** (21), 6813.
- 47 H. E. Katz, A. Dodabalapur, L. Torsi and D. Elder, *Chem. Mater.*, 1995, **7** (12), 2238.
- 48 A. Facchetti, Y. Deng, A. Wang, Y. Koide, H. Sirringhaus, T. J. Marks and R. H. Friend, *Angew. Chem. Int. Ed.*, 2000, **39** (24), 4547.
- 49 J. Kagan and S. K. Arora, *Heterocycles*, 1983, **20** (10), 1937.
- 50 G. Horowitz, D. Fichou, X. Peng and F. Garnier, *Synth. Met.*, 1991, **41-43**, 1127.
- 51 M. S. A. Abdou, X. Lu, Z. W. Xie, F. Orfino, M. J. Deen and S. Holdcroft, *Chem. Mater.*, 1995, **7** (4), 631.
- 52 H. E. Katz, L. Torsi and A. Dodabalapur, *Chem. Mater.*, 1995, **7** (12), 2235.

- 53 J. G. Laquindanum, H. E. Katz and A. J. Lovinger, *J. Am. Chem. Soc.*, 1998, **120** (4), 664.
- 54 J. G. Laquindanum, H. E. Katz, A. J. Lovinger and A. Dodabalapur, *Adv. Mater.*, 1997, **9** (1), 36.
- 55 H. E. Katz, *J. Mater. Chem.*, 1997, **7** (3), 369.
- 56 H. Sirringhaus, R. H. Friend, X.-C. Li, S. C. Morratti, A. B. Holmes and N. Feeder, *Appl. Phys. Lett.*, 1997, **71** (26) 3871.
- 57 X.-C. Li, H. Sirringhaus, F. Garnier, A. B. Holmes, S. C. Morratti, N. Feeder, W. Clegg, S. J. Teat and R. H. Friend, *J. Am. Chem. Soc.*, 1998, **120** (9), 2206.
- 58 J. J. Morrison, M. M. Murray, X.-C. Li, A. B. Holmes, S. C. Morratti, R. H. Friend and H. Sirringhaus, *Synth. Met.*, 1999, **102**, 987.
- 59 C. R. Kagan, D. B. Mitzi and C. D. Dimitrakopoulos, *Science*, 1999, **286**, 945.
- 60 P. G. Schouten, J. M. Warman, M. P. de Haas, M. A. Fox and H. L. Pan, *Nature*, 1991, **353**, 736.
- 61 Z. Bao, A. J. Lovinger and A. Dodabalapur, *Appl. Phys. Lett.*, 1996, **69** (20), 3066.
- 62 J. Salbeck, N. Yu, J. Bauer, F. Weissortel and H. Bestgen, *Synth. Met.*, 1997, **91**, 209.
- 63 A. W. Grice, A. Tajbakhsh, P. L. Burn and D. D. C. Bradley, *Adv. Mater.*, 1997, **9** (15), 1174.
- 64 C. J. Tonzola, M. M. Alam and S. A. Jenekhe, *Adv. Mater.*, 2002, **14** (15), 1086.
- 65 K. R. J. Thomas, J. T. Lin, Y.-T. Tao and C.-W. Ko, *Adv. Mater.*, 2000, **12** (24), 1949.
- 66 I. McCulloch, W. Zhang, M. Heeney, C. Bailey, M. Giles, D. Graham, M. Shkunov, D. Sparrowe and S. Tierney, *J. Mater. Chem.*, 2003, **13** (10), 2436.
- 67 P. Vlachos, B. Mansoor, M. P. Aldred, M. O'Neill and S. M. Kelly, *Chem. Commun.*, 2005, **23**, 2921.
- 68 K. Oikawa, H. Monobe, J. Takahashi, K. Tsuchiya, B. Heinrich, D. Guillon and Y. Shimizu, *Chem. Commun.*, 2005, **42**, 5337.

- 69 P. Strohmriegl, D. Hanft, M. Jandke and T. Pfeuffer, *Mat. Res. Soc. Symp. Proc.*, 2001, **709**, 31.
- 70 A. E. A. Contoret, S. R. Farrar, S. M. Kelly, J. E. Nicholls, M. O'Neill and G. J. Richards, *Synth. Met.*, 2001, **121**, 1629.
- 71 M. O'Neill and S. M. Kelly, *Adv. Mater.*, 2003, **15** (14), 1135.
- 72 M. S. Bayerl, T. Braig, O. Nuyken, D. C. Müller, M. Groß and K. Meerholz, *Macromol. Rapid Commun.*, 1999, **20** (4), 224.
- 73 K. L. Woon, M. O'Neill, G. J. Richards, M. P. Aldred, S. M. Kelly and A. M. Fox, *Adv. Mater.*, 2003, **15** (18), 1555.
- 74 P. Strohmriegl and J. V. Grazulevicius, *Adv. Mater.*, 2002, **14** (20), 1439.
- 75 M. Redecker, D. D. C. Bradley, M. Inbasekaran and E. P. Woo, *Appl. Phys. Lett.*, 1999, **74** (10), 1400.
- 76 H. Sirringhaus, R. J. Wilson, R. H. Friend, M. Inbasekaran, W. Wu, E. P. Woo, M. Grell and D. D. C. Bradley, *Appl. Phys. Lett.*, 2000, **77** (3), 406.
- 77 P. G. Schouten, J. M. Warman, M. P. de Haas, M. A. Fox and H. L. Pan, *Nature*, 1991, **353**, 736.
- 78 A. Facchetti, M. Mushrush, H. E. Katz and T. J. Marks, *Adv. Mater.*, 2003, **15** (1), 33.
- 79 A. Bernanose, M. Comte and P. Vouaux, *J. Chim. Phys.*, 1953, **50**, 64.
- 80 A. E. A. Contoret, S. R. Farrar, P. O. Jackson, S. M. Khan, L. May, M. O'Neill, J. E. Nicholls, S. M. Kelly and G. J. Richards, *Adv. Mater.*, 2000, **12** (13), 971.
- 81 J. Barche, S. Janietz, M. Ahles, R. Schmechel and H. von Seggern, *Chem. Mater.*, 2004, **16** (22), 4286.
- 82 A. E. A. Contoret, S. R. Farrar, M. O'Neill, J. E. Nicholls, G. J. Richards, S. M. Kelly and A. W. Hall, *Chem. Mater.*, 2002, **14** (4), 1477.
- 83 S. R. Farrar, A. E. A. Contoret, M. O'Neill, J. E. Nicholls, G. J. Richards and S. M. Kelly, *Phys. Rev. B*, 2002, **66** (12), 125107.
- 84 A. E. A. Contoret, S. R. Farrar, S. M. Khan, M. O'Neill, G. J. Richards, M. P. Aldred and S. M. Kelly, *J. Appl. Phys.*, 2003, **93** (3), 1465.
- 85 A. E. A. Contoret, S. R. Farrar, P. O. Jackson, M. O'Neill, J. E. Nicholls, S. M. Kelly and G. J. Richards, *Synth. Met.*, 2001, **121**, 1645.

- 86 P. J. Collings and M. Hird, *'Introduction to Liquid Crystals: Chemistry and Physics'*, G. W. Gray, J. W. Goodby and A. Fukuda (Eds.), Taylor & Francis, London (1997).
- 87 G. Friedel, *Ann. Phys.*, 1922, **18**, 273.
- 88 K. J. Toyne, *'Thermotropic Liquid Crystals'*, G. W. Gray (Ed.), John Wiley & Sons Ltd., Chichester (1987).
- 89 J. W. Goodby, *J. Mater. Chem.*, 1991, **1** (3), 307.
- 90 P. Balkwill, D. Bishop, A. Pearson and I. Sage, *Mol. Cryst. Liq. Cryst.*, 1985, **123**, 1.
- 91 M. R. C. Gerstenberger and A. Hass, *Angew. Chem. Int. Ed. Engl.*, 1981, **20** (8), 647.
- 92 P. G. de Gennes and J. Prost, *'The Physics of Liquid Crystals'* (2nd Ed), Oxford Science Publications, Oxford (1993).
- 93 D. Demus, in *'Handbook of Liquid Crystals Volume 1: Fundamentals'*, D. Demus, J. W. Goodby, G. W. Gray, H.-W. Spiess and V. Vill (Eds.), Wiley-VCH, Weinheim (1998).
- 94 G. W. Gray, in *'Molecular Structure and the Properties of Liquid Crystals'*, Academic Press Ltd., London (1962).
- 95 J. W. Goodby, *Mol. Cryst. Liq. Cryst. Lett. Sect.*, 1983, **92**, 171.
- 96 J. W. Goodby, *'Handbook of Liquid Crystals, Volume 2A: Low Molecular Weight Liquid Crystals I'*, D. Demus, J. W. Goodby, G. W. Gray, H.-W. Spiess and V. Vill (Eds.), Wiley-VCH, Weinheim (1998).
- 97 G. W. Gray and J. W. Goodby, *'Smectic Liquid Crystals - Textures and Structures'*, Leonard Hill, Glasgow and London (1984).
- 98 J. Billard, *'Liquid Crystals of One- and Two-Dimensional Order, Springer Series in Chemical Physics'*, W. Helfrich and G. Heppke (Eds.), Springer-Verlag, Berlin (1980).
- 99 A. W. Hall, J. Hollingshurst and J. W. Goodby, *'Handbook of Liquid Crystal Research'*, P. J. Collings and J. S. Patel (Eds.), Oxford University Press Inc., New York (1997).
- 100 D. G. McDonnell, *'Thermotropic Liquid Crystals'*, G. W. Gray (Ed.), John Wiley & Sons Ltd., Chichester (1987).

- 101 J. W. Goodby, '*Ferroelectric Liquid Crystals - Principals, Properties and Applications*', J. W. Goodby, R. Blinc, N. A. Clark, S. T. Lagerwall, M. A. Osipov, S. A. Pikin, T. Sakurai, K. Yoshino and B. Žekš (Eds.), Gordon & Breach, Philadelphia and Reading (1991).
- 102 J. Doucet, '*The Molecular Physics of Liquid Crystals*', G. R. Luckhurst and G. W. Gray (Eds.), Academic Press Ltd., London (1979).
- 103 A. J. Leadbetter, M. A. Mazid, and R. M. Richardson, '*Liquid Crystals*', S. Chandrasekhar (Ed.), Heydon & Sons Ltd., London (1980).
- 104 J. W. Goodby in '*Encyclopedia of Analytical Science*', A. Townshend, P. J. Worsfold, S. J. Haswell, R. Macrae, H. W. Werner and I. D. Wilson (Eds.), Academic Press Ltd., London (1995).
- 105 D. A. Skoog and J. J. Leary, '*Principles of Instrumental Analysis*' (4th Ed.), Saunders College Publishing, Philadelphia (1992).
- 106 P. W. Atkins, '*Physical Chemistry*' (5th Ed), Oxford University Press, Oxford (1994).
- 107 M. Funahashi and J.-I. Hanna, *Appl. Phys. Lett.*, 2000, **76** (18), 2574.
- 108 E. Peeters, M. P. T. Christiaans, R. A. J. Janssen, H. F. M. Schoo, H. P. J. M. Dekkers and E. W. Meijer, *J. Am. Chem. Soc.*, 1997, **119** (41), 9909.
- 109 M. Funahashi and J.-I. Hanna, *Appl. Phys. Lett.*, 1998, **73** (25), 3733.
- 110 H. Tokuhisa, M. Era and T. Tsutsui, *Adv. Mater.*, 1998, **10** (5), 404.
- 111 P. Vlachos, S. M. Kelly, B. Mansoor and M. O'Neill, *Chem. Commun.*, 2002, **8**, 874.
- 112 M. Funahashi and J.-I. Hanna, *Phys. Rev. Lett.*, 1997, **78** (11), 2184.
- 113 M. Funahashi and J.-I. Hanna, *Jpn. J. Appl. Phys.*, 1996, **35**, L703.
- 114 M. Funahashi and J.-I. Hanna, *Mol. Cryst. Liq. Cryst.*, 1997, **304**, 429.
- 115 S. Méry, D. Haristoy, J. F. Nicoud, D. Guillon, S. Diele, H. Monobe and Y. Shimizu, *J. Mater. Chem.*, 2002, **12** (1), 37.
- 116 D. Haristoy, S. Méry, B. Heinrich, L. Mager, J. F. Nicoud and D. Guillon, *Liq. Cryst.*, 2000, **27** (3), 321.
- 117 B. Košata, V. Kozmik, J. Svoboda, V. Novotná, P. Vaněk and M. Glogarová, *Liq. Cryst.*, 2003, **30** (5), 603.
- 118 D. J. Broer, H. Finkelmann and K. Kondo, *Macromol. Chem. & Phys.*, 1988, **189** (1), 185.
- 119 R. A. M. Himkmet, J. Lub and J. A. Higgins, *Polymer*, 1993, **34** (8), 1736.

- 120 D. J. Broer, *Mol. Cryst. Liq. Cryst.*, 1995, **261**, 513.
- 121 S. M. Kelly, *J. Mater. Chem.*, 1995, **5** (12), 2047.
- 122 A. P. Davey, R. G. Howard and W. J. Blau, *J. Mater. Chem.*, 1997, **7** (3), 417.
- 123 A. Bacher, P. G. Bentley, D. D. C. Bradley, L. K. Douglas, P. G. Glarvey, M. Grell, K. S. Whitehead and M. L. Turner, *J. Mater. Chem.*, 1999, **9** (12), 2985.
- 124 D. Hölter, H. Frey, R. Mülhaupt and J. E. Klee, *Adv. Mater.*, 1998, **10** (11), 864.
- 125 M. S. Bayerl, T. Braig, O. Nuyken, D. C. Müller, M. Groß and K. Meerholz, *Macromol. Rapid Commun.*, 1999, **20** (4), 224.
- 126 B. P. Hoag and D. L. Gin, *Macromolecules*, 2000, **33** (23), 8549.
- 127 A. E. A Contoret, S. R. Farrar, P. O. Jackson, S. M. Khan, L. May, M. O'Neill, J. E. Nicholls, S. M. Kelly and G. J. Richards, *Adv. Mater.*, 2000, **12** (13), 971.



Chapter Two



Aims of the Research



•

•



•

•

•

•

•

•

2.0 Aims of the Research

The overall aim of this research was to synthesise and evaluate novel organic liquid crystalline semiconductors to be used as the charge-transporting layer in organic semiconductor device applications. The primary focus of the work was the synthesis and evaluation of LMM liquid crystalline materials, which incorporate photopolymerisable (non-conjugated diene and methacrylate)^[1-2] and chemically polymerisable (oxetane)^[3-6] end-groups, attached by aliphatic spacer units of varying length, to an aromatic core. These organic materials could then be aligned in the liquid crystalline state and fixed into position by photo- or chemical-polymerisation to form thin-layer, insoluble, cross-linked, anisotropic, polymer networks by either a radical or ionic mechanism.

Cross-linked, liquid crystalline polymer networks offer many potential advantages when compared to small molecules or conjugated main chain polymers for the fabrication of multi-layer, organic semiconductor devices. These include the advantages associated with LMM compounds, such as ease of purification and deposition from solution using low cost techniques such as spin coating, inkjet printing and doctor blade techniques.

This approach would allow the fabrication of multi-layer, organic semiconductor devices, combining the advantages of LMM compounds, with those of aromatic main-chain polymers. In addition, it offers the possibility of high charge-transport due to the highly ordered nature of liquid crystalline polymer networks. This research is a continuation and further extension to OFETs of work carried out by the Organophotonics Group^[7] at the University of Hull, in which a similar technique has been used to fabricate organic light emitting diodes (OLEDs) and other groups^[8-10] who have also attempted to achieve high carrier mobility, through highly ordered materials, whilst maintaining the advantages of low-cost deposition techniques, principally, solution processing.

A secondary focus of this research was to identify potential structure-property relationships for the novel organic LMM materials synthesised, such as the

dependence of liquid crystalline and crystal-smectic transition temperatures and charge-transport or mobility on molecular structure. The correlation between molecular structure and charge-transporting properties was to be achieved by synthesising a series of related compounds with different central chromophores. This should enable clear comparisons of the efficiency of each of the chromophores to be established. Furthermore, the incorporation of different end-groups and aliphatic spacer unit lengths into a number of compounds with the same chromophore should allow their effect upon the physical properties stated above to be studied.

The nature of the central aromatic core, the polymerisable end-groups and the spacer lengths of the RMs was altered systematically in attempts to obtain low melting points, high clearing points and wide temperature ranges for the smectic and nematic mesophases observed and also to tune the physical properties of each of the materials. The main aromatic rings used, as constituent parts of the central molecular cores, throughout this research are shown in figure 2.1.

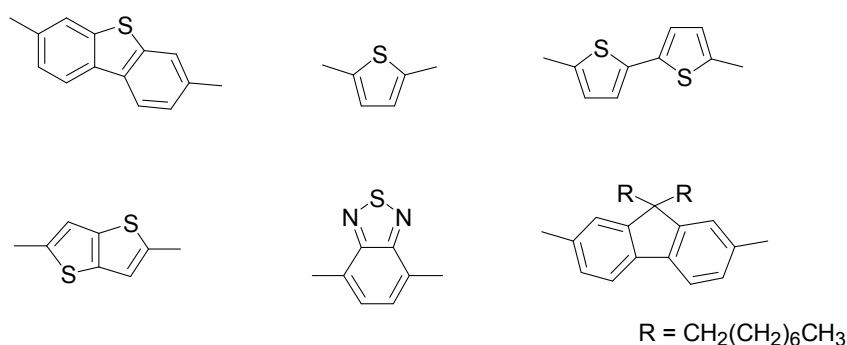


Figure 2.1 - The main aromatic rings used, as constituent parts of the central molecular cores, throughout this research

The molecular cores of the RMs detailed in this work only incorporate a small number of aromatic rings, firstly to allow increased solubility of the material and secondly to minimise the synthetic complexity and subsequent cost of any potential practical applications.

The presence of a 2,7-disubstituted-9,9-dialkylfluorene unit in the structure of specific liquid crystalline, LMM materials should ensure good solubility, induce lower liquid crystalline transition temperatures, especially the melting point, due to steric effects,

and, in addition, induce good charge-transporting properties of the materials. LCs incorporating the 2,7-disubstituted-9,9-dialkylfluorene unit tend to form nematic mesophases due to steric effects. Consequently materials containing these units tend to have lower viscosities than analogous materials forming smectic mesophases due to the absence of a layer structure. This was intended to allow the new nematic liquid crystalline semiconductors to be aligned more easily than the standard smectic semiconductors for practical devices. Fluorine atoms were also incorporated into the phenyl units in a lateral position, adjacent to the main core of certain RMs, in attempts to induce even lower melting points for these materials.

2.1 References

- 1 A. W. Hall, D. Lacey and P. I. Buxton, *Macromol. Rapid Commun.*, 1996, **17** (6), 417.
- 2 P. I. Buxton, A. W. Hall and D. Lacey, *Macromol. Chem. Phys.*, 1997, **198** (7), 2307.
- 3 E. J. Corey and N. Raju, *Tet. Lett.*, 1983, **24** (50), 5571.
- 4 Y. Kawakami, K. Takahashi and H. Hibino, *Macromolecules*, 1991, **24** (16), 4531.
- 5 Y. Kawakami, K. Takahashi, S. Nishiguchi and K. Toida, *Polymer Int.*, 1993, **31** (1), 35.
- 6 M. Motoi, K. Noguchi, A. Arano, S. Kanoh and A. Ueyama, *Bull. Chem. Soc. Jpn.*, 1993, **66** (6), 1778.
- 7 A. E. A. Contoret, S. R. Farrar, P. O. Jackson, S. M. Khan, L. May, M. O'Neill, J. E. Nicholls, S. M. Kelly and G. J. Richards, *Adv. Mater.*, 2000, **12** (13), 971.
- 8 H. Sirringhaus, R. J. Wilson, R. H. Friend, M. Inbasekarran, W. Wu, E. P. Woo, M. Grell and D. C. C. Bradley, *Appl. Phys. Lett.*, 2000, **77** (3), 406.
- 9 H. Sirringhaus, P. J. Brown, R. H. Friend, M. M. Nielsen, K. Bechgaard, B. M. W. Langeveld-Voss, A. J. H. Spiering, R. A. J. Janssen and E. W. Meijer, *Synth. Met.*, 2000, **111-112**, 129.
- 10 H. Sirringhaus, P. J. Brown, R. H. Friend, M. M. Nielsen, K. Bechgaard, B. M. W. Langeveld-Voss, A. J. H. Spiering, R. A. J. Janssen, E. W. Meijer, P. Herwig and D. M. de Leeuw, *Nature*, 1999, **401**, 685.



Chapter Three



Experimental



•

•



•

•

•

•

•

3.0 Experimental

3.1 Material Evaluation

¹H Nuclear Magnetic Resonance (NMR) Spectroscopy

The structures of intermediates and final products were confirmed by ¹H NMR spectroscopy using either a JEOL, JNM-LA FT NMR spectrometer (400 MHz) or a JEOL, JNM-ECP FT NMR spectrometer (400 MHz). Tetramethylsilane (TMS) was used as the internal standard unless otherwise stated. The following abbreviations are used to describe the splitting patterns:

s - singlet	d - doublet	t - triplet	quart - quartet
quint - quintet	dd - double doublet	dt - double triplet	tt - triple triplet
m - multiplet			

Infrared (IR) Spectroscopy

Infrared spectroscopy was carried out using a Perkin Elmer, Paragon 1000 Fourier Transform Infrared (FT-IR) spectrophotometer. IR spectra of liquids were obtained by inserting the material between two sodium chloride plates and IR spectra of solids were obtained using potassium bromide discs.

Mass Spectrometry (MS)

Mass spectra of intermediates and final products were recorded using either a Shimadzu QP 5050A, Gas Chromatograph Mass Spectrometer (GCMS), using an Electron Impact (EI) ionisation method at a source temperature of 350 °C, or a Finnigan-MAT 1020 GCMS. Mass spectra of certain materials, in a 2-(4-hydroxyphenylazo)benzoic acid (HABA) matrix, were obtained using a Bruker Reflex IV instrument. Only the most important or relevant peaks are included in the material

synthesis section. Where present, the mass ion of a particular material (intermediate or final product) is identified by (M^+). In addition, the base peak (most stable fragment) is identified by (M100).

Elemental Analysis

The purity of intermediates and final products was confirmed by elemental analysis (C, H, N and S), which was carried out using a Carlo Erba EA 1108 CHN Fisons instrument. The purity of certain intermediates was confirmed by capillary gas chromatography (GC), using a Varian CP-3380 gas chromatograph equipped with a Phenomenex, 15 m x 0.32 mm (internal diameter) x 0.25 μ m (phase thickness), ZB1 column.

Melting Points and Transition Temperatures

The melting points of intermediate materials were measured using either, a Linkam 350 hot-stage and control unit in conjunction with a Nikon E400 polarising microscope or a Mettler FP 52 hot-stage and FP 5 control unit in conjunction with an Olympus BH-2 polarising microscope. Melting point temperatures and enthalpies of transition of intermediates and final products exhibiting liquid crystalline mesophases were measured using a Perkin-Elmer DSC-7 Differential Scanning Calorimeter (DSC) in conjunction with a TAC 7/DX instrument control unit, using the peak measurement for the reported value of the transition temperature. The same instrument was also used to ascertain the melting points of certain intermediate compounds.

Calibration of the DSC was carried out using standard reference materials (indium, melting point onset = 156.60 $^{\circ}$ C, ΔH = 28.45 J/g and lead, melting point onset = 327.47 $^{\circ}$ C). A small amount of sublimed elemental sulfur was added to the aluminium pans of the compounds containing both the non-conjugated diene and methacrylate polymerisable end-groups, in order to prevent thermally induced polymerisation of these compounds during DSC analysis.

Chromatography for Purification and Purity Determination

Reaction progress was frequently monitored by either, thin layer chromatography (TLC), utilising aluminium-backed TLC plates coated with silica gel (60 F₂₅₄ Merck) for this purpose or capillary GC. Visualisation of the TLC plates was accomplished utilising either UV light or a cerium sulphate/ammonium molybdate stain^[1]. Purification of intermediates and final products was predominantly accomplished by column chromatography^[1] using silica gel (35-70 μ , 60 Å or 40-63 μ , 60 Å) obtained from Fluorochem, followed by recrystallisation from a suitable solvent or solvent mixture. Flash column chromatography^[1] was used less often and was carried out using the same types of silica gel.

All charge transport materials, i.e., those final products chosen for evaluation of their physical properties were further purified by passing the materials through a column of mixed anion and cation exchange resin (Dowex Monosphere MR-450 UPW) obtained from Supelco. The materials were then dried under vacuum and stored in aluminium cans. This further purification step was used to further reduce the amounts of ionic impurities present within these materials, which could lead to erroneous charge mobility values. For this final purification stage, all glass wear was thoroughly cleaned, rinsed with distilled water and dried in an oven at 100 °C for approximately 60 minutes.

Starting Materials

The majority of the starting materials and intermediates were obtained from either Alfa Aesar, Avocado, Fluorochem, Sigma-Aldrich, Strem Chem. Inc. or Supelco. Certain other materials were available internally from other research programmes.

Reagents and Reaction Solvents

All reagents and solvents that were purchased were used without further purification unless otherwise stated. Reaction solvents, such as diethyl ether and tetrahydrofuran, were initially stored over sodium wire and then freshly distilled, over sodium wire, under a dry, inert nitrogen atmosphere using benzophenone as the indicator,

immediately prior to use. Tetrahydrofuran was also freshly distilled over calcium hydride immediately prior to use. Dichloromethane was distilled over calcium hydride and stored over anhydrous molecular sieves (4 Å). DMF was dried and stored over anhydrous molecular sieves (4 Å). All other solvents were used as purchased.

N-Bromosuccinimide (NBS) was recrystallised from distilled water prior to use. All reactions were carried out under a dry, inert nitrogen atmosphere unless otherwise stated. All temperatures were measured internally. Some abbreviations that are commonly known and that are used in this work are listed below:

BDT	-	Bis(dithienothiophene)
BHT	-	2,6-Di- <i>tert</i> -butyl-4-methylphenol
<i>n</i> - BuLi	-	<i>n</i> – Butyllithium
Cr	-	Crystal
DCC	-	<i>N</i> , <i>N'</i> -Dicyclohexylcarbodiimide
DCM	-	Dichloromethane
DCU	-	Dicyclohexylurea
DHADT	-	α,ω -Dihexylanthradithiophene
DH-PTP	-	2,5-Bis(4- <i>n</i> -hexylphenyl)thiophene
DMAP	-	4-(<i>N</i> , <i>N'</i> -Dimethylamino)pyridine
DME	-	1,2-Dimethoxyethane
DMF	-	<i>N</i> , <i>N</i> -Dimethylformamide
DO-BDT	-	Dioctyl bis(dithienothiophene)
DSC	-	Differential scanning calorimetry
DTH-BDT	-	Dithiohexyl bis(dithienothiophene)
EI	-	Electron impact
FEM	-	Field effect mobility
FET	-	Field effect transistor
FT-IR	-	Fourier transform-infrared
GC	-	Gas chromatography
GCMS	-	Gas chromatography mass spectrometry
GR	-	Glass resin
HABA	-	2-(4-Hydroxyphenylazo)benzoic acid
HMDS	-	Hexamethyldisilazane

HOBT	-	1-Hydroxybenzotriazole
HOMO	-	Highest occupied molecular orbital
I	-	Isotropic liquid
IC	-	Integrated circuit
IR	-	Infra red
ITO	-	Indium tin oxide
LC	-	Liquid crystal
LCP	-	Liquid crystalline polymer
LDA	-	Lithium diisopropyl amide
Lit.	-	Literature
LMM	-	Low molar mass
LUMO	-	Lowest unoccupied molecular orbital
MO	-	Molecular orbital
MS	-	Mass spectrometry
N	-	Nematic phase
N [*]	-	Chiral nematic phase
NBS	-	<i>N</i> -Bromosuccinimide
NMR	-	Nuclear magnetic resonance
OFET	-	Organic field effect transistor
OLED	-	Organic light emitting diode
OTFT	-	Organic thin film transistor
PEDOT	-	Poly(dioxyethylene thienolene)
PM	-	Polymeric material
PPV	-	Polyphenylenevinylene
PSS	-	Polystyrene sulphonic acid
PTTP	-	5,5'-Bis(4-heptylphenyl)-2,2'-bithiophene
PTV	-	Polythienylenevinylene
RM	-	Reactive mesogen
RT	-	Room temperature
SEM	-	Scanning electron microscopy
Sm	-	Smectic phase
Sm [*]	-	Chiral smectic phase
TBAB	-	Tetrabutylammonium bromide
TFT	-	Thin film transistor

THF	-	Tetrahydrofuran
TLC	-	Thin layer chromatography
TMS	-	Tetramethyl silane
TOF	-	Time of flight
UV	-	Ultra violet

3.2 Experimental Discussion

The synthetic pathways to the reaction intermediates and final products are shown in schemes 1-15. A brief discussion of the synthesis involved in each scheme and some of the problems encountered are given below.

Scheme One

Dibenzothiophene **1** and cyanuric acid **3** were commercially available and were used without any further purification. The sulphone **2**^[2-7] was synthesised in high yield (82.6%) by the oxidation of compound **1** using hydrogen peroxide in glacial acetic acid. The dibromo compound **4**^[8-10] was synthesised in high yield (78.9%) by lithiation of compound **3**, using lithium hydroxide, followed by metal-halogen exchange, using liquid bromine. The 3,7-dibromodibenzothiophene-5,5-dioxide **5**^[4] was synthesised in good yield (67.4%) by the bromination of compound **2** using the brominating agent **4**, in concentrated sulphuric acid. Reduction of compound **5** using lithium aluminium hydride yielded 3,7-dibromodibenzothiophene **6**^[4, 7] in moderate yield (54.0%).

Scheme Two

The ω -bromoalkanoic acids **7** and **8**, 1,4-pentadien-3-ol **10** and the ω -bromoalkanoyl chlorides **11**, **12** and **13** were commercially available and used without further purification. The acid chloride **9** was synthesised in high yield (94.6%) from 7-bromoheptanoic acid **7** by the reaction with oxalyl chloride. The diene-esters **14**, **15**, **16** and **17** were obtained in moderate to high yields (44.8%, 77.0%, 75.2% and 70.7% respectively) from the appropriate acid chlorides by a condensation reaction with the secondary alcohol, 1,4-pentadien-3-ol **10**. The diene-ester **18** was produced in high yield (77.5%) by base-assisted esterification^[11], using DCC and DMAP, reacting the same secondary alcohol **10** with the commercially available 10-bromodecanoic acid **8**. The liquid bromo-diene-esters **14-18** were purified by column chromatography. They were not subsequently distilled due to the possibility of thermally induced polymerisation.

Scheme Three

The starting materials 4-bromophenol **19** and (s)-8-bromo-2,6-dimethyl-oct-2-ene **20** were commercially available and used without further purification. 4-Bromophenol **19** was alkylated with (s)-8-bromo-2,6-dimethyl-oct-2-ene **20** utilising the Williamson ether synthesis^[12-14] to give the ether **21**, which was purified by fractional distillation under reduced pressure, in high yield (94.1%). Lithiation of compound **21** with *n*-butyllithium at -78 °C followed by quenching with trimethyl borate and subsequent acid hydrolysis^[15], gave the phenyl boronic acid **22** in good yield (69.5%). The phenyl boronic acid **22**, was aryl-aryl cross-coupled with the di-bromide **6**, using the commercially available catalyst *tetrakis*(triphenylphosphine)palladium(0), utilising the Suzuki cross-coupling reaction^[16-18], to yield compound **23** in moderate yield (49.8%). The catalyst obtained from Strem Chem. Inc. proved to be more efficient in the cross-coupling reaction when compared to the same catalyst obtained from Sigma-Aldrich. The dealkylation of the ether **23** using boron tribromide^[19] at 0 °C, afforded the symmetric bis-phenol, compound **24**, in high yield (91.4%). The purification of compound **24** was the main synthetic problem of this scheme, as compound **24** was insoluble in most common solvents. Compound **24** was subsequently washed thoroughly with hot DCM to remove any starting material and/or mono-alkylated material. The ¹H NMR spectrum of compound **24** revealed no aliphatic protons, therefore it was used in the next step without any further purification. The ethers **25-29** were synthesised in moderate to good yields (60.9%, 54.2%, 52.0%, 56.4% and 62.7% respectively) by the alkylation of the diphenol **24** with the 1-vinyl-allyl ω-bromoalkanoic acid esters **14-18**, respectively, utilising the Williamson ether synthesis. The moderate yields obtained (54.2%, 52.0% and 56.4 %) for compounds **26-28** respectively, are potentially due to losses of each of the products during purification.

Scheme Four

The starting material 4-bromo-2-fluorophenol **30**, was commercially available and used without further purification. It was alkylated with (s)-8-bromo-2,6-dimethyl-oct-2-ene **20** utilising the Williamson ether synthesis to give the ether **31** in high yield (92.2%). Compound **31** was purified as described for compound **21** in scheme three. The aryl bromide **31** was converted into the corresponding phenyl boronic acid **32** in high yield (71.4%), as described for compound **22** in scheme three. Compound **32** was

aryl-aryl cross-coupled with the di-bromide **6**, utilising the Suzuki coupling reaction, as described for compound **23** in scheme three, to yield compound **33** in moderate yield (49.8%). The symmetric bis-phenol **34**, was synthesised in high yield (83.5%) by the dealkylation of the diether **33** using boron tribromide at 0 °C, as described for compound **24** in scheme three. Purification of the diphenol **34** was the main synthetic problem of this scheme, as compound **34** was insoluble in most common solvents. Treatment of compound **34** was as that described for compound **24** in scheme three. The ethers **35-39** were synthesised in moderate to high yields (59.1%, 69.6%, 63.8%, 56.9% and 75.0% respectively) by the reaction of the diphenol **34** with the 1-vinyl-allyl ω -bromoalkanoic acid esters **14-18** respectively, utilising the Williamson ether synthesis as described for compounds **25-29** in scheme three. The moderate yields obtained (59.1% and 56.9 %) for compounds **35** and **38** respectively, are potentially due to losses of each of the products during purification.

Scheme Five – a and b

Compounds **40** and **41** were commercially available and were used without further purification. Compounds **42** and **43** were synthesised in high yields (70.6% and 76.9% respectively) by the reaction of the ω -bromoalcohols **40** and **41** respectively, with methacryloyl chloride at 0 °C. The ethers **44** and **45** were synthesised in low yields (24.4% and 21.7% respectively) by the reaction of the diphenol **24** with the bromides **42** and **43** respectively, utilising the Williamson ether synthesis. Each of the methacrylates **44** and **45** were stabilised by the addition of BHT (approximately 10.0 wt%). BHT (inhibitor) was employed when alkylating compound **24** with compounds **42** and **43**, in order to prevent the spontaneous, thermal polymerisation of the methacrylate end-group. The non-conjugated diene end-group is not as sensitive as the methacrylate end-group towards thermal polymerisation. The low yields obtained (24.4% and 21.7% respectively) for compounds **44** and **45** are potentially due to losses of each of the products during purification. The ethers **46** and **47** were synthesised in low yields (31.7% and 22.7% respectively) by the reaction of the fluorinated phenol **34** with the bromides **42** and **43** respectively, utilising the Williamson ether synthesis as described for compounds **44** and **45** in scheme five a. BHT was again employed (approximately 10.0 wt%) when alkylating compound **34**, with compounds **42** and **43**, for the reason described above. The low yields obtained

(31.7% and 22.7% respectively) for compounds **46** and **47** are potentially due to losses of each of the products during purification.

Scheme Six – a and b

Compounds **48**, **49** and **50** were commercially available and were used without further purification. The oxetanes **51** and **52** were synthesised, according to the literature methods^[20-21], and subsequently purified by fractional distillation under reduced pressure in low to good yields (31.9% and 62.9% respectively), by reacting (3-methyloxetan-3-yl)methanol **48** with the appropriate α,ω -dibromoalkanes **49** and **50** respectively, in a two-phase system of hexane and aqueous sodium hydroxide in the presence of the phase transfer catalyst, TBAB^[22]. The ethers **53** and **54** were synthesised in moderate yield (59.0% and 55.0% respectively) by reacting compound **24** with the bromides **51** and **52** respectively, utilising the Williamson ether synthesis. The moderate yields obtained for compounds **53** and **54** are potentially due to losses of each of the products during purification. Compounds **55** and **56** were synthesised in moderate to good yields (51.4% and 60.5% respectively) by the reaction of the diphenol **34** with the bromides **51** and **52** respectively, utilising the Williamson ether synthesis as described for compounds **53** and **54** in scheme six a. The moderate yield obtained for the ether **55** is potentially due to losses of the product during purification.

Scheme Seven

The synthesis and purification of the arylbromide **21** is described in scheme three. Compounds **57** and **58** were commercially available and were used without further purification. Lithiation of (s)-1-bromo-4-(3,7-dimethyl-oct-6-enyloxy)benzene **21** with *n*-butyllithium at -78 °C followed by quenching with 2-isopropoxy-4,4,5,5-tetramethyl-1,3,2-dioxaborolane **57**, gave the boronate ester **59** in good yield (61.1%), the purification of which was achieved by column chromatography. The boronate ester **59** was cross-coupled with 2,5-dibromothiophene **58** utilising the Suzuki coupling reaction to yield the 2,5-diphenylthiophene **60** in good yield (68.2%). The attempted Suzuki coupling of compounds **58** and **59**, utilising 2 *M* sodium carbonate solution as the base and 1,2-dimethoxyethane as the solvent generated low yields of the required product **60**. Consequently, when coupling phenyl boronic esters and dibrominated thiophene moieties, the base and solvent employed were tripotassium phosphate and DMF respectively. The bis-phenol **61**, was synthesised in high yield

(91.2%) by dealkylation of the diether **60** using boron tribromide at 0 °C. Purification of the diphenol **61** was the main synthetic problem of this scheme, as it was insoluble in most common organic solvents. Treatment of compound **61** was as that described for compound **24** in scheme three. The diether **62** was synthesised in low yield (26.3%) by reaction of the diphenol **61** with the 1-vinyl-allyl ω -bromoalkanoic acid ester **17**, utilising the Williamson ether synthesis. The low yield obtained (26.3%) for compound **62** is potentially due to losses of the product during purification.

Scheme Eight

[2,2']-Bithiophene **63** was commercially available and was used without further purification. Bromination of compound **63**, in glacial acetic acid and chloroform, with two equivalent quantities of *N*-bromosuccinimide (NBS)^[23] (purified by recrystallisation from distilled water) gave 5,5'-dibromo-[2,2']-bithiophene **64** in high yield (90.6%) according to the literature method^[24]. NBS was the preferred brominating agent, rather than molecular bromine in this reaction, in an effort to selectively dibrominate the thiophene rings of compound **63**, and with monitoring of the reaction (TLC analysis), avoid further bromination of the thiophene moieties. Compound **65** was synthesised, in good yield (67.2%), by the Suzuki cross-coupling reaction between the boronate ester **59** and 5,5'-dibromo-[2,2']-bithiophene **64**. The branched alkyl chains were used to improve the solubility and consequently further facilitate the purification of the di-ether **65**. The dealkylation of compound **65** using boron tribromide at 0 °C, afforded the symmetric bis-phenol **66**, in high yield (97.1%). Purification by standard techniques was not possible due to the insolubility of the diphenol **66** and consequently the treatment of compound **66** was as that described for compound **24** in scheme three. The polymerisable products **67-70** were synthesised by the reaction of the bis-phenol **66**, with the bromo-diene-esters **17** and **18**, the methacrylate **42** and the oxetane **52** respectively, utilising the Williamson ether synthesis. Good to low yields of the ethers **67**, **68**, **69** and **70** were obtained (25.8%, 49.2%, 62.1% and 35.5% respectively). During the synthesis of the methacrylate **69** the product was stabilised by the addition of BHT (approximately 10.0 wt%). The low yields obtained (25.8% and 35.5%) for compounds **67** and **70** are potentially due to losses of the products during purification.

Scheme Nine

The synthesis of the fluorinated boronate ester **71**, from the ether **31** and 2-isopropoxy-4,4,5,5-tetramethyl-1,3,2-dioxaborolane **57**, was achieved in moderate yield (49.6%) and was carried out as that described for compound **59**, scheme seven. The diether **72** was synthesised, in good yield (60.1%), in the same way as that described for compound **65**, scheme eight. The branched alkyl chains attached to the phenyl rings were used to improve the solubility and therefore facilitate the purification of the diether **72**. The fluorine moieties, attached to the phenyl rings, were used to lower the melting points of the diether **72** and polymerisable products **74-77**. Ether cleavage of compound **72**, using boron tribromide at 0 °C, afforded the bis-phenol **73**, in high yield (87.2%). Purification by standard techniques was not possible due to the insolubility of the diphenol **73** and consequently the treatment of compound **73** was as that described for compound **24** in scheme three.

The polymerisable products **74-77**, were synthesised by the reaction of the bis-phenol **73**, with the 1-vinyl-allyl ω -bromoalkanoic acid esters **17** and **18**, the methacrylate **42** and the oxetane **52** respectively, utilising the Williamson ether synthesis. Moderate yields of the ethers **74**, **75**, **76** and **77** were obtained (40.4%, 55.9%, 57.7% and 44.8% respectively). During the synthesis of the methacrylate **76**, the product was stabilised by the addition of BHT (approximately 10.0 wt%).

Scheme Ten

3-Bromothiophene **78** and mercaptoacetic acid ethyl ester **80** were commercially available and were used without further purification. Compounds **79** and **81-84** were synthesised according to the literature methods^[25-26]. 3-Bromothiophene-2-carbaldehyde **79**^[25] was synthesised in high yield (79.0%) by lithiating compound **78** using LDA at 0 °C followed by quenching with *N*-formylpiperidine. Thieno[3,2-b]thiophene-2-carboxylic acid ester **81**^[25] was synthesised in high yield (79.7%) by the reaction of compounds **79** and **80** in the presence of potassium carbonate. The carboxylic acid **82**^[25] was synthesised in high yield (98.5%) by dealkylation and subsequent acidification of compound **81**, using 1 *M* lithium hydroxide solution and aqueous (20%) hydrochloric acid respectively. Decarboxylation of compound **82** using copper powder and quinoline yielded thieno[3,2-b]thiophene **83**^[25] in high yield (92.7%). Bromination of compound **83**, in glacial acetic acid and chloroform, with two equivalent quantities of NBS (purified by recrystallisation from distilled water)

gave 2,5-dibromothiopheno[3,2-b]thiophene **84**^[26] in good yield (63.8%). NBS was preferred as the brominating agent rather than molecular bromine in this reaction, for similar reasons as discussed for compound **64** in scheme eight.

Scheme Eleven

The diether **85** was synthesised, in moderate yield (48.4%), by the Suzuki cross-coupling reaction between the boronate ester **59** and 2,5-dibromothiopheno[3,2-b]thiophene **84**. The branched alkyl chains were used to improve the solubility and consequently further facilitate the purification of the diether **85**. Ether cleavage of the diether **85** using boron tribromide at 0 °C, afforded the symmetric bis-phenol **86**, in high yield (89.1%). Purification by standard techniques was not possible due to the insolubility of the diphenol **86** and consequently the treatment of compound **86** was as that described for compound **24** in scheme three.

The polymerisable products **87-90**, were synthesised by the reaction of the bis-phenol **86**, with the 1-vinyl-allyl ω -bromoalkanoic acid ester **18**, the methacrylates **42** and **43** and the oxetane **52** respectively, utilising the Williamson ether synthesis. Low yields of the ethers **87**, **88**, **89** and **90** were obtained (34.2%, 33.3%, 9.5% and 18.9% respectively). During the synthesis of the methacrylates **88** and **89** the products were stabilised by the addition of BHT (approximately 10.0 wt%). The low yields obtained (34.2%, 33.3%, 9.5% and 18.9%) for the ethers **87** to **90** respectively are potentially due to losses of the products during purification.

Scheme Twelve

The fluorinated diether **91** was synthesised from the fluorinated boronate ester **71** and 2,5-dibromothiopheno[3,2-b]thiophene **84** in moderate yield (45.2%) and was carried out as that described for compound **85**, scheme eleven. The branched alkyl chains attached to the phenyl rings were used to improve the solubility and therefore facilitate the purification of the diether **91**. The fluorine moieties, attached to the phenyl rings, were used to lower the melting points of the diether **91** and polymerisable products **93-96**. Ether cleavage of the diether **91**, using boron tribromide at 0 °C, afforded the bis-phenol **92**, in high yield (76.9%). Purification by standard techniques was not possible due to the insolubility of the diphenol **92** and consequently the treatment of compound **92** was as that described for compound **24** in scheme three.

The polymerisable products **93-96**, were synthesised by the reaction of the bis-phenol **92**, with the 1-vinyl-allyl ω -bromoalkanoic acid ester **18**, the methacrylates **42** and **43** and the oxetane **52** respectively, utilising the Williamson ether synthesis. Good to low yields of the ethers **93**, **94**, **95** and **96** were obtained (61.1%, 51.9%, 31.0% and 15.7% respectively). During the synthesis of the methacrylates **94** and **95**, the products were stabilised by the addition of BHT (approximately 10.0 wt%). The low yields obtained (31.0% and 15.7%) for the ethers **95** and **96** respectively are potentially due to losses of the products during purification.

Scheme Thirteen

(s)-Tributyl-[5-(3,7-dimethyl-oct-6-enyl)thiophen-2-yl]stannane **97**, was obtained from a previous research programme and used without further purification. (s)-3,7-Bis-[5-(3,7-dimethyl-oct-6-enyl)thiophen-2-yl]dibenzothiophene **98**, was synthesised, by a Stille coupling^[27] reaction between 3,7-dibromodibenzothiophene **6** and compound **97**, in good yield (63.6%).

Scheme Fourteen

The dibromofluorene **99**, benzo-[1,2,5]-thiadiazole **103** and 2-hydroxypyrimidine hydrochloride **105** were commercially available and used without further purification. The phenol **100** was synthesised in high yield (82.8%) from compound **99** by conversion to the boronic acid followed by oxidation using hydrogen peroxide. In order to avoid any potential radical reaction, the reaction mixture containing the hydrogen peroxide was washed thoroughly with a solution of saturated sodium metabisulphite. The ether **101** was prepared from the phenol **100** in high yield (93.0%) by reaction with 1-bromooctane utilising the Williamson ether synthesis. The boronic ester **102** was synthesised in moderate yield (48.6%) from the ether **101** using *n*-butyllithium in diethyl ether, at 0 °C, followed by quenching the resulting lithium salt with 2-isopropoxy-4,4,5,5-tetramethyl-[1,3,2]-dioxaborolane **57**. The reaction mixture was allowed to warm to RT and stirred at room temperature for a period of time in an attempt to allow complete conversion to the corresponding lithium salt, prior to quenching with compound **57** at -78 °C. 4,7-Dibromobenzo-[1,2,5]-thiadiazole **104** was synthesised in high yield (94.0%) by the bromination of compound **103** according to the literature method^[28]. 5-Bromo-2-chloropyrimidine **106** was synthesised in low yield (27.0%) from compound **105** according to the

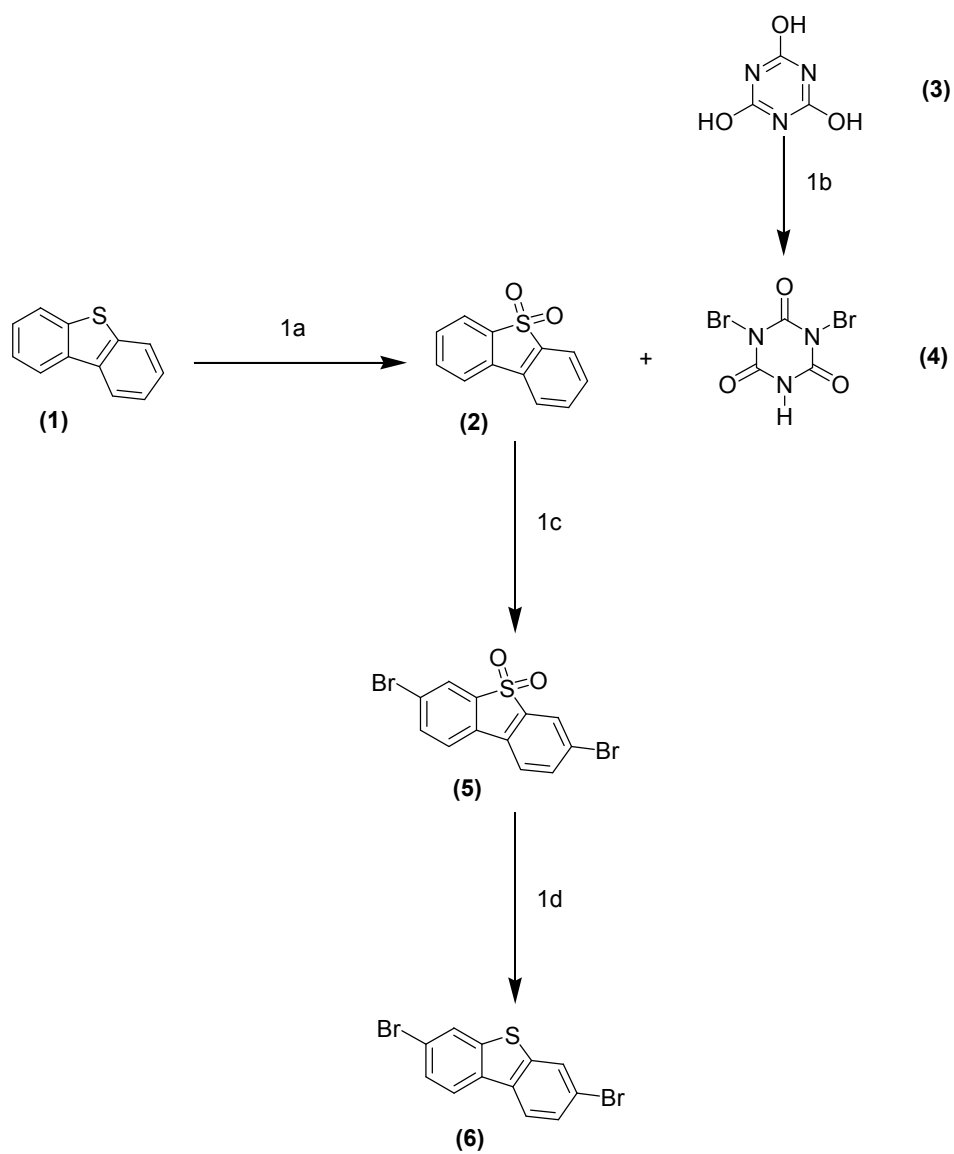
literature method^[29]. The diethers **107** and **108** were synthesised, in low yields (38.2% and 36.7% respectively), by the Suzuki cross-coupling reaction between the boronate ester **102** and compounds **104** and **106** respectively.

Scheme Fifteen

The starting materials 4-bromophenol **19** and 1-bromooctane **109** were commercially available and used without further purification. 4-Bromophenol **19** was alkylated with 1-bromooctane **109** utilising the Williamson ether synthesis to give the ether **110**, which was purified by fractional distillation under reduced pressure, in high yield (97.1%). A Stille coupling of the aryl-bromide **110** with the commercially available, tributylthiophene-2-ylstannane **111** produced 2-(4-octyloxyphenyl)thiophene **112** in moderate yield (53.2%). Compound **114** was synthesised in good yield (68.7%) by reaction of compound **112** with *n*-butyllithium in THF at -78 °C followed by the addition of tri-*n*-butyltin chloride^[30] **113**. The tin compound **114** was found to be sensitive to acidic conditions, undergoing destannylation in which the product converted back to the starting material **112**. Therefore compound **114** was not purified and fortunately, the crude material proved to be sufficiently pure for the next step. A Stille coupling of the tin compound **114** with the dibromofluorene **99** afforded the diether **115** in moderate yield (57.7%). Branched chains were not necessary for compound **115** because its solubility was high due to the lateral octyl chains at the 9-positions on the fluorene.

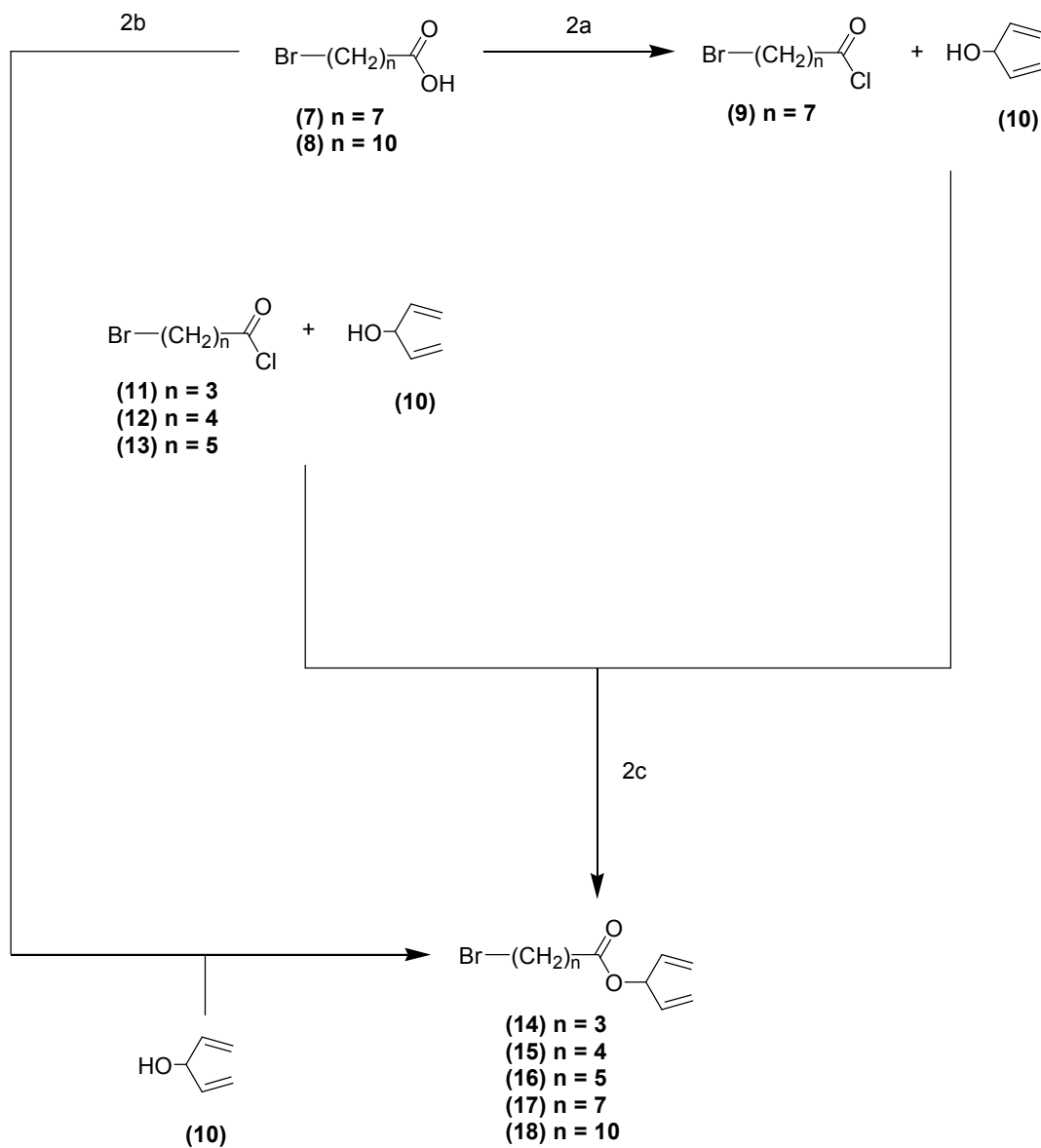
3.3 Reaction Schemes

Reaction Scheme 1



- 1a... Hydrogen peroxide, glacial acetic acid (reflux).
1b... (i) Lithium hydroxide, H_2O ; (ii) Br_2 .
1c... Concentrated H_2SO_4 .
1d... Lithium aluminium hydride, diethyl ether (reflux).

Reaction Scheme 2

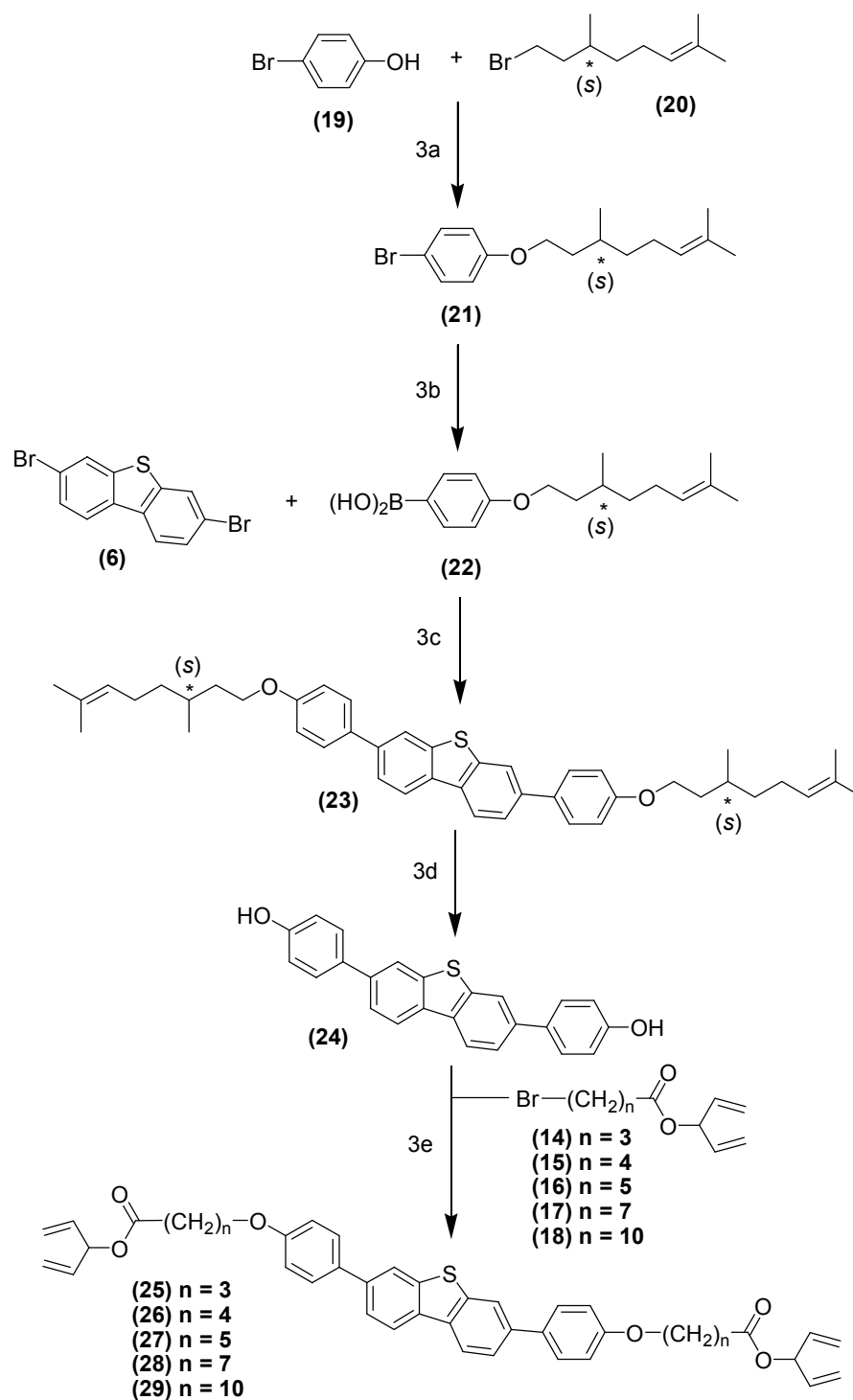


2a... $(\text{COCl})_2$, DMF, CHCl_3 .

2b... DMAP, DCC, DCM (0 °C).

2c... Triethylamine, DCM (0 °C).

Reaction Scheme 3



3a... K_2CO_3 , butanone (reflux).

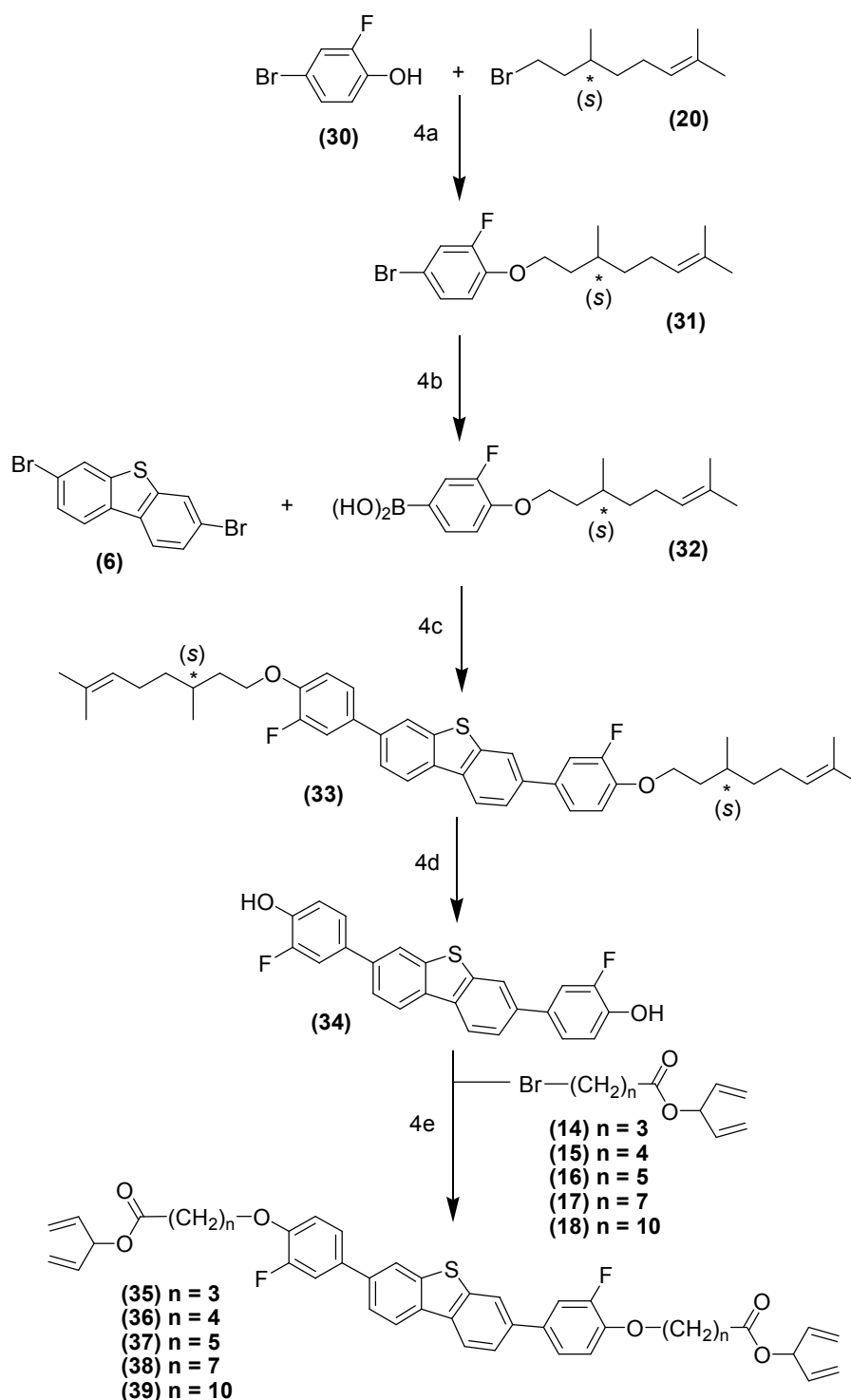
3b... (i) $n\text{-BuLi}$, $\text{B}(\text{OCH}_3)_3$, THF ($-78\text{ }^\circ\text{C}$); (ii) HCl (aq) (20%).

3c... $\text{Pd}(\text{PPh}_3)_4$, 2 M Na_2CO_3 (aq), 1,2-dimethoxyethane (reflux).

3d... (i) BBr_3 , DCM ($0\text{ }^\circ\text{C}$); (ii) H_2O (ice).

3e... K_2CO_3 , DMF ($90\text{ }^\circ\text{C}$).

Reaction Scheme 4



4a... K_2CO_3 , butanone (reflux).

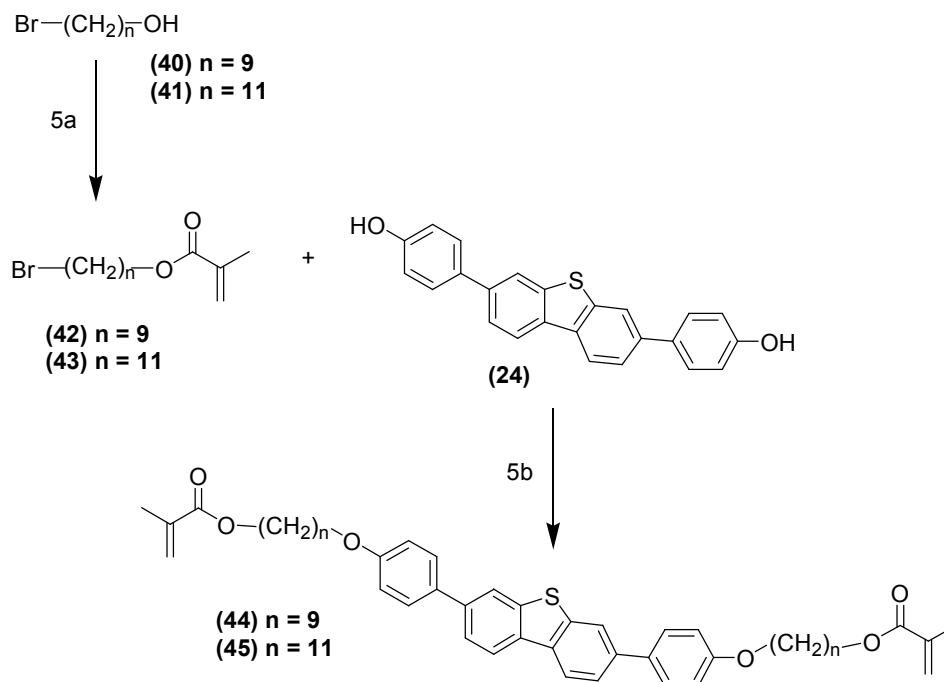
4b... (i) n -BuLi, $B(OCH_3)_3$, THF ($-78\text{ }^\circ\text{C}$); (ii) HCl (aq) (20%).

4c... $Pd(PPh_3)_4$, 2 M Na_2CO_3 (aq), 1,2-dimethoxyethane (reflux).

4d... (i) BBr_3 , DCM ($0\text{ }^\circ\text{C}$); (ii) H_2O (ice).

4e... K_2CO_3 , DMF ($90\text{ }^\circ\text{C}$).

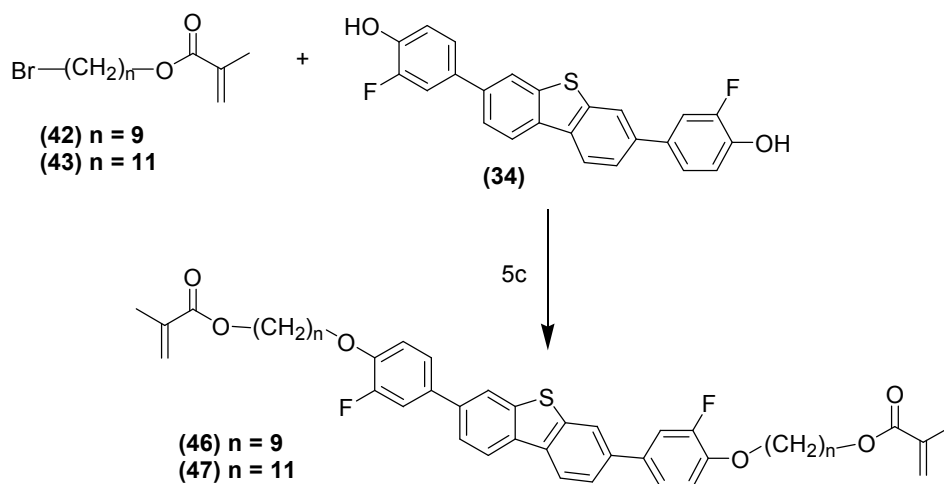
Reaction Scheme 5a



5a... Methacryloyl chloride, triethylamine, DCM (0 °C).

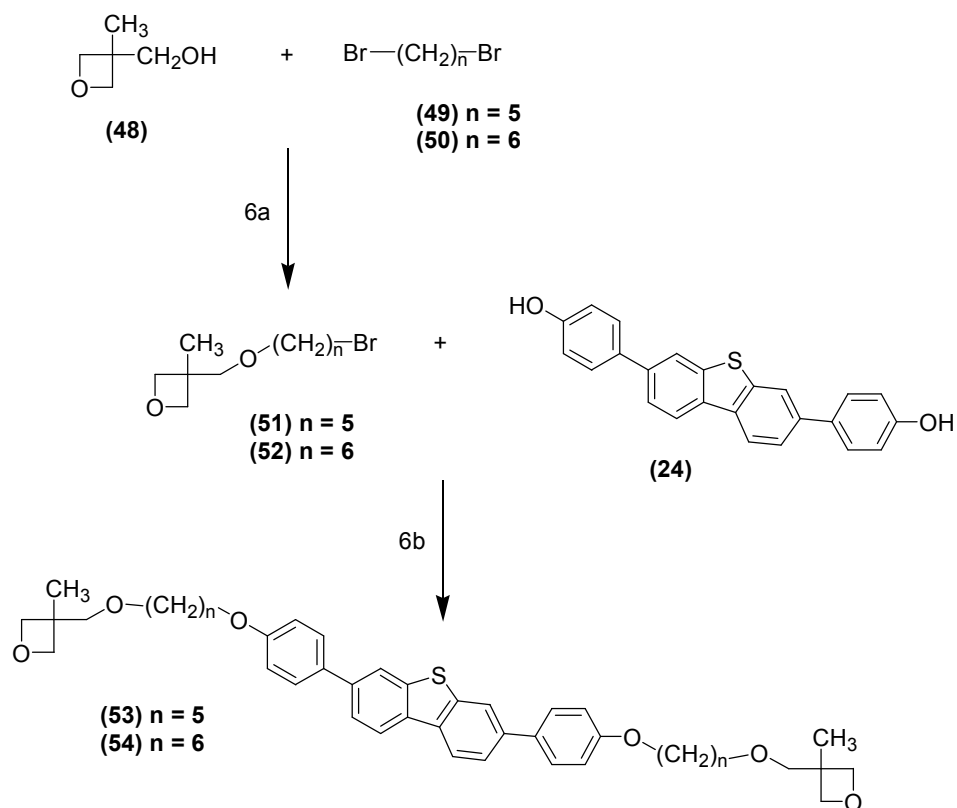
5b... K_2CO_3 , BHT, DMF (60 °C).

Reaction Scheme 5b



5c... K_2CO_3 , BHT, DMF (60 °C).

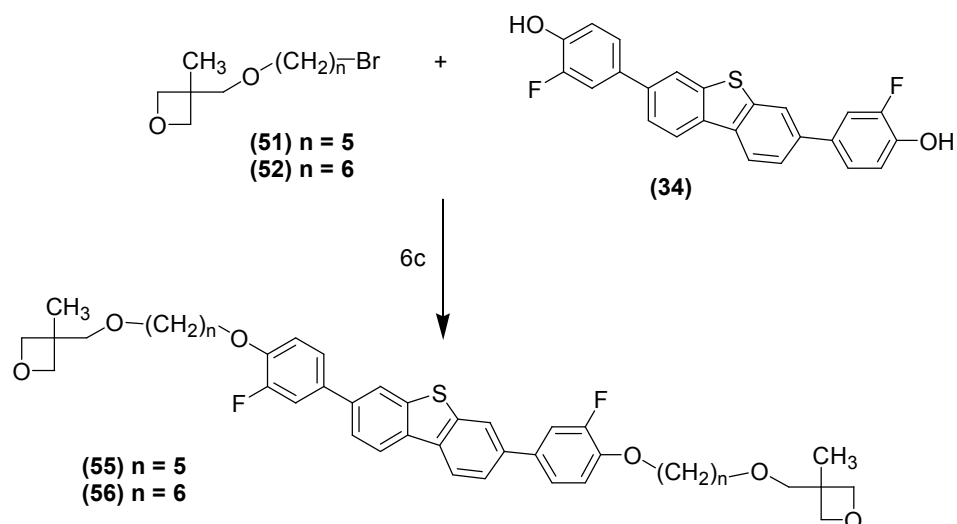
Reaction Scheme 6a



6a... 50% NaOH (aq), TBAB, hexane, H₂O (reflux).

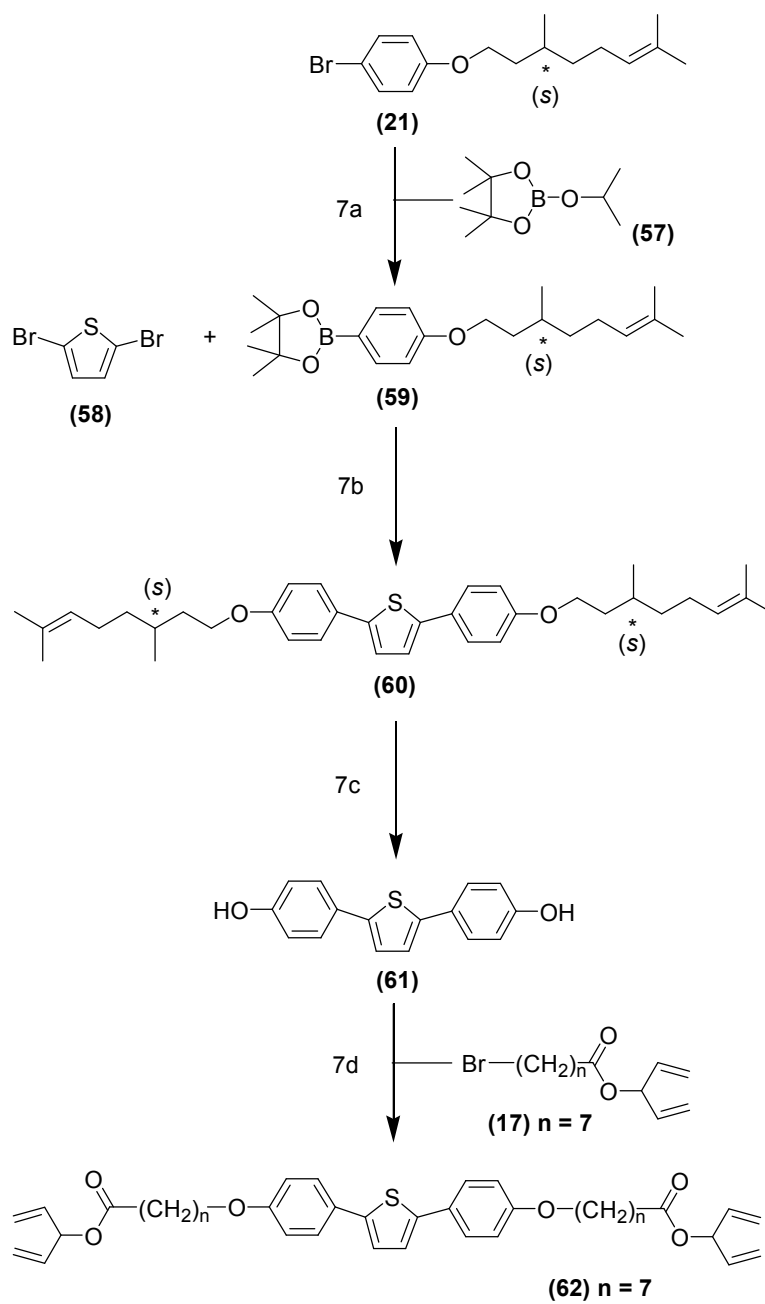
6b... K₂CO₃, DMF (90 °C).

Reaction Scheme 6b



6c... K₂CO₃, DMF (90 °C).

Reaction Scheme 7



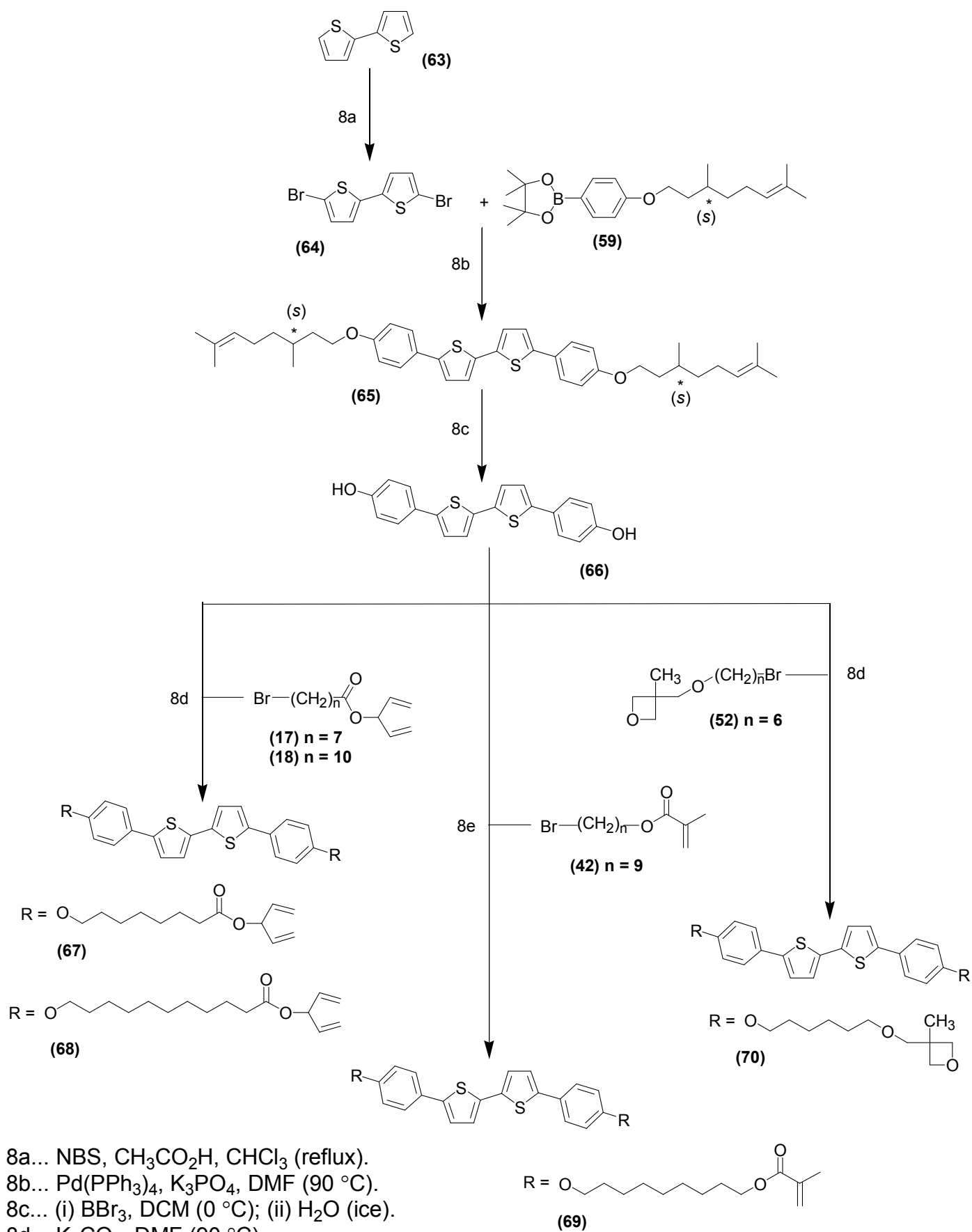
7a... *n*-BuLi, THF (-78 °C).

7b... $\text{Pd}(\text{PPh}_3)_4$, K_3PO_4 , DMF (90 °C).

7c... (i) BBr_3 , DCM (0 °C); (ii) H_2O (ice).

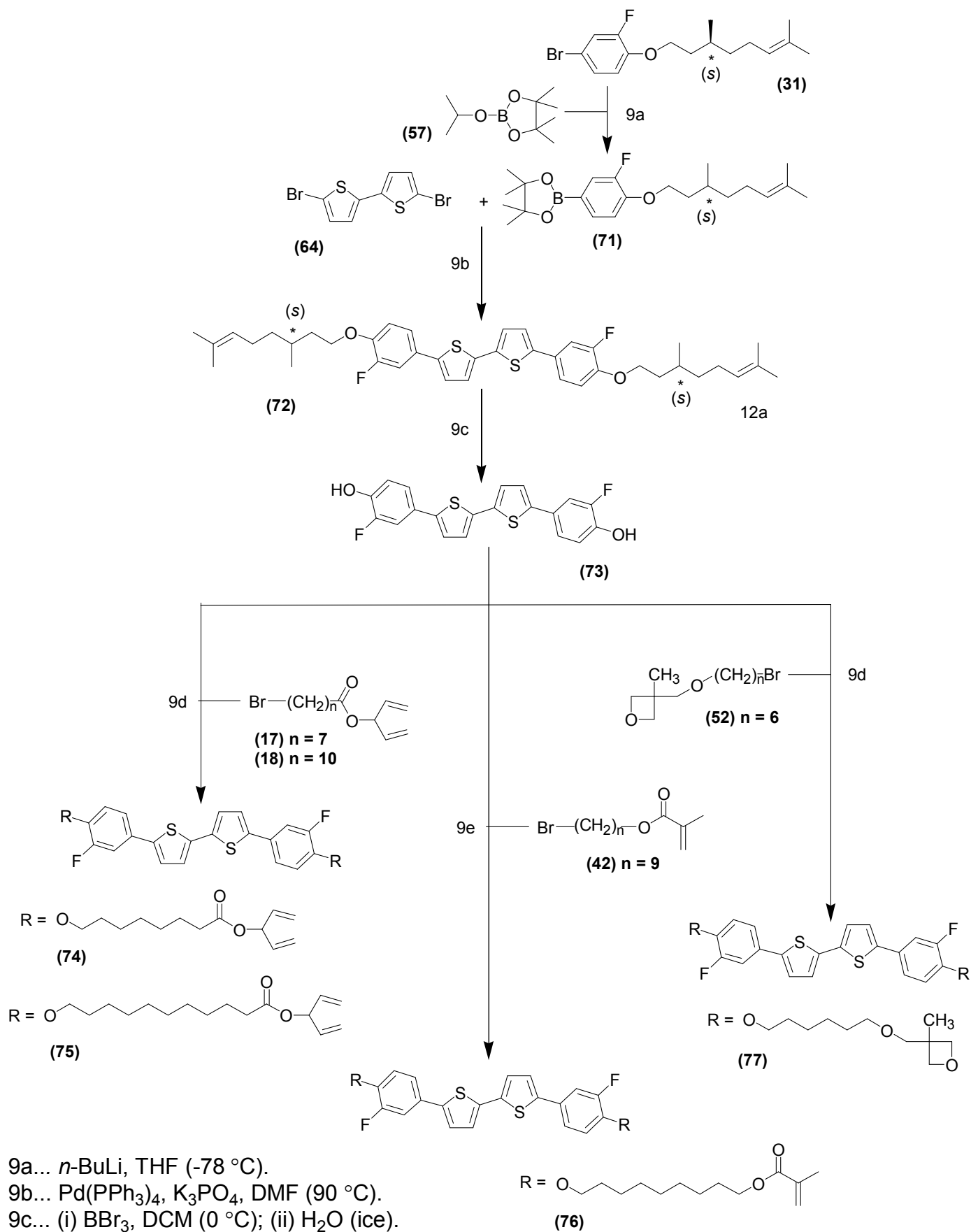
7d... K_2CO_3 , DMF (90 °C).

Reaction Scheme 8

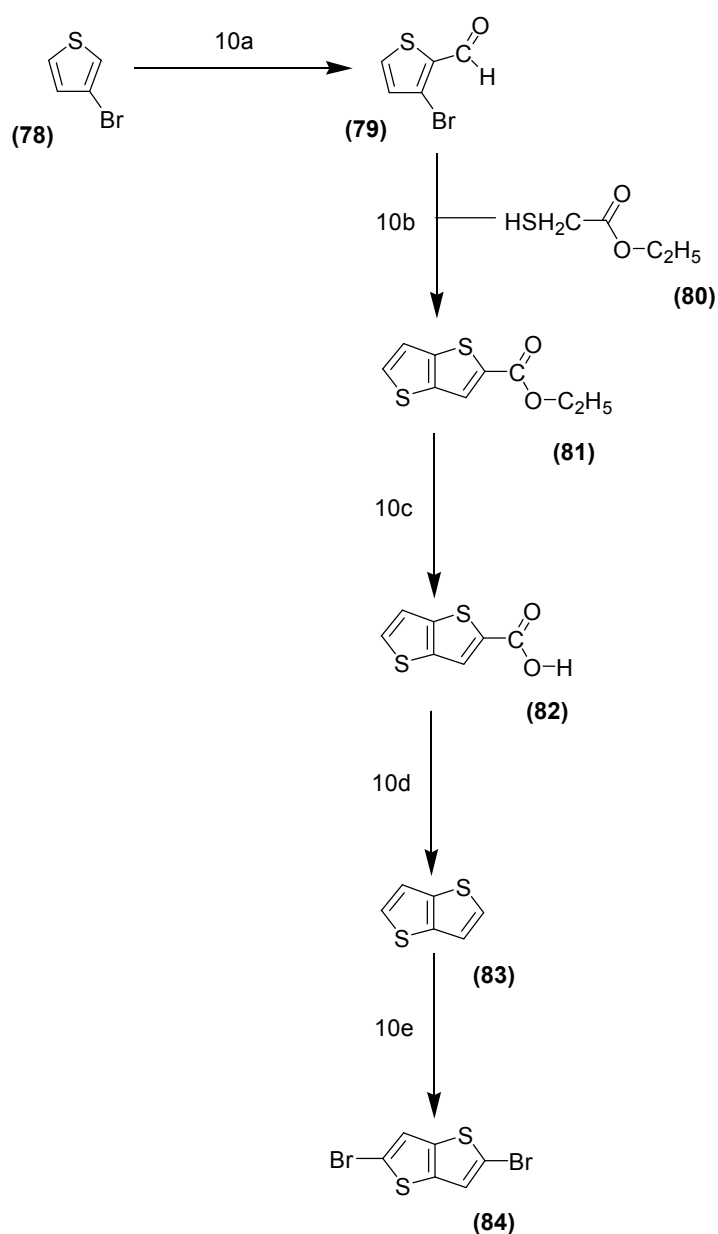


8a... NBS, CH₃CO₂H, CHCl₃ (reflux).
 8b... Pd(PPh₃)₄, K₃PO₄, DMF (90 °C).
 8c... (i) BBr₃, DCM (0 °C); (ii) H₂O (ice).
 8d... K₂CO₃, DMF (90 °C).
 8e... K₂CO₃, BHT, DMF (55 °C).

Reaction Scheme 9



Reaction Scheme 10



10a... (i) LDA, THF (0 °C); (ii) *N*-formylpiperidine.

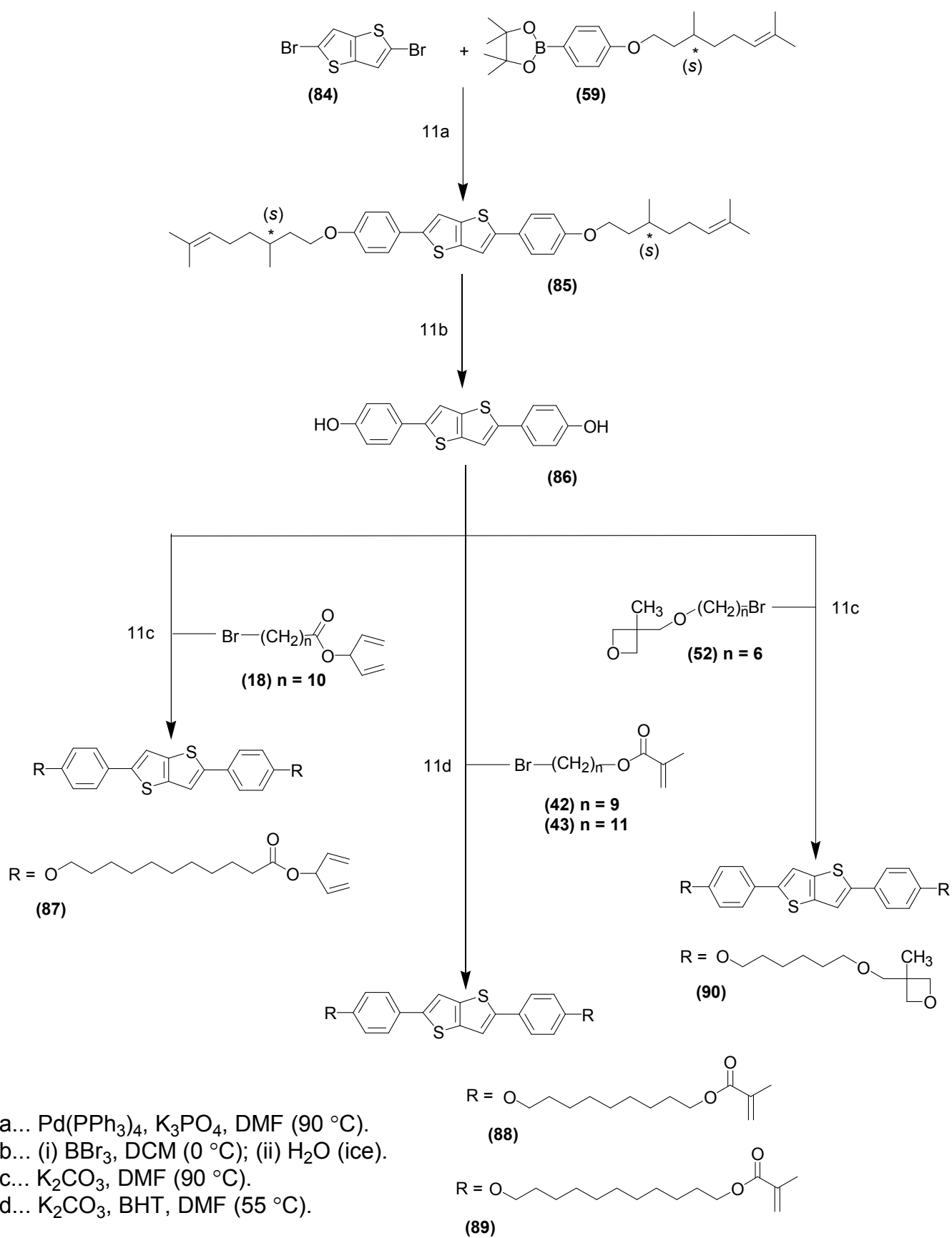
10b... K₂CO₃, DMF (RT).

10c... (i) 1 *M* Lithium hydroxide, THF (reflux); (ii) HCl (aq) (20 %).

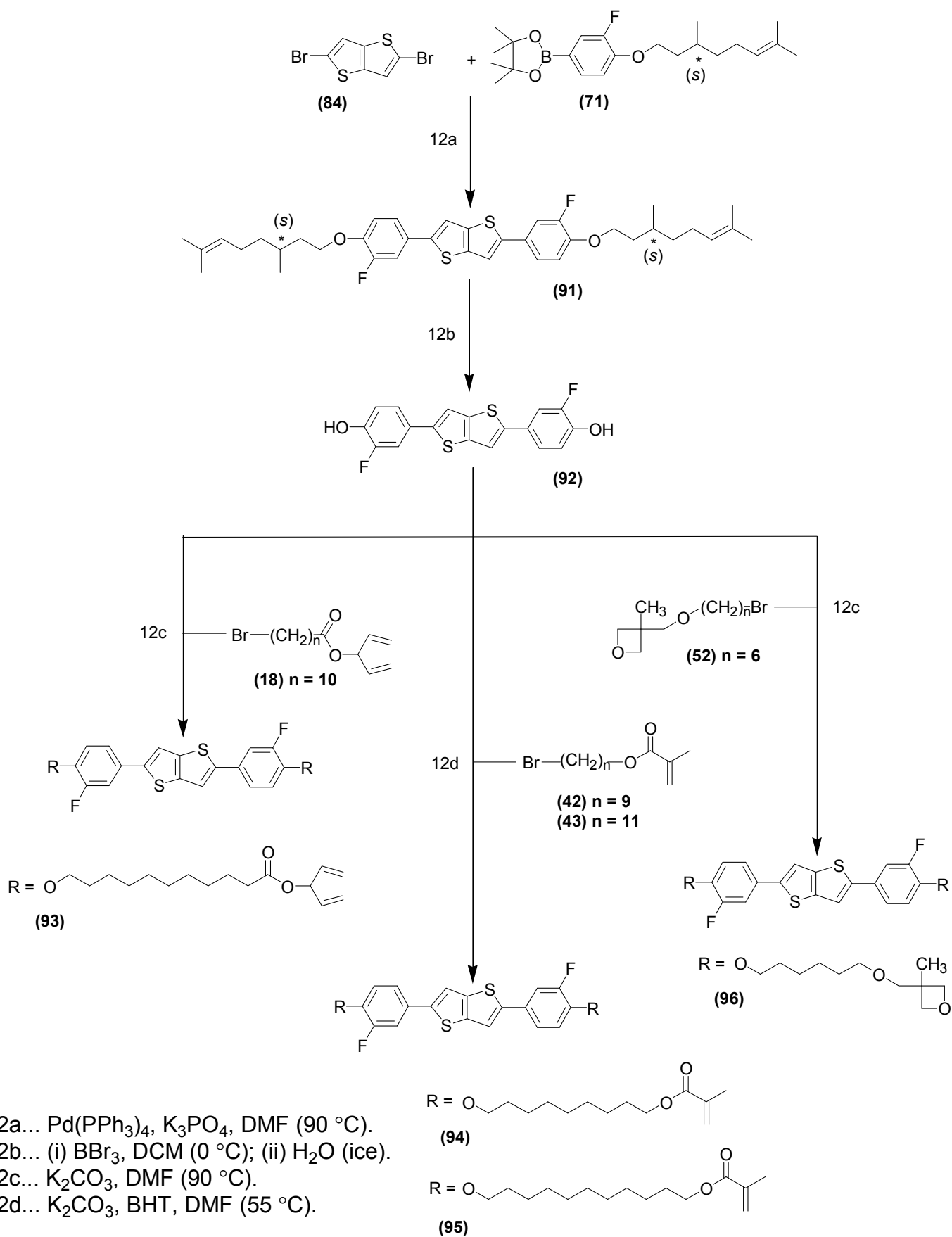
10d... Copper powder, quinoline (240 °C).

10e... NBS, CH₃CO₂H, CHCl₃ (RT).

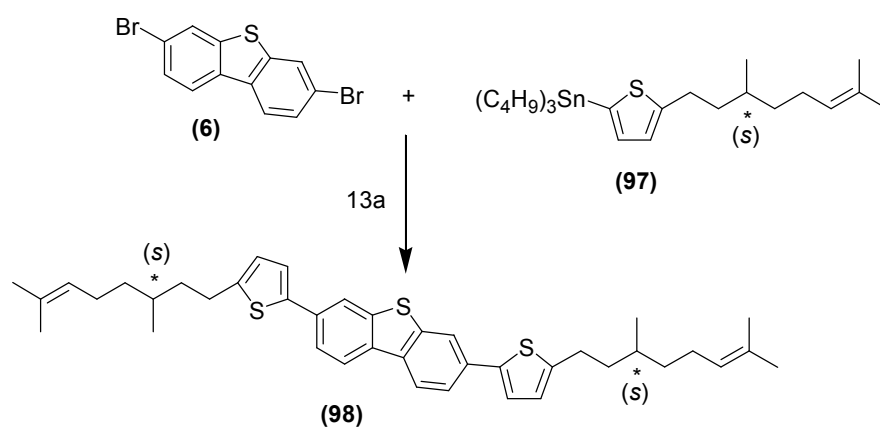
Reaction Scheme 11



Reaction Scheme 12

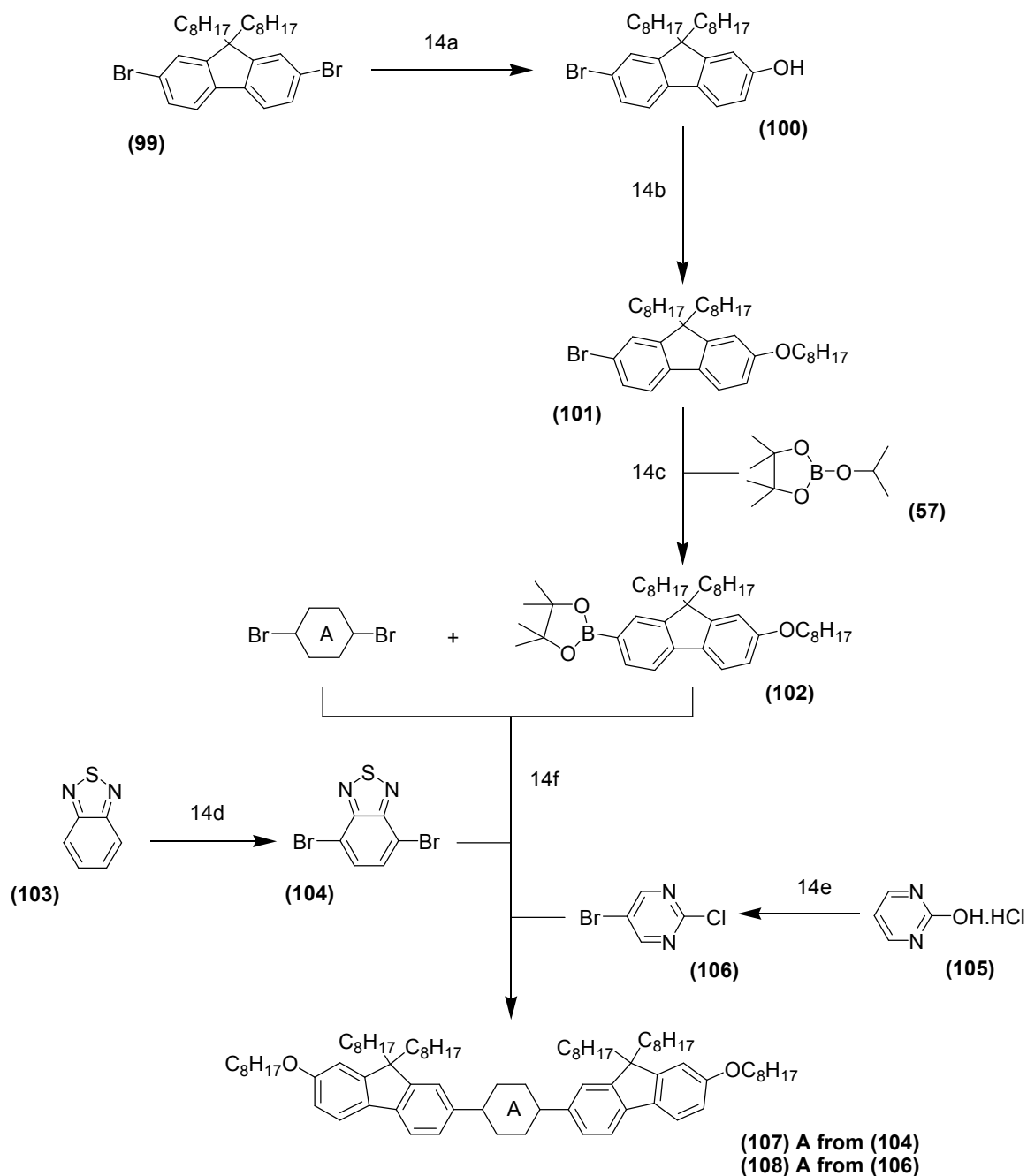


Reaction Scheme 13



13a... $\text{Pd}(\text{PPh}_3)_4$, DMF (90 °C).

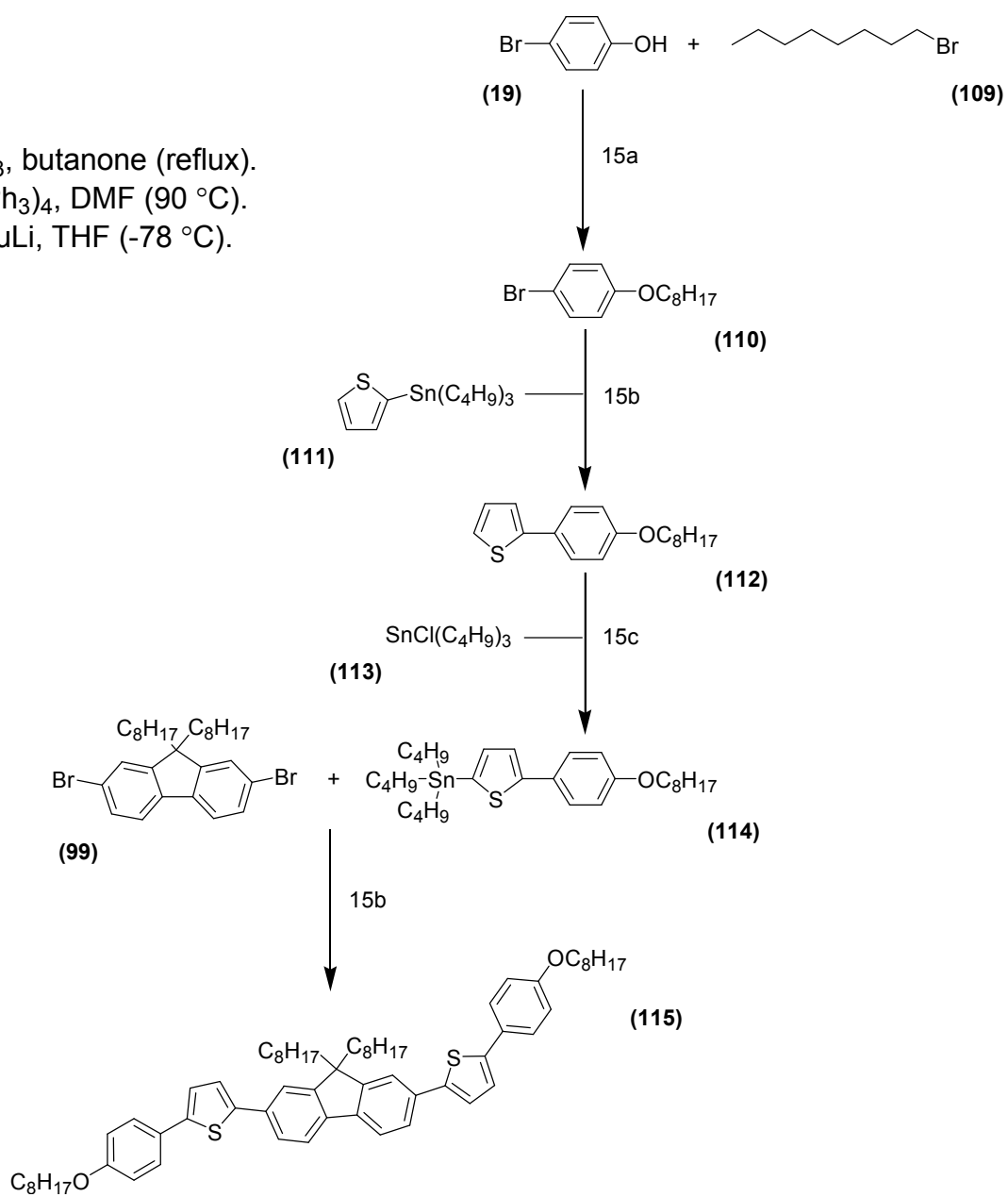
Reaction Scheme 14



- 14a... (i) *n*-BuLi, THF (-78 °C); (ii) B(OCH₃)₃; (iii) HCl (aq) (20 %); (iv) H₂O₂, diethyl ether (reflux).
 14b... C₈H₁₇Br, K₂CO₃, butanone (reflux).
 14c... *n*-BuLi, diethyl ether (RT).
 14d... HBr (aq) (48%), Br₂ (reflux).
 14e... (i) Br₂, H₂O; (ii) POCl₃, (CH₃)NC₆H₅ (reflux).
 14f... Pd(PPh₃)₄, K₃PO₄, DMF (90 °C).

Reaction Scheme 15

15a... K_2CO_3 , butanone (reflux).
 15b... $\text{Pd}(\text{PPh}_3)_4$, DMF ($90\text{ }^\circ\text{C}$).
 15c... (i) $n\text{-BuLi}$, THF ($-78\text{ }^\circ\text{C}$).



3.4 Material Synthesis

Dibenzothiophene-5,5-dioxide (**2**)

Dibenzothiophene (**1**) (25.04 g, 0.14 mol), glacial acetic acid (600 cm³) and hydrogen peroxide (35 w/w% solution in water) (130 cm³, 1.47 mol) were heated under reflux for 5 hours. The reaction mixture was then allowed to cool to RT and the precipitate filtered off. The crude solid was recrystallised from ethanol to yield 24.27 g (82.6%) of the desired product (white needles).

Melting point /°C: 239-241 (Lit. 232-233)^[2].

¹H NMR (CDCl₃) δ_H: 7.52 (2H, t), 7.63 (2H, t), 7.78 (2H, d, *J*=7.6 Hz), 7.82 (2H, d, *J*=7.6 Hz).

IR ν_{max} /cm⁻¹: 3084, 1578, 1508, 1480, 1452, 1289, 1167, 876, 758.

MS (m/z) (EI): 216 (M⁺) (M100), 187, 168, 160, 144, 128, 115, 85, 76, 63, 51.

Elemental analysis: Expected /% C 66.65, H 3.73, S 14.83.

Found /% C 66.66, H 3.65, S 15.13.

1,3-Dibromo-[1,3,5]triazine-2,4,6-trione (**4**)

Bromine (15 cm³, 46.79 g, 0.29 mol) was added to a stirred solution of cyanuric acid (**3**) (12.99 g, 0.10 mol) and lithium hydroxide (4.84 g, 0.20 mol) in distilled water. The reaction mixture was stirred vigorously for 2 hours and then placed into a refrigerator overnight. The resulting precipitate was filtered off and washed with distilled water until all excess of bromine had been removed. The crude solid was dried in a vacuum dessicator to yield 22.77 g (78.9%) of the desired product (pale orange solid).

Not analysed.

3,7-Dibromodibenzothiophene-5,5-dioxide (**5**)

1,3-Dibromo-[1,3,5]triazine-2,4,6-trione (**4**) (16.55 g, 0.06 mol) was added, as a powder, in one portion, to a stirred solution of dibenzothiophene-5,5-dioxide (**2**) (10.70 g, 0.05 mol) in concentrated (98%) sulphuric acid (420 cm³). The resultant reaction mixture was stirred vigorously at RT overnight. The milky white suspension was then poured onto ice (300 g) and allowed to stand until cool. The resulting solids were then filtered and washed successively with distilled water (200 cm³), potassium hydroxide solution (5%) (200 cm³) and distilled water (2 × 150 cm³). The crude solid

was recrystallised from chlorobenzene to yield 12.48 g (67.4%) of the desired product (off-white solid).

Melting point /°C: 316-322 (Lit. 288-290)^[4].

¹H NMR (CDCl₃) δ_H: 7.64 (2H, d, *J*=8.2 Hz), 7.77 (2H, d, *J*=8.2 Hz), 7.94 (2H, s).

IR ν_{max} /cm⁻¹: 3081, 1598, 1474, 1456, 1302, 1167, 880, 827, 575.

MS (m/z) (EI): 374 (M⁺) (M100), 296, 294, 267, 265, 216, 214, 186, 158, 150, 138, 109, 98, 75, 62.

Elemental analysis: Expected /% C 38.53, H 1.62, S 8.57.

Found /% C 38.83, H 1.70, S 8.84.

3,7-Dibromodibenzothiophene (6)

Lithium aluminium hydride (2.53g, 0.07 mol) was added, portion wise, to a stirred suspension of 3,7-dibromodibenzothiophene-5,5-dioxide (5) (12.44 g, 0.03 mol) in diethyl ether (160 cm³) at RT, so as to maintain a gentle reflux. Once the addition was complete, the reaction mixture was heated under reflux for a further hour. After cooling, the excess lithium aluminium hydride was carefully destroyed by the dropwise addition of distilled water (80 cm³). Concentrated (37%) hydrochloric acid was then added (25 cm³) to dissolve the thick precipitate that had formed. The diethyl ether was allowed to evaporate and the resulting mixture was filtered and washed with distilled water (2 × 100 cm³). The crude solid was recrystallised from chloroform to yield 6.15 g (54.0%) of the desired product (white needles).

Melting point /°C: 176-179 (Lit. 169-170)^[4].

¹H NMR (CDCl₃) δ_H: 7.57 (2H, d, *J*=8.4 Hz), 7.96 (2H, d, *J*=8.7 Hz), 7.98 (2H, s).

IR ν_{max} /cm⁻¹: 1572, 1474, 1446, 860, 796, 531.

MS (m/z) (EI): 342 (M⁺) (M100), 279, 264, 262, 219, 217, 200, 182, 138, 93, 69.

Elemental analysis: Expected /% C 42.14, H 1.77, S 9.37.

Found /% C 42.36, H 1.71, S 9.61.

8-Bromooctanoyl chloride (9)

Oxalyl chloride (19.10 g, 0.15 mol) in chloroform (30 cm³) was added dropwise to a stirred solution of 8-bromooctanoic acid (7) (16.79 g, 0.08 mol) and DMF (a few drops) in chloroform (100 cm³) at RT. The solution was stirred overnight, under

anhydrous conditions. The solution was concentrated and filtered to remove solid impurities, to yield 17.20 g (94.6%) of the desired product (yellow/orange oil).

Not analysed.

4-Bromobutanoic acid 1-vinyl-allyl ester (**14**)

A solution of 4-bromobutanoyl chloride (**11**) (24.13 g, 0.13 mol), in DCM (60 cm³), was added dropwise to a solution of penta-1,4-dien-3-ol (**10**) (11.19 g, 0.13 mol) and triethylamine (13.66 g, 0.14 mol) in DCM (100 cm³) at 0 °C. The solution was stirred for 1 hour at 0 °C and then stirred and allowed to reach RT overnight. The resulting reaction mixture was filtered to remove the white precipitate, triethylammonium chloride [HN⁺(C₂H₅)₃Cl⁻], that had formed and then the reaction mixture was washed with dilute hydrochloric acid (10%) (100 cm³), saturated potassium carbonate solution (100 cm³) and distilled water (4 × 100 cm³) then dried (MgSO₄) and concentrated to an orange/yellow oil. The product was purified by column chromatography [silica gel, DCM] to yield 13.58 g (44.8%) of the desired product (pale yellow oil).

Purity: >99% (GC).

¹H NMR (CDCl₃) δ_H: 2.19 (2H, quint), 2.55 (2H, t), 3.47 (2H, t), 5.24 (2H, dt), 5.30 (2H, dt), 5.72 (1H, tt), 5.80-5.88 (2H, m).

IR ν_{max} /cm⁻¹: 3089, 2988, 1736 (C=O), 1642, 1438, 1252, 1198, 1172, 987, 933, 739.

MS (m/z) (EI): 233 (M⁺), 219, 217, 201, 149, 121, 93, 84, 67 (M100).

Elemental analysis: Expected /% C 46.37, H 5.62.

Found /% C 46.25, H 5.92.

5-Bromopentanoic acid 1-vinyl-allyl ester (**15**)

A solution of 5-bromopentanoyl chloride (**12**) (10.39 g, 0.05 mol), in DCM (50 cm³), was added dropwise to a solution of penta-1,4-dien-3-ol (**10**) (4.55 g, 0.05 mol) and triethylamine (5.67 g, 0.06 mol) in DCM (80 cm³) at 0 °C. The solution was stirred for 1 hour at 0 °C and then stirred and allowed to reach RT overnight. The resulting reaction mixture was filtered to remove the white precipitate that had formed (triethylammonium chloride) and then the reaction mixture was washed with dilute hydrochloric acid (10%) (100 cm³), saturated potassium carbonate solution (100 cm³) and distilled water (4 × 100 cm³) then dried (MgSO₄) and concentrated to an

orange/yellow oil. The product was purified by column chromatography [silica gel, DCM] to yield 9.91 g (77.0%) of the desired product (pale yellow oil).

Purity: >99% (GC).

^1H NMR (CDCl_3) δ_{H} : 1.80 (2H, quint), 1.91 (2H, quint), 2.39 (2H, t), 3.41 (2H, t), 5.24 (2H, dt), 5.30 (2H, dt), 5.72 (1H, tt), 5.79-5.88 (2H, m).

IR ν_{max} / cm^{-1} : 3089, 2941, 2871, 1736 (C=O), 1641, 1418, 1253, 1171, 988, 933, 739.

MS (m/z) (EI): 247 (M^+), 231, 165, 163, 135, 84, 67 (M100).

Elemental analysis: Expected /% C 48.60, H 6.12.

Found /% C 48.75, H 6.34.

6-Bromohexanoic acid 1-vinyl-allyl ester (**16**)

A solution of 6-bromohexanoyl chloride (**13**) (10.92 g, 0.05 mol), in DCM (50 cm^3), was added dropwise to a solution of penta-1,4-dien-3-ol (**10**) (4.46 g, 0.05 mol) and triethylamine (5.57 g, 0.06 mol) in DCM (80 cm^3) at 0 °C. The solution was stirred for 1 hour at 0 °C and then stirred and allowed to reach RT overnight. The resulting reaction mixture was filtered to remove the white precipitate that had formed (triethylammonium chloride) and then the reaction mixture was washed with dilute hydrochloric acid (10%) (100 cm^3), saturated potassium carbonate solution (100 cm^3) and distilled water (4 \times 100 cm^3) then dried (MgSO_4) and concentrated to an orange/yellow oil. The product was purified by column chromatography [silica gel, DCM] to yield 10.04 g (75.2%) of the desired product (pale yellow oil).

Purity: >97% (GC).

^1H NMR (CDCl_3) δ_{H} : 1.49 (2H, quint), 1.68 (2H, quint), 1.88 (2H, quint), 2.37 (2H, t), 3.40 (2H, t), 5.23 (2H, dt), 5.30 (2H, dt), 5.72 (1H, tt), 5.80-5.88 (2H, m).

IR ν_{max} / cm^{-1} : 3089, 2940, 2865, 1737 (C=O), 1641, 1460, 1251, 1176, 986, 932, 737.

MS (m/z) (EI): 261 (M^+), 233, 219, 217, 179, 177, 151, 149, 133, 107, 97, 84, 69 (M100), 67.

8-Bromooctanoic acid 1-vinyl-allyl ester (**17**)

A solution of 8-bromooctanoyl chloride (**9**) (16.84 g, 0.07 mol), in DCM (60 cm^3), was added dropwise to a solution of penta-1,4-dien-3-ol (**10**) (5.97 g, 0.07 mol) and

triethylamine (7.39 g, 0.07 mol) in DCM (100 cm³) at 0 °C. The solution was stirred for 1 hour at 0 °C and then stirred and allowed to reach RT overnight. The resulting reaction mixture was filtered to remove the white precipitate that had formed (triethylammonium chloride) and then the reaction mixture was washed with dilute hydrochloric acid (10%) (100 cm³), saturated potassium carbonate solution (100 cm³) and distilled water (4 × 100 cm³) then dried (MgSO₄) and concentrated to an orange/brown oil. The product was purified by column chromatography [silica gel, DCM] to yield 14.26 g (70.7%) of the desired product (yellow oil).

Purity: >98% (GC).

¹H NMR (CDCl₃) δ_H: 1.32-1.36 (4H, m), 1.43 (2H, quint), 1.65 (2H, quint), 1.85 (2H, quint), 2.35 (2H, t), 3.40 (2H, t), 5.23 (2H, dt), 5.30 (2H, dt), 5.72 (1H, tt), 5.80-5.88 (2H, m).

IR ν_{max} /cm⁻¹: 3088, 2934, 2858, 1737 (C=O), 1641, 1464, 1236, 1172, 986, 932, 728.

MS (m/z) (EI): 289 (M⁺), 279, 261, 259, 207, 205, 163, 149, 135, 123, 107, 97, 84, 67 (M100).

11-Bromoundecanoic acid 1-vinyl-allyl ester (**18**)

DCC (10.89 g, 0.05 mol) in DCM (70 cm³) was added, in portions, to a stirred solution of 11-bromoundecanoic acid (**8**) (12.69 g, 0.05 mol), penta-1,4-dien-3-ol (**10**) (4.17 g, 0.05 mol) and DMAP (3.24 g, 0.03 mol) in DCM (250 cm³) at 0 °C. The reaction mixture was stirred and allowed to reach RT overnight. The bi-product, dicyclohexylurea (DCU), was filtered off and rinsed with DCM (2 × 100 cm³). The filtrate was concentrated under reduced pressure to give an orange/yellow oil and then purified by column chromatography [silica gel, DCM:hexane, 50%:50%] to yield a pale yellow oil (12.27 g, 77.5 %).

Purity: >98 % (GC).

¹H NMR (CDCl₃) δ_H: 1.29 (10H, s), 1.42 (2H, quint), 1.64 (2H, quint), 1.85 (2H, quint), 2.34 (2H, t), 3.40 (2H, t), 5.22 (2H, d, *J*=10.4 Hz), 5.30 (2H, d, *J*=17.1 Hz), 5.72 (1H, t), 5.79-5.88 (2H, m).

IR ν_{max} /cm⁻¹: 3088, 2929, 2856, 1740 (C=O), 1641, 1465, 1244, 1168, 986, 931, 723, 563.

MS (m/z) (EI): 331 (M⁺), 315, 313, 249, 247, 165, 149, 133, 123, 97, 83, 67 (M100), 41.

(s)-1-Bromo-4-(3,7-dimethyl-oct-6-enyloxy)benzene (**21**)

A mixture of 4-bromophenol (**19**) (16.20 g, 0.09 mol), (s)-8-bromo-2,6-dimethyl-oct-2-ene (**20**) (26.49 g, 0.12 mol) and potassium carbonate (21.81 g, 0.16 mol) in butanone (350 cm³) was heated under reflux for 48 hours. The cooled reaction mixture was filtered and the filtrate was concentrated under reduced pressure. The crude product (pale yellow liquid) was purified by fractional distillation under reduced pressure to yield 27.43 g (94.1%) of the desired product (colourless liquid).

Boiling point /°C: 125-135 @ 2 mm Hg.

¹H NMR (CDCl₃) δ_H: 0.94 (3H, d), 1.17-1.26 (2H, m), 1.34-1.43 (1H, m), 1.60 (3H, s), 1.68 (3H, s), 1.77-1.86 (2H, m), 1.92-2.08 (2H, m), 3.89-3.99 (2H, m), 5.10 (1H, t), 6.76 (2H, d, *J*=9.0 Hz), 7.35 (2H, d, *J*=9.0 Hz).

IR ν_{max} /cm⁻¹: 2914, 1591, 1578, 1488, 1286, 1244, 1171, 821, 801.

MS (m/z) (EI): 312 (M⁺), 310 (M⁺), 174, 172, 145, 143, 138, 123, 109, 95, 83, 69 (M100).

Elemental analysis: Expected /% C 61.74, H 7.45.

Found /% C 61.60, H 7.75.

(s)-4-(3,7-Dimethyl-oct-6-enyloxy)phenyl boronic acid (**22**)

n-Butyllithium in hexanes (42.50 cm³, 2.5 M, 0.11 mol) was added dropwise to a cooled (-78 °C) solution of (s)-1-bromo-4-(3,7-dimethyl-oct-6-enyloxy)benzene (**21**) (26.53 g, 0.09 mol) in sodium dried THF (260 cm³). The resulting solution was stirred at this temperature for 1 hour and then trimethyl borate (19.50 g, 0.19 mol) in sodium dried THF (40 cm³) was added dropwise to the reaction mixture whilst maintaining the temperature at -78 °C. The reaction mixture was allowed to warm to RT overnight and then dilute (20%) hydrochloric acid (500 cm³) was added and the resulting mixture was stirred for 1 hour and then extracted into diethyl ether (3 × 200 cm³). The combined ethereal extracts were washed with water (3 × 100 cm³) and dried (MgSO₄). After filtration the solvent was removed under reduced pressure to yield 16.37 g (69.5%) of the desired product (orange/yellow oil).

Not analysed.

(s)-3,7-Bis-[4-(3,7-dimethyl-oct-6-enyloxy)phenyl]dibenzothiophene (**23**)

Tetrakis(triphenylphosphine)palladium(0) (0.85 g, 7.40×10^{-4} mol) was added to a mixture of 3,7-dibromodibenzothiophene (**6**) (2.50 g, 7.31×10^{-3} mol), (s)-4-(3,7-dimethyl-oct-6-enyloxy)phenyl boronic acid (**22**), (7.13 g, 2.58×10^{-2} mol) and aqueous 2 M sodium carbonate solution (37 cm³) in 1,2-dimethoxyethane (100 cm³) at RT. The reaction mixture was then heated under reflux for 48 hours. The cooled reaction mixture was poured into distilled water (150 cm³) and extracted with dichloromethane (3×150 cm³) and the combined organic layers were washed with brine (2×150 cm³) and dried (MgSO₄). After filtration, the solution was concentrated onto silica gel for purification by column chromatography [silica gel, DCM:hexane, 20%:80%] followed by recrystallisation from a DCM:ethanol mixture (3:1) to yield 2.35 g (49.8%) of the desired product (white solid).

Transition temp. /°C: Cr 196 SmC* 243 SmA* 246 I.

¹H NMR (CDCl₃) δ_H: 0.98 (6H, d), 1.20-1.29 (4H, m), 1.38-1.47 (2H, m), 1.62 (6H, s), 1.70 (6H, s), 1.84-1.92 (4H, m), 1.97-2.09 (4H, m), 4.01-4.11 (4H, m), 5.12 (2H, t), 7.10 (4H, d, *J*=9.0 Hz), 7.62 (4H, d, *J*=8.7 Hz), 7.66 (2H, d, *J*=8.2 Hz), 8.01 (2H, s), 8.16 (2H, d, *J*=8.2 Hz).

IR ν_{max} /cm⁻¹: 2924, 1606, 1518, 1465, 1294, 1249, 1187, 873, 808.

MS (m/z) (EI): 644 (M⁺) (M100) (HABA matrix).

Elemental analysis: Expected /% C 81.94, H 8.13, S 4.97.

Found /% C 81.76, H 8.40, S 4.93.

3,7-Bis-(4-hydroxyphenyl)dibenzothiophene (**24**)

Boron tribromide (4.24 g, 1.60 cm³, 1.69×10^{-2} mol) in dichloromethane (20 cm³) was added dropwise to a cooled (0 °C), stirred solution of (s)-3,7-bis-[4-(3,7-dimethyl-oct-6-enyloxy)phenyl]dibenzothiophene (**23**) (2.71 g, 4.20×10^{-3} mol) in dichloromethane (130 cm³). The reaction mixture was stirred and allowed to reach RT overnight. The reaction mixture was then poured onto an ice/water mixture (300 g), DCM was added (200 cm³) and the resulting mixture stirred (2 hours). The precipitate was filtered off, washed with hot DCM (2×30 cm³) and pulled dry under vacuum to yield 1.43 g (91.4%) of the desired product (red/brown solid).

Melting point /°C: >329 (material decomposition).

^1H NMR (DMSO) δ_{H} : 6.89 (4H, d, $J=8.7$ Hz), 7.63 (4H, d, $J=8.7$ Hz), 7.72 (2H, d, $J=8.3$ Hz), 8.21 (2H, s), 8.33 (2H, d, $J=8.4$ Hz), 9.63 (2H, s-OH).

IR $\nu_{\text{max}}/\text{cm}^{-1}$: 3364, 1609, 1593, 1517, 1450, 1265, 1244, 836, 810.

MS (m/z) (EI): 368 (M^+), 202, 184, 130, 97, 82, 69, 55, 44, 40 (M100).

4-[4-(7-{4-[3-(1-Vinyl-allyloxycarbonyl)propoxy]phenyl}dibenzothiophene-3-yl)phenoxy]butanoic acid 1-vinyl-allyl ester (**25**)

A mixture of 3,7-bis-(4-hydroxyphenyl)dibenzothiophene (**24**) (0.25 g, 6.80×10^{-4} mol), 4-bromobutanoic acid 1-vinyl-allyl ester (**14**) (0.48 g, 2.06×10^{-3} mol) and potassium carbonate (0.35 g, 2.53×10^{-3} mol) in DMF (25 cm^3) was heated (90 $^{\circ}\text{C}$) for 24 hours. The excess potassium carbonate was filtered off from the cooled reaction mixture and rinsed with DCM (3 \times 30 cm^3). The solution was concentrated onto silica gel for purification by column chromatography [silica gel, ethyl acetate:hexane, 20%:80%] followed by recrystallisation from a DCM:ethanol mixture (1:1) to yield 0.28 g (60.9%) of the desired product (white solid).

Transition temp. / $^{\circ}\text{C}$: Cr 116 SmX 129 SmC 168 SmA 205 I.

^1H NMR (CDCl_3) δ_{H} : 2.10 (4H, quint), 2.54 (4H, t), 4.03 (4H, t), 5.17 (4H, dt), 5.25 (4H, dt), 5.68 (2H, tt), 5.74-5.82 (4H, m), 6.93 (4H, d, $J=8.7$ Hz), 7.54 (4H, d, $J=8.7$ Hz), 7.58 (2H, d, $J=8.4$ Hz), 7.94 (2H, s), 8.09 (2H, d, $J=8.4$ Hz).

IR $\nu_{\text{max}}/\text{cm}^{-1}$: 3086, 2935, 2873, 1734 (C=O), 1641, 1605, 1517, 1458, 1245, 1170, 982, 938, 836, 805, 721.

MS (m/z) (EI): 673 (M^+), 367, 293, 195, 167, 149 (M100), 127, 104, 97, 84, 67.

Elemental analysis: Expected /% C 74.97, H 5.99, S 4.77.
Found /% C 74.95, H 6.23, S 4.50.

5-[4-(7-{4-[4-(1-Vinyl-allyloxycarbonyl)butoxy]phenyl}dibenzothiophene-3-yl)phenoxy]pentanoic acid 1-vinyl-allyl-ester (**26**)

A mixture of 3,7-bis-(4-hydroxyphenyl)dibenzothiophene (**24**) (0.25 g, 6.80×10^{-4} mol), 5-bromopentanoic acid 1-vinyl-allyl ester (**15**) (0.54 g, 2.19×10^{-3} mol) and potassium carbonate (0.37 g, 2.68×10^{-3} mol) in DMF (25 cm^3) was heated (90 $^{\circ}\text{C}$) for 24 hours. The excess potassium carbonate was filtered off from the cooled

reaction mixture and rinsed with DCM ($3 \times 30 \text{ cm}^3$). The solution was concentrated onto silica gel for purification by column chromatography [silica gel, ethyl acetate:hexane, 20%:80%] followed by recrystallisation from a DCM:ethanol mixture (1:1) to yield 0.26 g (54.2%) of the desired product (off-white solid).

Transition temp. /°C: Cr 91 SmX 107 SmC 168 SmA 210 I.

^1H NMR (CDCl_3) δ_{H} : 1.86-1.89 (8H, m), 2.47 (4H, t), 4.04 (4H, t), 5.24 (4H, dt), 5.32 (4H, dt), 5.74 (2H, tt), 5.81-5.89 (4H, m), 7.00 (4H, d, $J=9.0 \text{ Hz}$), 7.62 (4H, d, $J=8.7 \text{ Hz}$), 7.65 (2H, d, $J=8.2 \text{ Hz}$), 8.01 (2H, s), 8.17 (2H, d, $J=8.2 \text{ Hz}$).

IR $\nu_{\text{max}}/\text{cm}^{-1}$: 3087, 2926, 2870, 1736 (C=O), 1640, 1606, 1517, 1458, 1247, 1166, 986, 928, 836, 806, 720.

MS (m/z) (EI): 701 (M^+), 681, 533, 438, 404, 367, 293, 231, 195, 149, 97, 83, 69, 67, 44 ($\text{M}100$).

Elemental analysis: Expected /% C 75.40, H 6.33, S 4.58.

Found /% C 75.66, H 6.39, S 4.29.

6-[4-(7-{4-[5-(1-Vinyl-allyloxycarbonyl)pentyl]oxy}phenyl)dibenzothiophene-3-yl)phenoxy]hexanoic acid 1-vinyl-allyl-ester (**27**)

A mixture of 3,7-bis-(4-hydroxyphenyl)dibenzothiophene (**24**) (0.25 g, 6.80×10^{-4} mol), 6-bromohexanoic acid 1-vinyl-allyl ester (**16**) (0.54 g, 2.07×10^{-3} mol) and potassium carbonate (0.37 g, 2.68×10^{-3} mol) in DMF (25 cm^3) was heated (90 °C) for 24 hours. The excess potassium carbonate was filtered off from the cooled reaction mixture and rinsed with DCM ($3 \times 30 \text{ cm}^3$). The solution was concentrated onto silica gel for purification by column chromatography [silica gel, ethyl acetate:hexane, 30%:70%] followed by recrystallisation from a DCM:ethanol mixture (1:1) to yield 0.26 g (52.0%) of the desired product (off-white solid).

Transition temp. /°C: Cr 107 SmX 116 SmC 167 SmA 206 I.

^1H NMR (CDCl_3) δ_{H} : 1.57 (4H, quint), 1.75 (4H, quint), 1.85 (4H, quint), 2.41 (4H, t), 4.02 (4H, t), 5.24 (4H, d, $J=10.4 \text{ Hz}$), 5.31 (4H, d, $J=17.2 \text{ Hz}$), 5.73 (2H, tt), 5.81-5.89 (4H, m), 7.00 (4H, d, $J=8.7 \text{ Hz}$), 7.62 (4H, d, $J=8.7 \text{ Hz}$), 7.66 (2H, d, $J=8.1 \text{ Hz}$), 8.01 (2H, s), 8.16 (2H, d, $J=8.2 \text{ Hz}$).

IR $\nu_{\text{max}}/\text{cm}^{-1}$: 2937, 2866, 1734 (C=O), 1640, 1605, 1516, 1457, 1245, 1184, 1162, 985, 926, 835, 806, 708.

MS (m/z) (EI): 729 (M^+), 681, 548, 438, 404, 352, 235, 195, 186, 97, 82, 69, 55, 44 (M_{100}).

Elemental analysis: Expected /% C 75.79, H 6.64, S 4.40.
Found /% C 76.00, H 6.85, S 4.16.

8-[4-(7-{4-[7-(1-Vinyl-allyloxycarbonyl)heptyloxy]phenyl}dibenzothiophene-3-yl)phenoxy]octanoic acid 1-vinyl-allyl-ester (**28**)

A mixture of 3,7-bis-(4-hydroxyphenyl)dibenzothiophene (**24**) (0.26 g, 7.10×10^{-4} mol), 8-bromooctanoic acid 1-vinyl-allyl ester (**17**) (0.60 g, 2.08×10^{-3} mol) and potassium carbonate (0.34 g, 2.46×10^{-3} mol) in DMF (25 cm³) was heated (90 °C) for 24 hours. The excess potassium carbonate was filtered off from the cooled reaction mixture and rinsed with DCM (3 \times 30 cm³). The solution was concentrated onto silica gel for purification by column chromatography [silica gel, ethyl acetate:hexane, 20%:80%] followed by recrystallisation from a DCM:ethanol mixture (1:1) to yield 0.31 g (56.4%) of the desired product (off-white solid).

Transition temp. /°C: Cr 116 SmX 134 SmC 168 SmA 206 I.

¹H NMR (CDCl₃) δ_H : 1.36-1.43 (8H, m), 1.50 (4H, quint), 1.67 (4H, quint), 1.81 (4H, quint), 2.36 (4H, t), 4.01 (4H, t), 5.23 (4H, dt), 5.31 (4H, dt), 5.73 (2H, tt), 5.80-5.89 (4H, m), 7.00 (4H, d, $J=8.7$ Hz), 7.61 (4H, d, $J=9.0$ Hz), 7.65 (2H, d, $J=8.4$ Hz), 8.01 (2H, s), 8.16 (2H, d, $J=8.2$ Hz).

IR ν_{max}/cm^{-1} : 3087, 2922, 2858, 1736 (C=O), 1641, 1605, 1518, 1464, 1243, 1171, 988, 930, 836, 806, 722.

MS (m/z) (EI): 785 (M^+), 576, 368, 352, 335, 312, 242, 213, 138, 110, 98, 84, 67 (M_{100}).

Elemental analysis: Expected /% C 76.50, H 7.19, S 4.08.
Found /% C 76.80, H 7.41, S 4.17.

11-[4-(7-{4-[10-(1-Vinyl-allyloxycarbonyl)decyloxy]phenyl}dibenzothiophene-3-yl)phenoxy]undecanoic acid 1-vinyl-allyl-ester (**29**)

A mixture of 3,7-bis-(4-hydroxyphenyl)dibenzothiophene (**24**) (0.25 g, 6.80×10^{-4} mol), 11-bromoundecanoic acid 1-vinyl-allyl ester (**18**) (0.67 g, 2.02×10^{-3} mol) and potassium carbonate (0.38 g, 2.75×10^{-3} mol) in DMF (25 cm³) was heated (90 °C) for 24 hours. The excess potassium carbonate was filtered off from the cooled

reaction mixture and rinsed with DCM ($3 \times 30 \text{ cm}^3$). The solution was concentrated onto silica gel for purification by column chromatography [silica gel, ethyl acetate:hexane, 20%:80%] followed by recrystallisation from a DCM:ethanol mixture (1:1) to yield 0.37 g (62.7%) of the desired product (off-white solid).

Transition temp. /°C: Cr 115 SmX 129 SmC 177 SmA 198 I.

^1H NMR (CDCl_3) δ_{H} : 1.24 (20H, s), 1.41 (4H, quint), 1.57 (4H, quint), 1.74 (4H, quint), 2.27 (4H, t), 3.94 (4H, t), 5.15 (4H, dt), 5.23 (4H, dt), 5.65 (2H, tt), 5.72-5.81 (4H, m), 6.93 (4H, d, $J=9.0 \text{ Hz}$), 7.54 (4H, d, $J=8.7 \text{ Hz}$), 7.58 (2H, d, $J=8.1 \text{ Hz}$), 7.94 (2H, s), 8.09 (2H, d, $J=8.1 \text{ Hz}$).

IR $\nu_{\text{max}}/\text{cm}^{-1}$: 3088, 2921, 2852, 1740 (C=O), 1641, 1605, 1517, 1466, 1247, 1166, 986, 922, 837, 806, 723.

MS (m/z) (EI): 869 (M^+), 681, 438, 404, 368, 289, 231, 195, 175, 149, 121, 112, 91, 83, 67 ($\text{M}100$).

Elemental analysis: Expected /% C 77.38, H 7.89, S 3.69.
Found /% C 77.52, H 8.07, S 3.42.

(s)-4-Bromo-1-(3,7-dimethyl-oct-6-enyloxy)-2-fluorobenzene (**31**)

A mixture of 4-bromo-2-fluorophenol (**30**) (20.66 g, 0.11 mol), (s)-8-bromo-2,6-dimethyl-oct-2-ene (**20**) (24.30 g, 0.11 mol) and potassium carbonate (21.86 g, 0.16 mol) in butanone (350 cm^3) was heated under reflux for 48 hours. The cooled reaction mixture was filtered and the filtrate was concentrated under reduce pressure. The crude product (orange liquid) was purified by fractional distillation under reduced pressure to yield 32.82 g (92.2%) of the desired product (colourless liquid).

Boiling point /°C: 126-134 @ 1.5 mm Hg.

^1H NMR (CDCl_3) δ_{H} : 0.95 (3H, d), 1.17-1.27 (2H, m), 1.34-1.43 (1H, m), 1.60 (3H, s), 1.68 (3H, s), 1.82-1.90 (2H, m), 1.94-2.06 (2H, m), 3.99-4.08 (2H, m), 5.10 (1H, t), 6.83 (1H, t), 7.15-7.26 (2H, m).

IR $\nu_{\text{max}}/\text{cm}^{-1}$: 2926, 1604, 1583, 1475, 1266, 1245, 1207, 1130, 858, 800.

MS (m/z) (EI): 330 (M^+), 328 (M^+), 192, 190, 163, 161, 138, 123, 109, 95, 83, 69 ($\text{M}100$).

Elemental analysis: Expected /% C 58.37, H 6.73.
Found /% C 58.43, H 7.00.

(s)-2-Fluoro-1-(3,7-dimethyl-oct-6-enyloxy)phenyl boronic acid (**32**)

n-Butyllithium in hexanes (47.00 cm³, 2.5 M, 0.12 mol) was added dropwise to a cooled (-78 °C) solution of (s)-4-bromo-1-(3,7-dimethyl-oct-6-enyloxy)-2-fluorobenzene (**31**) (32.36 g, 0.10 mol) in sodium dried THF (310 cm³). The resulting solution was stirred at this temperature for 1 hour and then trimethyl borate (22.50 g, 0.22 mol) in sodium dried THF (40 cm³) was added dropwise to the reaction mixture whilst maintaining the temperature at -78 °C. The reaction mixture was allowed to warm to RT over night and then dilute (20%) hydrochloric acid (500 cm³) was added and the resulting mixture was stirred for 1 hour and then extracted into diethyl ether (3 × 200 cm³). The combined ethereal extracts were washed with water (3 × 100 cm³) and dried (MgSO₄). After filtration the solvent was removed under reduce pressure to yield 20.64 g (71.4%) of the desired product (brown/orange oil).

Not analysed.

(s)-3,7-Bis-[4-(3,7-dimethyl-oct-6-enyloxy)-3-fluorophenyl]dibenzothiophene (**33**)

Tetrakis(triphenylphosphine)palladium(0) (0.85 g, 7.40 × 10⁻⁴ mol) was added to a mixture of 3,7-dibromodibenzothiophene (**6**) (2.50 g, 7.31 × 10⁻³ mol), (s)-2-fluoro-1-(3,7-dimethyl-oct-6-enyloxy)phenyl boronic acid (**32**) (7.13 g, 2.58 × 10⁻² mol) and aqueous 2 M sodium carbonate solution (37 cm³) in 1,2-dimethoxyethane (100 cm³) at RT. The reaction mixture was then heated under reflux for 48 hours. The cooled reaction mixture was poured into distilled water (150 cm³) and extracted with dichloromethane (3 × 150 cm³) and the combined organic layers were washed with brine (2 × 150 cm³) and dried (MgSO₄). After filtration, the solution was concentrated onto silica gel for purification by column chromatography [silica gel, DCM:hexane, 20%:80%] followed by recrystallisation from a DCM:ethanol mixture (3:1) to yield 2.35 g (49.8%) of the desired product (white solid).

Transition temp. /°C: Cr 145 SmC* 212 SmA* 227 I.

¹H NMR (CDCl₃) δ_H: 0.91 (6H, d), 1.21-1.30 (4H, m), 1.38-1.47 (2H, m), 1.62 (6H, s), 1.70 (6H, s), 1.88-1.95 (4H, m), 1.99-2.08 (4H, m), 4.09-4.18 (4H, m), 5.12 (2H, t), 7.07 (2H, t), 7.38-7.46 (4H, m), 7.64 (2H, d, *J*=8.0 Hz), 8.00 (2H, s), 8.18 (2H, d, *J*=8.0 Hz).

IR ν_{max} /cm⁻¹: 2965, 2914, 1618, 1528, 1467, 1312, 1283, 1239, 1188, 860, 802.

MS (m/z) (EI): 681 (M^+), 641, 438, 404, 370, 231, 195, 136, 97, 83, 69, 55, 44 (M100).

Elemental analysis: Expected /% C 77.61, H 7.40, S 4.71.

Found /% C 77.90, H 7.67, S 4.99.

3,7-Bis-(3-fluoro-4-hydroxyphenyl)dibenzothiophene (**34**)

Boron tribromide (2.86 g, 1.10 cm^3 , $1.14 \times 10^{-2} \text{ mol}$) in dichloromethane (20 cm^3) was added dropwise to a cooled (0°C), stirred solution of (s)-3,7-bis-[4-(3,7-dimethyl-oct-6-enyloxy)-3-fluorophenyl]dibenzothiophene (**33**) (1.94 g, $2.85 \times 10^{-3} \text{ mol}$) in dichloromethane (130 cm^3). The reaction mixture was stirred and allowed to reach RT overnight. The reaction mixture was then poured onto an ice/water mixture (300 g), DCM was added (200 cm^3) and the resulting mixture stirred (2 hours). The precipitate was filtered off, washed with hot DCM ($2 \times 30 \text{ cm}^3$) and pulled dry under vacuum to yield 0.96 g (83.5%) of the desired product (white solid).

Melting point $^\circ\text{C}$: >282 (material decomposition).

^1H NMR (DMSO) δ_{H} : 7.07 (2H, t), 7.49 (2H, dt), 7.65 (2H, dd), 7.78 (2H, d, $J=8.2 \text{ Hz}$), 8.29 (2H, s), 8.38 (2H, d, $J=8.1 \text{ Hz}$), 10.07 (2H, s-OH).

IR $\nu_{\text{max}}/\text{cm}^{-1}$: 3404, 1624, 1526, 1466, 1394, 1307, 1175, 1117, 860, 805.

MS (m/z) (EI): 404 (M^+) (M100), 375, 355, 202, 153, 141, 83, 69, 57, 40.

4-[2-Fluoro-4-(7-{3-fluoro-4-[3-(1-vinyl-allyloxycarbonyl)propoxy]phenyl}dibenzothiophene-3-yl)phenoxy]butanoic acid 1-vinyl-allyl ester (**35**)

A mixture of 3,7-bis-(3-fluoro-4-hydroxyphenyl)dibenzothiophene (**34**) (0.25 g, $6.20 \times 10^{-4} \text{ mol}$), 4-bromobutanoic acid 1-vinyl-allyl ester (**14**) (0.43 g, $1.85 \times 10^{-3} \text{ mol}$) and potassium carbonate (0.34 g, $2.46 \times 10^{-3} \text{ mol}$) in DMF (25 cm^3) was heated (90°C) for 24 hours. The excess potassium carbonate was filtered off from the cooled reaction mixture and rinsed with DCM ($3 \times 30 \text{ cm}^3$). The solution was concentrated onto silica gel for purification by column chromatography [silica gel, ethyl acetate:hexane, 20%:80%] followed by recrystallisation from a DCM:ethanol mixture (1:1) to yield 0.26 g (59.1%) of the desired product (white solid).

Transition temp. $^\circ\text{C}$: Cr 116 SmC 168 SmA 210 I.

^1H NMR (CDCl_3) δ_{H} : 2.19 (4H, quint), 2.63 (4H, t), 4.14 (4H, t), 5.24 (4H, dt), 5.32 (4H, dt), 5.75 (2H, tt), 5.80-5.90 (4H, m), 7.04 (2H, t), 7.37

(2H, dt), 7.42 (2H, dd), 7.61 (2H, d, $J=8.4$ Hz), 7.98 (2H, s), 8.15 (2H, d, $J=8.4$ Hz).

IR $\nu_{\max}/\text{cm}^{-1}$: 3086, 2936, 2880, 1735 (C=O), 1641, 1618, 1525, 1465, 1244, 1171, 984, 925, 865, 803, 712.

MS (m/z) (EI): 709 (M^+), 625, 555, 469, 403, 369, 346, 208, 105, 87, 67, 44 ($M100$).

Elemental analysis: Expected /% C 71.17, H 5.40, S 4.52.
Found /% C 71.44, H 5.44, S 4.82.

5-[2-Fluoro-4-(7-{3-fluoro-4-[4-(1-vinyl-allyloxycarbonyl)butoxy]phenyl}dibenzothiophene-3-yl)phenoxy]pentanoic acid 1-vinyl-allyl ester (**36**)

A mixture of 3,7-bis-(3-fluoro-4-hydroxyphenyl)dibenzothiophene (**34**) (0.25 g, 6.20×10^{-4} mol), 5-bromopentanoic acid 1-vinyl-allyl ester (**15**) (0.51 g, 2.06×10^{-3} mol) and potassium carbonate (0.37 g, 2.68×10^{-3} mol) in DMF (25 cm³) was heated (90 °C) for 24 hours. The excess potassium carbonate was filtered off from the cooled reaction mixture and rinsed with DCM (3 \times 30 cm³). The solution was concentrated onto silica gel for purification by column chromatography [silica gel, ethyl acetate:hexane, 20%:80%] followed by recrystallisation from a DCM:ethanol mixture (1:1) to yield 0.32 g (69.6%) of the desired product (white solid).

Transition temp. /°C: Cr 130 SmC 167 SmA 203 I.

¹H NMR (CDCl₃) δ_{H} : 1.84-1.95 (8H, m), 2.47 (4H, t), 4.10 (4H, t), 5.24 (4H, dt), 5.32 (4H, dt), 5.74 (2H, tt), 5.80-5.89 (4H, m), 7.04 (2H, t), 7.37 (2H, dt), 7.42 (2H, dd), 7.62 (2H, d, $J=8.3$ Hz), 7.99 (2H, s), 8.16 (2H, d, $J=8.4$ Hz).

IR $\nu_{\max}/\text{cm}^{-1}$: 3087, 2943, 2877, 1736 (C=O), 1640, 1619, 1526, 1466, 1241, 1168, 987, 928, 868, 804, 712.

MS (m/z) (EI): 737 (M^+), 491, 279, 167, 149 ($M100$), 113, 104, 84, 71, 57, 43.

Elemental analysis: Expected /% C 71.72, H 5.75, S 4.35.
Found /% C 71.84, H 5.88, S 4.12.

6-[2-Fluoro-4-(7-{3-fluoro-4-[5-(1-vinyl-allyloxycarbonyl)pentyl]oxy}phenyl)dibenzothiophene-3-yl]phenoxy]hexanoic acid 1-vinyl-allyl ester (**37**)

A mixture of 3,7-bis-(3-fluoro-4-hydroxyphenyl)dibenzothiophene (**34**) (0.25 g, 6.20×10^{-4} mol), 6-bromohexanoic acid 1-vinyl-allyl ester (**16**) (0.48 g, 1.84×10^{-3} mol) and potassium carbonate (0.34 g, 2.46×10^{-3} mol) in DMF (25 cm³) was heated (90 °C) for 24 hours. The excess potassium carbonate was filtered off from the cooled reaction mixture and rinsed with DCM (3 × 30 cm³). The solution was concentrated onto silica gel for purification by column chromatography [silica gel, ethyl acetate:hexane, 20%:80%] followed by recrystallisation from a DCM:ethanol mixture (1:1) to yield 0.30 g (63.8%) of the desired product (white solid).

Transition temp. /°C: Cr 123 SmC 169 SmA 202 I.

¹H NMR (CDCl₃) δ_H: 1.56 (4H, quint), 1.75 (4H, quint), 1.88 (4H, quint), 2.41 (4H, t), 4.08 (4H, t), 5.23 (4H, dt), 5.31 (4H, dt), 5.73 (2H, tt), 5.79-5.89 (4H, m), 7.03 (2H, t), 7.37 (2H, dt), 7.42 (2H, dd), 7.61 (2H, d, *J*=8.1 Hz), 7.98 (2H, s), 8.15 (2H, d, *J*=8.2 Hz).

IR ν_{max}/cm⁻¹: 3088, 2945, 2870, 1736 (C=O), 1641, 1619, 1523, 1465, 1233, 1164, 1130, 984, 925, 874, 800, 712.

MS (m/z) (EI): 765 (M⁺), 583, 404, 403, 370, 253, 138, 115, 91, 67, 44 (M100).

Elemental analysis: Expected /% C 72.23, H 6.06, S 4.19.

Found /% C 72.53, H 6.26, S 3.90.

8-[2-Fluoro-4-(7-{3-fluoro-4-[7-(1-vinyl-allyloxycarbonyl)heptyl]oxy}phenyl)dibenzothiophene-3-yl]phenoxy]octanoic acid 1-vinyl-allyl ester (**38**)

A mixture of 3,7-bis-(3-fluoro-4-hydroxyphenyl)dibenzothiophene (**34**) (0.25 g, 6.20×10^{-4} mol), 8-bromooctanoic acid 1-vinyl-allyl ester (**17**) (0.54 g, 1.87×10^{-3} mol) and potassium carbonate (0.34 g, 2.46×10^{-3} mol) in DMF (25 cm³) was heated (90 °C) for 24 hours. The excess potassium carbonate was filtered off from the cooled reaction mixture and rinsed with DCM (3 × 30 cm³). The solution was concentrated onto silica gel for purification by column chromatography [silica gel, ethyl acetate:hexane, 20%:80%] followed by recrystallisation from a DCM:ethanol mixture (1:1) to yield 0.29 g (56.9%) of the desired product (white solid).

Transition temp. /°C: Cr 123 SmC 168 SmA 190 I.

^1H NMR (CDCl_3) δ_{H} : 1.38 (8H, s), 1.49 (4H, quint), 1.67 (4H, quint), 1.85 (4H, quint), 2.36 (4H, t), 4.06 (4H, t), 5.23 (4H, d, $J=10.4$ Hz), 5.30 (4H, d, $J=17.5$ Hz), 5.72 (2H, tt), 5.79-5.89 (4H, m), 7.02 (2H, t), 7.35 (2H, dt), 7.41 (2H, dd), 7.59 (2H, d, $J=8.3$ Hz), 7.97 (2H, s), 8.13 (2H, d, $J=8.4$ Hz).

IR $\nu_{\text{max}}/\text{cm}^{-1}$: 3087, 2935, 2857, 1736 (C=O), 1641, 1618, 1526, 1465, 1242, 1172, 988, 929, 867, 804, 724.

MS (m/z) (EI): 821 (M^+), 612, 404, 403, 370, 276, 213, 119, 97, 79, 67, 44 ($\text{M}100$).

Elemental analysis: Expected /% C 73.14, H 6.63, S 3.91.

Found /% C 73.03, H 6.80, S 3.61.

11-[2-Fluoro-4-(7-{3-fluoro-4-[10-(1-vinyl-allyloxycarbonyl)decyloxy]phenyl}dibenzothiophene-3-yl)phenoxy]undecanoic acid 1-vinyl-allyl ester (**39**)

A mixture of 3,7-bis-(3-fluoro-4-hydroxyphenyl)dibenzothiophene (**34**) (0.25 g, 6.20×10^{-4} mol), 11-bromoundecanoic acid 1-vinyl-allyl ester (**18**) (0.61 g, 1.84×10^{-3} mol) and potassium carbonate (0.34 g, 2.46×10^{-3} mol) in DMF (25 cm^3) was heated (90 °C) for 24 hours. The excess potassium carbonate was filtered off from the cooled reaction mixture and rinsed with DCM (3 \times 30 cm^3). The solution was concentrated onto silica gel for purification by column chromatography [silica gel, ethyl acetate:hexane, 20%:80%] followed by recrystallisation from a DCM:ethanol mixture (1:1) to yield 0.42 g (75.0%) of the desired product (creamy-white solid).

Transition temp. /°C: Cr 130 SmC 169 SmA 199 I.

^1H NMR (CDCl_3) δ_{H} : 1.31 (20H, s), 1.49 (4H, quint), 1.64 (4H, quint), 1.85 (4H, quint), 2.34 (4H, t), 4.08 (4H, t), 5.23 (4H, dt), 5.30 (4H, dt), 5.72 (2H, tt), 5.79-5.89 (4H, m), 7.02 (2H, t), 7.37 (2H, dt), 7.42 (2H, dd), 7.62 (2H, d, $J=8.3$ Hz), 7.98 (2H, s), 8.16 (2H, d, $J=8.4$ Hz).

IR $\nu_{\text{max}}/\text{cm}^{-1}$: 3088, 2917, 2850, 1737 (C=O), 1640, 1621, 1526, 1466, 1237, 1172, 989, 922, 826, 809, 716.

MS (m/z) (EI): 905 (M^+), 751, 654, 404, 403, 370, 306, 277, 253, 162, 134, 105, 91, 67 ($\text{M}100$), 41.

Elemental analysis: Expected /% C 74.31, H 7.35, S 3.54.

Found /% C 74.53, H 7.60, S 3.28.

2-Methacrylic acid 9-bromononyl ester (**42**)

Triethylamine (4.19 g, 0.04 mol) in DCM (25 cm³) was added, dropwise, to a stirred solution of 9-bromononan-1-ol (**40**) (5.03 g, 0.02 mol) and 2-methylacryloyl chloride (2.46 g, 0.02 mol) in DCM (75 cm³) at 0 °C. The reaction mixture was stirred and allowed to reach RT overnight. The reaction mixture was then quenched by the addition of distilled water (200 cm³) and the aqueous phase was extracted with DCM (4 × 100 cm³). The combined organic extracts were washed with brine (150 cm³) dried (MgSO₄) and concentrated to a cloudy yellow oil and then purified by column chromatography [silica gel, DCM:hexane, 10%:90%] to yield 4.63 g (70.6%) of the desired product (pale yellow oil).

¹H NMR (CDCl₃) δ_H: 1.28-1.47 (10H, m), 1.67 (2H, quint), 1.85 (2H, quint), 1.94 (3H, s), 3.41 (2H, t), 4.14 (2H, t), 5.53-5.56 (1H, m), 6.08-6.11 (1H, m).

IR ν_{max} /cm⁻¹: 2930, 2856, 1720 (C=O), 1638, 1454, 1321, 1297, 1167, 562.

MS (m/z) (EI): 293 (M⁺), 291 (M⁺), 247, 206, 204, 150, 148, 87, 83, 69 (M100), 55.

Elemental analysis: Expected /% C 53.61, H 7.96.
Found /% C 53.59, H 8.20.

2-Methacrylic acid 11-bromoundecyl ester (**43**)

Triethylamine (3.53 g, 0.04 mol) in DCM (25 cm³) was added, dropwise, to a stirred solution of 11-bromoundecan-1-ol (**41**) (5.01 g, 0.02 mol) and 2-methylacryloyl chloride (2.31 g, 0.02 mol) in DCM (75 cm³) at 0 °C. The reaction mixture was stirred and allowed to reach RT overnight. The reaction mixture was then quenched by the addition of distilled water (200 cm³) and the aqueous phase was extracted with DCM (4 × 100 cm³). The combined organic extracts were washed with brine (150 cm³) dried (MgSO₄) and concentrated to a cloudy yellow oil and then purified by column chromatography [silica gel, DCM:hexane, 20%:80%] to yield 4.90 g (76.9%) of the desired product (pale yellow oil).

¹H NMR (CDCl₃) δ_H: 1.23-1.45 (14H, m), 1.65 (2H, quint), 1.82 (2H, quint), 1.93 (3H, s), 3.39 (2H, t), 4.12 (2H, t), 5.51-5.55 (1H, m), 6.06-6.10 (1H, m).

IR ν_{max} /cm⁻¹: 2929, 2855, 1720 (C=O), 1638, 1454, 1321, 1297, 1167, 563.

MS (m/z) (EI): 321 (M⁺), 319 (M⁺), 275, 150, 148, 109, 87, 83, 69 (M100), 55.

2-Methacrylic acid 9-[4-(7-{4-[9-(2-methacryloyloxy)nonyloxy]phenyl}
dibenzothiophene-3-yl)phenoxy]nonyl ester (**44**)

A mixture of 3,7-bis-(4-hydroxyphenyl)dibenzothiophene (**24**) (0.21 g, 5.70×10^{-4} mol), 2-methacrylic acid 9-bromononyl ester (**42**) (0.66 g, 2.27×10^{-3} mol), potassium carbonate (0.34 g, 2.46×10^{-3} mol) and 2,6-di-tertbutyl-4-methylphenol (BHT) (0.06 g, 2.70×10^{-4} mol) in DMF (25 cm³) was heated (60 °C) for 48 hours. The excess potassium carbonate was filtered off from the cooled reaction mixture and rinsed with DCM (3 × 30 cm³). The solution was concentrated onto silica gel for purification by column chromatography [silica gel, ethyl acetate:hexane, 30%:70%] followed by recrystallisation from a DCM:ethanol mixture (1:1) to yield 0.11 g (24.4%) of the desired product (white solid).

Transition temp. /°C: Cr 116 material polymerised.

¹H NMR (CDCl₃) δ_H: 1.29 (16H, s), 1.42 (4H, quint), 1.61 (4H, quint), 1.75 (4H, quint), 1.88 (6H, s), 3.95 (4H, t), 4.08 (4H, t), 5.46-5.49 (2H, m), 6.02-6.05 (2H, m), 6.94 (4H, d, *J*=9.0 Hz), 7.55 (4H, d, *J*=8.7 Hz), 7.59 (2H, d, *J*=8.2 Hz), 7.94 (2H, s), 8.10 (2H, d, *J*=8.2 Hz).

IR ν_{max} /cm⁻¹: 2933, 2854, 1716 (C=O), 1639, 1466, 1329, 1297, 1183, 936, 837, 806.

MS (m/z) (EI): 789 (M⁺), 579, 442, 382, 368, 214, 157, 121, 91, 69, 55, 40 (M100).

Elemental analysis: Expected /% C 76.11, H 7.66, S 4.06.
Found /% C 75.83, H 7.86, S 4.31.

2-Methacrylic acid 11-[4-(7-{4-[11-(2-methacryloyloxy)undecyloxy]phenyl}
dibenzothiophene-3-yl)phenoxy]undecyl ester (**45**)

A mixture of 3,7-bis-(4-hydroxyphenyl)dibenzothiophene (**24**) (0.20 g, 5.40×10^{-4} mol), 2-methacrylic acid 11-bromoundecyl ester (**43**) (0.80 g, 2.51×10^{-3} mol), potassium carbonate (0.32 g, 2.32×10^{-3} mol) and BHT (0.06 g, 2.70×10^{-4} mol) in DMF (25 cm³) was heated (60 °C) for 48 hours. The excess potassium carbonate was filtered off from the cooled reaction mixture and rinsed with DCM (3 × 30 cm³). The solution was concentrated onto silica gel for purification by column chromatography [silica gel, ethyl acetate:hexane, 30%:70%] followed by recrystallisation from a

DCM:ethanol mixture (1:1) to yield 0.10 g (21.7%) of the desired product (white solid).

Transition temp. /°C: Cr 116 material polymerised.

¹H NMR (CDCl₃) δ_H: 1.28-1.42 (24H, m), 1.49 (4H, quint), 1.68 (4H, quint), 1.82 (4H, quint), 1.95 (6H, s), 4.02 (4H, t), 4.14 (4H, t), 5.53-5.56 (2H, m), 6.08-6.11 (2H, m), 7.01 (4H, d, *J*=9.0 Hz), 7.62 (4H, d, *J*=9.0 Hz), 7.66 (2H, d, *J*=8.2 Hz), 8.01 (2H, s), 8.17 (2H, d, *J*=8.2 Hz).

IR ν_{max} /cm⁻¹: 2920, 2852, 1714 (C=O), 1638, 1466, 1329, 1298, 1183, 935, 837, 806.

MS (m/z) (EI): 845 (M⁺), 763, 607, 582, 404, 382, 368, 214, 195, 142, 109, 83, 69, 55 (M100).

Elemental analysis: Expected /% C 76.74, H 8.11, S 3.79.
Found /% C 76.45, H 8.35, S 3.49.

2-Methacrylic acid 9-[2-fluoro-4-(7-{3-fluoro-4-[9-(2-methacryloyloxy)nonyloxy]phenyl}dibenzothiophene-3-yl)phenoxy]nonyl ester (**46**)

A mixture of 3,7-bis-(3-fluoro-4-hydroxyphenyl)dibenzothiophene (**34**) (0.20 g, 5.00 × 10⁻⁴ mol), 2-methacrylic acid 9-bromononyl ester (**42**) (0.69 g, 2.37 × 10⁻³ mol), potassium carbonate (0.33 g, 2.39 × 10⁻³ mol) and BHT (0.07 g, 3.20 × 10⁻⁴ mol) in DMF (25 cm³) was heated (60 °C) for 48 hours. The excess potassium carbonate was filtered off from the cooled reaction mixture and rinsed with DCM (3 × 30 cm³). The solution was concentrated onto silica gel for purification by column chromatography [silica gel, ethyl acetate:hexane, 30%:70%] followed by recrystallisation from a DCM:ethanol mixture (1:1) to yield 0.13 g (31.7%) of the desired product (white solid).

Transition temp. /°C: Cr 120 material polymerised.

¹H NMR (CDCl₃) δ_H: 1.36 (16H, s), 1.50 (4H, quint), 1.68 (4H, quint), 1.86 (4H, quint), 1.95 (6H, s), 4.09 (4H, t), 4.15 (4H, t), 5.53-5.57 (2H, m), 6.08-6.12 (2H, m), 7.06 (2H, t), 7.39 (2H, dt), 7.44 (2H, dd), 7.64 (2H, d, *J*=8.3 Hz), 8.00 (2H, s), 8.18 (2H, d, *J*=8.4 Hz).

IR ν_{max} /cm⁻¹: 2931, 2854, 1709 (C=O), 1637, 1466, 1312, 1281, 1185, 946, 823, 802.

MS (m/z) (EI): 825 (M^+), 404, 374, 316, 280, 214, 195, 165, 154, 142, 126, 107, 83, 69, 55 (M_{100}).

Elemental analysis: Expected /% C 72.79, H 7.09, S 3.89.
Found /% C 73.00, H 7.18, S 3.59.

2-Methacrylic acid 11-[2-fluoro-4-(7-{3-fluoro-4-[11-(2-methacryloyloxy)undecyloxy]phenyl}dibenzothiophene-3-yl)phenoxy]undecyl ester (**47**)

A mixture of 3,7-bis-(3-fluoro-4-hydroxyphenyl)dibenzothiophene (**34**) (0.20 g, 5.00×10^{-4} mol), 2-methacrylic acid 11-bromoundecyl ester (**43**) (0.78 g, 2.44×10^{-3} mol), potassium carbonate (0.32 g, 2.32×10^{-3} mol) and BHT (0.07 g, 3.20×10^{-4} mol) in DMF (25 cm³) was heated (60 °C) for 48 hours. The excess potassium carbonate was filtered off from the cooled reaction mixture and rinsed with DCM (3 \times 30 cm³). The solution was concentrated onto silica gel for purification by column chromatography [silica gel, ethyl acetate:hexane, 30%:70%] followed by recrystallisation from a DCM:ethanol mixture (1:1) to yield 0.10 g (22.7%) of the desired product (white solid).

Transition temp. /°C: Cr 116 material polymerised.

¹H NMR (CDCl₃) δ_H : 1.28-1.42 (24H, m), 1.50 (4H, quint), 1.67 (4H, quint), 1.86 (4H, quint), 1.95 (6H, s), 4.09 (4H, t), 4.14 (4H, t), 5.53-5.56 (2H, m), 6.08-6.11 (2H, m), 7.06 (2H, t), 7.39 (2H, dt), 7.43 (2H, dd), 7.63 (2H, d, $J=8.4$ Hz), 8.00 (2H, s), 8.18 (2H, d, $J=8.2$ Hz).

IR ν_{\max} /cm⁻¹: 2916, 2851, 1715 (C=O), 1639, 1469, 1313, 1284, 1187, 942, 824, 803.

MS (m/z) (EI): 881 (M^+), 795, 643, 404, 374, 280, 214, 195, 142, 107, 83, 69, 55 (M_{100}).

Elemental analysis: Expected /% C 73.60, H 7.55, S 3.64.
Found /% C 73.90, H 7.82, S 3.62.

3-(5-Bromopentyloxymethyl)-3-methyloxetane (**51**)

A two-phase system of 1,5-dibromopentane (**49**) (33.86 g, 0.15 mol), (3-methyloxetan-3-yl)methanol (**48**) (5.13 g, 0.05 mol), tetrabutylammonium bromide (TBAB) (0.80 g 2.48×10^{-3} mol) and sodium hydroxide (32.50 g, 0.81 mol) in hexane (50 cm³) and water (50 cm³) was heated under reflux for 2 hours. Distilled water (100

cm³) was added to the cooled reaction mixture and extracted with hexane (3 × 100 cm³). The combined organic layers were dried (MgSO₄), filtered and the filtrate was concentrated under reduced pressure. The crude product (pale yellow liquid) was purified by fractional distillation under reduced pressure to yield 4.03 g (31.9%) of the desired product (colourless liquid).

Boiling point /°C: 94-106 @ 1.5 mm Hg.

¹H NMR (CDCl₃) δ_H: 1.31 (3H, s), 1.52 (2H, quint), 1.62 (2H, quint), 1.89 (2H, quint), 3.42 (2H, t), 3.44-3.50 (4H, m), 4.34 (2H, d, *J*=5.9 Hz), 4.50 (2H, d, *J*=5.6 Hz).

IR ν_{max} /cm⁻¹: 2935, 2863, 1461, 1379, 1362, 1264, 1245, 1116, 562.

MS (m/z) (EI): 253 (M⁺), 251 (M⁺), 222, 220, 151, 149 (M100), 109, 107, 85, 69, 55, 41.

Elemental analysis: Expected /% C 47.82, H 7.62.

Found /% C 47.79, H 7.87.

3-(6-Bromohexyloxymethyl)-3-methyloxetane (**52**)

A two-phase system of 1,6-dibromohexane (**50**) (35.89 g, 0.15 mol), (3-methyloxetan-3-yl)methanol (**48**) (5.03 g, 0.05 mol), TBAB (0.81 g 2.51 × 10⁻³ mol) and sodium hydroxide (32.50 g, 0.81 mol) in hexane (50 cm³) and water (50 cm³) was heated under reflux for 2 hours. Distilled water (100 cm³) was added to the cooled reaction mixture and extracted with hexane (3 × 100 cm³). The combined organic layers were dried (MgSO₄), filtered and the filtrate was concentrated under reduced pressure. The crude product (yellow liquid) was purified by fractional distillation under reduced pressure to yield 8.17 g (62.9%) of the desired product (colourless liquid).

Boiling point /°C: 101-118 @ 1.5 mm Hg.

¹H NMR (CDCl₃) δ_H: 1.31 (3H, s), 1.35-1.50 (4H, m), 1.60 (2H, quint), 1.87 (2H, quint), 3.41 (2H, t), 3.43-3.49 (4H, m), 4.34 (2H, d, *J*=5.6 Hz), 4.50 (2H, d, *J*=5.6 Hz).

IR ν_{max} /cm⁻¹: 2935, 2863, 1461, 1379, 1362, 1264, 1245, 1116, 562.

MS (m/z) (EI): 267 (M⁺), 265 (M⁺), 236, 234, 193, 191, 165, 163, 123, 121, 103, 83, 72, 55 (M100), 41.

Elemental analysis: Expected /% C 49.82, H 7.98.

Found /% C 50.12, H 8.23.

3, 7-Bis-{4-[5-(3-methyloxetan-3-ylmethylenoxy)pentyloxy]phenyl}dibenzo-
thiophene (**53**)

A mixture of 3,7-bis-(4-hydroxyphenyl)dibenzothiophene (**24**) (0.20 g, 5.40×10^{-4} mol), 3-(5-bromopentyloxymethyl)-3-methyloxetane (**51**) (0.62 g, 2.47×10^{-3} mol) and potassium carbonate (0.30 g, 2.17×10^{-3} mol) in DMF (25 cm³) was heated (90 °C) for 48 hours. The excess potassium carbonate was filtered off from the cooled reaction mixture and rinsed with DCM (3 × 30 cm³). The solution was concentrated onto silica gel for purification by column chromatography [silica gel, ethyl acetate:hexane, 30%:70%] followed by recrystallisation from a DCM:ethanol mixture (1:1) to yield 0.23 g (59.0%) of the desired product (off-white solid).

Transition temp. /°C: Cr 169 SmX 196 SmC 250 SmA 260 I.

¹H NMR (CDCl₃) δ_H: 1.32 (6H, s), 1.58 (4H, quint), 1.69 (4H, quint), 1.85 (4H, quint), 3.48-3.55 (8H, m), 4.03 (4H, t), 4.37 (4H, d, *J*=5.6 Hz), 4.52 (4H, d, *J*=5.9 Hz), 7.00 (4H, d, *J*=8.7 Hz), 7.62 (4H, d, *J*=9.0 Hz), 7.65 (2H, d, *J*=8.3 Hz), 8.01 (2H, s), 8.16 (2H, d, *J*=8.2 Hz).

IR ν_{max} /cm⁻¹: 2933, 2863, 1518, 1464, 1385, 1294, 1248, 1115, 977, 835, 805, 722.

MS (m/z) (EI): 709 (M⁺), 679, 537, 430, 404, 368, 339, 289, 170, 152, 121, 112, 85, 69, 55 (M 100).

Elemental analysis: Expected /% C 74.54, H 7.39, S 4.52.

Found /% C 74.58, H 7.63, S 4.24.

3, 7-Bis-{4-[6-(3-methyloxetan-3-ylmethylenoxy)hexyloxy]phenyl}dibenzo-
thiophene (**54**)

A mixture of 3,7-bis-(4-hydroxyphenyl)dibenzothiophene (**24**) (0.20 g, 5.40×10^{-4} mol), 3-(6-bromohexyloxymethyl)-3-methyloxetane (**52**) (0.72 g, 2.72×10^{-3} mol) and potassium carbonate (0.30 g, 2.17×10^{-3} mol) in DMF (25 cm³) was heated (90 °C) for 48 hours. The excess potassium carbonate was filtered off from the cooled reaction mixture and rinsed with DCM (3 × 30 cm³). The solution was concentrated onto silica gel for purification by column chromatography [silica gel, ethyl acetate:hexane, 50%:50%] followed by recrystallisation from a DCM:ethanol mixture (1:1) to yield 0.22 g (55.0%) of the desired product (off-white solid).

Transition temp. /°C: Cr 125 SmX 193 SmC 247 SmA 251 I.

^1H NMR (CDCl_3) δ_{H} : 1.31 (6H, s), 1.40-1.56 (4H, m), 1.64 (4H, quint), 1.82 (4H, quint), 3.45-3.52 (8H, m), 4.01 (4H, t), 4.36 (4H, d, $J=5.6$ Hz), 4.52 (4H, d, $J=5.6$ Hz), 7.00 (4H, d, $J=8.7$ Hz), 7.61 (4H, d, $J=8.7$ Hz), 7.65 (2H, d, $J=8.3$ Hz), 8.01 (2H, s), 8.15 (2H, d, $J=8.1$ Hz).

IR ν_{max} / cm^{-1} : 2936, 2863, 1517, 1464, 1392, 1295, 1245, 1117, 978, 836, 805, 721.

MS (m/z) (EI): 737 (M^+), 707, 552, 430, 368, 308, 289, 246, 170, 133, 120, 107, 97, 83, 69, 55 (M 100).

Elemental analysis: Expected /% C 74.97, H 7.66, S 4.35.

Found /% C 75.21, H 7.85, S 4.09.

3, 7-Bis-{3-fluoro-4-[5-(3-methyloxetan-3-ylmethylenoxy)pentyl]oxy}phenyl} dibenzothiophene (**55**)

A mixture of 3,7-bis-(3-fluoro-4-hydroxyphenyl)dibenzothiophene (**34**) (0.20 g, 5.00×10^{-4} mol), 3-(5-bromopentylmethyl)-3-methyloxetane (**51**) (0.74 g, 2.95×10^{-3} mol) and potassium carbonate (0.30 g, 2.17×10^{-3} mol) in DMF (25 cm^3) was heated (90 °C) for 48 hours. The excess potassium carbonate was filtered off from the cooled reaction mixture and rinsed with DCM (3 \times 30 cm^3). The solution was concentrated onto silica gel for purification by column chromatography [silica gel, ethyl acetate:hexane, 50%:50%] followed by recrystallisation from a DCM:ethanol mixture (1:1) to yield 0.19 g (51.4%) of the desired product (white solid).

Transition temp. /°C: Cr 108 SmX 124 SmC 201 SmA 215 I.

^1H NMR (CDCl_3) δ_{H} : 1.32 (6H, s), 1.59 (4H, m), 1.70 (4H, quint), 1.89 (4H, quint), 3.47-3.54 (8H, m), 4.10 (4H, t), 4.37 (4H, d, $J=5.6$ Hz), 4.52 (4H, d, $J=5.6$ Hz), 7.05 (2H, t), 7.38 (2H, dt), 7.43 (2H, dd), 7.63 (2H, d, $J=8.3$ Hz), 7.99 (2H, s), 8.17 (2H, d, $J=8.2$ Hz).

IR ν_{max} / cm^{-1} : 2939, 2864, 1528, 1467, 1395, 1282, 1236, 1130, 977, 835, 804, 709.

MS (m/z) (EI): 745 (M^+), 574, 404, 375, 246, 195, 141, 103, 85, 69, 55 (M 100).

Elemental analysis: Expected /% C 70.94, H 6.77, S 4.30.

Found /% C 70.79, H 6.70, S 4.04.

3, 7-Bis-{3-fluoro-4-[6-(3-methyloxetan-3-ylmethylenoxy)hexyloxy]phenyl}
dibenzothiophene (**56**)

A mixture of 3,7-bis-(3-fluoro-4-hydroxyphenyl)dibenzothiophene (**34**) (0.20 g, 5.00×10^{-4} mol), 3-(6-bromohexyloxymethyl)-3-methyloxetane (**52**) (0.76 g, 2.87×10^{-3} mol) and potassium carbonate (0.31 g, 2.24×10^{-3} mol) in DMF (25 cm³) was heated (90 °C) for 48 hours. The excess potassium carbonate was filtered off from the cooled reaction mixture and rinsed with DCM (3 × 30 cm³). The solution was concentrated onto silica gel for purification by column chromatography [silica gel, ethyl acetate:hexane, 50%:50%] followed by recrystallisation from a DCM:ethanol mixture (1:1) to yield 0.23 g (60.5%) of the desired product (white solid).

Transition temp. /°C: Cr 73 SmX 128 SmC 201 SmA 212 I.

¹H NMR (CDCl₃) δ_H: 1.31 (6H, s), 1.41-1.57 (8H, m), 1.64 (4H, quint), 1.87 (4H, quint), 3.45-3.53 (8H, m), 4.08 (4H, t), 4.36 (4H, d, *J*=5.9 Hz), 4.52 (4H, d, *J*=5.6 Hz), 7.04 (2H, t), 7.37 (2H, dt), 7.42 (2H, dd), 7.62 (2H, d, *J*=8.1 Hz), 7.98 (2H, s), 8.15 (2H, d, *J*=8.2 Hz).

IR ν_{max} /cm⁻¹: 2934, 2859, 1526, 1466, 1396, 1284, 1244, 1132, 978, 835, 804, 712.

MS (m/z) (EI): 773 (M⁺), 588, 430, 404, 246, 195, 170, 133, 107, 91, 83, 69, 55 (M 100).

Elemental analysis: Expected /% C 71.48, H 7.04, S 4.15.
Found /% C 71.20, H 7.34, S 3.88.

(s)-2-[4-(3,7-Dimethyl-oct-6-enyloxy)phenyl]-4,4,5,5-tetramethyl-[1,3,2]-
dioxaborolane (**59**)

n-Butyllithium in hexanes (40.16 cm³, 2.5 M, 0.10 mol) was added dropwise to a cooled (-78 °C) solution of (s)-1-bromo-4-(3,7-dimethyl-oct-6-enyloxy)benzene (**21**) (26.04 g, 0.08 mol) in sodium dried THF (250 cm³). The resulting solution was stirred at this temperature for 1 hour and then 2-isopropoxy-4,4,5,5-tetramethyl-[1,3,2]-dioxaborolane (**57**) (17.12 g, 0.09 mol) in sodium dried THF (30 cm³) was added dropwise to the reaction mixture whilst maintaining the temperature at -78 °C. Once the addition was complete, the reaction mixture was stirred and allowed to reach RT overnight. The reaction mixture was then quenched by the addition of distilled water (200 cm³), extracted into diethyl ether (3 × 150 cm³) and the combined ethereal

extracts were washed with brine (200 cm³) and dried (MgSO₄). After filtration the solution was concentrated and purified by column chromatography [silica gel, DCM:hexane, 40%:60%] to yield 18.32 g (61.1%) of the desired product (yellow/orange oil).

Purity: >97% (GC).

¹H NMR (CDCl₃) δ_H: 0.95 (3H, d), 1.17-1.26 (2H, m), 1.33 (12H, s), 1.36-1.44 (1H, m), 1.61 (3H, s), 1.68 (3H, s), 1.79-1.88 (2H, m), 1.92-2.08 (2H, m), 3.96-4.06 (2H, m), 5.10 (1H, t), 6.88 (2H, d, *J*=8.7 Hz), 7.74 (2H, d, *J*=8.7 Hz).

IR ν_{max} /cm⁻¹: 2929, 1605, 1569, 1458, 1356, 1276, 1247, 1176, 1143, 861, 832.

MS (m/z) (EI): 358 (M⁺), 331, 273, 220, 205, 163, 134, 121, 109, 95, 84, 69, 49 (M100).

(s)-2,5-Bis-[4-(3,7-dimethyl-oct-6-enyloxy)phenyl]thiophene (**60**)

Tetrakis(triphenylphosphine)palladium(0) (1.07 g, 9.30 × 10⁻² mol) was added to a mixture of 2,5-dibromothiophene (**58**) (2.62 g, 0.01 mol), (s)-2-[4-(3,7-dimethyl-oct-6-enyloxy)phenyl]-4,4,5,5-tetramethyl-[1,3,2]-dioxaborolane (**59**) (8.20 g, 0.02 mol) and tripotassium phosphate (5.49 g, 0.03 mol) in DMF (90 cm³) at RT. The reaction mixture was then heated (90 °C) for 48 hours. The cooled reaction mixture was poured into distilled water (150 cm³) and extracted with dichloromethane (3 × 150 cm³) and the combined organic layers were washed with brine (200 cm³) and dried (MgSO₄). After filtration, the solution was concentrated onto silica gel for purification by column chromatography [silica gel, DCM:hexane, 40%:60%] followed by recrystallisation from a DCM:ethanol mixture (3:1) to yield 3.84 g (68.2%) of the desired product (yellow solid).

Transition temp. /°C: Cr 100 I.

¹H NMR (CDCl₃) δ_H: 0.97 (6H, d), 1.19-1.28 (4H, m), 1.34-1.46 (2H, m), 1.62 (6H, s), 1.69 (6H, s), 1.81-1.90 (4H, m), 1.94-2.09 (4H, m), 3.97-4.08 (4H, m), 5.12 (2H, t), 6.91 (4H, d, *J*=9.0 Hz), 7.14 (2H, s), 7.53 (4H, d, *J*=9.0 Hz).

IR ν_{max} /cm⁻¹: 2966, 2927, 1608, 1501, 1476, 1458, 1252, 1179, 1115, 831, 798.

MS (m/z) (EI): 544 (M⁺), 406, 289, 268, 239, 137, 121, 95, 83, 69 (M100), 55.

Elemental analysis: Expected /% C 79.36, H 8.88, S 5.89.

Found /% C 79.10, H 9.04, S 6.00.

2,5-Bis-(4-hydroxyphenyl)thiophene (**61**)

Boron tribromide (6.81 g, 2.57 cm^3 , $2.72 \times 10^{-2} \text{ mol}$) in dichloromethane (20 cm^3) was added dropwise to a cooled (0°C), stirred solution of (s)-2,5-bis-[4-(3,7-dimethyl-oct-6-enyloxy)phenyl]thiophene (**60**) (3.70 g, $6.79 \times 10^{-3} \text{ mol}$) in dichloromethane (220 cm^3). The reaction mixture was stirred and allowed to reach RT overnight. The reaction mixture was then poured onto an ice/water mixture (350 g), DCM was added (400 cm^3) and the resulting mixture stirred (2 hours). The precipitate was filtered off, washed with hot DCM ($2 \times 30 \text{ cm}^3$) and pulled dry under vacuum to yield 1.66 g (91.2%) of the desired product (light green solid).

Melting point $^\circ\text{C}$: >239 (material decomposition).

^1H NMR (DMSO) δ_{H} : 6.80 (4H, d, $J=8.7 \text{ Hz}$), 7.25 (2H, s), 7.46 (4H, d, $J=8.7 \text{ Hz}$), 9.63 (2H, s-OH).

IR $\nu_{\text{max}}/\text{cm}^{-1}$: 3300, 1607, 1592, 1545, 1499, 1450, 835, 799.

MS (m/z) (EI): 268 (M^+), 239, 206, 189, 178, 165, 150, 137, 118, 102, 94 (M100), 77, 65, 55.

8-[4-(5-{4-[7-(1-Vinyl-allyloxycarbonyl)heptyloxy]phenyl}thiophen-2-yl)phenoxy]octanoic acid 1-vinyl-allyl ester (**62**)

A mixture of 2,5-bis-(4-hydroxyphenyl)thiophene (**61**) (0.15 g, $5.60 \times 10^{-4} \text{ mol}$), 8-bromooctanoic acid 1-vinyl-allyl ester (**17**) (0.74 g , $2.56 \times 10^{-3} \text{ mol}$) and potassium carbonate (0.31 g , $2.24 \times 10^{-3} \text{ mol}$) in DMF (20 cm^3) was heated (90°C) for 48 hours. The excess potassium carbonate was filtered off from the cooled reaction mixture and rinsed with DCM ($3 \times 30 \text{ cm}^3$). The solution was concentrated onto silica gel for purification by column chromatography [silica gel, DCM] followed by recrystallisation from a DCM:ethanol mixture (2:1) to yield 0.10 g (26.3%) of the desired product (yellow solid).

Transition temp. $^\circ\text{C}$: Cr 52 SmX 86 SmC 111 I.

^1H NMR (CDCl_3) δ_{H} : 1.32-1.52 (12H, m), 1.65 (4H, quint), 1.79 (4H, quint), 2.36 (4H, t), 3.97 (4H, t), 5.23 (4H, dt), 5.30 (4H, dt), 5.72 (2H, tt), 5.79-5.89 (4H, m), 6.90 (4H, d, $J=8.7 \text{ Hz}$), 7.14 (2H, s), 7.52 (4H, d, $J=8.7 \text{ Hz}$).

IR $\nu_{\text{max}}/\text{cm}^{-1}$: 3088, 2934, 2857, 1736 (C=O), 1639, 1607, 1502, 1468, 1250, 1179, 989, 931, 831, 797.

MS (m/z) (EI): 685 (M^+), 624, 534, 476, 374, 268, 239, 214, 121, 97, 83, 67 ($\text{M}100$), 55.

Elemental analysis: Expected /% C 73.65, H 7.65, S 4.68.
 Found /% C 73.94, H 7.89, S 4.40.

5,5'-Dibromo-[2,2']-bithiophene (**64**)

N-Bromosuccinimide (8.90 g, 50.00 mmol), freshly purified by recrystallisation from distilled water, was added slowly (over a period of 3 hours) to a solution of [2,2']-bithiophene (**63**) (4.13 g, 24.84 mmol) in acetic acid (50 cm^3) and chloroform (50 cm^3). Once the addition was complete, additional chloroform (15 cm^3) was added and the reaction mixture was heated under reflux for 1 hour. The solution was then allowed to cool to RT and any precipitated product filtered off. The filtrate was washed with sodium metabisulphite solution (100 cm^3) and distilled water (100 cm^3). The solution was concentrated to a pale green solid and combined with previously precipitated product and purified by recrystallisation from ethanol to yield 7.29 g (90.6%) of the desired product (pearly-white flakes).

Melting point / $^{\circ}\text{C}$: 147-149 (Lit. 149-151)^[24].

^1H NMR (CDCl_3) δ_{H} : 6.85 (2H, d, $J=3.9$ Hz), 6.96 (2H, d, $J=3.9$ Hz).

IR $\nu_{\text{max}}/\text{cm}^{-1}$: 1504, 1416, 1197, 970, 867, 795.

MS (m/z) (EI): 324 (M^+) ($\text{M}100$), 279, 245, 243, 201, 199, 164, 149, 120, 95, 83, 71, 41.

Elemental analysis: Expected /% C 29.65, H 1.24, S 19.79.
 Found /% C 29.83, H 1.21, S 19.70.

(s)-5,5'-Bis-[4-(3,7-dimethyl-oct-6-enyloxy)phenyl]-[2,2']-bithiophene (**65**)

Tetrakis(triphenylphosphine)palladium(0) (0.78 g, 6.80×10^{-2} mol) was added to a mixture of 5,5'-dibromo-[2,2']-bithiophene (**64**) (2.50 g, 7.72 mmol), (s)-2-[4-(3,7-dimethyl-oct-6-enyloxy)phenyl]-4,4,5,5-tetramethyl[1,3,2]dioxaborolane (**59**) (6.08 g, 16.97 mmol) and tripotassium phosphate (4.21 g, 19.83 mmol) in DMF (90 cm^3) at RT. The reaction mixture was then heated (90 $^{\circ}\text{C}$) for 48 hours. The cooled reaction mixture was poured into distilled water (150 cm^3) and extracted with dichloromethane (3 \times 150 cm^3) and the combined organic layers were washed with brine (200 cm^3) and

dried (MgSO₄). After filtration, the solution was concentrated onto silica gel for purification by column chromatography [silica gel, DCM:hexane, 40%:60%] followed by recrystallisation from a DCM:ethanol mixture (2:1) to yield 3.25 g (67.2%) of the desired product (yellow solid).

Transition temp. /°C: Cr 185 I.

¹H NMR (CDCl₃) δ_H: 0.97 (6H, d), 1.19-1.29 (4H, m), 1.36-1.46 (2H, m), 1.62 (6H, s), 1.69 (6H, s), 1.80-1.90 (4H, m), 1.97-2.08 (4H, m), 3.98-4.08 (4H, m), 5.11 (2H, t), 6.91 (4H, d, *J*=8.7 Hz), 7.11 (4H, s), 7.51 (4H, d, *J*=8.7 Hz).

IR ν_{max} /cm⁻¹: 2965, 2926, 1606, 1499, 1253, 1178, 826, 794.

MS (m/z) (EI): 626 (M⁺), 488, 350, 321, 292, 213, 138, 109, 95, 83, 69 (M100), 55.

Elemental analysis: Expected /% C 76.63, H 8.04, S 10.23.
Found /% C 76.78, H 8.22, S 10.46.

5,5'-Bis(4-hydroxyphenyl)-[2,2']-bithiophene (**66**)

Boron tribromide (4.98 g, 1.88 cm³, 19.89 mmol) in dichloromethane (20 cm³) was added dropwise to a cooled (0 °C), stirred solution of (s)-5,5'-bis-[4-(3,7-dimethyloct-6-enyloxy)phenyl]-[2,2']-bithiophene (**65**) (3.11 g, 4.96 mmol) in dichloromethane (250 cm³). The reaction mixture was stirred and allowed to reach RT overnight. The reaction mixture was then poured onto an ice/water mixture (350 g), DCM was added (400 cm³) and the resulting mixture stirred (2 hours). The precipitate was filtered off, washed with hot DCM (2 × 30 cm³) and pulled dry under vacuum to yield 1.69 g (97.1%) of the desired product (green solid).

Melting Point /°C: > 300 (material decomposition).

¹H NMR (DMSO) δ_H: 6.81 (4H, d, *J*=8.7 Hz), 7.24 (2H, d, *J*=3.7 Hz), 7.28 (2H, d, *J*=3.9 Hz), 7.48 (4H, d, *J*=8.7 Hz), 9.71 (2H, s-OH).

IR ν_{max} /cm⁻¹: 3402, 1607, 1531, 1498, 1444, 1376, 1251, 1175, 1107, 828, 795.

MS (m/z) (EI): 350 (M⁺) (M100), 321, 258, 213, 200, 175, 150, 137, 118, 94, 77, 69, 45.

8-[4-(5'-{4-[7-(1-Vinyl-allyloxycarbonyl)heptyloxy]phenyl}-[2,2']-bithiophene-5-yl)phenoxy]octanoic acid 1-vinyl-allyl-ester (**67**)

A mixture of 5,5'-bis(4-hydroxyphenyl)-[2,2']-bithiophene (**66**) (0.30 g, 8.60×10^{-2} mol), 8-bromooctanoic acid 1-vinyl-allyl ester (**17**) (0.88 g, 3.04×10^{-3} mol) and potassium carbonate (0.47 g, 3.40×10^{-3} mol) in DMF (10 cm³) was heated (90 °C) for 48 hours. The excess potassium carbonate was filtered off from the cooled reaction mixture and rinsed with DCM (3 \times 30 cm³). The solution was concentrated onto silica gel for purification by column chromatography [silica gel, DCM] followed by recrystallisation from a DCM:ethanol mixture (2:1) to yield 0.17 g (25.8%) of the desired product (yellow solid).

Transition temp. /°C: Cr 50 SmX 119 SmC 184 SmA 192 I.

¹H NMR (CDCl₃) δ_{H} : 1.33-1.51 (12H, m), 1.67 (4H, quint), 1.79 (4H, quint), 2.36 (4H, t), 3.97 (4H, t), 5.23 (4H, dt), 5.30 (4H, dt), 5.72 (2H, tt), 5.79-5.89 (4H, m), 6.90 (4H, d, $J=9.0$ Hz), 7.11 (4H, s), 7.51 (4H, d, $J=9.0$ Hz).

IR $\nu_{\text{max}}/\text{cm}^{-1}$: 2935, 2856, 1736 (C=O), 1640, 1606, 1500, 1449, 1254, 1178, 929, 828, 795.

MS (m/z) (EI): 767 (M⁺), 616, 557, 349, 321, 167, 138, 105, 91, 83, 67 (M100), 55.

Elemental analysis: Expected /% C 72.03, H 7.10, S 8.36.

Found /% C 72.25, H 7.24, S 8.18.

11-[4-(5'-{4-[10-(1-Vinyl-allyloxycarbonyl)decyloxy]phenyl}-[2,2']-bithiophene-5-yl)phenoxy]undecanoic acid 1-vinyl-allyl-ester (**68**)

A mixture of 5,5'-bis(4-hydroxyphenyl)-[2,2']-bithiophene (**66**) (0.25 g, 7.10×10^{-2} mol), 11-bromoundecanoic acid 1-vinyl-allyl ester (**18**) (0.71 g, 2.14×10^{-3} mol) and potassium carbonate (0.39 g, 2.82×10^{-3} mol) in DMF (10 cm³) was heated (90 °C) for 48 hours. The excess potassium carbonate was filtered off from the cooled reaction mixture and rinsed with DCM (3 \times 30 cm³). The solution was concentrated onto silica gel for purification by column chromatography [silica gel, DCM] followed by recrystallisation from a DCM:ethanol mixture (2:1) to yield 0.30 g (49.2%) of the desired product (yellow solid).

Transition temp. /°C: Cr 97 SmX 127 SmC 182 SmA 186 I.

^1H NMR (CDCl_3) δ_{H} : 1.30 (20H, s), 1.46 (4H, quint), 1.64 (4H, quint), 1.79 (4H, quint), 2.34 (4H, t), 3.98 (4H, t), 5.22 (4H, dt), 5.30 (4H, dt), 5.72 (2H, tt), 5.79-5.88 (4H, m), 6.90 (4H, d, $J=9.0$ Hz), 7.11 (4H, s), 7.51 (4H, d, $J=8.7$ Hz).

IR $\nu_{\text{max}}/\text{cm}^{-1}$: 2918, 2851, 1737 (C=O), 1640, 1607, 1501, 1474, 1258, 1178, 1114, 922, 831, 792.

MS (m/z) (EI): 851 (M^+), 564, 537, 424, 406, 321, 298, 261, 254, 186, 121, 109, 87, 73, 67, 55 ($\text{M}100$).

Elemental analysis: Expected /% C 73.37, H 7.82, S 7.53.
Found /% C 73.52, H 7.94, S 7.34.

2-Methacrylic acid 9-[4-(5'-{4-[9-(2-methacryloyloxy)nonyloxy]phenyl}-[2,2']-bithiophene-5-yl)phenoxy]nonyl ester (**69**)

A mixture of 5,5'-bis(4-hydroxyphenyl)-[2,2']-bithiophene (**66**) (0.30 g, 8.60×10^{-2} mol), 2-methacrylic acid 9-bromononyl ester (**42**) (0.89 g, 3.06×10^{-3} mol), BHT (0.07 g, 3.20×10^{-2} mol), and potassium carbonate (0.47 g, 3.40×10^{-3} mol) in DMF (10cm^3) was heated (55°C) for 48 hours. The excess potassium carbonate was filtered off from the cooled reaction mixture and rinsed with DCM ($3 \times 30\text{ cm}^3$). The solution was concentrated onto silica gel for purification by column chromatography [silica gel, DCM] followed by recrystallisation from a DCM:ethanol mixture (2:1) to yield 0.41 g (62.1%) of the desired product (yellow solid).

Transition temp. $^\circ\text{C}$: Cr 108 SmC 171 SmA 180 I.

^1H NMR (CDCl_3) δ_{H} : 1.35 (16H, s), 1.47 (4H, quint), 1.68 (4H, quint), 1.80 (4H, quint), 1.94 (6H, s), 3.98 (4H, t), 4.14 (4H, t), 5.53-5.56 (2H, m), 6.08-6.11 (2H, m), 6.91 (4H, d, $J=9.0$ Hz), 7.11 (4H, s), 7.51 (4H, d, $J=9.0$ Hz).

IR $\nu_{\text{max}}/\text{cm}^{-1}$: 2933, 2853, 1714 (C=O), 1640, 1500, 1332, 1252, 1180, 933, 831, 792.

MS (m/z) (EI): 771 (M^+) ($\text{M}100$), 685, 559, 473, 350, 321, 268, 195, 138, 109, 83, 69, 55.

Elemental analysis: Expected /% C 71.65, H 7.58, S 8.32.
Found /% C 71.42, H 7.76, S 8.05.

5, 5'-Bis-{4-[6-(3-methyloxetan-3-ylmethylenoxy)hexyloxy]phenyl}-[2,2']-bithiophene (**70**)

A mixture of 5,5'-bis(4-hydroxyphenyl)-[2,2']-bithiophene (**66**) (0.15 g, 4.30×10^{-2} mol), 3-(6-bromohexyloxymethyl)-3-methyloxetane (**52**) (0.75 g, 2.83×10^{-3} mol) and potassium carbonate (0.31 g, 2.24×10^{-3} mol) in DMF (20 cm³) was heated (90 °C) for 48 hours. The excess potassium carbonate was filtered off from the cooled reaction mixture and rinsed with DCM (3 × 30 cm³). The solution was concentrated onto silica gel for purification by column chromatography [silica gel, ethyl acetate:hexane, 60%:40%] followed by recrystallisation from a DCM:ethanol mixture (2:1) to yield 0.11 g (35.5%) of the desired product (yellow solid).

Transition temp. /°C: Cr 122 SmX 180 SmC 185 I.

¹H NMR (CDCl₃) δ_H: 1.31 (6H, s), 1.40-1.55 (8H, m), 1.63 (4H, quint), 1.81 (4H, quint), 3.45-3.51 (8H, m), 3.99 (4H, t), 4.36 (4H, d, *J*=5.9 Hz), 4.51 (4H, d, *J*=5.9 Hz), 6.91 (4H, d, *J*=8.7 Hz), 7.11 (4H, s), 7.52 (4H, d, *J*=8.7 Hz).

IR ν_{max} /cm⁻¹: 2936, 2864, 1606, 1500, 1448, 1282, 1253, 1179, 1115, 979, 830, 795.

MS (m/z) (EI): 719 (M⁺), 689, 625, 533, 350, 321, 289, 214, 138, 121, 104, 91, 83, 67, 55 (M 100).

Elemental analysis: Expected /% C 70.16, H 7.57, S 8.92.

Found /% C 70.00, H 7.71, S 9.14.

(s)-2-[4-(3,7-Dimethyl-oct-6-enyloxy)-3-fluorophenyl]-4,4,5,5-tetramethyl-[1,3,2]-dioxaborolane (**71**)

n-Butyllithium in hexanes (39.49 cm³, 2.5 M, 0.08 mol) was added dropwise to a cooled (-78 °C) solution of (s)-4-bromo-1-(3,7-dimethyl-oct-6-enyloxy)-2-fluorobenzene (**31**) (27.09 g, 0.08 mol) in sodium dried THF (260 cm³). The resulting solution was stirred at this temperature for 1 hour and then 2-isopropoxy-4,4,5,5-tetramethyl-[1,3,2]-dioxaborolane (**57**) (16.84 g, 0.09 mol) in sodium dried THF (30 cm³) was added dropwise to the reaction mixture whilst maintaining the temperature at -78 °C. Once the addition was complete, the reaction mixture was stirred and allowed to reach RT overnight. The reaction mixture was then quenched by the addition of distilled water (200 cm³), extracted into diethyl ether (3 × 150 cm³) and the combined ethereal extracts were washed with brine (200 cm³) and dried (MgSO₄).

After filtration the solution was concentrated and purified by column chromatography [silica gel, DCM:hexane, 40%:60%] to yield 15.35 g (49.6%) of the desired product (pale yellow oil).

Purity: >97% (GC).

^1H NMR (CDCl_3) δ_{H} : 0.96 (3H, d), 1.17-1.27 (2H, m), 1.35 (12H, s), 1.36-1.44 (1H, m), 1.60 (3H, s), 1.68 (3H, s), 1.83-1.91 (2H, m), 1.94-2.07 (2H, m), 4.00-4.14 (2H, m), 5.10 (1H, t), 6.94 (1H, t), 7.46-7.52 (2H, m).

IR ν_{max} / cm^{-1} : 2978, 2930, 1615, 1522, 1423, 1360, 1269, 1203, 1133, 966, 855, 740.

MS (m/z) (EI): 376 (M^+), 291, 238, 223, 152, 138, 123, 109, 95, 83, 69, (M100), 55.

(s)-5,5'-Bis-[4-(3,7-dimethyl-oct-6-enyloxy)-3-fluorophenyl]-[2,2']-bithiophene (**72**)

Tetrakis(triphenylphosphine)palladium(0) (0.55 g, 4.80×10^{-2} mol) was added to a mixture of 5,5'-dibromo-[2,2']-bithiophene (**64**) (1.76 g, 5.43 mmol), (s)-2-[4-(3,7-dimethyl-oct-6-enyloxy)-3-fluorophenyl]-4,4,5,5-tetramethyl-[1,3,2]-dioxaborolane (**71**) (4.51 g, 11.99 mmol) and tripotassium phosphate (2.88 g, 13.57 mmol) in DMF (60 cm^3) at RT. The reaction mixture was then heated (90 $^{\circ}\text{C}$) for 48 hours. The cooled reaction mixture was poured into distilled water (150 cm^3) and extracted with dichloromethane (3 \times 150 cm^3) and the combined organic layers were washed with brine (200 cm^3) and dried (MgSO_4). After filtration, the solution was concentrated onto silica gel for purification by column chromatography [silica gel, DCM:hexane, 40%:60%] followed by recrystallisation from a DCM:ethanol mixture (3:1) to yield 2.15 g (60.1%) of the desired product (yellow solid).

Transition temp. / $^{\circ}\text{C}$: Cr 144 I.

^1H NMR (CDCl_3) δ_{H} : 0.97 (6H, d), 1.19-1.28 (4H, m), 1.36-1.45 (2H, m), 1.61 (6H, s), 1.69 (6H, s), 1.84-1.93 (4H, m), 1.96-2.07 (4H, m), 4.01-4.13 (4H, m), 5.11 (2H, t), 6.96 (2H, t), 7.11 (4H, s), 7.25-7.35 (4H, m).

IR ν_{max} / cm^{-1} : 2914, 1617, 1537, 1504, 1452, 1276, 1131, 864, 798.

MS (m/z) (EI): 663 (M^+), 662, 524, 386, 289, 276, 138, 121, 109, 95, 83, 69 (M100), 55.

Elemental analysis: Expected /% C 72.47, H 7.30, S 9.67.

Found /% C 72.19, H 7.41, S 9.46.

5,5'-Bis(3-fluoro-4-hydroxyphenyl)-[2,2']-bithiophene (**73**)

Boron tribromide (5.26 g, 1.99 cm³, 21.03 mmol) in dichloromethane (20 cm³) was added dropwise to a cooled (0 °C), stirred solution of (s)-5,5'-bis-[4-(3,7-dimethyloct-6-enyloxy)-3-fluorophenyl]-[2,2']-bithiophene (**72**) (3.48 g, 5.25 mmol) in dichloromethane (230 cm³). The reaction mixture was stirred and allowed to reach RT overnight. The reaction mixture was then poured onto an ice/water mixture (350 g), DCM was added (400 cm³) and the resulting mixture stirred (2 hours). The precipitate was filtered off, washed with hot DCM (2 × 30 cm³) and pulled dry under vacuum to yield 1.77 g (87.2%) of the desired product (light green solid).

Melting Point /°C: > 278 (material decomposition).

¹H NMR (DMSO) δ_H: 6.99 (2H, t), 7.28 (4H, s), 7.38 (2H, s), 7.50 (2H, dd), 10.15 (2H, s-OH).

IR ν_{max} /cm⁻¹: 3355, 1620, 1535, 1501, 1436, 1389, 1291, 1115, 859, 794.

MS (m/z) (EI): 386 (M⁺), 360 (M100), 324, 267, 219, 195, 180, 155, 136, 121, 107, 88, 69, 45.

8-[2-Fluoro-4-(5'-{3-fluoro-4-[7-(1-vinyl-allyloxycarbonyl)heptyloxy]phenyl}-[2,2']-bithiophene-5-yl)phenoxy]octanoic acid 1-vinyl-allyl-ester (**74**)

A mixture of 5,5'-bis(3-fluoro-4-hydroxyphenyl)-[2,2']-bithiophene (**73**) (0.25 g, 6.50 × 10⁻² mol), 8-bromooctanoic acid 1-vinyl-allyl ester (**17**) (0.71 g, 2.46 × 10⁻³ mol) and potassium carbonate (0.36 g, 2.61 × 10⁻³ mol) in DMF (10cm³) was heated (90 °C) for 48 hours. The excess potassium carbonate was filtered off from the cooled reaction mixture and rinsed with DCM (3 × 30 cm³). The solution was concentrated onto silica gel for purification by column chromatography [silica gel, DCM] followed by recrystallisation from a DCM:ethanol mixture (2:1) to yield 0.21 g (40.4%) of the desired product (yellow solid).

Transition temp. /°C: Cr 141 SmC 154 I.

¹H NMR (CDCl₃) δ_H: 1.32-1.43 (8H, m), 1.49 (4H, quint), 1.67 (4H, quint), 1.83 (4H, quint), 2.36 (4H, t), 4.05 (4H, t), 5.23 (4H, dt), 5.30 (4H, dt), 5.72 (2H, tt), 5.79-5.89 (4H, m), 6.95 (2H, t), 7.11 (4H, s), 7.25-7.34 (4H, m).

IR $\nu_{\max}/\text{cm}^{-1}$: 2935, 2857, 1737 (C=O), 1641, 1537, 1504, 1429, 1277, 1173, 1131, 996, 864, 791.

MS (m/z) (EI): 803 (M^+), 653, 594, 386, 254, 195, 138, 121, 91, 83, 67 (M100), 55.

Elemental analysis: Expected /% C 68.80, H 6.53, S 7.99.
Found /% C 68.79, H 6.72, S 7.72.

11-[2-Fluoro-4-(5'-{3-fluoro-4-[10-(1-vinyl-allyloxycarbonyl)decyloxy]phenyl}-[2,2']-bithiophene-5-yl)phenoxy]undecanoic acid 1-vinyl-allyl-ester (**75**)

A mixture of 5,5'-bis(3-fluoro-4-hydroxyphenyl)-[2,2']-bithiophene (**73**) (0.15 g, 3.90×10^{-2} mol), 11-bromoundecanoic acid 1-vinyl-allyl ester (**18**) (0.68 g, 2.05×10^{-3} mol) and potassium carbonate (0.29 g, 2.10×10^{-3} mol) in DMF (20 cm³) was heated (90 °C) for 48 hours. The excess potassium carbonate was filtered off from the cooled reaction mixture and rinsed with DCM (3 \times 30 cm³). The solution was concentrated onto silica gel for purification by column chromatography [silica gel, DCM:hexane, 90%:10%] followed by recrystallisation from a DCM:ethanol mixture (2:1) to yield 0.19 g (55.9%) of the desired product (yellow solid).

Transition temp. /°C: Cr 79 SmX 140 SmC 144 I.

¹H NMR (CDCl₃) δ_{H} : 1.30 (20H, s), 1.47 (4H, quint), 1.62 (4H, quint), 1.83 (4H, quint), 2.34 (4H, t), 4.05 (4H, t), 5.23 (4H, dt), 5.30 (4H, dt), 5.72 (2H, tt), 5.79-5.89 (4H, m), 6.96 (2H, t), 7.12 (4H, s), 7.25-7.36 (4H, m).

IR $\nu_{\max}/\text{cm}^{-1}$: 2918, 2851, 1737 (C=O), 1619, 1538, 1505, 1474, 1428, 1281, 1172, 1133, 922, 868, 790.

MS (m/z) (EI): 887 (M^+), 737, 625, 539, 499, 386, 289, 214, 138, 121, 83, 67, (M100), 55.

Elemental analysis: Expected /% C 70.40, H 7.27, S 7.23.
Found /% C 70.28, H 7.52, S 7.04.

2-Methacrylic acid 9-[2-fluoro-4-(5'-{3-fluoro-4-[9-(2-methacryloyloxy)nonyloxy]phenyl}-[2,2']-bithiophene-5-yl)phenoxy]nonyl ester (**76**)

A mixture of 5,5'-bis(3-fluoro-4-hydroxyphenyl)-[2,2']-bithiophene (**73**) (0.25 g, 6.50×10^{-2} mol), 2-methacrylic acid 9-bromononyl ester (**42**) (0.60 g, 2.06×10^{-3} mol), BHT (0.07 g, 3.20×10^{-2} mol), and potassium carbonate (0.36 g, 2.61×10^{-3} mol) in

DMF (10cm³) was heated (55 °C) for 48 hours. The excess potassium carbonate was filtered off from the cooled reaction mixture and rinsed with DCM (3 × 30 cm³). The solution was concentrated onto silica gel for purification by column chromatography [silica gel, DCM] followed by recrystallisation from a DCM:ethanol mixture (2:1) to yield 0.30 g (57.7%) of the desired product (yellow solid).

Transition temp. /°C: Cr 106 SmX 116 SmC 129 N 140 I.

¹H NMR (CDCl₃) δ_H: 1.35 (16H, s), 1.48 (4H, quint), 1.68 (4H, quint), 1.83 (4H, quint), 1.94 (6H, s), 4.05 (4H, t), 4.14 (4H, t), 5.53-5.56 (2H, m), 6.08-6.11 (2H, m), 6.96 (2H, t), 7.12 (4H, s), 7.28-7.35 (4H, m).

IR ν_{max} /cm⁻¹: 2930, 2852, 1714 (C=O), 1640, 1538, 1505, 1481, 1300, 1192, 1133, 869, 809, 787.

MS (m/z) (EI): 807 (M⁺) (M100), 636, 597, 552 (HABA matrix).

Elemental analysis: Expected /% C 68.46, H 6.99, S 7.95.

Found /% C 68.28, H 7.25, S 8.12.

5, 5'-Bis-{3-fluoro-4-[6-(3-methyloxetan-3-ylmethylenoxy)hexyloxy]phenyl}-[2,2']-bithiophene (**77**)

A mixture of 5,5'-bis(3-fluoro-4-hydroxyphenyl)-[2,2']-bithiophene (**73**) (0.15 g, 3.90 × 10⁻² mol), 3-(6-bromohexyloxymethyl)-3-methyloxetane (**52**) (0.39 g, 1.47 × 10⁻³ mol) and potassium carbonate (0.22 g, 1.59 × 10⁻³ mol) in DMF (20cm³) was heated (90 °C) for 48 hours. The excess potassium carbonate was filtered off from the cooled reaction mixture and rinsed with DCM (3 × 30 cm³). The solution was concentrated onto silica gel for purification by column chromatography [silica gel, ethyl acetate:hexane, 50%:50%] followed by recrystallisation from a DCM:ethanol mixture (2:1) to yield 0.13 g (44.8%) of the desired product (golden yellow solid).

Transition temp. /°C: Cr 138 I.

¹H NMR (CDCl₃) δ_H: 1.31 (6H, s), 1.42-1.55 (8H, m), 1.64 (4H, quint), 1.85 (4H, quint), 3.45-3.51 (8H, m), 4.06 (4H, t), 4.36 (4H, d, *J*=5.9 Hz), 4.51 (4H, d, *J*=5.6 Hz), 6.95 (2H, t), 7.12 (4H, s), 7.28-7.36 (4H, m).

IR ν_{max} /cm⁻¹: 2937, 2868, 1617, 1538, 1504, 1466, 1299, 1273, 1134, 1110, 972, 872, 794.

MS (m/z) (EI): 755 (M^+), 754, 725, 570, 386, 350, 289, 214, 138, 121, 107, 91, 83, 69, 55 (M 100).

Elemental analysis: Expected /% C 66.82, H 6.94, S 8.49.

Found /% C 66.59, H 7.22, S 8.19.

3-Bromothiophene-2-carbaldehyde (**79**)

3-Bromothiophene (**78**) (30.00 g, 0.18 mol) in sodium dried THF (40 cm³) was added dropwise to a cooled (0 °C), stirred solution of LDA (93.00 cm³, 2 M, 0.19 mol) in sodium dried THF (270 cm³). The reaction mixture was stirred for 75 minutes at this temperature and then *N*-formylpiperidine (21.35 g, 0.19 mol) in sodium dried THF (40 cm³) was added dropwise. The reaction mixture was allowed to warm to RT overnight and then ammonium chloride (20%) (300 cm³) was added. The resulting mixture was stirred for 30 minutes and then extracted into diethyl ether (3 × 200 cm³). The combined ethereal extracts were washed with brine (2 × 200 cm³) and dried (MgSO₄). After filtration the solvent was removed under reduced pressure and the crude product (dark red liquid) was purified by fractional distillation under reduced pressure to yield 27.75 g (79.0%) of the desired product (pale yellow liquid).

Boiling point /°C: 54-83 @ 1.75 mm Hg (Lit. 113-115 @ 10.00 mm Hg)^[25].

Purity: >97% (GC).

¹H NMR (CDCl₃) δ_H: 7.15 (1H, d, *J*=5.0 Hz), 7.72 (1H, d, *J*=5.8 Hz), 9.99 (1H, s, CHO).

IR ν_{max} /cm⁻¹: 2939, 2853, 1666 (C=O), 1498, 1417, 1372, 1213, 1161, 888, 739.

MS (m/z) (EI): 191 (M^+), 189 (M^+), 167, 151, 131, 117, 105, 91 (M 100), 77, 65.

Thieno[3,2-*b*]thiophene-2-carboxylic acid ethyl ester (**81**)

3-Bromothiophene-2-carbaldehyde (**79**) (27.21 g, 0.14 mol) in DMF (50 cm³) was added dropwise to a stirred solution of mercaptoacetic acid ethyl ester (**80**) (17.47 g, 0.15 mol) and potassium carbonate (26.68 g, 0.19 mol) in DMF (230 cm³). The resulting mixture was then stirred for 72 hours at RT. The reaction mixture was then poured into distilled water (500 cm³) and extracted into DCM (3 × 200 cm³). The combined organic extracts were washed with brine (2 × 200 cm³) and dried (MgSO₄). After filtration the solvent was removed under reduced pressure and the crude product

(orange/yellow liquid) was purified by fractional distillation under reduced pressure to yield 24.09 g (79.7%) of the desired product (orange liquid).

Boiling point /°C: 115-126 @ 1.25 mm Hg (Lit. 120-125 @ 0.1 mm Hg)^[25].

¹H NMR (CDCl₃) δ_H: 1.39 (3H, t), 4.38 (2H, quart), 7.26 (1H, d, *J*=5.4 Hz), 7.56 (1H, d, *J*=5.4 Hz), 7.98 (1H, s).

IR ν_{max} /cm⁻¹: 2981, 2936, 1710 (C=O), 1509, 1458, 1285, 1244, 1163, 915, 838, 754.

MS (m/z) (EI): 214 (M⁺), 212, 197, 184, 167 (M100), 139, 95, 81, 69.

Elemental analysis: Expected /% C 50.92, H 3.80, S 30.21.

Found /% C 50.70, H 4.10, S 30.49.

Thieno[3,2-*b*]thiophene-2-carboxylic acid (**82**)

A stirred mixture of thieno[3,2-*b*]thiophene-2-carboxylic acid ethyl ester (**81**) (16.39g, 0.08 mol), aqueous lithium hydroxide (185cm³, 1 M, 0.19 mol) and THF (220cm³) was heated under reflux (3 hours) until TLC analysis indicated the absence of the starting material. The aqueous and organic phases were separated and the aqueous phase was extracted with diethyl ether (2 × 200 cm³). The organic phases were combined and the solvent was removed under reduce pressure. Dilute (20%) hydrochloric acid (300 cm³) was added to the residue and the resulting precipitate was filtered off, washed with distilled water (2 × 250 cm³) and dried in a vacuum dessicator to yield 14.02 g (98.5%) of the desired product (yellow solid).

Melting Point /°C: 233-234 (Lit. 221-222)^[25].

¹H NMR (CDCl₃) δ_H: 7.51 (1H, d, *J*=5.0 Hz), 7.93 (1H, d, *J*=5.1 Hz), 8.11 (1H, s), 13.24 (1H, s-COOH).

IR ν_{max} /cm⁻¹: 3440, 1657 (C=O), 1510, 1459, 1409, 1260, 1165, 922, 828, 728.

MS (m/z) (EI): 184 (M⁺) (M100), 167, 156, 139, 127, 106, 95, 84, 69.

Elemental analysis: Expected /% C 45.63, H 2.19, S 34.81.

Found /% C 45.79, H 2.12, S 34.99.

Thieno[3,2-*b*]thiophene (**83**)

A stirred solution of thieno[3,2-*b*]thiophene-2-carboxylic acid (**82**) (10.02g, 0.05 mol) and copper powder (2.53 g, 0.04 mol) in quinoline (100 cm³) was heated at 240°C in a Woods metal bath. When no further bubbles of carbon dioxide gas were observed

from the reaction mixture (after approximately 3 hours), it was allowed to cool to RT. TLC analysis was used to confirm the absence of the starting material. Diethyl ether (300 cm³) was added to the mixture and the majority of the quinoline was removed by repeated washing of the resulting solution with dilute (1 M) hydrochloric acid (7 × 100 cm³). The solvent was removed under reduce pressure and the residue was purified by column chromatography [silica gel, DCM:hexane, 50%:50%] followed by recrystallisation from hexane to yield 7.07 g (92.7%) of the desired product (yellow crystalline solid).

Melting Point /°C: 55-56 (Lit. 55-56)^[25].

¹H NMR (CDCl₃) δ_H: 7.28 (2H, d, *J*=5.0 Hz), 7.40 (2H, d, *J*=5.0 Hz).

IR ν_{max} /cm⁻¹: 1620, 1563, 1442, 1347, 1189, 919, 880, 781.

MS (m/z) (EI): 140 (M⁺) (M100), 96, 84, 69, 45.

Elemental analysis: Expected /% C 51.39, H 2.88, S 45.73.

Found /% C 51.60, H 2.88, S 45.55.

2,5-Dibromothieno[3,2-*b*]thiophene (**84**)

N-Bromosuccinimide (12.34 g, 69.33 mol) (freshly purified by recrystallisation from distilled water) was added slowly (over a period of 2 hours) to a solution of thieno[3,2-*b*]thiophene (**83**) (4.86 g, 34.66 mmol) in acetic acid (50 cm³) and chloroform (50 cm³). Once the addition was complete, additional chloroform (60 cm³) was added and the reaction mixture was stirred at RT for a further 90 minutes. Any precipitated product after this period was filtered off. The filtrate was then poured into distilled water (150 cm³) and the aqueous phase extracted with chloroform (3 × 100 cm³). The combined organic phases were then washed with sodium metabisulphite solution (150 cm³) and distilled water (150 cm³). The solution was concentrated to a green/white solid and combined with previously precipitated product (white solid) and purified by recrystallisation from ethanol to yield 6.59 g (63.8%) of the desired product (green/grey needles).

Melting point /°C: 129-133 (Lit. 129.5-131.0)^[26].

¹H NMR (CDCl₃) δ_H: 7.18 (2H, s).

IR ν_{max} /cm⁻¹: 1625, 1448, 1327, 1162, 842, 804, 504.

MS (m/z) (EI): 300 (M⁺), 298 (M⁺) (M100), 296 (M⁺), 219, 217, 149, 138, 93, 81, 69, 57.

Elemental analysis: Expected /% C 24.18, H 0.68, S 21.52.

Found /% C 24.38, H 0.60, S 21.30.

(s)-2,5-Bis-[4-(3,7-dimethyl-oct-6-enyloxy)phenyl]thieno[3,2-*b*]thiophene (**85**)

Tetrakis(triphenylphosphine)palladium(0) (0.58 g, 5.00×10^{-2} mol) was added to a mixture of 2,5-dibromothieno[3,2-*b*]thiophene (**84**) (1.75 g, 5.87 mmol), (s)-2-[4-(3,7-dimethyl-oct-6-enyloxy)phenyl]-4,4,5,5-tetramethyl-[1,3,2]-dioxaborolane (**59**) (4.63 g, 12.92 mmol) and tripotassium phosphate (3.15 g, 14.70 mmol) in DMF (60 cm³) at RT. The reaction mixture was then heated (90 °C) for 48 hours. The cooled reaction mixture was poured into distilled water (150 cm³) and extracted with dichloromethane (3 × 150 cm³) and the combined organic layers were washed with brine (200 cm³) and dried (MgSO₄). After filtration, the solution was concentrated onto silica gel for purification by column chromatography [silica gel, DCM:hexane, 40%:60%] followed by recrystallisation from a DCM:ethanol mixture (3:1) to yield 1.71 g (48.4%) of the desired product (yellow solid).

Transition temp. /°C: Cr 229 I.

¹H NMR (CDCl₃) δ_H: 0.90 (6H, d), 1.12-1.21 (4H, m), 1.29-1.39 (2H, m), 1.55 (6H, s), 1.62 (6H, s), 1.73-1.83 (4H, m), 1.89-2.03 (4H, m), 3.91-4.01 (4H, m), 5.04 (2H, t), 6.85 (4H, d, *J*=8.7 Hz), 7.19 (2H, s), 7.47 (4H, d, *J*=9.0 Hz).

IR ν_{max} /cm⁻¹: 2966, 2926, 1606, 1523, 1471, 1287, 1253, 1172, 828, 812.

MS (m/z) (EI): 601 (M⁺), 600, 462, 324, 289 (M100), 230, 138, 121, 110, 91, 81, 69, 55.

Elemental analysis: Expected /% C 75.95, H 8.05, S 10.67.

Found /% C 75.74, H 8.27, S 10.39.

2,5-Bis-[4-hydroxyphenyl]thieno[3,2-*b*]thiophene (**86**)

Boron tribromide (4.84 g, 1.83 cm³, 19.32 mmol) in dichloromethane (20 cm³) was added dropwise to a cooled (0 °C), stirred solution of (s)-2,5-bis-[4-(3,7-dimethyl-oct-6-enyloxy)phenyl]thieno[3,2-*b*]thiophene (**85**) (2.90 g, 4.83 mmol) in dichloromethane (280 cm³). The reaction mixture was stirred and allowed to reach RT overnight. The reaction mixture was then poured onto an ice/water mixture (350 g), DCM was added (400 cm³) and the resulting mixture stirred (2 hours). The precipitate

was filtered off, washed with hot DCM ($2 \times 30 \text{ cm}^3$) and pulled dry under vacuum to yield 1.40 g (89.1%) of the desired product (purple solid).

Melting Point /°C: > 282 (material decomposition).

^1H NMR (DMSO) δ_{H} : 6.83 (4H, d, $J=8.7$ Hz), 7.50 (4H, d, $J=8.7$ Hz), 7.63 (2H, s), 9.71 (2H, s-OH).

IR ν_{max} / cm^{-1} : 3369, 2938, 1609, 1523, 1474, 1441, 1382, 1252, 1174, 984, 811.

MS (m/z) (EI): 324 (M^+) (M100), 295, 263, 245, 203, 175, 162, 137, 118, 109, 89, 77, 69, 45.

11-[4-(5-{4-[10-(1-Vinyl-allyloxycarbonyl)decyloxy]phenyl}thieno[3,2-*b*]thiophen-2-yl)phenoxy]undecanoic acid 1-vinyl-allyl-ester (**87**)

A mixture of 2,5-bis-[4-hydroxyphenyl]thieno[3,2-*b*]thiophene (**86**) (0.15 g, 4.60×10^{-2} mol), 11-bromoundecanoic acid 1-vinyl-allyl ester (**18**) (0.67 g, 2.02×10^{-3} mol) and potassium carbonate (0.30 g, 2.17×10^{-3} mol) in DMF (20 cm^3) was heated (90 °C) for 48 hours. The excess potassium carbonate was filtered off from the cooled reaction mixture and rinsed with DCM ($3 \times 30 \text{ cm}^3$). The solution was concentrated onto silica gel for purification by column chromatography [silica gel, DCM:hexane, 90%:10%] followed by recrystallisation from a DCM:ethanol mixture (2:1) to yield 0.13 g (34.2%) of the desired product (light green solid).

Transition temp. /°C: Cr 100 SmX2 179 SmX1 227 I.

^1H NMR (CDCl_3) δ_{H} : 1.30 (20H, s), 1.46 (4H, quint), 1.64 (4H, quint), 1.79 (4H, quint), 2.34 (4H, t), 3.98 (4H, t), 5.23 (4H, dt), 5.30 (4H, dt), 5.72 (2H, tt), 5.79-5.89 (4H, m), 6.92 (4H, d, $J=8.7$ Hz), 7.33 (2H, s), 7.54 (4H, d, $J=8.7$ Hz).

IR ν_{max} / cm^{-1} : 2918, 2850, 1740 (C=O), 1640, 1606, 1523, 1472, 1290, 1258, 1172, 1114, 921, 834, 812.

MS (m/z) (EI): 825 (M^+), 574, 324, 214, 195, 149, 121, 109, 91, 83, 67 (M100), 55.

Elemental analysis: Expected /% C 72.78, H 7.82, S 7.77.
Found /% C 72.61, H 8.02, S 7.50.

2-Methacrylic acid 9-[4-(5-{4-[9-(2-methacryloyloxy)nonyloxy]phenyl}thieno[3,2-*b*]thiophen-2-yl)phenoxy]nonyl ester (**88**)

A mixture of 2,5-bis-[4-hydroxyphenyl]thieno[3,2-*b*]thiophene (**86**) (0.25 g, 7.70×10^{-2} mol), 2-methacrylic acid 9-bromononyl ester (**42**) (0.67 g, 2.30×10^{-3} mol), BHT (0.07 g, 3.20×10^{-2} mol) and potassium carbonate (0.43 g, 3.11×10^{-3} mol) in DMF (10 cm³) was heated (55 °C) for 48 hours. The excess potassium carbonate was filtered off from the cooled reaction mixture and rinsed with DCM (3 × 30 cm³). The solution was concentrated onto silica gel for purification by column chromatography [silica gel, DCM] followed by recrystallisation from a DCM:ethanol mixture (2:1) to yield 0.19 g (33.3%) of the desired product (light green solid).

Transition temp. /°C: Cr 116 SmX2 169 SmX1 215 I.

¹H NMR (CDCl₃) δ_H: 1.35 (16H, s), 1.47 (4H, quint), 1.68 (4H, quint), 1.80 (4H, quint), 1.95 (6H, s), 3.99 (4H, t), 4.14 (4H, t), 5.53-5.56 (2H, m), 6.08-6.11 (2H, m), 6.92 (4H, d, *J*=8.7 Hz), 7.33 (2H, s), 7.54 (4H, d, *J*=8.7 Hz).

IR ν_{max} /cm⁻¹: 2935, 2854, 1715 (C=O), 1640, 1606, 1523, 1472, 1288, 1186, 1114, 933, 834, 812.

MS (m/z) (EI): 745 (M⁺) (M100), 576, 534 (HABA matrix).

Elemental analysis: Expected /% C 70.93, H 7.58, S 8.61.

Found /% C 70.99, H 7.62, S 8.34.

2-Methacrylic acid 11-[4-(5-{4-[11-(2-methacryloyloxy)undecyloxy]phenyl}thieno[3,2-*b*]thiophen-2-yl)phenoxy]undecyl ester (**89**)

A mixture of 2,5-bis-[4-hydroxyphenyl]thieno[3,2-*b*]thiophene (**86**) (0.30 g, 9.30×10^{-2} mol), 2-methacrylic acid 11-bromoundecyl ester (**43**) (0.89 g, 2.79×10^{-3} mol), BHT (0.07 g, 3.20×10^{-2} mol), and potassium carbonate (0.51 g, 3.69×10^{-3} mol) in DMF (10 cm³) was heated (55 °C) for 24 hours. The excess potassium carbonate was filtered off from the cooled reaction mixture and rinsed with DCM (3 × 30 cm³). The solution was concentrated onto silica gel for purification by column chromatography [silica gel, DCM] followed by recrystallisation from a DCM:ethanol mixture (2:1) to yield 0.07 g (9.5%) of the desired product (yellow solid).

Transition temp. /°C: Cr 116 SmX2 169 SmX1 206 I.

¹H NMR (CDCl₃) δ_H: 1.35 (24H, s), 1.47 (4H, quint), 1.67 (4H, quint), 1.80 (4H, quint), 1.94 (6H, s), 3.99 (4H, t), 4.14 (4H, t), 5.53-5.56 (2H,

m), 6.08-6.11 (2H, m), 6.92 (4H, d, $J=8.7$ Hz), 7.33 (2H, s), 7.54 (4H, d, $J=8.7$ Hz).

IR ν_{\max} / cm^{-1} : 2934, 2852, 1715 (C=O), 1640, 1606, 1523, 1472, 1288, 1256, 1185, 934, 834, 812.

MS (m/z) (EI): 801 (M^+), 561, 323, 295, 233, 195, 164, 149, 138, 121, 104, 83, 69, 55 ($M100$).

Elemental analysis: Expected /% C 71.96, H 8.05, S 8.00.
Found /% C 71.70, H 8.30, S 7.77.

2, 5-Bis-{4-[6-(3-methyloxetan-3-ylmethylenoxy)hexyloxy]phenyl}thieno[3,2-*b*]thiophene (**90**)

A mixture of 2,5-bis-[4-hydroxyphenyl]thieno[3,2-*b*]thiophene (**86**) (0.25 g, 7.70×10^{-2} mol), 3-(6-bromohexyloxymethyl)-3-methyloxetane (**52**) (0.75 g, 2.83×10^{-3} mol) and potassium carbonate (0.43 g, 3.11×10^{-3} mol) in DMF (10 cm^3) was heated (90 °C) for 48 hours. The excess potassium carbonate was filtered off from the cooled reaction mixture and rinsed with DCM (3 \times 30 cm^3). The solution was concentrated onto silica gel for purification by column chromatography [silica gel, ethyl acetate:hexane, 60%:40%] followed by recrystallisation from a DCM:ethanol mixture (2:1) to yield 0.10 g (18.9%) of the desired product (yellow solid).

Transition temp. /°C: Cr 157 SmX1 239 I.

^1H NMR (CDCl_3) δ_{H} : 1.31 (6H, s), 1.40-1.55 (8H, m), 1.61 (4H, quint), 1.81 (4H, quint), 3.44-3.51 (8H, m), 3.99 (4H, t), 4.35 (4H, d, $J=5.9$ Hz), 4.51 (4H, d, $J=5.6$ Hz), 6.92 (4H, d, $J=8.7$ Hz), 7.33 (2H, s), 7.54 (4H, d, $J=8.7$ Hz).

IR ν_{\max} / cm^{-1} : 2935, 2863, 1605, 1523, 1469, 1287, 1255, 1173, 1114, 981, 833, 813.

MS (m/z) (EI): 693 (M^+) (M 100), 665, 636, 608, 508, 324, 295, 214, 139, 107, 83, 69, 55.

Elemental analysis: Expected /% C 69.33, H 7.56, S 9.25.
Found /% C 69.15, H 7.74, S 9.34.

(s)-2,5-Bis-[4-(3,7-dimethyl-oct-6-enyloxy)-3-fluorophenyl]thieno[3,2-*b*]thiophene
(**91**)

Tetrakis(triphenylphosphine)palladium(0) (0.49 g, 4.20×10^{-2} mol) was added to a mixture of 2,5-dibromothieno[3,2-*b*]thiophene (**84**) (1.50 g, 5.03 mmol), (s)-2-[4-(3,7-dimethyl-oct-6-enyloxy)-3-fluorophenyl]-4,4,5,5-tetramethyl-[1,3,2]-dioxaborolane (**71**) (4.17 g, 11.08 mmol) and tripotassium phosphate (2.74 g, 12.58 mmol) in DMF (60 cm³) at RT. The reaction mixture was then heated (90 °C) for 48 hours. The cooled reaction mixture was poured into distilled water (150 cm³) and extracted with dichloromethane (3 × 150 cm³) and the combined organic layers were washed with brine (200 cm³) and dried (MgSO₄). After filtration, the solution was concentrated onto silica gel for purification by column chromatography [silica gel, DCM:hexane, 40%:60%] followed by recrystallisation from a DCM:ethanol mixture (3:1) to yield 1.45 g (45.2%) of the desired product (yellow solid).

Transition temp. /°C: Cr 194 I.

¹H NMR (CDCl₃) δ_H: 0.97 (6H, d), 1.19-1.29 (4H, m), 1.36-1.46 (2H, m), 1.61 (6H, s), 1.69 (6H, s), 1.85-1.94 (4H, m), 1.95-2.09 (4H, m), 4.06-4.15 (4H, m), 5.11 (2H, t), 6.80 (2H, t), 7.29-7.38 (6H, m).

IR ν_{max} /cm⁻¹: 2965, 2914, 1613, 1530, 1475, 1277, 1233, 1124, 860, 808.

MS (m/z) (EI): 637 (M⁺), 636, 498, 360 (M100), 331, 289, 250, 138, 121, 91, 83, 69, 55.

Elemental analysis: Expected /% C 71.66, H 7.28, S 10.07.

Found /% C 71.50, H 7.27, S 9.89.

2,5-Bis-(3-fluoro-4-hydroxyphenyl)thieno[3,2-*b*]thiophene (**92**)

Boron tribromide (4.33 g, 1.64 cm³, 17.28 mmol) in dichloromethane (20 cm³) was added dropwise to a cooled (0 °C), stirred solution of (s)-2,5-bis-[4-(3,7-dimethyl-oct-6-enyloxy)-3-fluorophenyl]thieno[3,2-*b*]thiophene (**91**) (2.75 g, 4.32 mmol) in dichloromethane (280 cm³). The reaction mixture was stirred and allowed to reach RT overnight. The reaction mixture was then poured onto an ice/water mixture (350 g), DCM was added (400 cm³) and the resulting mixture stirred (2 hours). The precipitate was filtered off, washed with hot DCM (2 × 30 cm³) and pulled dry under vacuum to yield 1.20 g (76.9%) of the desired product (green solid).

Melting Point /°C: > 265 (material decomposition).

^1H NMR (DMSO) δ_{H} : 7.01 (2H, t), 7.31 (2H, d), 7.52 (2H, d), 7.73 (2H, s), 10.17 (2H, s-OH).

IR ν_{max} / cm^{-1} : 3392, 1624, 1528, 1477, 1433, 1370, 1295, 1214, 1112, 861, 807, 785.

MS (m/z) (EI): 360 (M^+) (M100), 331, 311, 295, 268, 219, 180, 155, 136, 107, 93, 81, 69, 45.

11-[2-Fluoro-4-(5-{3-fluoro-4-[10-(1-vinyl-allyloxycarbonyl)decyloxy]phenyl}thieno[3,2-*b*]thiophen-2-yl)phenoxy]undecanoic acid 1-vinyl-allyl-ester (**93**)

A mixture of 2,5-bis-(3-fluoro-4-hydroxyphenyl)thieno[3,2-*b*]thiophene (**92**) (0.15 g, 4.20×10^{-2} mol), 11-bromoundecanoic acid 1-vinyl-allyl ester (**18**) (0.63 g, 1.90×10^{-3} mol) and potassium carbonate (0.29 g, 2.10×10^{-3} mol) in DMF (20 cm^3) was heated (90 °C) for 48 hours. The excess potassium carbonate was filtered off from the cooled reaction mixture and rinsed with DCM (3 \times 30 cm^3). The solution was concentrated onto silica gel for purification by column chromatography [silica gel, DCM:hexane, 90%:10%] followed by recrystallisation from a DCM:ethanol mixture (2:1) to yield 0.22 g (61.1%) of the desired product (yellow solid).

Transition temp. /°C: Cr 74 SmX1 188 I.

^1H NMR (CDCl_3) δ_{H} : 1.30 (20H, s), 1.47 (4H, quint), 1.64 (4H, quint), 1.83 (4H, quint), 2.34 (4H, t), 4.06 (4H, t), 5.22 (4H, d, $J=10.4$ Hz), 5.30 (4H, d, $J=17.4$ Hz), 5.72 (2H, tt), 5.79-5.89 (4H, m), 6.97 (2H, t), 7.28-7.37 (6H, m).

IR ν_{max} / cm^{-1} : 2918, 2850, 1739 (C=O), 1618, 1532, 1473, 1280, 1235, 1168, 1123, 920, 865, 800.

MS (m/z) (EI): 861 (M^+), 795, 711, 360, 289, 214, 195, 121, 109, 91, 83, 67 (M100), 55.

Elemental analysis: Expected /% C 69.74, H 7.26, S 7.45.

Found /% C 69.48, H 7.56, S 7.42.

2-Methacrylic acid 9-[2-fluoro-4-(5-{3-fluoro-4-[9-(2-methacryloyloxy)nonyloxy]phenyl}thieno[3,2-*b*]thiophen-2-yl)phenoxy]nonyl ester (**94**)

A mixture of 2,5-bis-(3-fluoro-4-hydroxyphenyl)thieno[3,2-*b*]thiophene (**92**) (0.25 g, 6.90×10^{-2} mol), 2-methacrylic acid 9-bromononyl ester (**42**) (0.69 g, 2.37×10^{-3} mol), BHT (0.07 g, 3.20×10^{-2} mol) and potassium carbonate (0.38 g, 2.75×10^{-3}

mol) in DMF (10cm³) was heated (55 °C) for 48 hours. The excess potassium carbonate was filtered off from the cooled reaction mixture and rinsed with DCM (3 × 30 cm³). The solution was concentrated onto silica gel for purification by column chromatography [silica gel, DCM] followed by recrystallisation from a DCM:ethanol mixture (2:1) to yield 0.28 g (51.9%) of the desired product (yellow solid).

Transition temp. /°C: Cr 139 SmX2 177 SmX1 185 I.

¹H NMR (CDCl₃) δ_H: 1.35 (16H, s), 1.49 (4H, quint), 1.68 (4H, quint), 1.84 (4H, quint), 1.95 (6H, s), 4.06 (4H, t), 4.14 (4H, t), 5.53-5.56 (2H, m), 6.08-6.11 (2H, m), 6.97 (2H, t), 7.29-7.38 (6H, m).

IR ν_{max} /cm⁻¹: 2923, 2856, 1703 (C=O), 1636, 1531, 1470, 1272, 1181, 1132, 798.

MS (m/z) (EI): 781 (M⁺) (M100), 611, 570 (HABA matrix).

Elemental analysis: Expected /% C 67.66, H 6.97, S 8.21.

Found /% C 67.43, H 7.08, S 7.96.

2-Methacrylic acid 11-[2-fluoro-4-(5-{3-fluoro-4-[11-(2-methacryloyloxy)undecyloxy]phenyl}thieno[3,2-*b*]thiophen-2-yl)phenoxy]undecyl ester (**95**)

A mixture of 2,5-bis-(3-fluoro-4-hydroxyphenyl)thieno[3,2-*b*]thiophene (**92**) (0.25 g, 6.90 × 10⁻² mol), 2-methacrylic acid 11-bromoundecyl ester (**43**) (0.86 g, 2.69 × 10⁻³ mol), BHT (0.07 g, 3.20 × 10⁻² mol), and potassium carbonate (0.38 g, 2.75 × 10⁻³ mol) in DMF (10cm³) was heated (55 °C) for 48 hours. The excess potassium carbonate was filtered off from the cooled reaction mixture and rinsed with DCM (3 × 30 cm³). The solution was concentrated onto silica gel for purification by column chromatography [silica gel, DCM] followed by recrystallisation from a DCM:ethanol mixture (2:1) to yield 0.18 g (31.0%) of the desired product (yellow solid).

Transition temp. /°C: Cr 127 SmX2 173 SmX1 179 I.

¹H NMR (CDCl₃) δ_H: 1.30 (24H, s), 1.48 (4H, quint), 1.67 (4H, quint), 1.84 (4H, quint), 1.94 (6H, s), 4.06 (4H, t), 4.14 (4H, t), 5.53-5.56 (2H, m), 6.08-6.11 (2H, m), 6.97 (2H, t), 7.29-7.38 (6H, m).

IR ν_{max} /cm⁻¹: 2921, 2854, 1703 (C=O), 1637, 1531, 1471, 1307, 1274, 1177, 801.

MS (m/z) (EI): 837 (M⁺), 771, 751, 597, 360, 279, 214, 138, 110, 83, 69 (M100), 55.

Elemental analysis: Expected /% C 68.87, H 7.47, S 7.66.

Found /% C 69.00, H 7.70, S 7.37.

2, 5-Bis-{3-fluoro-4-[6-(3-methyloxetan-3-ylmethylenoxy)hexyloxy]phenyl}thieno-[3,2-*b*]thiophene (**96**)

A mixture of 2,5-bis-(3-fluoro-4-hydroxyphenyl)thieno[3,2-*b*]thiophene (**92**) (0.25 g, 6.90×10^{-2} mol), 3-(6-bromohexyloxymethyl)-3-methyloxetane (**52**) (0.83 g, 3.13×10^{-3} mol) and potassium carbonate (0.38 g, 2.75×10^{-3} mol) in DMF (10 cm³) was heated (90 °C) for 48 hours. The excess potassium carbonate was filtered off from the cooled reaction mixture and rinsed with DCM (3 × 30 cm³). The solution was concentrated onto silica gel for purification by column chromatography [silica gel, ethyl acetate:hexane, 60%:40%] followed by recrystallisation from a DCM:ethanol mixture (2:1) to yield 0.08 g (15.7%) of the desired product (yellow solid).

Transition temp. /°C: Cr 191 I.

¹H NMR (CDCl₃) δ_H: 1.31 (6H, s), 1.41-1.59 (8H, m), 1.64 (4H, quint), 1.85 (4H, quint), 3.45-3.51 (8H, m), 4.07 (4H, t), 4.31 (4H, d, *J*=5.6 Hz), 4.51 (4H, d, *J*=5.6 Hz), 6.97 (2H, t), 7.28-7.37 (6H, m).

IR ν_{max} /cm⁻¹: 2938, 2864, 1616, 1531, 1474, 1307, 1278, 1123, 979, 860, 802.

MS (m/z) (EI): 729 (M⁺), 728, 698, 672, 644, 544, 442, 359 (M 100), 331, 282, 155, 121, 83, 72, 55.

Elemental analysis: Expected /% C 65.91, H 6.91, S 8.80.

Found /% C 65.88, H 6.81, S 9.09.

(s)-3,7-Bis-[5-(3,7-dimethyl-oct-6-enyl)thiophen-2-yl]dibenzothiophene (**98**)

Tetrakis(triphenylphosphine)palladium(0) (0.22 g, 1.90×10^{-2} mol) was added to a solution of 3,7-dibromodibenzothiophene (**6**) (0.78 g, 2.28 mmol) and (s)-tributyl-[5-(3,7-dimethyl-oct-6-enyl)thiophen-2-yl]stannane (**97**) (2.55 g, 4.99 mmol) in DMF (30 cm³) at RT. The reaction mixture was then heated (90 °C) for 48 hours. The cooled reaction mixture was poured into distilled water (100 cm³), extracted with dichloromethane (3 × 100 cm³) and the combined organic layers were washed with brine (150 cm³) and dried (MgSO₄). After filtration, the solution was concentrated onto silica gel for purification by column chromatography [silica gel, DCM:hexane,

20%:80%] followed by recrystallisation from a DCM:ethanol mixture (3:1) to yield 0.91 g (63.6%) of the desired product (light green solid).

Transition temp. /°C: Cr 187 I

¹H NMR (CDCl₃) δ_H: 0.94 (6H, d), 1.15-1.25 (4H, m), 1.33-1.44 (2H, m), 1.60 (6H, s), 1.67 (6H, s), 1.70-1.80 (2H, m), 1.91-2.06 (4H, m), 2.76-2.92 (4H, m), 5.10 (2H, t), 6.77 (2H, d, *J*=3.6 Hz), 7.22 (2H, d, *J*=3.6 Hz), 7.63 (2H, d, *J*=8.3 Hz), 7.98 (2H, s), 8.04 (2H, d, *J*=8.4 Hz).

IR ν_{max} /cm⁻¹: 2965, 2915, 1594, 1487, 1451, 1376, 1218, 970, 822, 799.

MS (m/z) (EI): 625 (M⁺), 624, 539, 499, 387, 374, 329, 277, 214, 200, 187, 146, 115, 99, 83, 69, 55, 40 (M100).

Elemental analysis: Expected /% C 76.87, H 7.74, S 15.39.

Found /% C 76.99, H 8.00, S 15.27.

7-Bromo-9,9-dioctyl-9*H*-fluoren-2-ol (**100**)

n-Butyllithium in hexanes (22.00 cm³, 2.5 *M*, 0.06 mol) was added dropwise to a cooled (-78 °C) solution of 2,7-dibromo-9,9-dioctyl-9*H*-fluorene (**99**) (30.0 g, 0.06 mol) in sodium dried THF (300 cm³). The resulting solution was stirred at this temperature for 1 hour and then trimethyl borate (56.86 g, 0.55 mol) was added dropwise to the mixture whilst maintaining the temperature at -78 °C. Once the addition was complete, the reaction mixture was stirred and allowed to reach RT overnight. Dilute (20%) hydrochloric acid (350 cm³) was added and the resulting mixture was stirred for 1 hour and then extracted into diethyl ether (2 × 200 cm³). The combined ethereal extracts were washed with water (2 × 150 cm³), dried (MgSO₄) and concentrated to a pale yellow oil. Diethyl ether (250 cm³) and hydrogen peroxide (35%, 100 cm³) were added and the solution heated under gentle reflux for 3 hours with vigorous stirring. The ethereal layer was separated, washed with saturated sodium metabisulphite solution (100 cm³), dilute hydrochloric acid (20%, 100 cm³) and water (2 × 100 cm³), dried (MgSO₄) and concentrated to a red/orange oil. The crude product was concentrated onto silica gel for purification by column chromatography [silica gel, hexane (eluting unreacted starting material) followed by DCM:hexane, 50%:50% (eluting product)] to yield 22.00 g (82.8%) of the desired product (brown/green oil, which crystallised to a green solid on standing).

Melting point /°C: 71-73.

^1H NMR (CDCl_3) δ_{H} : 0.59 (4H, quint), 0.83 (6H, t), 1.00-1.25 (20H, m), 1.82-1.94 (4H, m), 4.98 (1H, s-OH), 6.76-6.81 (2H, m), 7.37-7.45 (3H, m), 7.51 (1H, d, $J=8.8$ Hz).

IR $\nu_{\text{max}}/\text{cm}^{-1}$: 3305, 2924, 1616, 1569, 1489, 1456, 1357, 1242, 1168, 1062, 961, 866, 807, 585.

MS (m/z) (EI): 486 (M^+) ($\text{M}100$), 484 (M^+), 406, 292, 261, 207, 194, 181, 176, 71, 57, 43.

2-Bromo-9,9-dioctyl-7-octyloxy-9*H*-fluorene (**101**)

A mixture of 7-bromo-9,9-dioctyl-9*H*-fluoren-2-ol (**100**) (27.55 g, 0.06 mol), 1-bromooctane (**109**) (11.54 g, 0.06 mol) and potassium carbonate (15.67 g, 0.11 mol) in butanone (350 cm^3) was heated under reflux for 48 hours. The cooled reaction mixture was filtered and the filtrate was concentrated under reduce pressure. The crude product (pale orange oil) was concentrated onto silica gel for purification by column chromatography [silica gel, DCM:hexane 20%:80%] to yield 31.55 g (93.0%) of the desired product (pale yellow oil, which crystallised to an off-white, waxy solid on standing).

Melting point / $^{\circ}\text{C}$: 39-40.

^1H NMR (CDCl_3) δ_{H} : 0.59 (6H, quint), 0.82 (6H, t), 0.89 (3H, t), 1.00-1.24 (20H, m), 1.25-1.42 (8H, m), 1.49 (2H, quint), 1.77-1.93 (4H, m), 4.00 (2H, t), 6.81-6.88 (2H, m), 7.36-7.46 (3H, m), 7.53 (1H, d, $J=8.2$ Hz).

IR $\nu_{\text{max}}/\text{cm}^{-1}$: 2921, 1607, 1564, 1457, 1253, 1172, 882, 816, 753, 594.

MS (m/z) (EI): 598 (M^+), 596 (M^+) ($\text{M}100$), 519, 484, 404, 292, 259, 194, 181, 84, 69, 57, 43.

Elemental analysis: Expected /% C 74.34, H 9.61.

Found /% C 74.33, H 9.68.

2-(9,9-Dioctyl-7-octyloxy-9*H*-fluoren-2-yl)-4,4,5,5-tetramethyl-[1,3,2]-dioxaborolane (**102**)

n-Butyllithium in hexanes (16.00 cm^3 , 2.5 *M*, 0.04 mol) was added dropwise to a cooled (0 $^{\circ}\text{C}$) solution of 2-bromo-9,9-dioctyl-7-octyloxy-9*H*-fluorene (**101**) (21.00 g, 0.04 mol) in sodium dried diethyl ether (280 cm^3). The resulting solution was stirred at this temperature for 1 hour and then the mixture was allowed to warm to RT. The

mixture was stirred at RT for 1 hour and cooled again to -78 °C. The resulting solution was stirred at this temperature for 30 minutes and then 2-isopropoxy-4,4,5,5-tetramethyl-[1,3,2]-dioxaborolane (**57**) (7.63 g, 0.04 mol) in sodium dried diethyl ether (20 cm³) was added rapidly to the reaction mixture. Once the addition was complete, the reaction mixture was stirred and allowed to reach RT overnight. The reaction mixture was then quenched by the addition of distilled water (150 cm³), extracted into diethyl ether (3 × 150 cm³) and the combined ethereal extracts were washed with brine (2 × 150 cm³) and dried (MgSO₄). After filtration the crude product (pale orange oil) was concentrated onto silica gel for purification by column chromatography [silica gel, hexane (eluting unreacted starting material) followed by DCM:hexane, 20%:80% (eluting product)] to yield 11.00 g (48.6%) of the desired product (pale green/yellow viscous oil).

¹H NMR (CDCl₃) δ_H: 0.58 (6H, quint), 0.81 (6H, t), 0.89 (3H, t), 0.98-1.23 (20H, m), 1.25-1.41 (20H, m), 1.49 (2H, quint), 1.77-2.03 (4H, m), 4.01 (2H, t), 6.83-6.88 (2H, m), 7.56-7.62 (2H, m), 7.69 (1H, s), 7.77 (1H, d, *J*=7.5 Hz).

IR ν_{max}/cm⁻¹ : 2911, 1610, 1558, 1495, 1475, 1287, 963, 909, 849, 819.

MS (m/z) (EI): 645 (M⁺), 644 (M100), 484, 406, 292, 194, 165, 101, 83, 71, 57, 43.

4,7-Dibromo-benzo-[1,2,5]-thiadiazole (**104**)

Bromine (63.93 g, 20.50 cm³, 0.40 mol) was added to a solution of benzo-[1,2,5]-thiadiazole (**103**) (10.01 g, 0.07 mol) in hydrobromic acid (47 %, 130 cm³) and the resulting solution was heated under reflux for 2.5 hours. The cooled reaction mixture reaction mixture was filtered and the solid product washed with water (4 × 100 cm³) and pulled dry under vacuum. The crude product was purified by recrystallisation from an ethanol:DCM (3:1) mixture to yield 20.30 g (94.0%) of the desired product (orange needles).

Melting point /°C: 183-185 (Lit. 184-185)^[28].

¹H NMR (CDCl₃) δ_H: 7.74 (2H, s).

IR ν_{max}/cm⁻¹: 3050, 1576, 1476, 1310, 1184, 936, 875, 825, 587.

MS (m/z) (EI): 296 (M⁺), 294 (M⁺) (M100), 292 (M⁺), 215, 213, 134, 101, 83, 75, 51, 46.

Elemental analysis: Expected /% C 24.51, H 0.69, N 9.53, S 10.91.

Found /% C 24.71, H 0.53, N 9.78, S 10.75.

5-Bromo-2-chloropyrimidine (**106**)

Bromine (67.00 g, 21.48 cm³, 0.42 mol) was added dropwise to a solution of 2-hydroxypyrimidine hydrochloride (**105**) (50.04 g, 0.38 mol) in water (200 cm³). The resulting solution was stirred at room temperature for 1 hour and then the water and excess of bromine were removed under reduced pressure to yield a dry, pale orange solid. Phosphorous oxychloride (360 cm³) and *N,N*-dimethylaniline (20 cm³) were added and the resulting mixture was heated under reflux for 4 hours. The cooled reaction mixture was poured carefully on to ice (400 g) and then extracted into diethyl ether (4 × 100 cm³). The combined organic layers were washed with water (150 cm³) and dried (MgSO₄). After filtration, the solvent was removed under reduce pressure and the crude product was recrystallised from ethanol to yield 19.68 g (27.0%) of the desired product (white needles).

Melting point /°C: 78-79 (Lit. 79)^[29].

¹H NMR (CDCl₃) δ_H: 8.69 (2H, s).

IR ν_{max} /cm⁻¹: 1702, 1576, 1532, 1436, 1394, 1156, 1008, 759, 631.

MS (m/z) (EI): 196 (M⁺), 194 (M⁺) (M100), 192(M⁺), 176, 167, 157, 143, 121, 104, 84, 71, 49, 41.

Elemental analysis: Expected /% C 24.84, H 1.04, N 14.48.

Found /% C 25.06, H 0.87, N 14.25.

4,7-Bis(9,9-dioctyl-7-octyloxy-9*H*-fluoren-2-yl)benzo-[1,2,5]-thiadiazole (**107**)

Tetrakis(triphenylphosphine)palladium(0) (0.95 g, 8.22 × 10⁻⁴ mol) was added to a mixture of 2-(9,9-dioctyl-7-octyloxy-9*H*-fluoren-2-yl)-4,4,5,5-tetramethyl-[1,3,2]-dioxaborolane (**102**) (4.41 g, 6.80 × 10⁻³ mol), 4,7-dibromo-benzo-[1,2,5]-thiadiazole (**104**) (1.00g, 3.40 × 10⁻³ mol) and tripotassium phosphate (1.90 g, 9.00 × 10⁻³ mol) in DMF (70 cm³) at RT. The reaction mixture was then heated (90 °C) for 48 hours. The cooled reaction mixture was poured into distilled water (100 cm³) and extracted with dichloromethane (3 × 150 cm³) and the combined organic layers were washed with brine (2 × 150 cm³) and dried (MgSO₄). After filtration, the solution was concentrated onto silica gel for purification by column chromatography [silica gel, DCM:hexane, 20%:80%] to yield 1.52 g (38.2%) of the desired product (bright orange oil).

^1H NMR (CDCl_3) δ_{H} : 0.79 (12H, t), 0.90 (6H, t), 1.02-1.24 (48H, m), 1.27-1.44 (20H, m), 1.51 (4H, quint), 1.79-2.09 (8H, m), 4.04 (4H, t), 6.87-6.94 (4H, m), 7.65 (2H, d, $J=7.9$ Hz), 7.76 (2H, d, $J=7.9$ Hz), 7.86 (2H, s), 7.90 (2H, s), 8.00 (2H, d, $J=7.9$ Hz).

IR $\nu_{\text{max}}/\text{cm}^{-1}$: 2904, 1607, 1506, 1452, 1248, 1103, 1045, 894, 816, 723.

MS (m/z) (EI): 1170 (M^+) ($\text{M}100$) (HABA matrix).

Elemental analysis: Expected /% C 82.13, H 9.99, N 2.39, S 2.74.

Found /% C 82.32, H 10.17, N 2.19, S 2.53.

2,5-Bis(9,9-dioctyl-7-octyloxy-9*H*-fluoren-2-yl)pyrimidine (**108**)

Tetrakis(triphenylphosphine)palladium(0) (0.70 g, 6.06×10^{-4} mol) was added to a mixture of 2-(9,9-dioctyl-7-octyloxy-9*H*-fluoren-2-yl)-4,4,5,5-tetramethyl-[1,3,2]-dioxaborolane (**102**) (3.44 g, 5.30×10^{-3} mol), 5-bromo-2-chloropyrimidine (**106**) (0.51 g, 2.6×10^{-3} mol) and tripotassium phosphate (1.53 g, 7.20×10^{-3} mol) in DMF (70 cm^3) at RT. The reaction mixture was then heated (90 $^{\circ}\text{C}$) for 48 hours. The cooled reaction mixture was poured into distilled water (100 cm^3) and extracted with dichloromethane (3 \times 150 cm^3) and the combined organic layers were washed with brine (2 \times 150 cm^3) and dried (MgSO_4). After filtration, the solution was concentrated onto silica gel for purification by column chromatography [silica gel, DCM:hexane, 20%:80%] to yield 1.08 g (36.7%) of the desired product (pale yellow oil).

^1H NMR (CDCl_3) δ_{H} : 0.68 (12H, quint), 0.80 (12H, t), 0.90 (6H, t), 1.00-1.23 (40H, m), 1.25-1.43 (16H, m), 1.51 (4H, quint), 1.79-2.14 (8H, m), 4.04 (4H, t), 6.87-6.93 (2H, m), 7.53 (2H, s), 7.57 (2H, d, $J=7.8$ Hz), 7.72 (2H, d, $J=7.9$ Hz), 8.42 (2H, s), 8.50 (2H, d, $J=8.0$ Hz), 9.08 (2H, s).

IR $\nu_{\text{max}}/\text{cm}^{-1}$: 2967, 1614, 1538, 1454, 1103, 1041, 918, 877, 804.

MS (m/z) (EI): 1114 (M^+) ($\text{M}100$) (HABA matrix).

Elemental analysis: Expected /% C 84.11, H 10.50, N 2.52.

Found /% C 84.30, H 10.22, N 2.45.

1-Bromo-4-octyloxybenzene (**110**)

A mixture of 4-bromophenol (**19**) (25.05 g, 0.15 mol), 1-bromooctane (**109**) (28.50 g, 0.15 mol) and potassium carbonate (28.04 g, 0.20 mol) in butanone (310 cm^3) was heated under reflux for 48 hours. The cooled reaction mixture was filtered and the

filtrate was concentrated under reduced pressure. The crude product (pale yellow liquid) was purified by fractional distillation under reduced pressure to yield 40.11 g (97.1%) of the desired product (colourless liquid).

Boiling point /°C: 106-132 @ 2 mm Hg.

Purity: >98% (GC).

^1H NMR (CDCl_3) δ_{H} : 0.89 (3H, t), 1.22-1.38 (8H, m), 1.45 (2H, quint), 1.76 (2H, quint), 3.90 (2H, t), 6.76 (2H, d, $J=9.0$ Hz), 7.35 (2H, d, $J=9.0$ Hz).

IR ν_{max} / cm^{-1} : 2912, 1591, 1558, 1480, 1259, 1169, 819, 600.

MS (m/z) (EI): 286 (M^+), 284 (M^+), 185, 174 ($\text{M}100$), 172, 157, 155, 145, 143, 133, 119, 93, 83, 71, 57, 43.

2-(4-Octyloxyphenyl)thiophene (**112**)

A mixture of 1-bromo-4-octyloxybenzene (**110**) (30.08 g, 0.11 mol), tributylthiophene-2-ylstannane (**111**) (40.70 g, 0.11 mol) and *tetrakis*-(triphenylphosphine)-palladium (0) (0.98 g, 8.48×10^{-4} mol) in DMF (150 cm^3) was heated (90 °C) for 24 hours. The mixture was allowed to cool to RT and the solution was treated (stirred for 3 hours at RT) with a saturated potassium fluoride solution (100 cm^3) to destroy any tin side products^[31-32]. The mixture was extracted with hexane (3 \times 150 cm^3) and the combined organic layers were washed with brine (200 cm^3), dried (MgSO_4), filtered and concentrated under reduced pressure. The crude product was concentrated onto silica gel for purification by column chromatography [silica gel, hexane] followed by recrystallisation from ethanol to yield 16.18 g (53.2%) of the desired product (pearly/white flakes).

Melting point /°C: 68-70.

^1H NMR (CDCl_3) δ_{H} : 0.89 (3H, t), 1.24-1.36 (8H, m), 1.46 (2H, quint), 1.79 (2H, quint), 3.98 (2H, t), 6.90 (2H, d, $J=8.8$ Hz), 7.05 (1H, dd), 7.20 (2H, m), 7.52 (2H, d, $J=8.8$ Hz).

IR ν_{max} / cm^{-1} : 3067, 2929, 1606, 1569, 1502, 1476, 1289, 1252, 1181, 1115, 1076, 1026, 854.

MS (m/z) (EI): 288 (M^+), 244, 216, 176 ($\text{M}100$), 147, 131, 115, 84, 69, 55, 41.

Elemental analysis: Expected /% C 74.95, H 8.39, S 11.12.

Found /% C 74.92, H 8.38, S 10.98.

2-[(4-Octyloxyphenyl)-5-tributylstannyl]thiophene (**114**)

n-Butyllithium in hexanes (29.00 cm³, 2.5 M, 0.07 mol) was added dropwise to a cooled (-78 °C) solution of 2-(4-octyloxyphenyl)thiophene (**112**) (15.61 g, 0.05 mol) in sodium dried THF (250 cm³). The resulting solution was stirred at this temperature for 1 hour and then tri-*n*-butyltin chloride (**113**) (29.39 g, 0.09 mol) was added dropwise to the reaction mixture whilst maintaining the temperature at -78 °C. The reaction mixture was then allowed to warm to RT over night. Water (100 cm³) was added and the product was then extracted into diethyl ether (3 × 100 cm³). The combined ethereal extracts were dried (MgSO₄), filtered and concentrated under reduced pressure to yield a pale brown oil (21.47 g, 68.7%). The product was not purified further.

¹H NMR (CDCl₃) δ_H: 0.85-0.95 (12H, m), 1.11 (6H, t), 1.25-1.50 (16H, m), 1.54-1.69 (8H, m), 3.96 (2H, t), 6.88 (2H, d, *J*=8.8 Hz), 7.10 (1H, d, *J*=3.3 Hz), 7.31 (1H, d, *J*=3.3 Hz), 7.53 (2H, d, *J*=8.8 Hz).

IR ν_{max} /cm⁻¹: 2955, 2925, 2854, 1609, 1569, 1506, 1472, 1279, 1248, 1176, 1073, 828.

MS (m/z) (EI): 578 (M⁺), 521, 465, 407, 291, 269, 235, 213, 176, 145, 115, 94, 71, 57, 43 (M100).

2,7-Bis(5-{4-[octyloxy]phenyl}thien-2-yl)-9,9-dioctylfluorene (**115**)

Tetrakis(triphenylphosphine)-palladium (0) (1.05 g, 9.09 × 10⁻⁴ mol) was added to a mixture of 2,7-dibromo-9,9-dioctyl-9*H*-fluorene (**99**) (5.01 g, 9.14 × 10⁻³ mol) and 2-[(4-octyloxyphenyl)-5-tributylstannyl]thiophene (**114**) (11.74 g, 2.03 × 10⁻² mol) in DMF (80 cm³) at RT. The reaction mixture was then heated (90 °C) for 48 hours. The mixture was allowed to cool to RT and the solution was treated (stirred for 3 hours at RT) with a saturated potassium fluoride solution (100 cm³) to destroy any tin side products. The reaction mixture was then extracted with dichloromethane (3 × 150 cm³) and the combined organic layers were washed with brine (2 × 150 cm³) and dried (MgSO₄). After filtration, the solution was concentrated onto silica gel for purification by column chromatography [silica gel, DCM:hexane, 20%:80%] followed by recrystallisation from a DCM:ethanol mixture (1:1) to yield 5.08 g (57.7%) of the desired product (green/yellow solid).

Transition temp. /°C: T_g -3 Cr 56 N 91 I.

^1H NMR (CDCl_3) δ_{H} : 0.70 (4H, quint), 0.79 (6H, t), 0.90 (6H, t), 1.00-1.22 (20H, m), 1.24-1.41 (16H, m), 1.48 (4H, quint), 1.81 (4H, quint), 1.98-2.07 (4H, m), 3.99 (4H, t), 6.93 (4H, d, $J=8.6$ Hz), 7.20 (2H, d, $J=3.8$ Hz), 7.34 (2H, d, $J=3.8$ Hz), 7.54-7.63 (6H, m), 7.68 (4H, d, $J=8.6$ Hz).

IR ν_{max} / cm^{-1} : 3069, 2949, 2923, 2846, 1607, 1569, 1490, 1472, 1276, 1248, 1177, 1027, 825, 793.

MS (m/z) (EI): 963 (M^+) ($\text{M}100$) (HABA matrix).

Elemental analysis: Expected /% C 81.03, H 9.00, S 6.66.
Found /% C 81.14, H 9.15, S 6.50.

3.5 References

- 1 L. M. Harwood, C. J. Moody and J. M. Percy, '*Experimental Organic Chemistry: Preparative and Microscale*' (2nd Ed.), Wiley-Blackwell, New York (1998).
- 2 H. Gilman and D. L. Esmay, *J. Am. Chem. Soc.*, 1952, **74** (8), 2021.
- 3 R. B. Lacount and S. Friedman, *J. Org. Chem.*, 1977, **42** (16), 2751.
- 4 H. Sirringhaus, R. H. Friend, C. Wang, J. Leuninger and K. Müllen, *J. Mater. Chem.*, 1999, **9** (9), 2095.
- 5 R. M. Acheson and J. K. Stubbs, *J. Chem. Soc. Perkin Trans. 1*, 1972, 899.
- 6 J. P. A. Castrillon and H. H. Szmant, *J. Org. Chem.*, 1967, **32** (4), 976.
- 7 R. Gerdil and E. A. C. Lucken, *J. Am. Chem. Soc.*, 1965, **87** (2), 213.
- 8 Z. P. Demko, M. Bartsch and K. B. Sharpless, *Org. Lett.*, 2000, **2** (15), 2221.
- 9 W. Gottardi, *Monatsh. Chem.*, 1967, **98** (2), 507.
- 10 K. Morita, *J. Chem. Soc. Japan, Pure Chem. Sec.*, 1958, **31** (3), 347.
- 11 B. Neises and W. Steglich, *Angew. Chem. Int. Ed. Engl.*, 1978, **17** (7), 522.
- 12 A. Williamson, *Justus Liebigs Ann. Chem.*, 1851, **77**, 37.
- 13 R. D. Stephens and C. E. Castro, *J. Org. Chem.*, 1963, **28** (12), 3313.
- 14 H. Feuer and J. Hooz, '*The Chemistry of the Ether Linkage*', S. Patai (Ed.), Wiley-Interscience, New York (1967).
- 15 G. W. Gray, M. Hird, D. Lacey and K. J. Toyne, *J. Chem. Soc. Perkin Trans. 2*, 1989, **12**, 2041.
- 16 N. Miyaura, T. Yanagi and A. Suzuki, *Synth. Commun.*, 1981, **11** (7), 513.
- 17 A. Suzuki, *Pure & Appl. Chem.*, 1994, **66** (2), 213.
- 18 N. Miyaura and A. Suzuki, *Chem. Rev.*, 1995, **95** (7), 2457.
- 19 J. F. W. McOmie, M. L. Watts and D. E. West, *Tetrahedron*, 1968, **24** (5), 2289.
- 20 M. Motoi, H. Suda, K. Shimamura, S. Nagahara, M. Takei and S. Kanoh, *Bull. Chem. Soc. Jpn.*, 1988, **61** (5), 1653.
- 21 Y.-H. Lu and C.-S. Hsu, *Macromolecules*, 1995, **28** (5), 1673.
- 22 A. Bhattacharjee, P. Chattopadhyay, A. P. Kundu and R. Mukhopadhyay, *Indian J. Chem.*, 1996, **35**, 69.

- 23 R. M. Kellog, A. P. Schapp, E. T. Harper and H. Wynberg, *J. Org. Chem.*, 1968, **33** (7), 2902.
- 24 R. M. Kellog, A. P. Schapp and H. Wynberg, *J. Org. Chem.*, 1969, **34** (2), 343.
- 25 L. S. Fuller, B. Iddon and K. A. Smith, *J. Chem. Soc. Perkin Trans. 1*, 1997, **22**, 3465.
- 26 A. Bugge, *Acta Chem. Scand.*, 1969, **23** (8), 2704.
- 27 J. K. Stille, *Angew. Chem. Int. Ed. Engl.*, 1986, **25** (6), 508.
- 28 K. Pilgram, M. Zupan and R. Skiles, *J. Heterocycl. Chem.*, 1970, **7** (3), 629.
- 29 M. Hird, K. J. Toyne and G. W. Gray, *Liq. Cryst.*, 1993, **14** (3), 741.
- 30 P. Vlachos, *Ph.D. Thesis, University of Hull*, 2003.
- 31 J. E. Leibner and J. Jacobus, *J. Org. Chem.*, 1979, **44** (3), 449.
- 32 C. J. Salomon, G. O. Danelon and O. A. Mascaretti, *J. Org. Chem.*, 2000, **65** (26), 9220.



Chapter Four



Results and Discussion



:



:

:
:
:

4.0 Results and Discussion

The mesomorphic behaviour and the liquid crystalline transition temperatures of the compounds synthesised in this PhD programme are illustrated in the following tables, 4.1-4.6 and 4.8-4.10.

The charge-carrier mobility measurements cited in this section of the thesis were carried out by members of the organic semiconductor group at E. Merck, Chilworth, UK, on compounds prepared in their laboratories. The homologous compounds prepared during this thesis were kept at Merck for a considerable period. However, no charge-carrier mobility measurements were carried out due to a lack of manpower at Chilworth for several years. A reorganisation of the organic semiconductor activities within Merck then resulted in most of the organic semiconductor group leaving Merck. They were only returned to the University of Hull, when it was clear that no manpower was available to carry out the necessary measurements. As a result, no charge-carrier mobility data is available for any of the compounds synthesised in this thesis.

For both polymeric and small molecular type materials, the critical factor for charge-carrier mobility is the exchange interaction between the molecules and the overlap of adjacent molecular orbitals. Such an interaction is weak in amorphous layers, but can be high in ordered systems, at least in specific directions where π - π stacking occurs^[1]. Consequently, the primary aim is to enhance this exchange interaction, within the transport direction, by specific control over the structural order within a material.

Supramolecular organisation of the organic semiconducting moieties in a thin film environment can be enhanced through the utilisation of liquid crystalline mesophases. Thermotropic (and lyotropic) phases can induce highly ordered, closely packed structures, leading to high mobilities within the domain boundaries^[2]. The formation of crystal-smectic phases could create large domains, which are advantageous for charge-transport, in that elimination of grain boundaries leads to less charge-carrier trapping. The lamellar morphology exhibited by smectic mesophases represents an optimum, as it brings together the π -conjugated component of the

molecules in close contact, which facilitates the inter-molecular charge-transport hopping mechanism.

Crystal-smectic phases containing an extended delocalised π -electron system are attractive candidates for organic semiconductor applications. Charge-carrier mobility of thin-film semiconductors can be enhanced by self-assembly into closely packed microstructures with long-range order due to the creation of large domains, with control of molecular alignment being achieved within the mesophase. High-order smectic phases offer three-dimensionally organised lamellae, which can be further orientated by surface treatments.

Calamitic LCs can align with their director orthogonal to the substrate surface, referred to as homeotropic alignment, or parallel to the surface, referred to as planar alignment. In most OFET device structures, charge-transport occurs within a thin, planar region, close to the semiconductor/insulator interface^[3]. Therefore, it is necessary to ensure that the charge-transport component of the liquid crystalline molecules is aligned within the charge-transport layer such that the distances between the π -electron orbitals of adjacent molecules are minimal and in the plane of the device to allow charge-transport in the plane of the substrate. This can be achieved by homeotropic alignment of a smectic or a nematic phase where the long molecular axes are aligned orthogonal to the substrate surface.

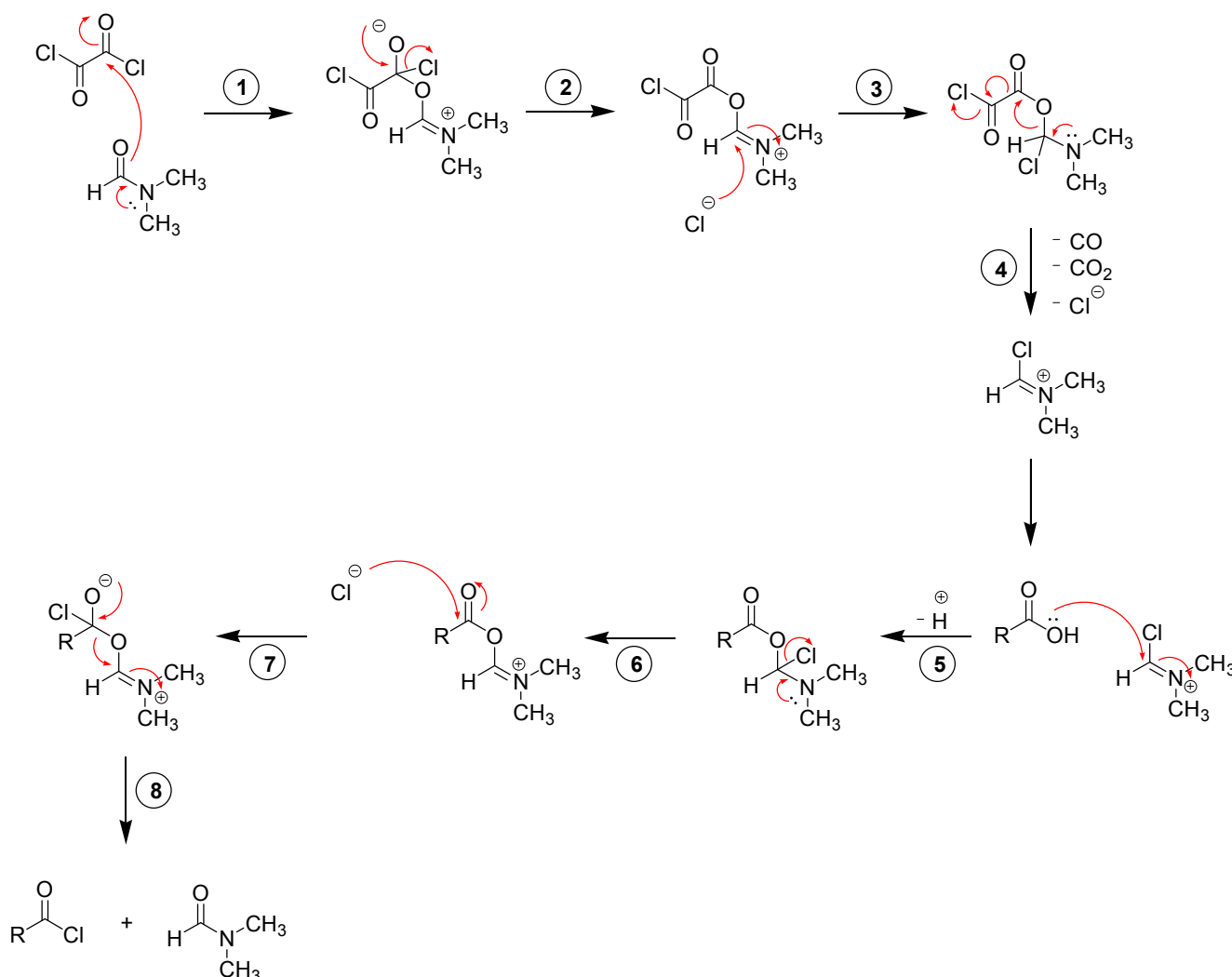
Aligned liquid crystalline phases are promoted by the use of interfacial, or alignment, layers such as hexamethyldisilazane (HMDS) or rubbed polyimide. Homeotropic alignment layers, such as HMDS, are generally hydrophobic in nature, and the low energy aliphatic tails of the molecules are thermodynamically driven to this interface to minimise the interfacial energy. In essence, the liquid crystalline phases do not wet the surface and so homeotropic alignment of the phase results as a consequence of this dewetting process. In addition, the use of alignment layers also promotes the formation of large area domains, or monodomains, in which the monodomain persists throughout the area of the alignment layer. As phase or grain boundaries generally cause charge-carrier trapping in organic semiconductors, the formation of monodomains is advantageous in optimising charge-carrier mobilities.

The liquid crystalline phases of known organic semiconductors are usually formed over a relatively small temperature range and at temperatures higher than that of the desired operating temperature of an OFET using that specific material. This means that there is a good chance that the liquid crystalline organic semiconductor will crystallise at room temperature and thereby generate crystal grain boundaries between domains. These boundaries will disrupt the alignment of the liquid crystalline mesophase and act as traps for electric charge-carriers and thereby lower the efficiency of the material as a conduction layer. A possible solution to overcome this problem is to fix the order present in the liquid crystalline phase by forming polymer networks. Such a conversion can be achieved by attaching reactive end-groups, such as diene (conjugated and non-conjugated), methacrylate or oxetane groups, to a molecule forming so-called RMs, which can then be permanently photo- or thermo-chemically cross-linked in the liquid crystalline phase (see section 1.6.2).

RM semiconductors typically comprise a conjugated aromatic core, which dictates the HOMO and LUMO energy levels, aliphatic spacers attached to each end of the aromatic core, which provide solubility in common organic solvents and lowers the melting point so that LC phases can be observed, and a reactive end-group capable of polymerisation at the end of each of the two spacers. This polymerisation creates an inert, intractable and insoluble cross-linked, ordered polymer network that is unchanged on thermal cycling and is impervious to exposure to solvents in any further processing steps. Short, conjugated aromatic cores would typically lead to low lying HOMO energy levels. Consequently such cores, and the materials synthesised from them, are unlikely to be susceptible to electrochemical oxidation under ambient conditions, which would, in turn, enhance their storage stability and potential device lifetime.

In the remainder of this Results and Discussion section we report the mesomorphic behaviour and liquid crystalline transition temperatures of several classes of RMs designed and synthesised as organic semiconductors for potential use as the functional charge-carrier layer in OFETs.

4.1 Reaction Scheme Two



Scheme 1 - A proposed mechanism for the DMF catalysed synthesis of the acid chloride, compound **9**, from the carboxylic acid, compound **7** and oxalyl chloride

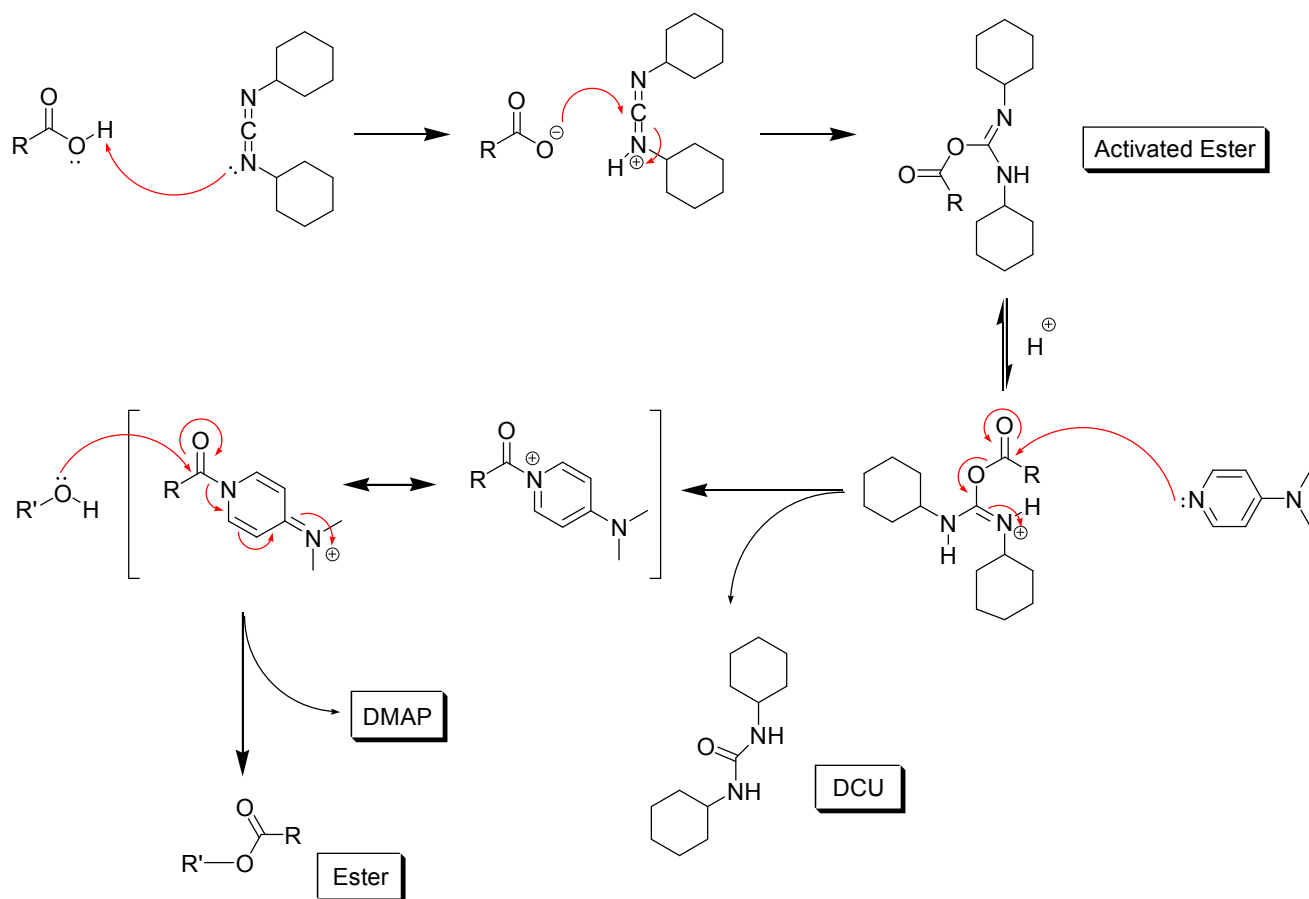
Scheme 1 shows an alternative method for synthesising acid chlorides, using oxalyl chloride in addition to catalytic DMF, which is a modification of the thionyl chloride (SOCl_2) method for making acyl chlorides. The oxalyl chloride reacts with the DMF generating a highly electrophilic cationic intermediate in addition to carbon monoxide and carbon dioxide. As with the SOCl_2 reaction, the by-products are all gases.

The first two steps are simply a nucleophilic substitution of Cl at the carbonyl group, going via a tetrahedral intermediate. Nucleophiles can attack the C=N bond (step 3) much as they might attack a C=O bond. The reactive intermediate is highly electrophilic and reacts rapidly with the carboxylic acid, producing another intermediate, which intercepts Cl⁻ to give the acyl chloride and regenerating the DMF in the process. This method is usually used for valuable acyl chlorides, as oxalyl chloride is much more expensive than thionyl chloride. DMF, will nonetheless, also catalyse acyl chloride formation using thionyl chloride.

The diene-ester, compound **18**, was readily synthesised from the commercially available ω-bromoalkanoic acid, compound **8** and the secondary alcohol, 1,4-pentadien-3-ol, compound **10**. The method used to esterify these two components employed *N,N'*-dicyclohexylcarbodiimide (DCC) and *N,N'*-dimethylaminopyridine (DMAP). This method is known as the Steglich esterification and was first described by Wolfgang Steglich in 1978^[4]. It is an adaptation of an older method for the formation of amides utilising DCC and 1-hydroxybenzotriazole (HOBT)^[5].

The advantages of this method are the mild conditions in which the reaction is carried out and the production of *N,N'*-dicyclohexylurea (DCU) as the hydrated by-product, which is easily removed by filtration. A proposed mechanism for this reaction is given in scheme 2. The scheme shows that the reaction between the carboxylate anion and DCC yields an activated ester intermediate. Subsequent nucleophilic attack from the phenol gives the desired ester and the insoluble by-product, DCU.

This reaction generally takes place at room temperature and is usually carried out in DCM. However, for insoluble components, then DMF is recommended^[6]. The disadvantage to this is that DCU is soluble in DMF. Because the reaction is mild, esters can be obtained that are inaccessible through other methods, for example esters of the sensitive 1,4-dihydroxybenzoic acid.



Scheme 2 - A proposed mechanism for the DCC/DMAP esterification of the ω -bromoalkanoic acid, compound **8** and the secondary alcohol, 1,4-pentadien-3-ol, compound **10** to form the diene-ester, compound **18**

The Steglich esterification is a mild reaction, which allows the conversion of sterically demanding and acid labile substrates, the mechanism of which is described below. DCC and the carboxylic acid react to form an O-acylisourea intermediate, which is more reactive than the corresponding free carboxylic acid. The alcohol can then attack this activated carboxylic acid intermediate to form the stable DCU and corresponding ester.

In practice, the reaction of carboxylic acids, DCC and amines proceeds without problems to the corresponding amides due to amines being very nucleophilic. If the esterification is slow however, a side-reaction occurs diminishing the yield or complicating purification of the final product. This side-reaction is a 1,3-rearrangement of the O-acyl intermediate to an N-acyl urea, which is unable to further react with the alcohol. To suppress this reaction, the addition of DMAP

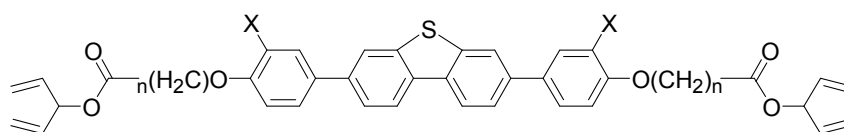
(approximately 5 mol%), acting as an acyl transfer reagent, is crucial for the efficient ester formation.

N-Acylureas, which may be quantitatively isolated in the absence of any nucleophile, are the side products of an acyl migration that takes place slowly. Strong nucleophiles such as amines react readily with the O-acylisourea and therefore no additives are required. A common explanation of the DMAP acceleration suggests that DMAP, being a stronger nucleophile than the alcohol, reacts with the O-acylisourea leading to a reactive amide or “active ester”. This intermediate cannot form intramolecular side products but reacts rapidly with alcohols, which subsequently form the ester.

4.2 Reaction Schemes Three and Four

The mesomorphic behaviour and liquid crystalline transition temperatures (°C) of the 3,7-bis-{4-[ω -(vinylallyloxycarbonyl)-*n*-alkyloxy]phenyl}dibenzothiophenes **25-29** and **35-39** are shown in Table 4.1.

Table 4.1 Chemical structures and liquid crystalline transition temperatures (°C) for the 3,7-bis-{4-[ω -(vinylallyloxycarbonyl)-*n*-alkyloxy]phenyl}dibenzothiophenes **25-29** and **35-39**



Compound	X	n	Cr	SmX		SmC		SmA		I	
25	H	3	●	116	●	129	●	168	●	205	●
26	H	4	●	91	●	107	●	168	●	210	●
27	H	5	●	107	●	116	●	167	●	206	●
28	H	7	●	116	●	134	●	168	●	206	●
29	H	10	●	115	●	129	●	177	●	198	●
35	F	3	●	116		-	●	168	●	210	●
36	F	4	●	130		-	●	167	●	203	●
37	F	5	●	123		-	●	169	●	202	●
38	F	7	●	123		-	●	168	●	190	●
39	F	10	●	130		-	●	169	●	199	●

SmX denotes an unidentified ordered smectic mesophase

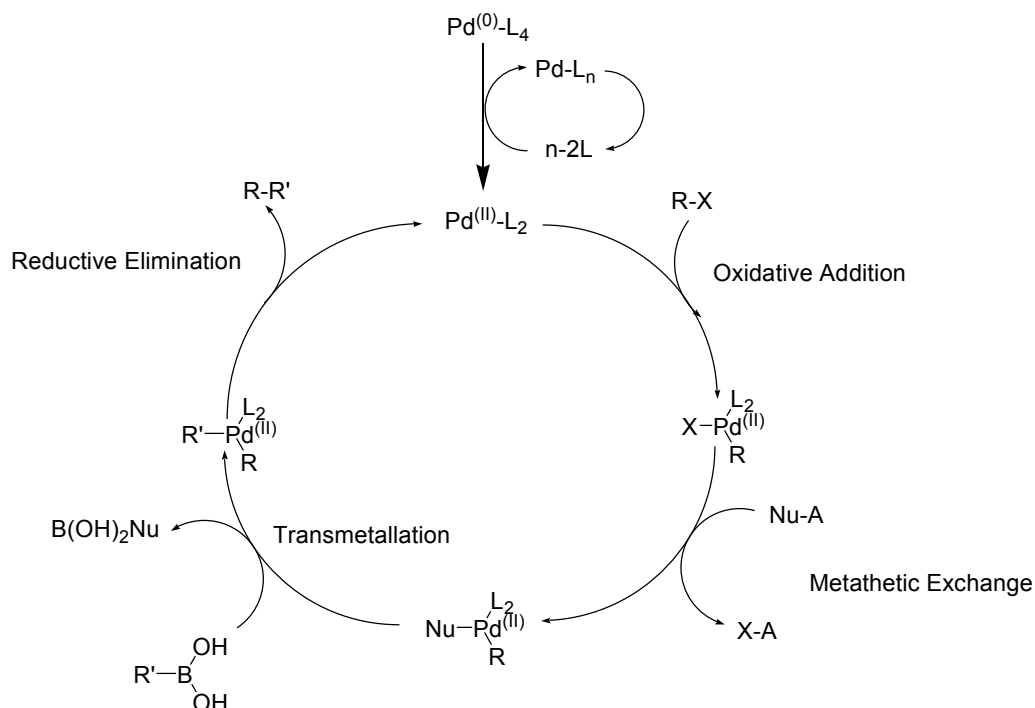
The non-conjugated diene RMs **25-29** shown in table 4.1, exhibit enantiotropic SmA and SmC mesophases in addition to a further unidentified ordered smectic phase, SmX. The liquid crystalline transition temperatures of the compounds **25-29** are all relatively high, probably due to significant intermolecular van der Waals forces of attraction between the rigid, planar and highly conjugated aromatic molecular cores of adjacent molecules. The liquid crystalline transition temperatures of the homologues **25-29** generally decrease with the increasing number of methylene units (*n*) in the spacers between the conjugated aromatic chromophore and the photo-polymerisable, non-conjugated, diene end-groups.

These aliphatic spacers serve to weaken the van der Waals forces of attraction between the aromatic cores and thereby induce lower melting points than otherwise could have been expected for such rigid, planar and highly conjugated molecules. The probability of the aliphatic chains adopting non-linear conformations with non-antiperiplanar conformations at carbon-carbon single bonds between methylene units (-CH₂-) will also increase with chain length, which would also serve to lower the liquid crystalline transition temperatures of these compounds.

In attempts to further reduce the liquid crystalline transition temperatures fluorine atoms were incorporated in a lateral position in the non-conjugated diene RMs **25-29** to produce the corresponding fluoro-substituted compounds **35-39**, also shown in table 4.1. The clearing points of the compounds **35-39** are sometimes higher, but mostly lower than those of the analogous non-fluoro-substituted compounds **25-29**, which have a hydrogen atom instead of a fluorine atom in the same position on the aromatic core.

The presence of fluorine atoms generally tends to increase the intermolecular distance and decrease the van der Waals forces of attraction between the molecular cores. This normally results in lower liquid crystalline transition temperatures. The melting points, however, tend generally to increase with the presence of the fluorine atoms in a lateral position, which is unusual. However, it is difficult to predict the melting points of organic compounds as they depend on a number of factors. Another consequence of the addition of the fluorine atoms is the absence of the ordered smectic phase, SmX, for the fluoro-substituted compounds **35-39**. None of the above materials exhibited a glassy state. These facts can also be attributed to steric interactions associated with the fluorine atoms in a lateral position on the molecular core.

The intermediate compounds **23** and **33**, leading to the RMs, compounds **25-29** and **35-39** respectively, were synthesised by a Suzuki cross-coupling reaction utilising the dibromide, compound **6** and the phenyl boronic acids, compounds **22** and **32** respectively. A proposed general catalytic cycle for the Suzuki cross-coupling reaction is given in scheme 3^[7], the mechanism of which is very similar to that for the Stille coupling reaction.



Scheme 3 - A proposed general catalytic cycle for the Suzuki coupling of the dibromide, compound **6** with the phenyl boronic acids, compounds **22** and **32** to form compounds **23** and **33** respectively

Since first being published by Akira Suzuki and his group in 1979^[8], the Suzuki coupling of a boronic acid with a halide has developed into one of the most important cross-coupling reactions. The Suzuki cross-coupling reaction is an extremely versatile methodology for the generation of carbon-carbon bonds. This originally was a reaction of an aryl-boronic acid with an aryl-halide catalysed by palladium. Recent catalyst and method developments, however, have broadened the possible applications of the Suzuki coupling reaction enormously, so that the scope of the reaction partners is not restricted to aryls, but includes alkyl, alkenyl, alkynyl, allyl, benzyl and vinyl boronic acids and halides, with sterically demanding substrates being well tolerated. Potassium trifluoroborates and organoboranes or boronate esters may also be used in place of the boronic acids. Some pseudohalides, for example triflates, may also be used as coupling partners.

The major difference between the Suzuki coupling mechanism and that of the Stille coupling (see section 4.5) is that the boronic acid must be activated, for example with

base, usually sodium or potassium ethoxide or hydroxide. The activation of the boron atom enhances the polarisation of the organic ligand, and facilitates transmetallation. If the starting materials are substituted with base labile groups, for example esters, powdered KF affects this activation while leaving the base labile groups unaffected. In part due to the stability, ease of purification and low toxicity of the boronic acid and boronate ester compounds, there is currently wide spread interest in applications of the Suzuki coupling reaction, with new developments and refinements being reported constantly.

By analogy to the other cross-coupling reactions, the catalytic cycle of Suzuki coupling reaction involves three basic steps. Firstly, oxidative addition of the halide to the palladium(0) complex generating a palladium(II) intermediate. Secondly, transmetallation between the palladium(II) intermediate and the boronic acid or boronate ester. Thirdly, the expulsion of the required product, by reductive elimination, regenerating the palladium(0) catalyst in the process.

The efficiency of palladium originates from its ability, when zero valent, to activate C-X bonds, where X = Cl, Br, I or O, by an oxidative addition which provides an organopalladium (II) complex, which is prone to react with nucleophiles^[9-10]. A large variety of palladium (0) catalysts or precursors can be used for this reaction, however Pd (0) L₄, where L = phosphine is the most commonly used, since it tends to be air stable. Palladium (II) complexes along with a reducer, can also be used^[11].

Oxidative addition of a suitable halide (see above) to a Pd (0) complex gives a stable trans-σ-palladium (II) complex^[12]. The reaction proceeds with complete retention of stereochemistry for alkenyl halides and with inversion of stereochemistry for allylic and benzylic halides. Oxidative addition is often the rate-limiting step in the catalytic cycle^[7]. The mechanism of the oxidative addition step is characterised by means of electrochemical techniques such as steady state voltammetry, transient voltammetry, cyclic voltammetry or reaction kinetics^[11], as the metal is oxidised.

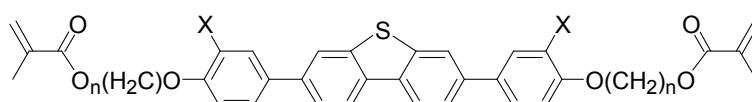
The transmetallation step between the organopalladium (II) complex and the organoboron compound does not usually proceed in the absence of base due to the low nucleophilicity of the organic group on the boron atom^[7]. However the

nucleophilicity can be enhanced by quarternisation of the boron with negatively charged bases giving the corresponding “ate” complex^[13], which undergo clean coupling reactions with organic halides^[14].

4.3 Reaction Schemes Five a and b

The melting points (°C) of the 3,7-bis{4-[ω -(methacryloxy)-*n*-alkyloxy]phenyl}dibenzothiophenes **44-47** are shown in Table 4.2.

Table 4.2 Chemical structures and melting points (°C) for the 3,7-bis{4-[ω -(methacryloxy)-*n*-alkyloxy]phenyl}dibenzothiophenes **44-47**



Compound	X	n	Cr	SmX	SmC	SmA	I		
44	H	9	●	116	●	polymerised	-	-	●
45	H	11	●	116	●	polymerised	-	-	●
46	F	9	●	120	●	polymerised	-	-	●
47	F	11	●	116	●	polymerised	-	-	●

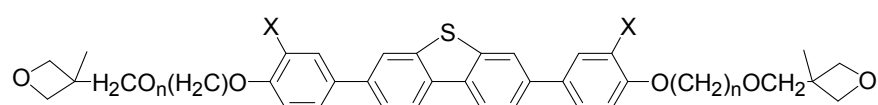
It was not possible to measure the transition temperatures of the mesophases of the compounds **44-47**, listed in table 4.2, or identify any potential smectic phases beyond reasonable doubt, as the materials polymerised during optical polarising microscopy and also during DSC measurements, that is the spontaneous thermally-initiated polymerisation of the methacrylate end-groups occurred during the attempted DSC and microscopy measurements. As a consequence, it is reasonable to assume that the methacrylate end-group is too thermally reactive to survive the elevated temperatures required during thin-film processing and subsequent OFET device manufacture and thus not likely to be a suitable polymerisable end-group for semiconductor device applications. This phenomenon has been observed by other research groups^[15].

It is also possible that some thermal instability of the methacrylate end-group could occur on recrystallisation of the compounds in table 4.2 from hot solvent, reducing their chemical purity. However, the elemental analysis results for compounds **44-47** (see section 3.4) have shown them to be chemically pure, with no initial polymerisation, prior to the microscopy or DSC measurements being carried out.

4.4 Reaction Schemes Six a and b

The mesomorphic behaviour and liquid crystalline transition temperatures (°C) of the 3,7-bis-{4-[ω-(3-methyloxetan-3-ylmethylenoxy)-*n*-alkyloxy]phenyl} dibenzothiophenes **53-56** are shown in Table 4.3.

Table 4.3 Chemical structures and liquid crystalline transition temperatures (°C) for the 3,7-bis-{4-[ω-(3-methyloxetan-3-ylmethylenoxy)-*n*-alkyloxy]phenyl} dibenzothiophenes **53-56**



Compound	X	n	Cr	SmX	SmC	SmA	I				
53	H	5	●	169	●	196	●	250	●	260	●
54	H	6	●	125	●	193	●	247	●	251	●
55	F	5	●	108	●	124	●	201	●	215	●
56	F	6	●	73	●	128	●	201	●	212	●

SmX denotes an unidentified ordered smectic mesophase

The oxetanes **53-56**, shown in Table 4.3, exhibit enantiotropic SmA and SmC mesophases, in addition to a further unidentified ordered smectic phase, SmX. The liquid crystalline transition temperatures of compounds **53-56** are all relatively high, except for the melting point of compound **56**. This is probably due to high intermolecular van der Waals forces of attraction between the aromatic molecular cores of the adjacent molecules. The liquid crystalline transition temperatures of the pairs of compounds **53-54** and **55-56** generally decrease with increasing number of methylene units (*n*) in the spacers between the aromatic chromophore and the chemically-polymerisable oxetane end-group. More homologues would be needed in order to determine whether this is a general trend. None of materials **53-56** exhibit an observable glassy state before recrystallisation occurs on cooling the smectic phases in a DSC.

The presence of fluorine atoms in a lateral position further lowers the liquid crystalline transition temperatures, without the loss of liquid crystallinity, of compounds **55** and **56** compared to compounds **53** and **54**, which have hydrogen atoms in the same position as the fluorine atoms. This can again be attributed to steric effects as the presence of fluorine atoms generally tends to increase the intermolecular distance and decrease the van der Waals forces of attraction between the molecular cores. However, the compounds **55** and **56** still possess the additional ordered smectic phase, SmX, despite the presence of the fluorine atoms in a lateral position on the molecular core.

Although it is difficult to make direct comparisons between the liquid crystalline transition temperatures of the non-conjugated dienes **25-29** and **35-39** and the oxetanes **53-56** due to the different shape of the terminal polymerisable groups, the oxetanes **53-56** appear to exhibit higher transition temperatures than those of the non-conjugated dienes **25-29** and **35-39**, see tables 4.1 and 4.3. This may be attributable to the smaller size of the oxetane group compared to that of the non-conjugated pentadiene end-group.

Studies of dioxetane polymerisation, *via* a cationic ring-opening mechanism, have shown a relatively fast and clean polymerisation^[16-18]. In addition, oxetanes have been found to show less polymerisation shrinkage than other polymerisable end-groups^[19]. Typically, free radical polymerisation requires the absence of oxygen, whereas this is not necessary for cationic polymerisation, making the oxetane system attractive for producing ordered polymer networks.

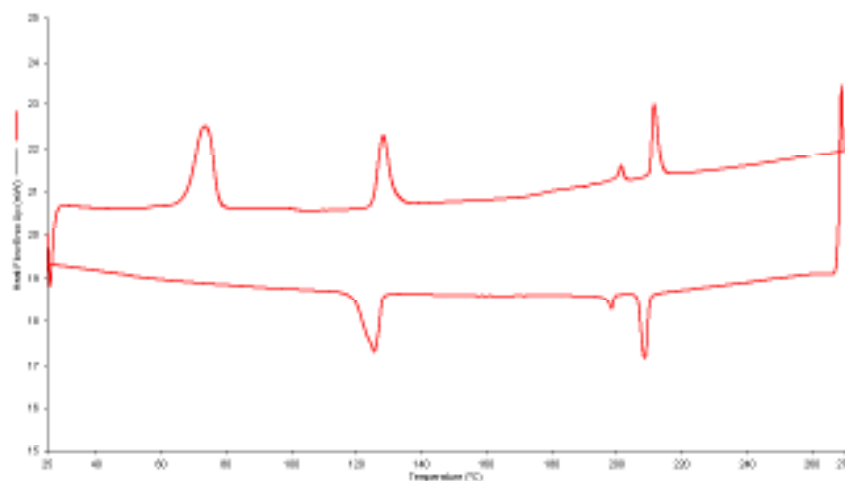


Figure 4.1 - DSC thermogram as a function of temperature for compound **56** (scan rate 10 °C/minute)

The DSC trace, figure 4.1, confirms the liquid crystalline transition temperatures of compound **56** (see table 4.3). The optical appearance between crossed polarisers of the SmA mesophase exhibited by compound **56** can be seen in picture 4.1.

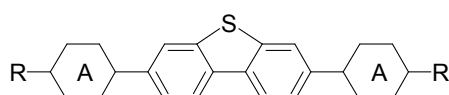



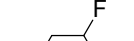
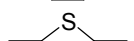
Picture 4.1 - The focal conic texture of the SmA mesophase of compound **56** at 212 °C

4.5 Reaction Schemes Three, Four and Thirteen

The mesomorphic behaviour and liquid crystalline transition temperatures (°C) of the 3,7-disubstituted dibenzothiophenes **23**, **33** and **98** are shown in Table 4.4.

Table 4.4 Chemical structures and liquid crystalline transition temperatures (°C) for the 3,7-disubstituted dibenzothiophenes **23**, **33** and **98**



Compound	A	R	Cr	SmC*	SmA*	I			
23		-OC ₂ H ₄ CH(CH ₃)C ₂ H ₄ CH=C(CH ₃) ₂	●	196	●	243	●	246	●
33		-OC ₂ H ₄ CH(CH ₃)C ₂ H ₄ CH=C(CH ₃) ₂	●	145	●	212	●	227	●
98		-C ₂ H ₄ CH(CH ₃)C ₂ H ₄ CH=C(CH ₃) ₂	●	187	-	-	-	-	●

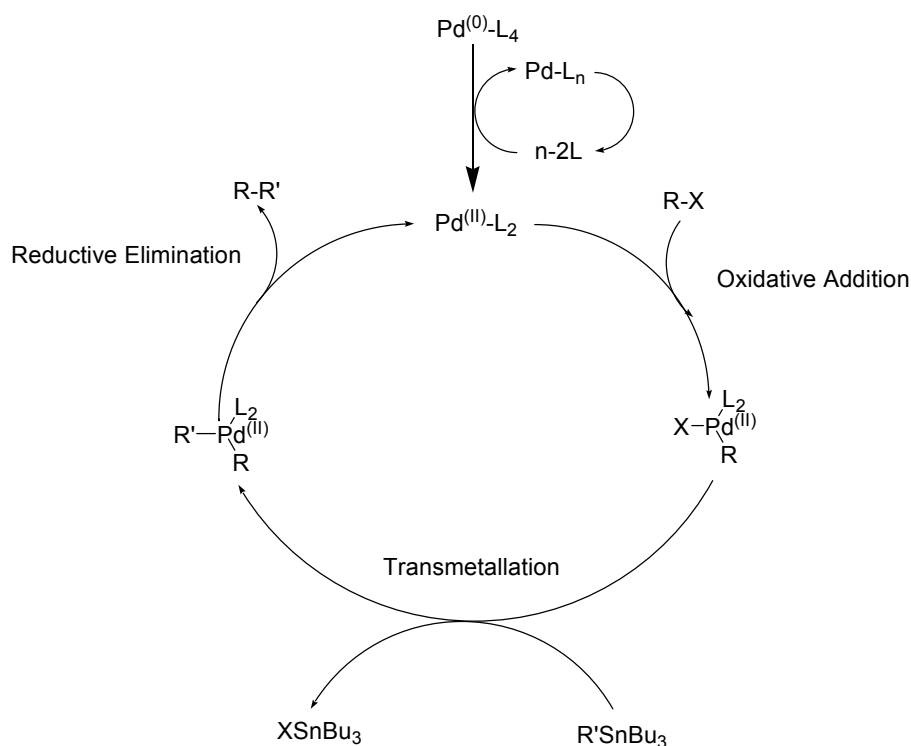
SmC* and SmA* denote chiral smectic C and chiral smectic A mesophases respectively

Compounds **23** and **33**, shown in table 4.4, exhibit enantiotropic SmA* and SmC* mesophases, but no ordered smectic phases. The presence of fluorine atoms in a lateral position in compound **33** results in a reduction of the melting and clearing points by 51 °C and 19 °C, respectively, compared to the values for the corresponding transition temperatures of the non-substituted analogue **23**. This is probably due to steric effects, as the presence of the fluorine atoms in a lateral position tends to increase the intermolecular distance and decreases the van der Waals forces of attraction between the molecular cores.

The presence of a thiophene ring, linked via a carbon-carbon bond to the branched chain rather than through an ether linkage, in the analogous material compound **98**, eliminates any potential mesomorphic behaviour, probably due to the non-linear and

non-co-axial nature of the 2,5-carbon-carbon bonds connecting the thiophene ring to the phenyl rings of the thiophene analogue **98**. Compound **98** was synthesised via a Stille coupling reaction utilising the dibromide, compound **6** and compound **97**. A proposed general catalytic cycle for the Stille coupling reaction is given in scheme 4.

Since the first reported use in the late 1970's the Stille coupling reaction^[20] has proven to be a versatile carbon-carbon bond forming reaction between stannanes, as the metallic component, and halides and pseudohalides, with very few limitations on the R groups. Well-elaborated methods allow the preparation of different products from a range of halides and stannanes. The main drawback is the toxicity of the tin compounds used and their low polarity, which makes them poorly soluble in water. Stannanes are stable, but boronic acids and their derivatives undergo much the same chemistry in the Suzuki coupling reaction (see section 4.2). Improvements in the Suzuki coupling reaction have lead to the same versatility without the drawbacks of using tin compounds.



Scheme 4 - A proposed general catalytic cycle for the Stille coupling of the dibromide, compound **6** and compound **97** to form compound **98**

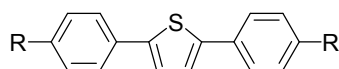
The mechanism involves the oxidative addition of a suitable halide or pseudohalide, such as a triflate, to give a palladium intermediate. This then undergoes a transmetallation reaction with the organostannane, giving an organopalladium intermediate in which both components are σ -bound. This complex then undergoes a reductive elimination step, releasing the product and regenerating the palladium (0) catalyst in the process.

The reaction occurs regardless of whether a halide is used in place of a triflate. However, triflates have been more widely used as they are readily prepared from phenols or enolisable aldehydes or ketones. In these reactions, the presence of a source of halide (typically LiCl) is generally required. This may be because the triflate is a counter ion and is not bound to the metal as a ligand. If transmetallation is to occur, some other ligand must be added to give the necessary square planar geometry.

4.6 Reaction Scheme Seven

The mesomorphic behaviour and liquid crystalline transition temperatures (°C) of the 2,5-(4-disubstituted-phenyl)thiophenes **60** and **62** and the reference compound **M1** are collated in Table 4.5.

Table 4.5 Chemical structures and liquid crystalline transition temperatures (°C) for the 2,5-(4-disubstituted-phenyl)thiophenes **60** and **62** and the reference compound **M1**



Compound	R	Cr	SmX	SmC	I
M1	-C ₆ H ₁₃	• 144	-	-	•
60	-OC ₂ H ₄ CH(CH ₃)C ₂ H ₄ CH=C(CH ₃) ₂	• 100	-	-	•
62	-OC ₇ H ₁₄ CO ₂ CH(CH=CH ₂) ₂	• 52	• 86	• 111	•

M1 Cr = 144°C^[21]

SmX denotes an unidentified ordered smectic mesophase

Compounds **M1**^[21] - 2,5-bis(4-*n*-hexylphenyl)thiophene (DH-PTP) and **60**, shown in table 4.5, were found not to exhibit any liquid crystalline mesophases. This is probably due to a combination of high melting point, low aspect ratio, i.e., length-to-breath ratio, and additionally, in the case of compound **60**, the high degree of branching of the side-chains, which hinders effective packing of the molecules, consequently weakening the van der Waals forces of attraction between the aromatic cores of the adjacent molecules. Compound **62**, however, exhibits an enantiotropic SmC mesophase, in addition to a further unidentified ordered smectic phase, SmX.

The occurrence of liquid crystalline mesophases in compound **62** appears to be a direct consequence of the branched, non-conjugated diene groups at the ends of the terminal chains lowering the melting point compared to those of the non-reactive materials **M1** and **60** thereby allowing these phases to be observed. The lower melting point is most likely due to steric effects attributable to the bulky reactive, non-

conjugated diene end-groups as is the absence of a glassy state on cooling from the smectic phases below the melting point.

M1 was part of a wider study synthesising and characterising a new series of *n*-hexyl-substituted thiophene oligomers, in which the number of central thiophene units was increased from 1 to 4, designed for solution processable OFETs, which were relatively easy to synthesise and could be readily deposited by both sublimation at moderate temperatures and casting from solution in xylenes. **M1**, although not liquid crystalline, is thermally stable and films have been shown to adopt microstructures with lattice spacings, suggestive of molecular alignment^[21]. The morphologies of the vacuum-evaporated films were featureless. However, the morphologies of the solution-cast films varied considerably, with highly interconnected crystallites of various shapes and sizes [as shown by Scanning Electron Microscopy (SEM)]. It was found that incorporation of phenylene units into the thiophene backbone results in a small lowering of the HOMO energy. It was also shown that this reduction in the HOMO energy is accompanied by a reduction in the off current, thus increasing device on/off ratios^[22].

M1 and its analogues were targeted and prepared because they were anticipated to combine the high mobility characteristics typically exhibited by thiophene-phenylene oligomers with the improved solubility/film processability and close packing tendencies associated with α,ω -alkyl chain substitution^[23-24]. Straightforward syntheses, thermal stability, and solution processability make these oligomers very attractive candidates for low cost molecular electronic applications. The oligomers are readily purified by recrystallisation rather than high vacuum sublimation and can be stored for several months in air with no apparent decomposition or discolouration^[21].

M1 has been shown to exhibit high *p*-type charge-carrier mobility for such a small material with a limited conjugated molecular core. **M1** can be readily deposited by both sublimation at moderate temperatures and casting from solution in xylenes. **M1** has shown mobilities and on/off ratios of $10^{-5} \text{ cm}^2 \text{ V}^{-1} \text{ s}^{-1}$ and 60 respectively from solution-cast films in xylene on ITO/GR (glass resin) substrates and mobilities and on/off ratios of $0.01 \text{ cm}^2 \text{ V}^{-1} \text{ s}^{-1}$ and 2500 and $0.01 \text{ cm}^2 \text{ V}^{-1} \text{ s}^{-1}$ and 3000 at RT and 50 °C, respectively, from vacuum-deposited films on Si/SiO₂ substrates that had been

pretreated with HMDS prior to film growth. Pretreatment of the silicon substrates with HMDS vapour creates a lipophilic monolayer coating, prior to vacuum deposition of the material film. Mobilities and on/off ratios of $10^{-5} \text{ cm}^2 \text{ V}^{-1} \text{ s}^{-1}$ and 30 and $10^{-4} \text{ cm}^2 \text{ V}^{-1} \text{ s}^{-1}$ and 200 at RT and 50 °C respectively from vacuum-deposited films on Si/SiO₂ substrates, with no HMDS pre-treatment, were also observed.

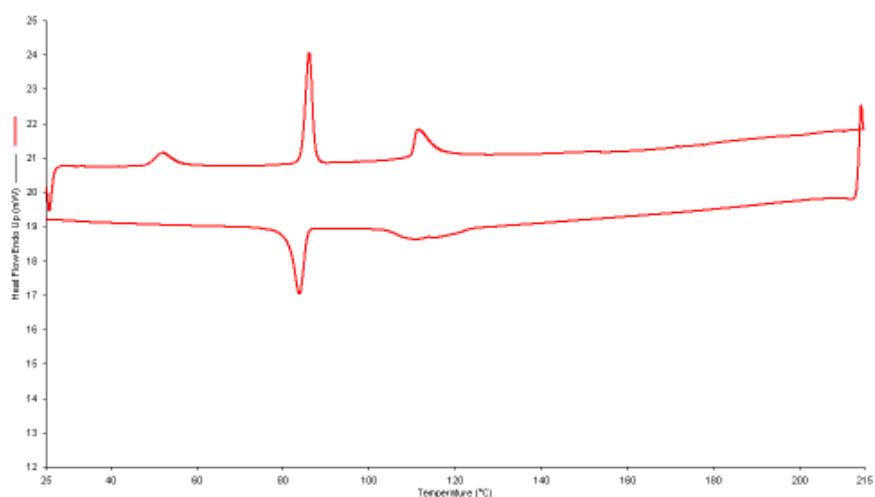


Figure 4.2 - DSC thermogram as a function of temperature for compound **62** (scan rate 10 °C/minute)

The DSC trace, figure 4.2, confirms the liquid crystalline transition temperatures of compound **62** (see table 4.5).

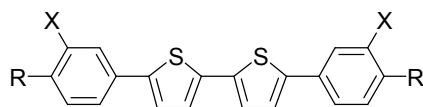
4.7 Reaction Schemes Eight and Nine

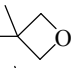
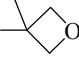
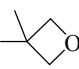
The mesomorphic behaviour and liquid crystalline transition temperatures (°C) of the 5,5'-(3,4-disubstituted-phenyl)-[2,2']-bithiophenes **65**, **67-70**, **72** and **74-77** and the reference compounds **M2-M7** are collated in Table 4.6.

Homologues with the same aromatic core as that of the symmetrical *bis* phenyl-bithiophenes, shown in table 4.6, have previously been shown to exhibit high hole mobility values with an advantageous HOMO energy value (5.13 eV)^[22]. The compounds in table 4.6 were synthesised in order to investigate their mesomorphic behaviour, liquid crystalline transition temperatures and charge transport properties for potential use as the active layer in OFETs using small molecules as organic semiconductors.

The non-polymerisable reference compound **M2** (*bis*-5,5'-(4-heptylphenyl)-2,2'-bithiophene - PTPP), with two terminal heptyl chains, shown in table 4.6, exhibits enantiotropic SmA and SmC mesophases, in addition to a further ordered SmG mesophase (SmX = SmG)^[25-26]. Compound **65**, a non-polymerisable analogue of compound **M2** with branching methyl groups in the alkoxy spacers, does not exhibit any observable liquid crystalline mesophases. The high degree of chain branching in the side-chains of compound **65** will hinder effective packing of the molecules. This significant steric effect probably weakens the van der Waals forces of attraction between the aromatic cores of adjacent molecules. The combined effect of four branching methyl groups in the terminal alkoxy chains of compound **65** leads to a relatively low melting point for a compound with four aromatic rings in the molecular core.

Table 4.6 Chemical structures and liquid crystalline transition temperatures (°C) for the 5,5'-(3,4-disubstituted-phenyl)-[2,2']-bithiophenes **65**, **67-70**, **72** and **74-77** and the reference compounds **M2-M7**



Compound	X	R	Cr	SmX	SmC	SmA	N	I
M2^b	H	-C ₇ H ₁₅	• 76	• 226	• 232	• 233	-	•
65	H	-OC ₂ H ₄ CH(CH ₃)C ₂ H ₄ CH=C(CH ₃) ₂	• 185	-	-	-	-	•
M3^b	H	-C ₄ H ₈ CO ₂ CH(CH=CH ₂) ₂	• 75	• 174	-	-	-	•
M4	H	-OC ₅ H ₁₀ CO ₂ CH(CH=CH ₂) ₂	• 135	• 196 [#]	-	-	-	•
67	H	-OC ₇ H ₁₄ CO ₂ CH(CH=CH ₂) ₂	• 50	• 119	• 184	• 192	-	•
68	H	-OC ₁₀ H ₂₀ CO ₂ CH(CH=CH ₂) ₂	• 97	• 127	• 182	• 186	-	•
M5	H	-C ₆ H ₁₂ O ₂ CC(CH ₃)=CH ₂	• 53	• 92	-	-	-	•
M6	H	-OC ₆ H ₁₂ O ₂ CC(CH ₃)=CH ₂	• 104	• 204 [#]	-	-	-	•
69	H	-OC ₉ H ₁₈ O ₂ CC(CH ₃)=CH ₂	• 108	-	• 171	• 180	-	•
M7^a	H	-C ₆ H ₁₂ OCH ₂ - 	• 83	• 144 [#]	-	-	-	•
70	H	-OC ₆ H ₁₂ OCH ₂ - 	• 122	• 180	• 185	-	-	•
72	F	-OC ₂ H ₄ CH(CH ₃)C ₂ H ₄ CH=C(CH ₃) ₂	• 144	-	-	-	-	•
74	F	-OC ₇ H ₁₄ CO ₂ CH(CH=CH ₂) ₂	• 141	-	• 154	-	-	•
75	F	-OC ₁₀ H ₂₀ CO ₂ CH(CH=CH ₂) ₂	• 79	• 140	• 144	-	-	•
76	F	-OC ₉ H ₁₈ O ₂ CC(CH ₃)=CH ₂	• 106	• 116	• 129	-	• 140	•
77	F	-OC ₆ H ₁₂ OCH ₂ - 	• 138	-	-	-	-	•

Notes for Table 4.6:

SmX denotes an unidentified ordered smectic mesophase

a denotes measured on cooling cycle and *b* denotes measured on heating cycle

M2 Cr-SmG = 140 °C; SmG-SmC = 226 °C; SmC-SmA = 232 °C; SmA = 233 °C^[25-26]

M3 Cr-SmG = 75 °C; SmG-I = 174 °C^[15]

M4 [#]Cr-SmG = 135 °C; SmG-SmB = 187 °C; SmB-I = 196 °C^[27]

M5 Cr-SmG = 53 °C; SmG-I = 92 °C^[15]

M6 [#]Cr-SmG = 104 °C; SmG-SmB = 187 °C; SmB-I = 204 °C^[27]

M7 [#]Cr-SmG = 83 °C; SmG-SmB = 93 °C; SmB-I = 144 °C^[15, 25-27]

The polymerisable compound **M3** consisting of the PTPP molecular core, C4 aliphatic spacers linked directly to the phenyl rings by carbon-carbon single bonds and incorporating a non-conjugated diene group at the end of the aliphatic spacers, exhibits a low melting point and an ordered SmG mesophase^[15]. The related non-conjugated diene **M4**^[27], but consisting of C5 aliphatic spacers linked *via* ether linkages to the phenyl rings, exhibits a higher melting point (+60 °C). This increase is observed despite an increase of one methylene unit in the spacers, which often leads to lower melting points. The higher melting point of compound **M4** compared to that of **M3** is probably attributable to greater forces of attraction between molecules of the alkoxy-substituted compound **M4** than between the related alkyl-substituted compound **M3**. The presence of the oxygen atoms increases the length of the aromatic core and thus the length-to-breadth ratio as well as the degree of conjugation and the anisotropy of polarisability. Compound **M4** also exhibits two ordered smectic phases, SmG and SmB^[27].

The compounds **67** and **68** are homologues of compound **M4**, i.e., they both have the same non-conjugated diene end-group attached to the molecular core by an alkoxy spacer. However, they differ in the aliphatic space length; C7 for compound **67** and C10 for compound **68**. In contrast to the C5 homologue **M4**, which only exhibits ordered smectic phases (SmG and SmB) according to the literature^[27], compounds **67** and **68** both exhibit enantiotropic SmA and SmC mesophases, in addition to a further unidentified ordered smectic mesophase, SmX. We suspect that the phases of compound **M4** have been incorrectly assigned. Uncharacteristically, the C7 homologue **67** exhibits a lower melting point (-47 °C) than that of the C10 homologue

68. The C10 homologue **68** has a lower clearing point than that of the C7 homologue **67**, as expected, due to the longer spacers between the aromatic chromophore and the polymerisable non-conjugated diene end-groups.

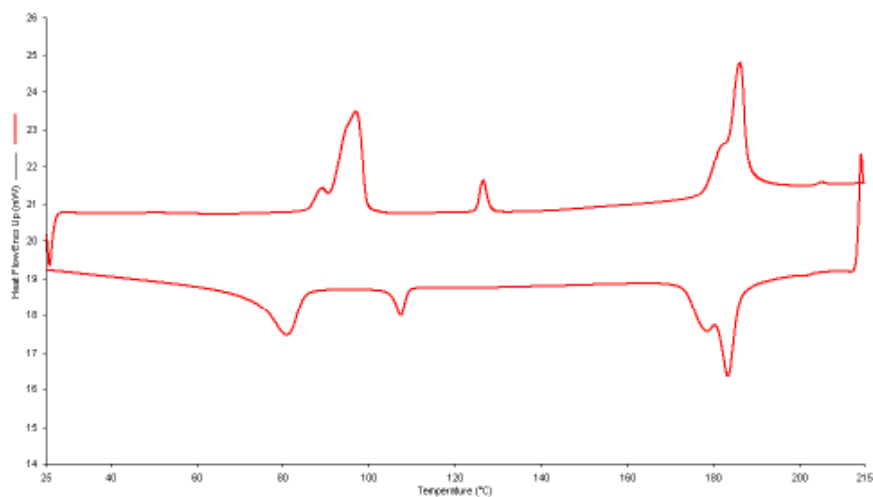
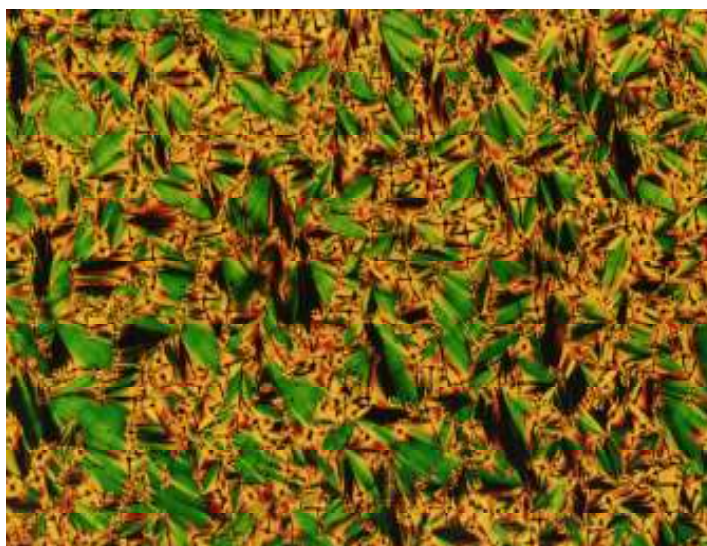


Figure 4.3 - DSC thermogram as a function of temperature for compound **68** (scan rate 10 °C/minute)

The DSC trace, figure 4.3, confirms the liquid crystalline transition temperatures of compound **68** (see table 4.6). The optical appearance between crossed polarisers of the SmA mesophase exhibited by compound **68** can be seen in picture 4.2.



Picture 4.2 - The SmA mesophase of compound **68** at 186 °C

The related compounds **M5**^[15] and **M6**^[27] both have the same methacrylate end-group and a C6 aliphatic spacer. However, they differ in the way that the two spacers are linked to the phenyl rings. The hexyl spacers of compound **M5** are linked directly through carbon-carbon single bonds to the phenyl rings, whereas the spacers of compound **M6** are linked *via* ether linkages to the phenyl rings. Compound **M5** has significantly lower melting and clearing points (51 and 112 °C, respectively) when compared to those of **M6**. Both compounds exhibit ordered SmG mesophases, with compound **M6** exhibiting an additional ordered SmB mesophase.

Compound **69** differs from compound **M6** only in the length of the spacers, with compound **69** having C9 spacers. The C6 homologue **M6** exhibits a slightly lower melting point (-4 °C) than that of the C9 homologue **69**. However compound **69** has a lower clearing point, as expected, due to the longer spacers between the aromatic chromophore and the polymerisable methacrylate end-groups. Compound **69** exhibits enantiotropic SmC and SmA mesophases, but no additional ordered smectic phases. We suspect that the phases of compound **M6** may have been incorrectly assigned^[27] and may well be SmA and SmC mesophases.

The oxetanes **M7**^[15, 25-27] and compound **70** both have the same oxetane end-group and C6 aliphatic spacers. However, they also differ in the way that the two spacers are linked to the phenyl rings. The spacers of compound **M7** are linked directly to the phenyl rings, whereas the spacers of compound **70** are linked *via* ether linkages to the phenyl rings. Compound **M7** exhibits significantly lower melting and clearing points (-39 and -41 °C, respectively) compared to those of compound **70**. Compound **M7** exclusively exhibits ordered SmG and SmB mesophases, whereas compound **70** exhibits an enantiotropic SmC mesophase and an additional unidentified ordered smectic mesophase, SmX.

In attempts to produce compounds with lower liquid crystalline transition temperatures and especially the melting point, fluorine atoms were incorporated in a lateral position in the compounds **65** and **67-70** to produce the analogous fluoro-substituted compounds **72** and **74-77**, respectively. Generally, the liquid crystalline transition temperatures of the fluoro-substituted compounds **72** and **74-77** are lower than the corresponding values of the analogous non-fluoro-substituted compounds **65**

and **67-70**. These differences can probably be attributed in the usual way to steric effects associated with the presence of fluorine atoms in a lateral position in the fluoro-substituted compounds **72** and **74-77**. Compounds **74** and **77** exhibit higher melting points than those of **67** and **70**. However, it is difficult to predict the melting point of organic compounds as they depend on a number of factors.

The fluoro-substituted compound **72** with branched citronellyloxy terminal chains, like the corresponding non-fluoro-substituted compound **65** with the same terminal chains, does not exhibit any observable liquid crystalline mesophases. This is again probably due to the high degree of chain branching in the side chains of compound **72**, which hinder effective packing of the molecules. The presence of fluorine atoms in compound **77** in a lateral position eliminate any observable mesomorphic behaviour. The presence of fluorine atoms in a lateral position in compound **74** results in the absence of both the ordered smectic, SmX and SmA mesophases.

The fluoro-substituted compound **75** also does not possess a SmA mesophase. Interestingly, the presence of fluorine atoms in compound **76** eliminates the SmA mesophase, but induces a nematic mesophase, probably due to steric effects associated with the fluorine atoms eliminating a layer structure at elevated temperatures. This could be of significant importance. The vast majority of known liquid crystalline organic semiconductors only exhibit smectic mesophases. A nematic mesophase would be easier to align on a device substrate and could still exhibit a high charge-carrier mobility.

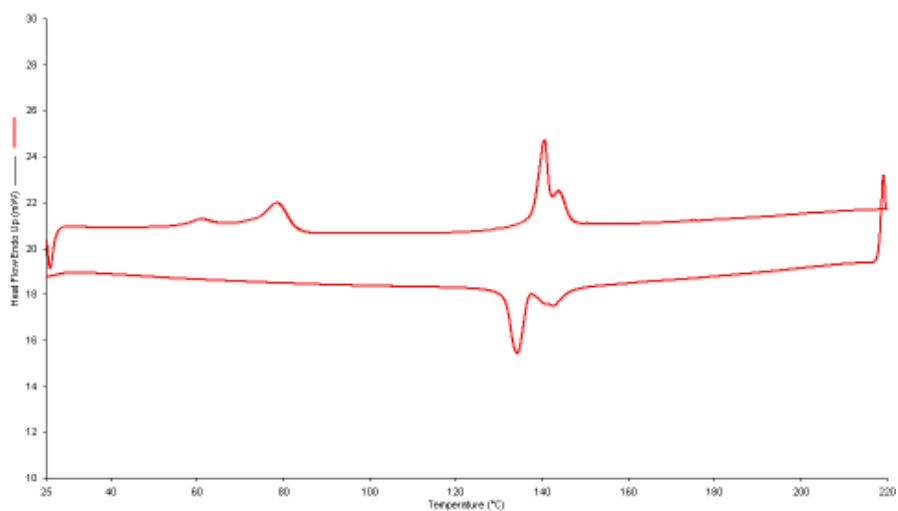
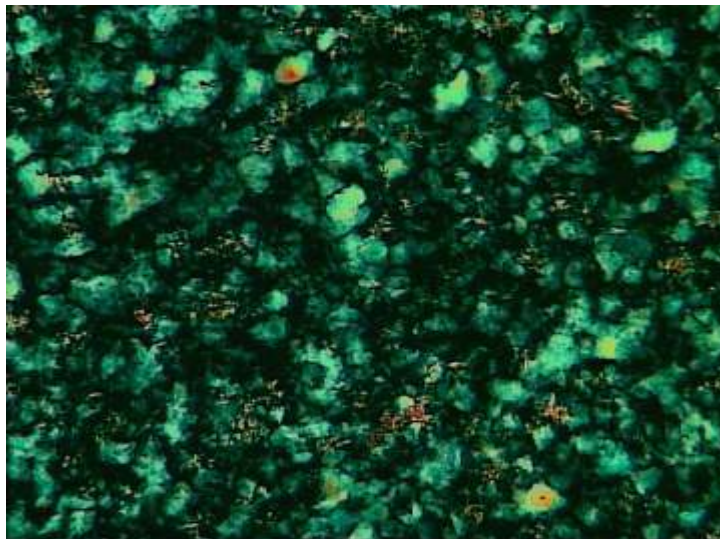


Figure 4.4 - DSC thermogram as a function of temperature for compound **75** (scan rate 10 °C/minute)

The DSC trace, figure 4.4, confirms the liquid crystalline transition temperatures of compound **75**. The optical appearance between cross polarisers of the SmX mesophase exhibited by compound **75** can be seen in picture 4.3.



Picture 4.3 - The SmX mesophase of compound **75** at 139 °C

Although direct comparisons cannot be made between the compounds shown in table 4.6, due to the materials incorporating different alkyl spacer chain lengths and different polymerisable groups at the end of the spacers, it is generally observed that

the incorporation of the non-conjugated diene end-group serves to suppress the melting point and liquid crystalline transition temperatures in comparison to both the methacrylate and oxetane analogues, as well as reducing the clearing point, although less significantly. However, this is not always shown to be the case, particularly with fluorine atoms incorporated in a lateral position, see table 4.6. This may be attributed to its more sterically bulky shape, lowering transition temperatures by interfering with the organisation of the molecules. Another consequence of the melting point suppression is that the highest order smectic phases are also exhibited by the non-conjugated diene RMs. Also the non-conjugated diene RMs generally tend to have a larger mesophase temperature range when compared with the methacrylate and oxetane RMs. None of the materials **65**, **67-70**, **72** and **74-77** and the reference compounds **M2-M7** detailed in table 4.6 exhibit a glassy state.

4.7.1 Charge-Carrier Mobility

The hole and/or electron mobility of the nematic phase of calamitic RMs is usually low, i.e., in the range of 10^{-5} - 10^{-3} $\text{cm}^2 \text{V}^{-1} \text{s}^{-1}$ and much lower than that of highly ordered smectic mesophases^[28]. The high order SmG phase formed by the non-polymerisable reference compound **M2** with a PTPP molecular core shows excellent electron and hole mobility values, approaching 10^{-1} $\text{cm}^2 \text{V}^{-1} \text{s}^{-1}$, see table 4.7. Comparing the value for the charge-transport of the non-polymerisable reference compound **M2** with that of RMs, e.g., the PTPP-diene **M3** and the PTPP-oxetane **M7**, a lower value for the mobility of the polymerisable analogues is observed, see table 4.7. The PTPP-oxetane **M7** values were obtained in the SmB mesophase and relatively high values for the mobility ($\approx 10^{-2}$ $\text{cm}^2 \text{V}^{-1} \text{s}^{-1}$) for both holes and electrons, were found.

Table 4.7 Summary of the mobilities for PTPP and its analogues^[26]

Material	$\mu_{\text{hole}} (\text{cm}^2 \text{V}^{-1} \text{s}^{-1})$	$\mu_{\text{electron}} (\text{cm}^2 \text{V}^{-1} \text{s}^{-1})$	Mesophase
PTPP (M2)	4.4×10^{-2} (at 175 °C)	7.1×10^{-2} (at 175 °C)	SmG
PTPP-diene (non-polymerised) (M3)	6.6×10^{-3} (at 140 °C)	1.7×10^{-4} (at 140 °C)	SmG
PTPP-diene (polymerised)	7.1×10^{-4} (at 15 °C)	7.5×10^{-4} (at 15 °C)	
PTPP-oxetane (non-polymerised)	9.5×10^{-3} (at 140 °C)	7.5×10^{-3} (at 140 °C)	SmB
PTPP- oxetane (M7)	1.6×10^{-2} (at 15 °C)	2.8×10^{-2} (at 15 °C)	
PTPP- oxetane (polymerised)	3.3×10^{-2} (at 140 °C)	2.4×10^{-2} (at 140 °C)	

It appears that the oxetane end-group in compound **M7** tends to have a much smaller effect on charge-transport compared to that of the non-conjugated diene end-group in compound **M3**. The presence of the non-conjugated diene end-group clearly effects the electron transport more significantly than that of hole transport, see table 4.7. This may be due to stabilisation of the charged species on the highly-polar, non-conjugated diene moiety, which leads to a much lower charge mobility.

When the hole transport of the two RMs **M3** and **M7** is compared, it can be seen that the higher order present in the SmG mesophase of the diene **M3** has no compensating effect on the mobility, when compared to that measured in the less ordered SmB mesophase of the oxetane **M7**. This is in contrast to the general transport behaviour

observed in calamitic liquid crystalline systems, which show an improvement in mobility as the material forms higher order mesophases. The higher the order of the mesophase, the better the π -overlap between neighbouring molecules and the higher the subsequent carrier mobility^[28-29].

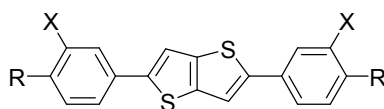
Post-polymerisation results have shown to yield long range charge-transport in both systems over a large temperature range, including RT, with comparable values for the mobility to those of the RM mesophases before polymerisation. In the case of the PTTP-oxetane **M7**, the electron mobility was found to be temperature dependent whereas the hole mobility showed a weak temperature dependence. In contrast, the PTTP-diene **M3** shows temperature independent hole and electron mobility^[26]. The electron mobility in PTTP-diene **M3** is higher in the polymer network formed after polymerisation than in the precursor RM mesophase. This provides further evidence that the non-conjugated diene end-group acts as a chemical trap for electrons. This is in contrast to the data for hole transport, which shows a lower magnitude of mobility after the polymerisation of the RM **M3**. This may be attributable to trapping due to the residues from the photoinitiator [Irgacure 651 (2,2-dimethoxy-1,2-diphenyl-ethan-1-one), Ciba Geigy] used. Consequently, non-conjugated diene containing RMs are unsuitable where ambipolar transport is required.

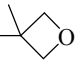
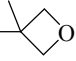
In the case of the polymerised PTTP-oxetane **M7** there are only small changes in both the electron and hole mobility in the polymer network formed after polymerisation compared to that of the precursor RM mesophase, although the mobility is measured at different temperatures for the RM and the polymer network. The values determined for the oxetane **M7** and its polymer network approach the values measured for the reference PTTP compound **M2**. The cationic photoinitiator used in the oxetane polymerisation reaction [Omnicat 550 (10-biphenyl-4-yl-2-isopropyl-9-oxo-9H-thioanthen-10-ium hexafluorophosphate), IGM resins] does not appear to effect charge-transport, this is in contrast to what is observed for the non-conjugated diene **M7**, where a free radical photoinitiator was used, see above. Therefore, it appears reasonable to assume that the choice of photoinitiator used in the polymerisation reaction may well affect the magnitude of the charge transport^[30].

4.8 Reaction Schemes Eleven and Twelve

The mesomorphic behaviour and liquid crystalline transition temperatures (°C) of the 2,5-(3,4-disubstituted-phenyl)thieno[3,2-*b*]thiophenes **85**, **87-90**, **91** and **93-96** are collated in Table 4.8.

Table 4.8 Chemical structures and liquid crystalline transition temperatures (°C) for the 2,5-(3,4-disubstituted-phenyl)thieno[3,2-*b*]thiophenes compounds **85**, **87-90**, **91** and **93-96**)



Compound	X	R	Cr	SmX2	SmX1	I
85	H	$-\text{OC}_2\text{H}_4\text{CH}(\text{CH}_3)\text{C}_2\text{H}_4\text{CH}=\text{C}(\text{CH}_3)_2$	• 229	-	-	•
87	H	$-\text{OC}_{10}\text{H}_{20}\text{CO}_2\text{CH}(\text{CH}=\text{CH}_2)_2$	• 100	• 179	• 227	•
88	H	$-\text{OC}_9\text{H}_{18}\text{O}_2\text{CC}(\text{CH}_3)=\text{CH}_2$	• 116	• 169	• 215	•
89	H	$-\text{OC}_{11}\text{H}_{22}\text{O}_2\text{CC}(\text{CH}_3)=\text{CH}_2$	• 116	• 169	• 206	•
90	H	$-\text{OC}_6\text{H}_{12}\text{OCH}_2$ 	• 157	-	• 239	•
91	F	$-\text{OC}_2\text{H}_4\text{CH}(\text{CH}_3)\text{C}_2\text{H}_4\text{CH}=\text{C}(\text{CH}_3)_2$	• 194	-	-	•
93	F	$-\text{OC}_{10}\text{H}_{20}\text{CO}_2\text{CH}(\text{CH}=\text{CH}_2)_2$	• 74	-	• 188	•
94	F	$-\text{OC}_9\text{H}_{18}\text{O}_2\text{CC}(\text{CH}_3)=\text{CH}_2$	• 139	• 177	• 185	•
95	F	$-\text{OC}_{11}\text{H}_{22}\text{O}_2\text{CC}(\text{CH}_3)=\text{CH}_2$	• 127	• 173	• 179	•
96	F	$-\text{OC}_6\text{H}_{12}\text{OCH}_2$ 	• 191	-	-	•

SmX2 and SmX1 denote unidentified ordered smectic mesophases

Compound **85** was found not to exhibit any liquid crystalline mesophases. The high degree of chain branching in the side chains of compound **85** probably hinders effective packing of the molecules. This effect dilutes the van der Waals forces of attraction between the aromatic cores of adjacent molecules. The melting point of compound **85** is high, although the combined effect of four branching methyl groups in the chain should lead to relatively low melting points for such compounds with three aromatic rings, one of which is fused, in the aromatic core. Unfortunately, the presence of the branching methyl groups in the terminal alkoxy chains also decreases the tendency for mesophase formation.

The non-conjugated diene, compound **87**, containing no branching methyl groups in the terminal alkoxy chains, was found to exhibit two enantiotropic unidentified ordered smectic mesophases, SmX2 and SmX1. The related compounds **88** and **89** both have polymerisable methacrylate end-groups, rather than a non-conjugated diene end-groups, but differ in the aliphatic spacer lengths, C9 alkoxy chains for compound **88** and C11 alkoxy chains for compound **89**. Both compounds possess identical melting points (Cr-SmX2) and smectic-smectic transition temperatures (SmX2-SmX1), with compound **89** having a slightly lower clearing point (206 °C) than that of compound **88** (215 °C). The oxetane, compound **90**, exhibits an enantiotropic unidentified ordered smectic mesophase, SmX1, with relatively high melting (157 °C) and clearing (239 °C) points. The rigid, planar and highly conjugated nature of the thieno[3,2-*b*]thiophene molecular core probably makes it difficult to induce liquid crystallinity with low liquid crystalline transition temperatures.

However, in an attempt to produce analogous compounds, but with lower liquid crystalline transition temperatures, especially the melting point, fluorine atoms were incorporated in a lateral position in the compounds **85** and **87-90** to produce the corresponding fluoro-substituted compounds **91** and **93-96**, respectively, see table 4.8. Generally, the liquid crystalline transition temperatures, including the melting and clearing points, of the fluoro-substituted compounds **91** and **93-96** are lower than those of the corresponding non-fluoro substituted compounds **85** and **87-90**. This is again probably due to steric effects associated with the presence of the fluorine atoms incorporated in a lateral position. This was not the case for the methacrylates, compounds **94** and **95**, whose melting point (Cr-SmX2) and smectic-smectic

transition temperature (SmX2-SmX1) are actually higher than the corresponding values for the non-fluoro substituted methacrylate compounds **88** and **89**. The fluoro-substituted compound **91**, like the non-fluoro substituted compound **85**, does not exhibit any observable liquid crystalline mesophases, again probably due to the high degree of branching associated with the methyl groups in the alkoxy side chains which hinders effective packing of adjacent molecules. The presence of fluorine atoms in the non-conjugated diene, compound **93**, results in the loss of an ordered smectic mesophase. The presence of fluorine atoms in the oxetane, compound **96**, in a lateral position, eliminates any observable mesomorphic behaviour; cf the corresponding non-fluoro substituted oxetane, compound **90**, which exhibits an unidentified ordered smectic phase (SmX1) at an elevated temperature.

Although direct comparisons cannot be made between the compounds shown in table 4.8, due to the materials incorporating different alkyl spacer chain lengths and different polymerisable groups at the end of the spacers, it is generally observed that the incorporation of the non-conjugated diene end-group serves to suppress the melting point of the materials in comparison to both the methacrylate and oxetane analogues. However, the liquid crystalline transition temperatures and clearing points tend to, in general, be slightly higher. It is also observed that, as in the case of the [2,2']-bithiophenes, table 4.6, the non-conjugated diene RMs generally tend to have a larger mesophase temperature range when compared with the methacrylate and oxetane RMs. None of the materials detailed in table 4.8 exhibit an observable glassy state on cooling in the DSC evaluations of these materials.

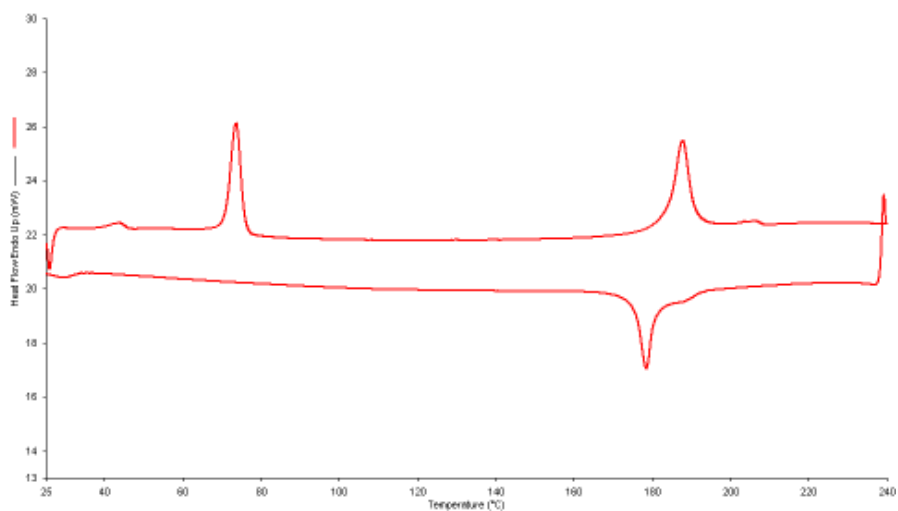
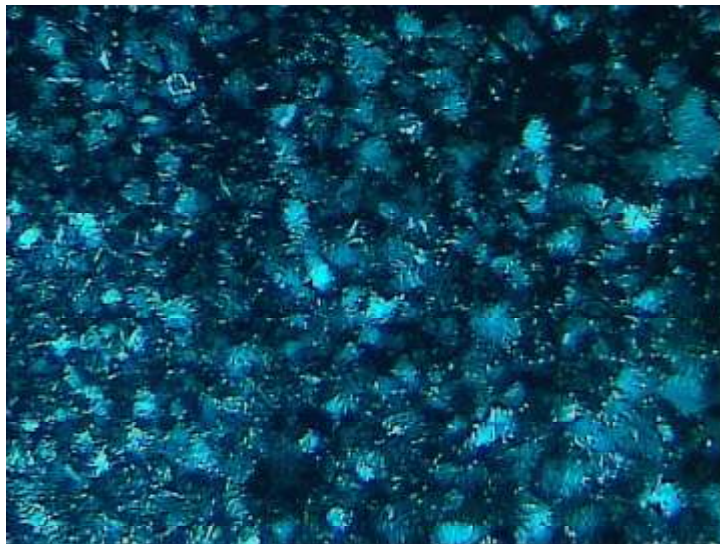


Figure 4.5 - DSC thermogram as a function of temperature for compound **93** (scan rate 10 °C/minute)

The DSC trace, figure 4.5, confirms the liquid crystalline transition temperatures of compound **93**. The optical appearance between cross polarisers of the SmX mesophase exhibited by compound **93** can be seen in picture 4.4.

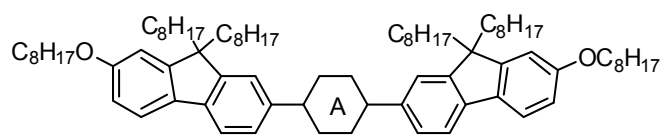


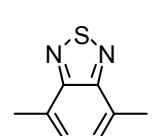
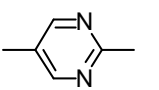
Picture 4.4 - The SmX mesophase of compound **93** at 188 °C

4.9 Reaction Scheme Fourteen

The melting points (°C) of the difluorenes **107** and **108** are shown in Table 4.9.

Table 4.9 Chemical structures and melting points (°C) for the heterocyclic difluorenes **107** and **108**



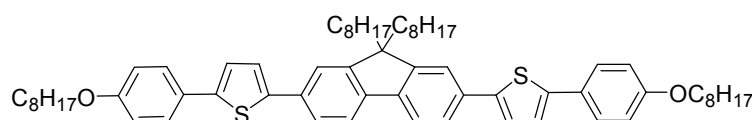
Compound	A	Cr	I
107			oil
108			oil

Compounds **107** and **108** were found not to exhibit any liquid crystalline mesophases. This is probably due to a combination of the length of the alkyl chains at the bridging benzylic position (9-position) on the fluorene aromatic cores and the non-linear molecular shape of the materials. However, the length of the alkyl chains at the bridging benzylic position of the fluorene aromatic cores tends to have a strong influence on the transition temperatures of polyfluorene homopolymers, and is probably the major reason why compounds **107** and **108** do not exhibit any observable liquid crystalline mesophases.

4.10 Reaction Scheme Fifteen

The mesomorphic behaviour and liquid crystalline transition temperatures (°C) of the 2,7-disubstituted-(5-{4-[octyloxy]phenyl}thien-2-yl)-9,9-dioctylfluorene **115** are shown in Table 4.10.

Table 4.10 Chemical structure and liquid crystalline transition temperatures (°C) for the 2,7-disubstituted-(5-{4-[octyloxy]phenyl}thien-2-yl)-9,9-dioctylfluorene **115**



Compound	Tg	Cr	N	I
115	• -3	• 56	• 91	•

Compound **115** exhibits a relatively low melting point (56 °C) and a nematic mesophase, due to the presence of the two long C8 alkyl chains at the 9-position on the fluorene aromatic core which increase the intermolecular distance and consequently lower the van der Waals forces of attraction between the aromatic cores. In addition to which, a glass transition temperature was also exhibited. Most 2,7-disubstituted-9,9-dialkylpolyfluorenes exhibit a high glass transition temperature that allows the polymer to be quenched to form a nematic glass at or above room temperature, in which the liquid crystalline order is preserved. However, the glass transition temperature for compound **115** is present at -3 °C and therefore unsuitable for practical applications.

Fluorene-based polymers and compounds have been reported extensively and have been shown to exhibit good hole-transporting properties^[31-32]. Compound **115** was synthesised with straight C8 alkyl chains at the peripheries of the molecule, unfortunately, due to time constraints, this material was unable to be synthesised as a RM.

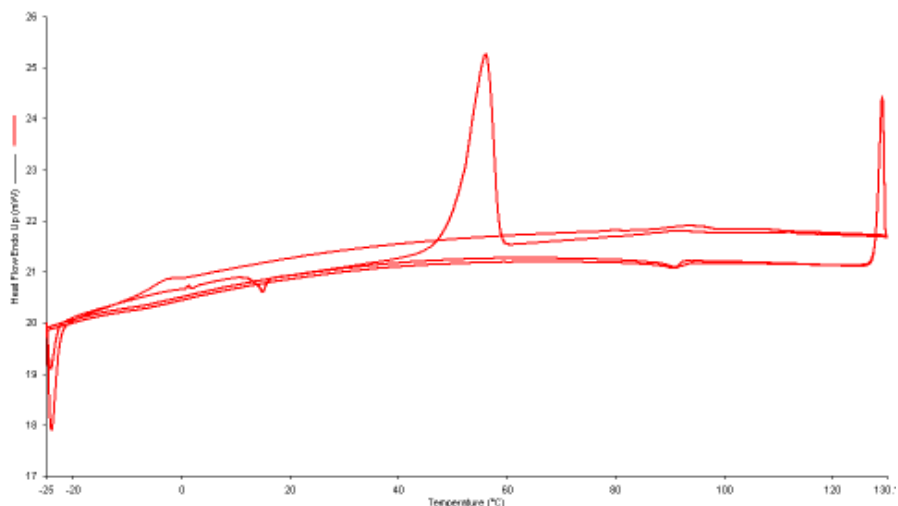
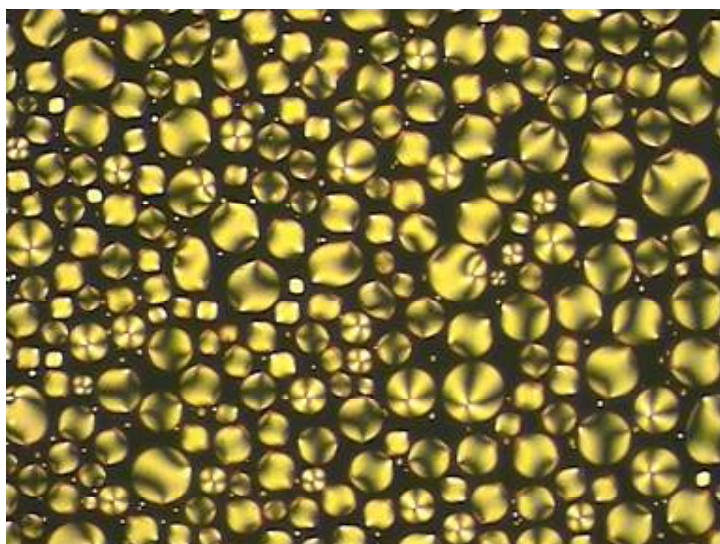


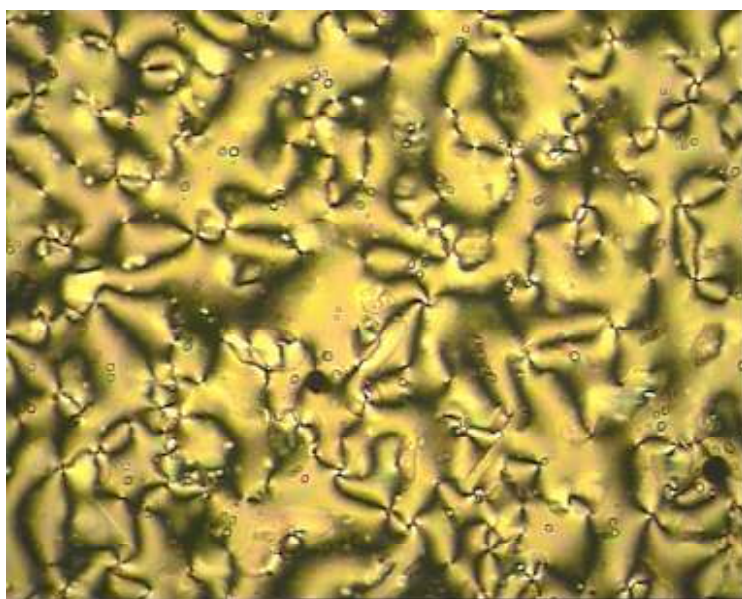
Figure 4.6 - DSC thermogram as a function of temperature for compound **115** (scan rate 10 °C/minute)

The DSC trace, figure 4.6, confirms the liquid crystalline transition temperatures of compound **115**. The large melting transition peak and the relatively small monotropic nematic-isotropic peak is characteristic of a nematic LC. A second order transition peak is observed on cooling and heating at -3 °C, which is characteristic of a glass transition temperature due to a shift in the baseline. On heating above the glass transition temperature the compound does not crystallise readily and no transitions are observed until the clearing point.

The optical appearance between crossed polarisers of the nematic mesophase exhibited by compound **115** can be seen in pictures 4.5 and 4.6. Droplets, characteristic of a nematic phase are observed as well as 2-point and four-point brushes. The droplets are formed on cooling the isotropic liquid above the nematic phase.



Picture 4.5 - The droplet texture of the nematic mesophase of compound **115** formed by slow cooling (1 °C/minute) from the clearing point to the onset of the nematic phase



Picture 4.6 - The texture of the nematic mesophase of compound **115** at 90 °C

4.11 Cyclic Voltammetry (CV)

Table 4.11 The ionisation potential (IP) and electron affinity (EA) of the RMs **29**, **39**, **62**, **68**, **75**, **87** and **93**

Compound	IP ^a (eV) \pm 0.02	E _g ^b (eV) \pm 0.04	EA ^c (eV) \pm 0.06	Comment
29	5.78	2.65	3.86	Reversible
39	5.97	2.72	3.25	Reversible
62	5.50	2.68	2.82	Reversible
68	5.48	2.63	2.85	Reversible
75	5.59	2.66	2.93	Reversible
87	5.54	2.92	2.62	Reversible
93	5.67	2.95	2.72	Reversible

^aFrom CV ^bFrom optical absorption spectrum ^cFrom IP - E_g

Efficient OFETs and OTFTs require hole injection materials with low ionisation potentials (IPs) and electron injection materials with high electron affinities (EAs). The standard strategy to increase or decrease the IP of a molecule is to include electron withdrawing or donating groups respectively in to its aromatic core. The IP tends not to be sensitive to the spacer length of the aliphatic end-chain spacer units. Table 4.11 shows the measured IPs of some selected RMs that were synthesised in this PhD programme.

The IPs of the RMs were measured electrochemically by CV using a computer-controlled scanning potentiostat (Solartron 1285). 1 mM of the compound was dissolved in 5 cm³ of an electrolytic solution (0.1 M tetrabutylammonium hexafluorophosphate in dichloromethane). The solution was placed in a standard three-electrode electrochemical cell. A glassy carbon electrode was used as the working electrode and a silver/silver chloride (3 M NaCl and saturated Ag/Cl)) and a platinum wire formed the reference and counter electrodes respectively. The

electrolyte was recrystallised twice before use and oxygen contamination was avoided by purging the solution with dry argon before each measurement.

The measured potentials were corrected to an internal ferrocene reference added at the end of each measurement. A typical scan rate of 20 mV s^{-1} was used. Two scans were performed to check the reproducibility. A value for the reduction potential was unable to be measured because of the limited working range of the electrolyte. However, EA was estimated by subtraction of the optical bandedge, taken as the energy of the onset of absorption of the compound, from the IP. This approximation however, does not include a correction for the exciton binding energy.

The efficiency of a semiconductor is determined by the band-gap (E_g) of a compound. A reduction in the magnitude of the E_g results in a more proficient semiconductor, that is, less energy is required to promote electrons, either thermally or through an applied field, from the valence band to the conduction band and hence conduct electricity. The dibenzothiophene materials, compounds **29** and **39**, containing 5 aromatic rings in the core, 3 of which are fused, serves to extend the conjugation and generally reduces the E_g , have E_g values of 2.65 and 2.72 eV respectively. The incorporation of non-fused thiophene rings in to the cores of compounds **62** (thiophenes) and **68** and **75** ([2,2']-bithiophenes), which contain 3 and 4 aromatic rings respectively in the cores, have E_g values of 2.68, 2.63 and 2.66 eV respectively. The materials incorporating 4 aromatic rings, two of which are fused thiophene rings, compounds **87** and **93** (thieno[3,2-b]thiophenes) have E_g values of 2.92 and 2.95 eV respectively. The two electron-withdrawing fluorine atoms that are present in the cores of compounds **39**, **75** and **93** increased the IP by 0.19, 0.11 and 0.13 eV respectively, over the non-fluorinated analogues, compounds **29**, **68** and **87**. The lower IPs exhibited by the compounds **62** and **68** compared to compounds **29**, **39**, **87** and **93** can be attributed to the presence of the non-fused thiophene rings, in addition to the electron-rich nature of sulphur. However, this was not shown to be the case for compound **75**, which exhibited a higher IP (0.05 eV) than compound **87**.

4.12 References

- 1 J. Barche, S. Janietz, M. Ahles, R. Schmechel and H. von Segern, *Chem. Mater.*, 2004, **16** (22), 4286.
- 2 I. McCulloch, W. Zhang, M. Heeney, C. Bailey, M. Giles, D. Graham, M. Shkunov, D. Sparrowe and S. Tierney, *J. Mater. Chem.*, 2003, **13** (10), 2436.
- 3 A. Dodabalapur, L. Torsi and H. E. Katz, *Science*, 1995, **268**, 270.
- 4 B. Neises and W. Steglich, *Angew. Chem. Int. Ed. Engl.*, 1978, **17** (7), 522.
- 5 J. C. Sheehan and G. P. Hess, *J. Am. Chem. Soc.*, 1955, **77** (4), 1067.
- 6 N. Miyaura and A. Suzuki, *J. Chem. Soc., Chem. Commun.*, 1979, **19**, 866.
- 7 N. Miyaura and A. Suzuki, *Chem. Rev.*, 1995, **95** (7), 2457.
- 8 N. Miyaura, K. Yamada and A. Suzuki, *Tet. Lett.*, 1979, **20** (36), 3437.
- 9 J. F. Fauvarque and A. J. Jutland, *J. Organomet. Chem.*, 1977, **132** (2), C17.
- 10 A. Gillie and J. K. Stille, *J. Am. Chem. Soc.*, 1980, **102** (15), 4933.
- 11 C. Amatore and A. J. Jutland, *J. Organomet. Chem.*, 1999, **576** (1-2), 254.
- 12 R. F. Heck, '*Palladium Reagents in Organic Synthesis*', Academic Press Inc., New York (1985).
- 13 A. Pelter, K. Smith and H. C. Brown, '*Borane Reagents*', Academic Press Inc., New York (1988).
- 14 A. O. Aliprantis and J. W. Canary, *J. Am. Chem. Soc.*, 1994, **116** (15), 6985.
- 15 I. McCulloch, C. Bailey, K. Genevicius, M. Heeney, M. Shkunov, D. Sparrowe, S. Tierney, W. Zhang, R. Baldwin, T. Kreouzis, J. W. Andreasen, D. W. Breiby and M. N. Nielsen, *Phil. Trans. R. Soc. A*, 2006, **364**, 2779.
- 16 H. Sasaki and J. V. Crivello, *J. Macromol Sci. Part A: Pure & Appl. Chem.*, 1992, **29** (10), 915.
- 17 O. Nuyken, R. Böhner and C. Erdmann, *Macromol. Symp.*, 1996, **107**, 125.
- 18 J. V. Crivello and H. Sasaki, *J. Macromol Sci. Part A: Pure & Appl. Chem.*, 1993, **30** (2-3), 189.
- 19 J. Lub, V. Recaj, L. Puig, P. Forcén and C. Luengo, *Liq. Cryst.*, 2004, **31** (12), 1627.

- 20 J. K. Stille, *Angew. Chem. Int. Ed. Engl.*, 1986, **25** (6), 508.
- 21 M. Mushrush, A. Facchetti, M. Lefenfeld, H. E. Katz and T. J. Marks, *J. Am. Chem. Soc.*, 2003, **125** (31), 9414.
- 22 X. M. Hong, H. E. Katz, A. J. Lovinger, B.-C. Wang and K. Raghavachari, *Chem. Mater.*, 2001, **13** (12), 4686.
- 23 F. Garnier, A. Yassar, R. Hajlaoui, G. Horowitz, F. Deloffre, B. Servet, S. Ries and P. Alnot, *J. Am. Chem. Soc.*, 1993, **115** (19), 8716.
- 24 D. Fichou, *J. Mater. Chem.*, 2000, **10** (3), 571.
- 25 T. Kreozis, R. J. Baldwin, M. Shkunov, I. McCulloch, M. Heeney and W. Zhang, *Appl. Phys. Lett.*, 2005, **87** (17), 172110.
- 26 R. J. Baldwin, T. Kreouzis, M. Shkunov, M. Heeney, W. Zhang and I. McCulloch, *J. Appl. Phys.*, 2007, **101** (2), 023713.
- 27 M. Heeney, W. Zhang, S. Tierny, D. Sparrowe, M. Shkunov and I. McCulloch, *USA Patent Appl.*, 20050184274, (2005).
- 28 M. Funahashi and J.-I. Hanna, *Phys. Rev. Lett.*, 1997, **78** (11), 2184.
- 29 M. Funahashi and J.-I. Hanna, *Appl. Phys. Lett.*, 1998, **73** (25), 3733.
- 30 M. Funahashi and J.-I. Hanna, *Chem. Phys. Lett.*, 2004, **397** (4-6), 319.
- 31 D. E. Loy, B. E. Koene and M. E. Thompson, *Adv. Funct. Mater.*, 2002, **12** (4), 245.
- 32 M. Redecker, D. D. C. Bradley, M. Inbasekaran and E. P. Woo, *Appl. Phys. Lett.*, 1999, **74** (10), 1400.



Chapter Five



Conclusions



•

•



•

•

•

•

•

5.0 Conclusions

The research efforts for this thesis were focused on liquid crystalline organic semiconductors that should have been, at least in theory, relatively easy to synthesise, purify and subsequently characterise. However, purification of the desired compounds and many reaction intermediates proved difficult and many syntheses had to be repeated several times before the desired final products could be isolated with the required purity. This was primarily due to a lack of solubility of many of the reaction intermediates. However, in spite of these synthetic difficulties, a wide range of charge-transporting RMs for organic semiconductor device applications, have been successfully synthesised. Many of the compounds exhibit liquid crystalline mesophases over significant temperature ranges. The materials synthesised have enabled relationships between molecular structure, especially the nature of the polymerisable end-group, and the mesomorphic behaviour and liquid crystalline transition temperatures to be established.

The determination of a correlation between molecular structure and charge transporting properties was intended to be facilitated by the synthesis of the series of related compounds with different central chromophores, spacer groups and polymerisable end-groups, enabling clear comparisons of the efficiency of each of the chromophores and polymerisable end-groups before and after polymerisation to be established. However, no charge-carrier transport properties (TOF measurements) were attained for any of the RMs synthesised in this thesis, see results and discussion section. Provisional results from our collaborators at Merck have, however, been included in this thesis.

The first series of compounds to be synthesised incorporated a disubstituted dibenzothiophene aromatic ring system. This class of materials generally exhibits smectic mesophases (SmA and SmC) and an additional unidentified ordered smectic mesophase (SmX) at elevated temperatures and over wide temperature ranges. The differences in the structure of the materials, such as the presence of different spacer lengths and/or end-groups and the introduction of fluorine atoms in the 2-position on the phenyl rings, to lower the melting points of materials, did not lead to a loss of

mesomorphic behaviour, although the unidentified ordered smectic phase was lost when the fluorine atoms were present in the molecular core.

The diphenyl-substituted thiophene materials exhibit a smectic mesophase (SmC) and an unidentified ordered smectic mesophase (SmX) when photo-polymerisable non-conjugated diene end-groups are present in the materials structure. A series of disubstituted [2,2']-bithiophenes and thieno[3,2-b]thiophenes were also synthesised. The [2,2']-bithiophene class of materials also exhibit smectic mesophases (SmA and SmC) and an additional unidentified ordered smectic mesophase (SmX) over large temperature ranges. This class of materials also exhibits a nematic mesophase when photo-polymerisable methacrylate end-groups are incorporated, in lateral position, and fluorine atoms incorporated adjacent to the molecular core, into the materials structure. The thieno[3,2-b]thiophene class of materials exhibit two unidentified ordered smectic mesophases (SmX2 and SmX1) again over significant temperature ranges. The liquid crystalline transition temperatures were significantly lower for each class of material, i.e., the [2,2']-bithiophenes and the thieno[3,2-b]thiophenes, in the presence of branched photo- and chemically-polymerisable groups at the ends of the spacers and fluorine atoms in the 2-position on the phenyl rings in the materials structures.

Benzo-2,1,3-thiadiazole and pyrimidine heterocyclic rings with fluorene units were synthesised. However these materials do not exhibit any observable liquid crystalline mesophases, probably due to the length of the C8 alkyl chains at the bridging benzylic position (9-position) on the fluorene aromatic cores. A disubstituted, fluorene-based, liquid crystalline material was synthesised (compound **115**) with a straight C8 alkyl chain at the peripheries of the molecule, which exhibited a nematic mesophase. Unfortunately, due to time constraints, this material was unable to be synthesised as a RM.

LCs incorporating the 2,7-disubstituted-9,9-dialkylfluorene unit tend to form nematic mesophases due to steric effects. Consequently materials containing these units tend to have lower viscosities than analogous materials forming smectic mesophases due to the absence of a layer structure. This was intended to allow the new nematic liquid

crystalline semiconductors to be aligned more easily than the standard smectic semiconductors for practical devices.

Unfortunately, apart from the disubstituted fluorene-based material (compound **115**) which exhibits a glass transition temperature at -3 °C, there was no evidence for the formation of stable glasses, at or above room temperature, by any of the other materials synthesised. The formation of a stable glass by a material is an attractive property for organic semiconductors, as it would allow device fabrication based on anisotropic polymer networks to be carried out at or above room temperature.

From this work, it has been observed that the liquid crystalline transition temperatures can be manipulated by synthetically altering the structure of the RMs. This has been successfully achieved by changing the central aromatic chromophore, the number of methylene units in the spacers between the aromatic chromophore and the polymerisable end-groups, the polymerisable end-groups themselves and the introduction of fluorine atoms in the 2-position on the phenyl rings of specific materials.